DEVELOPMENT OF THE ULTRA-HIGH-FREQUENCY RADIO RANGE

PART III

A VISUAL-AURAL ULTRA-HIGH-FREQUENCY RADIO RANGE WITH SIMULTANEOUS VOICE

By

Radio Development Section
Technical Development Division

Technical Development Report No 49

June 1945

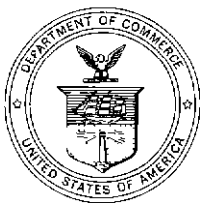

U S DEPARTMENT OF COMMERCE
CIVIL AERONAUTICS ADMINISTRATION
WASHINGTON, D C

UNITED STATES DEPARTMENT OF COMMERCE

HENRY A WALLACE, *Secretary*

CIVIL AERONAUTICS ADMINISTRATION

THEODORE P WRIGHT, *Administrator*

CONTENTS

TABLE INDEX

DEVELOPMENT OF THE ULTRA-HIGH-FREQUENCY RADIO RANGE

PART III - A VISUAL-AURAL ULTRA-HIGH-FREQUENCY RADIO RANGE WITH SIMULTANEOUS VOICE

SUMMARY

This report describes the development of an ultra-high-frequency two-course visual radio range with sector identification and simultaneous voice It treats the basic principles of the various components of this type of range, such as the mechanical modulator, radio-frequency bridges, antenna systems, and tie lines

The latter part of the report covers further simplification of the antenna system and various methods of applying simultaneous voice to this range A navigational aid was developed which provided two visual courses, two aural courses to give sector identification, station identification, and a simultaneous voice feature for weather information and airway traffic control The receiving and transmitting equipment which was used in this development is described, and the results of flight tests are given

This radio range was developed to demonstrate improved methods in air navigation which would simplify the orientation problem The field patterns are arranged so that the pilot is continuously informed as to the quadrant he is in by a combination of visual and aural indications These principles were demonstrated and proved to be a great step forward in the simplification of the navigation problem

INTRODUCTION

Previous reports[1,2] describe the application of ultra-high frequencies to radio range problems The systems described in these reports produce four aural courses similar to those of the low-frequency range systems now in use The major disadvantage of the four-course aural range is that a complicated and lengthy orientation procedure is necessary if the pilot wishes to determine in what quadrant he is located In bad weather it is necessary that a pilot be immediately aware of his location so that a minimum of maneuvering is necessary to reach his destination Previously, systems have been proposed to supply quadrant identification for the low-frequency ranges [3,4] These systems have not been adopted because of their added complexity

An approach to the problem of supplying information to the pilot as to his bearing with respect to the range station has been made at the ultra-high frequencies in the development of an omnidirectional radio range [5]

---

[1]J C Hromada, "Preliminary Report on a Four Course Ultra-High-Frequency Radio Range," CAA Technical Development Report No 3, January 1938

[2]J C Hromada and P B King, "Development of the Ultra-High-Frequency Radio Range Part I - The Ultra-High-Frequency Aural Radio Range," CAA Technical Development Report No 42, June 1944

[3]F W Dunmore, "A Method of Providing Course and Quadrant Identification with the Radio Range Beacon System," National Bureau of Standards Journal of Research, Vol 11, September 1933

[4]Francis Pope, U S Patent 2,187,097

[5]D G. C Luck, "An Omnidirectional Radio-Range System," RCA Review, July 1941 and January 1942

Further developments in the omnidirectional type of range are now in progress and, at this writing, it is yet to be determined whether this type of range will provide the same degree of accuracy and reliability as the two-course visual range

In May 1939, a subcommittee of the Radio Technical Committee for Aeronautics conducted an experimental program with a Link Trainer which was equipped to simulate a four-course aural range, a two-course visual range with sector identification, and an omnidirectional range It was the unanimous decision of the group of pilots who participated in these tests that the two-course visual range with sector identification was the preferred type of range

In August 1939, a contract was awarded to the International Telephone Development Co , Inc , for the development of the two-course visual range with sector identification The system was completed and accepted by the Civil Aeronautics Administration in September 1941 Another development contract was awarded to the International Telephone and Radio Manufacturing Corporation in the fall of 1941 for the addition of a simultaneous voice feature to the system This system was completed and accepted in July 1942 During this period, engineers of the Radio Development Section constructed a simultaneous two-course range with voice and sector identification, some of the features of which were used by the International Telephone and Radio Manufacturing Corporation in the construction of their range

This report treats the basic principles of a two-course visual radio range with sector identification and simultaneous voice The development of the methods used to obtain these basic requirements is described, and flight data of the completed systems are given

THEORETICAL DISCUSSION

Theory of Radiating System

The basic field patterns which are necessary to produce a two-course visual radio range with sector identification are shown in figure 1 Two overlapping bean-shaped patterns, one of which is modulated with 150 cycles and the other with 90 cycles, form the visual courses which extend, say, east and west If the receiver is connected to a visual indicator, the indicator will point to one side when north of the course and to the other side when south of the course When located directly on course, the indicator will point to the center With this arrangement, there is no ambiguity as to whether a pilot is north or south of the course.

Another pair of bean-shaped patterns modulated at 1020 cycles is oriented at right angles to the visual cardioids. The aural patterns are keyed in an interlocked D-U rhythm, the D signal appearing to the east of the range station and the U signal to the west of the range station A station identification is also given at regular intervals with the antenna phase-reversing relay locked first on one side and then on the other side By observing the visual indicator and listening to the aural signal, the pilot can immediately establish the quadrant in which he is located In addition, the intersection of the aural patterns forms two aural courses running north and south which can also be used for navigational purposes

In a practical setup, the patterns shown in figure 1 represent only the modulation on a circular carrier field pattern Continuous carrier makes it possible to use a receiver with automatic volume control, the advantages of which will be discussed later in the report Also, the addition of simultaneous voice to the range was planned from the beginning of the project, which further emphasized the necessity of radiating a circular carrier pattern

The basic antenna configuration used to produce the bean patterns is shown in figure 2 The three-loop array consists of a center loop which radiates a circular pattern and a pair of antiphased loops which radiate a cloverleaf-shaped pattern These loops are spaced on either side of the center loop at a distance S electrical degrees

The expression for the relative field due to the outside radiators, assuming unit current represented by $\sin\omega t$ in each radiator, is

$$E_0 = 2 \sin (S \sin \theta) \cos \omega t, \qquad (1)$$

where θ is measured from the normal to the line of antennas

The field due to the center antenna with current represented by $\cos\omega t$ is circular and is represented by

$$E_c = k \cos \omega t, \qquad (2)$$

where k is the ratio of the current in the center loop to the current in either of the side loops.

Since the current in the center antenna is phased at 90° to the current in the side antennas, the field due to the array is

$$E = k \pm 2 \sin (S \sin \theta), \qquad (3)$$

the sign of the field due to the side antennas depending upon whether the relative phase of the current in one of the side antennas leads or lags the current in the center antenna by 90°

Figure 3 shows the circular and the cloverleaf patterns for an array with S = 120° and various values of k The combined pattern of the array for various values of k is shown in figure 4 The right hand pattern is formed when the phase progression in the three antennas from left to right is + 90°, 0°, − 90° Similarly, the left hand pattern is formed by the opposite phase progression, − 90°, 0°, + 90° Thus, to reverse the position of the bean pattern it is only necessary to reverse the phase of either the center or of the side antennas

The effect of k on the number and size of the minor lobes also is shown in figure 4 In this figure patterns are shown when k is 1 0, 1 4, 1 73, 1 86, 2 0, and 2 5 When the field from the center antenna equals the maximum field from the side antennas, k will be equal to 2 and there will be one minor lobe When the field from the center antenna equals the field from the side antennas at right angles to the course, k will equal 2 sin (S sin 90) or 1 732, and there will be two minor lobes For values of k between 1 732 and 2, there will be three minor lobes since the circle will intersect each half of the cloverleaf pattern in four places For the case where there are three minor lobes, each of these lobes will be smaller than for the case where there are only one or two minor lobes. When k is less than 1 732 there will be one minor lobe whose size progressively increases as k is decreased When k is greater than 2, there will be no minor lobes

Figure 5 shows the effect of the spacing, S, with a constant current ratio, k = 2 In this figure graphs are shown for S = 90°, 105°, 120°, 140°, 160°, and 180°

Two characteristics of the bean patterns are of interest, the sharpness of the pattern intersections and the clearance between the patterns at angles other than in the vicinity of the course. Course sharpness has been arbitrarily defined as the ratio in decibels of the two patterns at 1 5° off course

$$\text{Sharpness} = \frac{k + 2 \sin (S \sin 1\ 5^\circ)}{k - 2 \sin (S \sin 1\ 5^\circ)} \qquad (4)$$

$$= \frac{k + 2 \sin (0\ 026\ S)}{k - 2 \sin (0\ 026\ S)}$$

For small angles, $\sin \Delta = \Delta$ where the angle is expressed in radians

$$\text{Sharpness} = \frac{k + 0\ 00091\ S}{k - 0\ 00091\ S} \qquad (5)$$

where S is given in electrical degrees

Figure 6 shows the variation in course sharpness as k is changed, for values of S corresponding to 120°, 140°, and 160°

The pattern clearance must be such that the visual indicator in the airplane does not leave its extreme position except when approaching the vicinity of the course If it is desired that the visual indicator show full-scale deflection at 10° off course, then at any angle in the quadrant the pattern clearance must be equal to or greater than the ratio at 10°, if the pointer is to remain off scale at angles greater than 10°

$$\text{Clearance} \geqslant \frac{k + 2 \sin (S \sin 10°)}{k - 2 \sin (S \sin 10°)} \qquad (6)$$

$$\geqslant \frac{k + 2 \sin (0.1736\ \ S)}{k - 2 \sin (0\ 1736\ \ S)}.$$

There are either one or two points in each quadrant where the minor lobes are a maximum and, hence, the clearance is a minimum. One of these points is at right angles to the course and the clearance is equal to $\frac{k + 2 \sin S}{k - 2 \sin S}$ whenever k is greater than 2 sin S The other point of minimum clearance occurs whenever k is less than 2 and is located at the angle where the cloverleaf pattern has its maximum value, or $\sin (S \sin \theta) = 1$ This angle is $\sin^{-1} \frac{(90)}{S}$ and the clearance at this point is $\frac{k + 2}{k - 2}$

The most desirable pattern, if it could be obtained, is a cardioid since there would be no minor lobes in the field pattern In order to obtain a true cardioid, the spacing S would have to be 90° or less This is a difficult condition to achieve in practice because of the physical size of the loops. At 100° spacing the corners of adjacent loops almost touch and, for this reason, a minimum spacing of 120° has been decided upon in order to reduce the mutual coupling between the antenna elements The maximum spacing must be less than 180°, since with 180°spacing, four courses would be obtained instead of two. In the final design, a spacing of 120° was decided upon since it gave a physically realizable array, the field patterns of which most nearly approached cardioids

In designing the three-element array two parameters must be considered, the spacing S and the relative current ratio k. Since it was decided to use a 120° spacing, it is only necessary to examine the effect of changing k The sharpness and clearance are governed by the following relations

$$\text{Sharpness at } 1\ 5° \text{ off course} = \frac{k + 0\ 11}{k - 0\ 11} \qquad (7)$$

$$\text{Clearance at right angles to course} = \frac{k + 1\ 732}{k - 1\ 732} \qquad (8)$$

$$\text{Clearance at } 48\,6^\circ \text{ (angle at which cloverleaf has its maximum value)} = \frac{k+2}{k-2} \qquad (9)$$

The limiting ratio on the clearance is the pattern ratio at 10°, or

$$\text{Clearance} = \frac{k + 0\ 71}{k - 0\ 71} \qquad (10)$$

When maximum clearance for all angles is desired, the value of k may be solved graphically by plotting $\frac{k + 1.732}{k - 1\ 732}$ and $\frac{k+2}{k-2}$ against k and determining the point of intersection The optimum value of k will always lie between 2 and 2 sin S and will give a pattern with three minor lobes

$$2 > k > 2 \sin S$$

These curves have been plotted for S=120° and are shown in figure 7 Since we are interested only in the minimum clearance, it is necessary to plot only the minimum values of these curves In figure 8 similar curves have been prepared for values of S corresponding to 120°, 140°, and 160°

The value of k for which the clearance will be a maximum can be solved for analytically by equating the clearance at right angles to the course and the clearance at the angle where the cloverleaf is a maximum.

$$\frac{K + 2 \sin S}{k - 2 \sin S} = \frac{2 + k}{2 - k} \qquad (11)$$

Solving for k,

$$k = 2\sqrt{\sin S} \qquad (12)$$

For a spacing of 120°, this gives a value of 1 86 for k if maximum clearance is to exist in the quadrants This is the desired condition for the aural system, that is, the background signal should be a minimum except when the course is approached If any of the minor lobes were of an appreciable size, the background signal would start to come up at one of the minor lobes and the pilot might gain the impression that he was approaching the course intersection

For the visual array, it is not necessary that maximum clearance exist in the quadrants as long as the full-scale deflection of the visual indicator is obtained Referring to figure 7, it can be seen that when k is greater than 1 2, the visual indicator will deflect full scale at all angles more than 10° away from the course

A more important consideration is the effect of k on the total visual percentage modulation as the azimuth angle changes, remembering that percentage modulation is a function of the shape of the bean patterns since the carrier field pattern is circular Since the two patterns are of different frequency, it is necessary to add the absolute magnitudes of each pattern without regard to the algebraic sign The modulation on the visual course due to both patterns will be 2k since the side radiators contribute no signal at that angle.

At any other angle then,

$$M(\theta) = \left[k + 2 \sin (S \sin \theta)\right] + \left[k - 2 \sin (S \sin \theta)\right] \qquad (13)$$

The first term always has a positive sign for positive values of θ, regardless of the value of k The second term is positive for values of k greater than 2 and negative for some values of θ when k is less than 2 For values of k greater than 2 the terms can be added algebraically

$$M(\theta) = 2k \qquad (14)$$

Thus, as long as $k \geq 2$ the percentage modulation at any angle will be constant and will be equal to the percentage modulation on the visual course

When k is less than 2, the second term will be negative when

$$k < 2 \sin (S \sin \theta)$$

and the percentage modulation will be

$$M'(\theta) = 4 \sin (S \sin \theta), \tag{15}$$

or in terms of the on-course percentage,

$$\frac{M'(\theta)}{M(\theta)} = \frac{2 \sin (S \sin \theta)}{k} \tag{16}$$

The limiting angles where this relation holds can be found by letting

$$k = 2 \sin (S \sin \theta')$$

and the limiting angles are

$$\theta' = \sin^{-1}\left[\frac{\sin^{-1}\frac{k}{2}}{S}\right] \tag{17}$$

$$\theta' = \sin^{-1}\left[\frac{180 - \sin^{-1}\frac{k}{2}}{S}\right] \tag{18}$$

Between the limiting angles, equation (15) must be used to compute the percentage modulation, while for any other angle, equation (14) is valid Figure 9 shows a plot of $M(\theta)$ and $M'(\theta)$ against θ for various values of k, when the total modulation on course is 40 percent

In order to decide on a value of k for the visual system, a compromise must be made between course sharpness, modulation envelope, and pattern clearance Table I shows the effect of k on the characteristics of the visual bean patterns

TABLE I

THE EFFECT OF CURRENT RATIOS ON PATTERN CHARACTERISTICS

k (ratio)	Sharpness at 1 5° (db)	Clearance at 10° (db)	Clearance at 48 6° (db)	Clearance at 90° (db)	On-Course Signal / Max Signal (ratio)	Max Percent Mod / Percent Mod on Course (ratio)
1 0	1 94	15 4	9 5	11 4	0 333	2 00
1 4	1 36	9 7	15 1	19 5	0 412	1 43
1 732	1 10	7 6	22 8	∞	0 465	1.15
1 86	1 02	7 0	28 8	28 8	0 482	1 07
2 0	0 97	6 4	∞	22 8	0 500	1 00
2 5	0 76	5 1	19 1	14 8	0 556	1 00

A value of $k = 2$ was finally chosen for the visual system This gives a constant percentage modulation in any direction, a high average clearance at angles other than in the vicinity of the course, and a reasonably high value of course sharpness The restriction that the percentage modulation of the visual signals remain constant

is rather important since it permits using a maximum value of visual modulation without encountering overmodulation at some angles Obviously, the restriction has no meaning for the aural system because only one of the aural patterns is present at a given instant, whereas both visual patterns exist simultaneously As explained previously, a value of k=1 86 was chosen for the aural system since it gave maximum pattern clearance

In order to adjust the array, it is necessary to know what effect phase will have on the patterns In the systems described in this report, the phase between the various antennas is a function of the length of transmission line feeding the antennas and, having once been adjusted, will remain at that value Assuming the outer antennas are correctly phased at 180° to each other, it is desired to know what the patterns will be when the phase of the center antenna with respect to the side antennas is other than 90° If ϕ is the angle by which the phase of the center antenna differs from 90°, the field patterns become

$$E = \sqrt{[k \cos \phi \pm 2 \sin (S \sin \theta)]^2 + [k \sin \phi]^2}$$

which reduces to

$$E = 2\sqrt{\frac{k^2}{4} + k \cos \phi \sin (S \sin \theta) + \sin^2 (S \sin \theta)} \qquad (19)$$

Figure 10 shows the field patterns when $k = 2$ and $S = 120°$ for values of ϕ = 0° , 10° , 30°, 50°, 70°, and 90°, respectively Figure 11 shows one-half of the field pattern for values of ϕ= 0°, 10°, 30°, 50°, 70°, and 90° plotted on one graph By examining these curves it can be seen that the field is constant on course and changes slowly with ϕ in the direction of the maximum signal However, the relative field changes quite rapidly with phase in the directions of minimum signal, which provides a simple method of correctly adjusting the phase If a sensitive field detector is placed on a radial where the field should be zero when the phase between the center and side loops is correct, the phase may be adjusted for a null reading on the field detector For the case under consideration ($k = 2$, $S = 120°$) the minimum in the field pattern is located 48 6° from the course After the phase adjustments are completed, the field pattern will have the shape of the solid curve ($\phi = 0$) in figure 11.

Several other factors are of interest in adjusting the antenna array, particularly with regard to the side radiators In the foregoing discussion, it has been assumed that the outer radiators were fed 180° out of phase This was achieved by a crossover in the line feeding one of the antennas, as shown in figure 2 Actually, because of small differences in the loops, the phase may deviate slightly from 180° In this case, the field due to the two side radiators becomes

$$E = 2 \cos \left[\frac{\delta}{2} - S \sin \theta\right] \qquad (20)$$

where δ is the phase difference between the two antennas

When $\delta = 180°$, this reduces to

$$E = \sin (S \sin \theta)$$

For values of δ other than 180°, the minima of the cloverleaf pattern will not be reciprocal, as shown in figure 12 for $S = 120°$ and δ=150°, but will deviate from the normal to the array by the angle $\sin^{-1}\left[\frac{180° - \delta}{2S}\right]$ Since the courses are located at the cloverleaf nulls, the courses will not be aligned and will bend toward the radiator whose phase is lagging Referring to figure 2, let us assume that the nulls bend toward loop No. 1 In order to align the nulls and, consequently, the courses, the point of tap AB, where the outside loops are fed, must be moved along transmission line CD-EF toward loop No 1 This operation can be checked quite easily by making measurements with a field detector at a radius of 200 feet along a circle which has been staked out

An alternate method can be used for aligning the nulls By changing the

length of the building-out section on one of the outside loops by a small amount, the phase of the current in that loop can be changed a considerable amount without appreciably changing the magnitude of the current This is somewhat more convenient than moving the point of tap AB, providing the nulls are not displaced by too great an amount. For instance, if the nulls bend toward loop No. 1, reciprocal alignment can be obtained either by decreasing the length of the building-out section on loop No. 1 or by increasing the length of the building-out section on loop No 2 Conversely, the opposite procedure should be followed if the nulls bend in the other direction

Another essential requirement with regard to the antenna system is the condition for non-parasitic operation of the radiators. Because of the symmetry of the system, the outer antennas cannot induce current in the center antenna since the fields produced by the outer radiators are equal and opposite at the center of the system and thus cancel out Unless precautions are taken, the center loop will induce parasitic current in the outer loops, producing a carrier pattern which will no longer be circular and which under most conditions will have a variable instantaneous phase angle with azimuth. This is a highly undesirable condition since distortion on the voice and aural signals would be introduced at various azimuth angles due to overmodulation or phase distortion

Referring to figure 2, loop No 2 will induce parasitic current in loop No 1 and loop No 3 The voltages appearing at CD and EF will be in phase, and since there is a crossover in the line feeding loop No 1, the voltage at AB will be zero This means that the impedance at AB is zero insofar as the parasitic action is concerned The amount and relative phase of the parasitic current flowing in the loop are functions of the spacing, the self-impedance of the loop, and the impedance appearing across the terminals of the loop. The effective impedance across the loop consists of a shorted length of line AB-CD in parallel with the building-out section across CD, connected through a length of transmission line from the loop terminals to CD If this impedance is made very high, the loop will be effectively detuned for parasitic operation and no induced current can flow. If θ_1 is the electrical length of transmission line from the ends of the loop to CD, θ_2 is the length of the building-out section across CD, and θ_3 is the length of line AB-CD, it can be shown that the following relation will hold for the condition of zero parasitic current (See Appendix I)

$$\tan \theta_3 = \frac{\tan \theta_2}{\tan \theta_1 \tan \theta_2 - 1} \qquad (21)$$

The lengths θ_1 and θ_2 are a function of the self-impedance of the loop and the characteristic impedance of the transmission line Adjustment is accomplished by energizing loop No 1 with the other loops removed from the vicinity and by varying the length of the building-out section, θ_2, and its position θ_1, so that no reflections are present on the line AB-CD The loop is now correctly adjusted for the case where it is driven

The remaining adjustment is that of line length AB-CD, θ_3, which can be calculated and adjusted experimentally To make this adjustment, a driven loop is placed 120° away from loop No 1 and a current indicator is placed on one of the elements of loop No 1 A short is placed on line AB-CD and its position changed until the current indicator reads zero The line is then cut at the short and joined to loop No 3 after the same adjustments have been repeated for loop No. 3. For the particular radiators used in this development, θ_3 was slightly shorter than one-half wavelength. Radiators having a different self-impedance would require different values of θ_1, θ_2, and θ_3

When the outer loops are being connected at AB, care should be taken to reverse the line to one of the loops This may be checked with a field detector by determining whether there is a null normal to the line of radiators If there is a null, the connection is correct, but if there is maximum signal normal to the array, the loops are being fed in phase and the connection to one of them should be reversed for correct operation

Theory of the Mechanical Modulator

The basic elements of the two-course visual range are essentially the same as those of the instrument landing localizer [6] The method of simultaneously producing the 90- and 150-cycle patterns and the method of modulation are identical, although the localizer antenna configuration is somewhat more complex

The operation of the mechanical modulator can best be explained by reference to figure 13 which shows the schematic diagram of the modulator The modulator does not supply additional power but functions by effectively placing an impedance in series with the transmission line, the value of the impedance being varied at such a rate as to modulate the carrier at the desired audio frequency The unmodulated carrier leaves the transmitter at H and enters the lower bridge of the modulator at A, where it divides equally and leaves at B and C The current passing through lines BE and CF is modulated at 150 cycles and 90 cycles, respectively, by the coupled sections which introduce varying impedances into the lines at I and J

The signal appearing at E consists of carrier and 150-cycle sidebands, while the signal appearing at F consists of carrier and 90-cycle sidebands The two carriers will arrive at G in phase and combine to supply carrier to the center antenna, but because of the crossover between F and H the carriers will arrive at H 180° out of phase and will cancel out Since the two sets of sidebands are of different frequencies, they can neither combine nor cancel and will divide equally at E and F. Equal 90-cycle and 150-cycle sidebands will appear at G and H The 150-cycle sidebands at G will be in phase with those at H, while the 90-cycle sidebands at G will be 180° out of phase from those at H because of the crossover between F and H.

It may be seen that because of the action of the upper bridge, the proper phase relations are obtained in the loops Assuming that the lengths of transmission line from the modulator to the antennas are correct, the phase progression from left to right in the three antennas for one set of sidebands will be $+90°$, $0°$, $-90°$, while for the other set of sidebands the phase progression will be $-90°$, $0°$, $+90°$ Thus, the two patterns will exist simultaneously, one pattern representing the 150-cycle sidebands and the opposite pattern representing the 90-cycle sidebands Also, since modulated carrier is fed to the center antenna, the carrier pattern will be circular and the two bean patterns will correspond to percentage modulation of the carrier

Several other factors are of interest in regard to the upper bridge In order to prevent interaction between the modulation channels, none of the energy appearing at E should appear at F, and vice versa This condition will be obtained if the four arms of the bridge are made equal and the impedance at G matches the impedance at H Thus, if energy is introduced at E, equal amounts of energy will appear at F, but because of the crossover in one arm of the bridge the energy will be 180° out of phase and will cancel Therefore, when point E is used as a reference, a virtual short circuit will exist at F, and since the circuit is symmetrical, the converse will be true.

The electrical length of the arms of the upper bridge, as well as of other bridges used in various systems described in this report, has an optimum value so that the lines terminated at E and F may be matched. When the loads connected to G and H are equal to the characteristic impedance, Z_o, the impedance looking into E and F should also be Z_o This condition will be obtained when each arm of the bridge has an electrical length of 0 152 wavelength. (See Appendix II)

Although the mechanical modulator is designed to operate into a matched transmission line, a certain amount of mismatch can be tolerated without producing

---

[6] H I Metz, "The CAA-RTCA Instrument Landing System Part I - Development and Installation, " CAA Technical Development Report No 35, October 1943

any ill effects It is important, however, that the impedance at G equal the impedance at H regardless of whether or not the impedance at these points is equal to the characteristic impedance One convenient way of achieving this in practice is to energize the upper bridge at E, remove the transmission line feeding F, and place a sensitive voltage detector across F The impedance at H is adjusted to give a null reading of voltage, thus indicating that the bridge is balanced

The coupled sections which modulate the carrier signals are alternately tuned and detuned by toothed discs which rotate between condenser plates attached to the ends of the coupled sections. The toothed rotors are attached to opposite ends of the shaft of an 1800 r p m synchronous motor The rotors have three and five teeth, respectively, and produce the 90 cycle and 150-cycle modulation frequencies. The method of operation is such that with modulation peaks the rotors are fully meshed, thus detuning the sections and permitting maximum power to flow through the transmission lines When the rotors are unmeshed the sections are tuned to resonance and prevent any flow of energy beyond the open ends of the coupled section Since the modulator supplies no power but produces a form of downward modulation, the transmitter must supply the peak modulated carrier at normal plate voltage. The particular type of transmission line modulation used is such that the output tank circuit of the transmitter must have good voltage regulation under widely varying conditions of load if good wave form is to be obtained

The action of coupled sections has been treated quite thoroughly in the literature[7,8] so that no attempt will be made here to discuss the theoretical relationships. From the standpoint of a practical application, the coupled section can be considered as introducing two virtual generators in series with the line directly below the open ends of the section In figure 13, the effect of the coupled sections is concentrated wholly in the immediate region of points I and J on the transmission lines BE and CF. When the sections are tuned to resonance, an apparent open circuit occurs in the lines at points I and J, and complete reflection takes place so that no energy passes beyond these points When the sections are completely detuned they have no effect on the lines, and all of the energy is propagated along the lines BE and CF For other tuning conditions, the amount of energy which passes along the lines is varied so as to produce the desired shape of modulation envelope

For the modulator used in this development, the effect of the coupled sections on the line can be considered as analogous to that produced by the introduction of capacitive reactances in series with each of the lines at points I and J. The phase and magnitude of the reflected wave produced by the virtual generators are identical to those produced by introducing capacitive reactance in the line. Actually, of course, the modulator could be made to operate in such a way as to produce an equivalent inductive reactance in series with the line This would mean that the section would be detuned in the opposite direction to that now used At present, the operation of the coupled section is such that when power is prevented from flowing along the line, that is, at the minimum of the modulation cycle, the section is one-quarter wavelength long electrically, its length being adjusted for the resonant condition when the condenser rotors are fully unmeshed from the stator When the rotor is meshed so as to detune the section, the section is effectively made electrically longer, producing the effect of introducing capacitive reactance in the line. This can be shown from a consideration of the relationships given in reference 7

The equivalent circuit of the modulating system is shown for one modulation channel in figure 14. The upper bridge has been replaced by a load and the lower bridge plus the transmitter replaced by a generator The upper figure shows the cir-

---

[7]A. Alford, "Coupled Networks in Radio-Frequency Circuits," Proceedings of the I R.E , pp 55-69, February 1941

[8]R. King, "The Application of Low-Frequency Circuit Analysis to the Problem of Distributed Coupling in Ultra-High-Frequency Circuits," Proceedings of the I.R.E., pp. 715-724, November 1939.

cuit as actually used, while the lower figure shows how the interaction between the section and the line may be represented in terms of lumped circuits When the reactance of the equivalent series condenser is zero the energy is transmitted without reflection, while for infinite reactance complete reflection takes place and no energy is transmitted. For intermediate values of capacitive reactance, varying amounts of reflection would occur, modulating the amplitude of the carrier in accordance with the changing reactance

While a system as shown in the equivalent circuit or a system using a variable condenser connected across the line would give the same results as the circuit using coupled sections, in practice it would be difficult to obtain the range of reactance values necessary to obtain complete modulation The coupled section acts as a step-up transformer to control the energy in the main line, and since the Q of the coupled section is quite high, a large change in current can be produced with a small change in capacitance. The transformation ratio is a function not only of the distance between the plane of the section and the plane of the main line but also of the spacing of the conductors of the main line and the section The actual spacing used was determined empirically and is more or less a compromise between several factors If the step-up ratio is too low, complete modulation will be difficult, whereas if the step-up ratio is too high, the currents and voltages in the coupled sections will increase, resulting in a loss of power in the section, as well as making it difficult to maintain balance in the circuit.

The shapes of the rotors and coupled section stators were designed to produce 90-cycle and 150-cycle modulations with a minimum of harmonic distortion Since, because of fringing, it was difficult to calculate the shape of the condenser plates which would give a sinusoidal wave shape, it was necessary to design them experimentally

The lower bridge or cross-modulation bridge, as it is often called, serves to prevent interaction between the two modulating channels The radio-frequency power from the transmitter enters the lower bridge at A where it divides equally and flows to the modulating channels BE and CF Since the modulating system dissipates no power, energy which does not reach the upper bridge will be reflected back into the transmitter or into the opposite modulating channel This last-mentioned condition will cause cross modulation which will distort the output wave form and produce broad courses The cross-modulation bridge effectively isolates the two modulation channels so that any disturbance in one channel will not affect the opposite channel.

The operation of the lower bridge can be explained by reference to figure 13 The reflected 150-cycle energy will enter the bridge at B, where it will divide into equal parts which progress toward A and D If the impedance at D is the same as that looking into the transmitter at A, the two waves will arrive at C with their magnitudes equal and with a phase difference of 180° due to the crossover between D and C The waves will therefore cancel at C and no energy will be transmitted from B to C It can also be shown that the reciprocal relationship is true and that no energy will be transmitted from C to B Little energy will be lost in the cross-modulation impedance, provided the transmitter output tank and coupling circuit have low losses The impedance at A looking toward the transmitter is essentially reactive, therefore, the cross-modulation impedance will also be reactive, thus dissipating no energy other than the circuit losses The cross-modulation impedance consists of a tuned circuit which is adjusted in operation to give minimum interaction between the two channels

The length of the lower bridge elements and the distances from the open end of the coupled sections to the lower bridge have optimum dimensions of one-quarter wavelength for most efficient operation When both modulating channels are drawing the same amount of energy, there will be zero voltage at the cross-modulation impedance and the bridge arms CD and BD will be equivalent to a pair of short-circuited quarter-wave lines of high impedance connected across B and C The energy will then divide at A and reach the modulating channels without incurring any additional losses due to reflection from the bridge circuit At the time when neither modulating channel is drawing any power, the voltage at the cross-modulation impedance will be zero,

hence, the power dissipated due to circuit losses will be comparatively small since voltage does not appear at the cross-modulation impedance except during portions of the modulation cycle.

When one of the coupled sections is tuned to transmit no energy, an effective open circuit is produced at I or J, and since BI and CJ are one-quarter wavelength long, an effective short circuit will be produced at B or C If the 150-cycle section is tuned to resonance, the effective short will be located across B. Because of the fact that the bridge elements are also one-quarter wavelength, line BA will apply a very high impedance across A and will allow all of the energy to flow into the 90-cycle channel. This is the condition which will produce the largest voltage and power loss at the cross-modulation impedance. Under actual conditions the power loss in the cross-modulation impedance has been found to be negligible.

The line from the transmitter to the lower bridge has an optimum length when no energy is passing through either channel For the condition of maximum power, a matching section is placed across the line between A and H in order to remove reflections from the line. When minimum power is being transmitted to the modulation channels, effective short circuits are produced across B and C, giving rise to a very high impedance looking into A If the length of line between A and H were made an odd number of one-quarter wavelengths without the matching section in the circuit, a short circuit would appear across H and it would appear to the transmitter as though it were working into a very high impedance load For any other length of line, a reactive impedance would be coupled into the plate tank, causing excessive plate dissipation when no energy is being supplied to the antennas and thus reducing the over-all efficiency during the modulation cycle

In tuning up the modulator and transmitter, the coupled sections are first short-circuited near the open end so that they are completely detuned and allow maximum power to flow into the antennas It is assumed, of course, that the antenna system has previously been adjusted and that the lines being fed from the upper bridge have been matched A building-out section is then placed on the line feeding the lower bridge to remove standing waves from the line The plate tank of the transmitter is then tuned for minimum plate current and the output coupling circuit tuned for maximum output No further adjustments to the transmitter are necessary after this point. The short circuits are then removed from both coupled sections and the toothed rotors turned by hand until the rotors and stators of both coupled sections are fully unmeshed. The coupled sections are then tuned with the movable shorting bar to prevent energy from flowing beyond the coupled sections This can be readily checked with an r-f indicating instrument placed on the antenna side of each modulating channel. The tuning of the coupled sections is rather sharp, therefore, care must be exercised in moving the shorting bar when adjusting for complete cut-off.

The length of line from the mechanical modulator to the transmitter is determined for the cut-off condition and is so adjusted as to give minimum plate current This adjustment is not particularly critical and when made will result in minimum plate heating of the final amplifier stage Before setting the percentage modulation on each channel, it is necessary to tune the cross-modulation network for minimum interaction between the two channels. A convenient method of making this adjustment is to place a diode rectifier across the line feeding the center antenna and observe the rectified audio voltage on an oscilloscope The 90-cycle channel is short-circuited at the antenna side, the 150-cycle coupled section is short-circuited at the open end, and the cross-modulation network is adjusted to give minimum deflection on the oscilloscope The circuit is then adjusted to prevent interaction from the 90-cycle channel into the 150-cycle channel. The reciprocal relation will hold and can be checked readily by short-circuiting the 150-cycle channel and the 90-cycle coupled section Another convenient way of adjusting the cross modulation is to place a wave analyzer across the diode output and adjust for a minimum on the 240-cycle component when everything is running and there are no shorts on either the channels or the coupled sections

The percentage modulation on each channel can now be adjusted, since any changes made in one channel will have no effect on the opposite channel When the

mechanical modulator is used for localizer applications, the total percentage modulation will be close to 100 percent. Since the carrier divides equally into the two channels, each channel can be modulated 100 percent, and the total carrier will be modulated somewhat less than 100 percent due to the fact that the two modulations are of different frequencies. For radio range applications, the total modulation for the visual system must be considerably less than 100 percent since space must be left for the voice and aural modulations. The percentage modulation in each channel will vary from 40 to 80 percent, depending on the particular type of system used to combine the voice and aural modulations with the visual modulation

The depth of modulation in the channel will depend upon the tuning of the coupled section and the spacing of the stator plates Normally, the rotor is turned by hand until it is fully unmeshed from the stator When the tuning short circuit is positioned to give complete cut-off, 100 percent modulation will be obtained To decrease the modulation depth, the section is slightly detuned by moving the shorting bar away from the open ends of the coupled section. Fine adjustments can be made with a metal tab located near the shorting bar To decrease the percentage modulation, the metal tab is rotated out from the conductors of the coupled section.

The percentage modulation can be measured directly in each channel by placing an r-f indicator on the antenna side of the channel. The rotor is slowly turned by hand and the maximum and the minimum deflections of the indicator are noted The percentage modulation, m, can be determined from the following relation,

$$m = \frac{E_{max} - E_{min}}{E_{max} + E_{min}} \times 100$$

and conversely, the ratio of the minimum to the maximum deflection in terms of the modulated percentage is given by,

$$\frac{E_{min}}{E_{max}} = \frac{100 - m}{100 + m}$$

Since the nature of the modulation system is such that the maximum deflection will be almost constant regardless of the modulation depth, it is only necessary to calculate the minimum deflection for the desired percentage modulation and to adjust the short-circuiting bar or metal tab to give the calculated deflection Maximum deflection is obtained when the rotors are fully meshed and minimum deflection when the rotors are fully unmeshed

The wave form of either modulating frequency may readily be observed on the oscilloscope by shorting the opposite coupled section In order to obtain the best wave shape, it may be necessary to make some slight readjustments in the spacing of the stator plates, in which case the movable short circuit on the coupled section should be readjusted in order to keep the same modulation percentage It is important that each channel be modulated the same amount if the visual courses are to be in reciprocal alignment The percentage modulation of one channel relative to the other can be checked by short-circuiting first one coupled section and then the other and noting the deflection on the oscilloscope in each case

Although it was pointed out previously that the overlapping bean-shaped patterns represent only percentage modulation on the carrier, it is possible to obtain static patterns which may be measured with a field detector. In order to do this, both coupled sections are short-circuited and a short circuit is placed on the undesired channel For example, if it is desired to set up the 90-cycle bean pattern, the 150-cycle channel should be short-circuited, and vice versa. Since only one side of the upper bridge is supplied with carrier energy, all three antennas are excited at the same amplitude ratio and phase as they are when the mechanical modulator is operating normally. With only one pattern present, it is much simpler to phase the array than under dynamic conditions

DEVELOPMENT OF THE VISUAL-AURAL SYSTEMS

Tests on 109 9 Megacycles

The basic elements of the two-course range with sector identification were evolved as a result of the instrument landing development The first experiments with aural sector identification applied to the visual two-course localizer were conducted at Indianapolis during the fall of 1939 The three-loop localizer installation was used for the visual system and a set of three loops, located halfway between the localizer loops and the counterpoise and oriented at right angles to the visual loops, was used for the aural sector identification.

The aural antennas were fed from a balanced modulator which produced 1020-cycle sidebands In order to prevent interaction between the visual and the aural systems which would cause the visual indicator to fluctuate with the D-U keying, it was necessary to use a tie line between the two center antennas The tie line prevented any visual energy from reaching the aural balanced modulator, and vice versa If the tie line was not used, visual energy would feed into the aural transmitter and overload the tubes and also would couple visual power into the aural antennas and be keyed simultaneously with the aural signals

The preliminary experiments and flights with the equipment operating on 109 9 megacycles showed that the tie line could be adjusted to prevent interaction between the aural and the visual systems It was also found that the percentage modulation on the visual system would have to be reduced for radio range applications if excessive distortion of the aural signal as evidenced by cross-modulation products were to be eliminated

These experiments concluded the first part of the program and proved that the system was practical

125-Megacycle Visual-Aural Range Using the Six-Loop Array

The next stage of development utilized equipment operating on 125 megacycles with the six-loop array mounted on a 30-foot tower and counterpoise The frequency band of 119-126 megacycles had been allocated to the CAA for radio range applications,[9] and previous tests[10] had proven the desirability of locating the antenna system on a tower in order to increase the service radius of the radio range For these reasons, it was desired to design an experimental radio range which would be satisfactory when applied to the airways It was also desired to have a working installation which could be demonstrated to various groups interested in the use of ultra-high frequencies for air navigation

The most difficult problem in this development was the choice of a suitable antenna system and circuit arrangement which would prevent interaction between the visual and the aural systems without producing any crossovers or false courses at high angles. Both the transmitting and the receiving equipments used for the visual-aural range development were of standard design and did not possess any particularly novel features. Figure 15 shows the 30-foot tower and counterpoise with the building which houses the transmitting equipment located directly underneath Figure 16 is a view of the equipment, the main transmitter being at the left, the 1020-cycle sideband generator and keyer at the right, and the mechanical modulator in the center

---

[9] L H Simson, "National Allocation Plan for Assigning Radio-Range Frequencies in the Band 119-126 Megacycles," CAA Technical Development Report No 28, May 1941

[10] P. B King and T A Kouchnerkavich, "Development of the Ultra-High-Frequency Radio Range, Part II - Testing of UHF Radio Ranges on Towers," CAA Technical Development Report No 43, July 1944

The arrangement of antennas that was first tried on 125 megacycles was similar to the one used on 109 9 megacycles except that it was constructed in a more permanent fashion. The three visual loops were located in line and spaced one-half wavelength above the counterpoise The three aural loops were located in a line at right angles to the line of the visual antennas and spaced one-quarter wavelength above the counterpoise

A block diagram of the equipment and the antenna system is shown in figure 17. Although single lines are shown, two-wire balanced, shielded transmission line is actually used throughout the whole system. The principles of the mechanical modulator and the antenna arrays, with the exception of the tie line, have already been described The method of feeding the aural array is somewhat different from that used to supply energy to the visual antennas since the aural antennas have to carry only one pair of sideband modulation frequencies. All of the visual antennas have to carry both pairs of sideband modulation frequencies in order to set up both bean-shaped patterns simultaneously, while the carrier is supplied only to the center visual antenna which provides a circular carrier pattern In addition, the phase of one pair of sideband modulation frequencies in the side visual loops has to be reversed with respect to the other pair of sideband modulation frequencies, while both pairs of sideband modulation frequencies are fed to the center visual loop in phase with each other As previously explained, these conditions are automatically satisfied by the upper bridge circuit

The aural antennas produce only one bean pattern at a time, so that all three loops can be directly fed from the 1020-cycle sideband generator Appropriate means are required for controlling the relative power and phase of the side aural antennas The two aural bean patterns are obtained by changing the phase of the current in the side antennas by 180 degrees with a double-pole double-throw relay which reverses the line to the side antennas in accordance with the D-U keying rhythm.

The installation of either a visual system or an aural system by itself would be a comparatively simple and straightforward procedure. However, when it is desired to operate both systems simultaneously on the same tower, mutual coupling between the two systems causes some difficulty In order to eliminate the mutual coupling, it was proposed to place each antenna system on a separate tower, but because of added equipment and technical difficulties, this idea was abandoned

When all six antennas are placed on a counterpoise with the center of each array on the same vertical axis, the largest degree of coupling takes place between the two center loops. Because of symmetry, each pair of side antennas induces no current in the center antenna or in the other pair of side antennas Also, each center antenna induces no current in either pair of side antennas since the length of line to each side loop is adjusted to prevent the flow of parasitic current Although a horizontal loop has zero radiation field in the vertical direction, the induction field from one center loop induces considerable current in the other center loop since they are separated by only one-quarter wavelength

The mutual coupling between the two antennas manifests itself by two undesirable conditions First, parasitic current is induced in the visual loop by the aural loop, and vice versa Second, as a result of this parasitic current, energy from the visual system is fed into the aural system and energy from the aural system is fed into the visual system In order to prevent the flow of energy between the two systems, a tie line between the two center antennas was introduced As will be shown later, the tie line can also be used to control the parasitic current in the center antennas

The operation of the tie line may be understood readily by referring to figure 18 which shows only the transmission lines feeding the center antennas which are mounted one above the other Let us first consider the case where power is fed into the visual loop Because of mutual coupling between the loops, energy will appear in the aural loop and flow toward the aural transmitter. At point B, however, the tie line will feed energy of the same magnitude but with opposite phase to that of the induced current, thus producing a voltage node at B and preventing the flow of

visual energy into the aural transmitter Since the circuit is symmetrical, the reciprocal relation will be true and none of the aural energy will flow into the visual transmitter

The magnitude of the current in the tie line at point B depends upon the transfer impedance between A and B The transfer impedance is determined by the length of the tie line and by the length of the building-out section connected across the tie line Since the transfer impedance is purely reactive, the phase of the tie-line current can differ from the applied voltage at A by 90° either leading or lagging Thus, in order to control the phase of the current at B, it is necessary to vary the length of line between A and C While a reasonable amount of care is necessary in the adjustment of the tie line, it is not critical or difficult to make

The tie line was located arbitrarily during the first experiments; that is, point B was chosen at a convenient location and the position of point A was varied so as to effect a balance.

The first step when tuning the range was to balance the tie line so that any further adjustments in either the visual or the aural system could be made without reacting on the other system After this, the relative current and phase in the side antennas were adjusted The final patterns were checked by taking field-strength measurements on the ground at a radius of 200 feet.

When flight tests were made with this set-up, it was found that the aural patterns had poor clearance and several reversals of the signal at high angles when the visual course was flown It was found that these difficulties were due both to the wide spacing (135°) of the side aural loops and to parasitic current in the upper visual center loop Because of parasitic current, the center antennas produced a field pattern in the vertical plane which was quite different from the pattern due to the side antennas This accounted for discrepancies between the observed horizontal pattern on the ground and the results obtained in flight tests

Further investigation showed that the parasitic current in one of the center loops could be eliminated This was accomplished by positioning the tie line at such a point that the reactance reflected into the unfed loop would detune it for parasitic currents If the center aural loop was energized and the tie line correctly balanced, a virtual short would exist at point A. After the tie line was balanced in order to prevent aural parasitic current in the visual center loop when the aural center loop was driven, it was found that length BD was such as to cause visual parasitic current to flow in the aural loop when the visual loop was driven.

When the tie line was relocated, the spacing of the side aural antennas was reduced to 100° in order to more nearly approximate a cardioid pattern in the horizontal plane. The side aural loops were also elevated to a height halfway between the two center loops. This was necessary because of the physical size of the loops, since the three aural loops would have touched each other if they had been placed at the same level

Flight tests of this arrangement showed that the aural patterns were satisfactory and produced no sector reversals except at very high angles directly above the station It was also found that the visual indications were free of sector reversals below a vertical angle of 45° Some flights were made with only the visual system operating and with the lower center aural loop shorted out so as to prevent the flow of visual parasitic current Under these conditions, the region of sector reversals on the visual system was limited to vertical angles above 64° from the horizontal

In order to definitely establish that the high angle crossovers and reversals were caused by parasitic current in the center loops, vertical field patterns of the array elements were taken This was done by recording the output of a receiver which had a manual volume control Numerous flights were made at constant altitude on a radial through the station in the vertical plane which passes through the visual array Figure 19A is a representative recording of the flights made when the two side visual

antennas only were energized It will be noted that the vertical field pattern is comparatively smooth and gives but one lobe on either side of the vertical axis The departure from symmetry in the two lobes is due to the effect of the airplane, since the receiving antenna was mounted on the top of the fuselage

Figure 19B shows a representative recording of the flights made when the center visual antenna only was energized The effect of the lower loop operating parasitically is quite marked and shows up by producing a very deep null at a vertical angle of 42° on each side of the station Inasmuch as the radiated field is reversed by 180° every time the field pattern passes through a minimum, it is apparent that sector reversals should exist above 42° This is further confirmed by the fact that theoretically two lobes will be produced in the vertical plane by two antennas spaced above a reflecting surface at distances of one-quarter wavelength and one-half wavelength, respectively

These flights, as well as some other experiments which will be discussed later, proved that high angle sector reversals were primarily due to visual parasitic current flowing in the lower aural loop It was therefore desirable to modify the circuit in order to prevent parasitic action in both of the center loops This was done by locating points A and B so that both center loops were detuned when either loop was driven In order to accomplish this, it was necessary to use a tie line with a transfer impedance which contained a resistive term and a reactive term As a result, the input impedance of the tie line contained a resistive component which dissipated power with a consequent loss in efficiency This loss in efficiency is not as great as it appears, however, because the field in the horizontal plane is increased by an improved distribution of energy in the vertical plane, when no parasitic current flows in either center loop

A schematic sketch of the dissipative tie line is shown in figure 20 The adjustment procedure is somewhat different from that for the reactive tie line Points A and B are determined by exciting one loop and placing a short on the transmission line which connects to the other loop The position of the short which results in minimum parasitic current in the non-driven loop is then determined This is done for each center antenna and the tie line is connected between the two transmission lines at the positions where the shorts were located The tie line is next adjusted to prevent interaction between the two systems; that is, when voltage is applied at point A, there should be zero voltage at point B and, reciprocally, when voltage is applied at point B, there should be zero voltage at poirt A This adjustment also automatically satisfies the requirements for non-parasitic operation since a virtual short will appear at the end of the tie line opposite the end which is driven

In balancing the tie line, there are three variables which have to be adjusted, namely, the length of line EF, the length of line BF, and the length of the building-out section across point E. These three adjustments make it possible to obtain almost any desired value of transfer impedance between points A and B For convenience, the resistance across point F was made equal to the characteristic impedance of the transmission line, although this is by no means a necessary condition. A wide range of input impedances could be obtained for a given value of transfer impedance Also, the input impedance at one end of the tie line is not necessarily the same as that at the other end of the tie line. In fact, the input impedances were arranged so a greater percentage of aural power than visual power was dissipated.

Comparatively little power is needed from the aural sideband generator in order to give the same distance range as the visual signals; therefore, from the standpoint of power efficiency it is more desirable to dissipate a higher percentage of aural power than visual power, which includes all of the carrier power as well as half of the visual sideband power The order of power magnitude in the center visual antenna is about 150 watts, while the power in the center aural antenna is approximately 3 watts The power lost in the visual system is about 10 percent of the total visual power, whereas the power lost in the aural system is considerably greater than half of the total aural power Because of the small amounts of power involved, it is difficult to make accurate measurements on the aural system.

When the resistive tie line was installed, the spacing on the side visual loops was reduced from 135° to 120° Previous flights had shown that although the visual pattern clearance was good at most of the points around the station, it was not entirely satisfactory when the plane was flying in the center of the 150-cycle sector, due to the second harmonic of 90 cycles passing through the 150-cycle filter The 120° spacing increased the clearance and produced a more suitable pattern in general

A schematic diagram of the complete circuit arrangement is shown in figure 21. The double lines on the diagram represent the balanced two-wire shielded transmission line used throughout the system to feed the r-f energy to the antennas and various circuit elements. Building-out sections or stubs[11] are used to match the various circuits to the characteristic impedance of the two-wire transmission line so standing waves are removed from the line. In one or two places stubs are used to mismatch the line in order to obtain the correct power distribution between two circuits which are fed from the same source Line phasers are used to obtain the correct phase relations between the antennas, and to adjust the phase of the 1020-cycle sidebands with respect to the carrier The phasers, which are constructed of telescoping tubing in much the same manner as a trombone slide, vary the relative phase by changing the actual length of line in the circuit The size and the spacing of the telescoping tubing are designed so as to make the characteristic impedance of the phaser the same as that of the transmission line.

In several places, it will be noticed that a one-quarter wavelength stub is connected across the line. These stubs have no effect on the circuit but serve merely to correct conditions of unbalance. A one-quarter wavelength stub presents infinite impedance to balanced currents and zero impedance to unbalanced currents so that it effectively forces a balance at the point where it is connected across the line. These balancing stubs are most useful in eliminating unbalance occurring at the energy source Unbalance in circuit components, such as antennas, phasers, etc , can best be eliminated by careful design and construction, with particular attention being directed toward obtaining a symmetrical layout

Adjustments of the transmission line circuits feeding the antennas can be made without difficulty provided proper attention is paid to the sequence in which the various operations are made. Each of the six antennas was first matched to its respective transmission line This was done on the ground by locating the loop to be matched at a height above ground which was identical to the height to be used above the counterpoise Each loop was matched to its own line with none of the other loops in the vicinity. Then, the three visual loops were mounted on the counterpoise and the side loops adjusted for non-parasitic action when the center loop was driven After this, the three aural loops were mounted and the above procedure repeated

The transmission lines from the antennas to the transmitter were connected and matched and the proper location of the tie line was determined The tie line was balanced by adjustment of the current stub and the two phasers shown in figure 21 It was necessary to match the line feeding the center aural antenna again since connecting the tie line introduced a disturbance on the line feeding the center aural antenna No further adjustments were required on the line feeding the center visual antenna after the tie line was connected The visual antenna transmission lines were matched into the upper bridge of the mechanical modulator Next, the phase of the visual antenna currents was adjusted and the mechanical modulator was tuned. The current distribution in the aural antennas was adjusted with the aid of an inductively coupled radio-frequency meter The relative phase was adjusted in the same manner as previously described The main transmitter instead of the sideband generator was used as the power source in making these adjustments since the power output of the sideband generator was insufficient to give a reading. The correct phase re-

---

[11] E J. Sterba and C B Feldman, "Transmission Lines for Short-Wave Radio Systems," Proceedings of the I R E , pp. 1163-1202, July 1932

lationship between the main carrier and the sideband generator output was determined by varying the sideband generator output phaser so as to give maximum 1020-cycle output with minimum distortion in a monitor. (See Appendix III)

Suppressor Array

As previously discussed, the difficulties due to reversals at high vertical angles were greatly minimized by elimination of parasitic current in the center antennas However, it was impossible to completely eliminate reversals and oscillation of the visual indicator above vertical angles of 70°. In order to determine the effect of antenna height above ground, flights were made on a 125-megacycle portable two-course range with loops that were about $2\frac{1}{2}$ wavelengths above ground and one-quarter wavelength above a counterpoise. Flights were also made on a 109 9-megacycle localizer with loops which were one-half wavelength above ground. These flights showed that a certain amount of course reversal took place at very high vertical angles regardless of the height of the antennas above the counterpoise or above ground. Since theoretical considerations of the antenna system offered no explanation concerning this phenomenon, it was decided that stray radiation was causing the high angle reversals.

The pattern in the vertical plane of the loop antenna is a figure-of-eight with maximum intensity directed along the horizontal and zero signal being radiated directly upward Directly over the station no direct signal is received; therefore, any stray signal which is radiated from the outer sheath of the transmission line or from the equipment will predominate In addition to this, the receiver operates on automatic volume control so that its sensitivity is greatly increased when in the cone-of-silence area over the range station As a result of these two factors, the effect of a small amount of spurious signal is greatly magnified and causes oscillation of the visual indicator when the flight is over the station

The order of magnitude of the visual indicator deviation was such that a pilot would attempt to follow the course discontinuities when flying over the station at high altitudes and, as a result, would find himself in one of the quadrants rather than on the reciprocal course. At low altitudes, the visual pointer would vary so rapidly that there would be no possibility of misconstruing the indication. It was decided that it would be more desirable to have no signal at all over the station than to have false indications, since the pilot would merely hold his heading when the signal faded out and keep that heading until he encountered the reciprocal course.

To eliminate this difficulty it was proposed to suppress the stray radiation directly over the station and to hold the receiver in automatic volume control by means of an unmodulated signal directed upward in a manner similar to that of the 75-megacycle cone-of-silence marker.[12] This suppressor signal differed in frequency from that of the range carrier by 25 kilocycles so that no audible beat would be heard and no phase interference between the two signals would occur to produce further minima and maxima in the vertical field pattern.

The first suppressor arrangement used a transmitter which supplied 40 watts on 124.975 megacycles and an antenna array of four half-wave dipoles These dipoles were spaced one-quarter wave above the ground and were arranged in the form of a cross One pair of in-phase coaxial half-wave elements were fed in quadrature to the other pair of in-phase elements to give a circular field pattern Flights made with this arrangement showed the suppressor operation to be fairly satisfactory, although it was found that the cone in which the suppressor functioned was somewhat too broad and that the power output of the suppressor transmitter was not sufficient for the amount of main carrier power (150 watts)

---

[12] W. E. Jackson and H I. Metz, "The Development, Adjustment, and Application of the Z-Marker," CAA Technical Development Report No. 14, July 1938.

Greater directivity in the vertical plane was obtained by doubling the number of antenna elements This not only decreased the cone angle in which the suppressor was effective but increased the effective power radiated directly upward so it was not necessary to increase the output power of the suppressor transmitter The new suppressor array consisted of eight half-wave dipoles arranged as shown in figures 22 and 23 and spaced one-quarter wavelength above a counterpoise The four north-south antennas were fed in phase, and in phase quadrature with the four east-west antennas This arrangement gave very satisfactory results inasmuch as the cone of the suppressor has a much more definite and longer cone-of-silence than the present low-frequency four-course aural ranges.

Numerous recordings were made to show both the effect of the suppressor array and the effect of eliminating the parasitic current in the lower center loop These recordings of the visual indication were made flying over the station perpendicular to the visual courses For an ideal cone indication, the visual indicator should move smoothly without reversing direction from one side to the other, or vice versa

Figure 24A shows a recording taken without the suppressor transmitter operating and with parasitic current flowing in the lower loop The visual indicator oscillated several times before it definitely reversed itself The amplitude of the oscillation was such that the visual pointer deflected more than full scale Figure 24B shows the improvement when the suppressor transmitter was turned on This considerably decreased the amplitude of oscillation, although not sufficiently to be entirely satisfactory. In order to increase the ratio of the suppressor transmitter power to the power of the main transmitter, the plate voltage was reduced on the main transmitter Figure 24C is the result of a flight test made under these conditions, showing that further improvement could be obtained by effectively increasing the amount of suppressor signal with respect to the main signal In order to limit the visual pointer oscillation to the order of magnitude shown in figure 24C, it would be necessary to have a suppressor transmitter with a power output comparable to that of the main transmitter

By eliminating the parasitic current in the lower loop, still further improvement was obtained, as shown in figures 25A, 25B, and 25C These flight tests were made in the same manner as the previous tests except for a difference in altitude The latter tests were made at 2000 feet instead of 1000 feet Figure 25A is almost identical to figure 24A since the conditions of operation were the same, that is, both recordings were taken without the suppressor transmitter operating and with parasitic current flowing in the lower loop Figure 25B shows the very marked improvement obtained by detuning the lower loop so as to prevent the flow of parasitic current, while figure 25C shows the additional improvement obtained by turning on the suppressor transmitter in addition to eliminating the parasitic current

The results of figure 25C are quite satisfactory and provide the nearest approach to the ideal condition The visual indicator pointer moved smoothly from full-scale position to the center of the scale where it remained for a short interval and then traveled smoothly to the opposite full-scale position. This operation is preferable to the previous conditions where the visual indicator oscillated several times

Extensive flight tests showed that a nominal amount of power supplied to the suppressor array would give a satisfactory cone-of-silence provided the parasitic current in the lower center loop was eliminated. The suppressor transmitter had to supply about one-fifth as much power as that supplied by the main transmitter Later tests on a two-course range utilizing a different system showed similar results for the suppressor action, and these will be discussed more thoroughly in the discussion of the flight tests.

Some tests were also conducted to determine if the suppressor system could furnish aural and visual indications similar to those now produced by the 75-megacycle cone-of-silence marker. To accomplish this, the suppressor transmitter was modulated with 3000 cycles while the output of the range receiver was connected to the audio filters and rectifier of the standard marker receiver. Under these conditions, the marker light operated in almost the same manner as when the regular 75-megacycle cone-

of-silence marker was supplying the signal. The duration of indication was slightly less than with the standard Z marker, and the marker light went out briefly when the airplane was directly over the station This was due to the vertical pick-up characteristic of the horizontal loop receiving antenna Since the time these tests were made, another type of receiving antenna has been used which will receive signals straight downward so that the light will not go out when the plane is directly over the station However, a simultaneous voice feature has been added since these tests so voice frequencies are included in the receiver output. This necessitates another filter to prevent speech components from operating the marker light. Because of added complications, it was decided to abandon the idea of using the suppressor system for Z-marker indications since the present 75-megacycle marker systems adequately supplied the desired information without the necessity of interlocking the range and marker indications.

Demonstrations

In the Introduction to this report, it was stated that tests in the Link Trainer showed the two-course visual range with sector identification to be the most desirable type of range from the standpoint of having the simplest navigation procedure. The equipment described so far was built specifically for the purpose of showing that the navigation system as set up in the Link Trainer could be duplicated in practice and for the purpose of having a workable system to demonstrate under actual flight conditions This work completed the original contract with the International Telephone Development Co., Inc , which was performed in cooperation with Civil Aeronautics Administration engineers. In the fall of 1941, demonstrations were given to various interested groups, some of which included representatives from various divisions of the Civil Aeronautics Administration, Radio Technical Commission for Aeronautics, the Air Line Pilots Association, and representatives from the various airlines.

It was the unanimous decision of these groups that the visual-aural ultra-high-frequency radio range system be adopted for installation on the airways to supersede the four-course low-frequency ranges now used to define the airways It was further recommended that a number of the low-frequency ranges be kept in service for direction finding purposes. It was also recommended by these groups that the sector identification be continuously interlocked in order to provide a pair of aural courses at right angles to the visual courses and that simultaneous voice services be provided without the necessity of interrupting the aural or visual services.

DEVELOPMENT OF VISUAL AND AURAL SYSTEMS WITH SIMULTANEOUS VOICE

It was originally planned to provide simultaneous voice with visual courses by transmitting voice in lieu of the 1020-cycle quadrant and station identification aural signals which were transmitted once every 30 seconds, inasmuch as it was believed that an interruption of these signals would not be objectionable. With this arrangement, it would be comparatively simple to transmit speech by supplying voice sidebands to the lower center antenna only, after the aural sidebands had been removed This could easily be accomplished by short-circuiting the line to the side aural antennas and modulating the aural sideband generator with speech instead of 1020 cycles. However, the recommendation made by the Radio Technical Commission for Aeronautics that all three facilities be continuously available considerably complicated the problem of supplying voice transmission It became necessary to devise a system which would either allow the sidebands of all three services to be transmitted from the same center of radiation or utilize a separate carrier for the transmission of voice.

Separate Carrier Tests - System No 1

The possibility of using a separate carrier which differed in frequency from the main carrier by about 20 kilocycles had previously been examined for the aural part of the system This was done by replacing the sideband generator with a separate 30-watt transmitter which had a carrier frequency 20 kilocycles below the visual transmitter and modulated at 1020 cycles. Since the difference in frequency was very small, the tie line remained balanced and the other circuits remained in tune There was no

necessity of adjusting the relative phase between the aural and the visual systems since they were on different frequencies The difference in frequency was insufficient to give any difficulty due to receiver response

Flight tests made with this arrangement showed that the method could be made to work but that it possessed several disadvantages The biggest disadvantage was the fluctuation of the visual indicator with the D-6 keying This occurs when the airplane is off the visual or aural courses, since the total received carrier fluctuates except when the plane is on the aural course and changes the effective modulation of the visual frequencies When the airplane is on the visual course, the indicator receives no visual modulation energy, so a change in total carrier level will have no effect on the indicator The excessive indicator fluctuation was due to the large amount of aural carrier that was necessary with the two-carrier method in comparison to the small amount of aural sideband power that was necessary with the sideband generator

Although the two-carrier method did not offer many advantages as a substitute for the sideband generator it did offer advantages when used for transmitting voice In this case, the carrier could be left on continuously so that there was no variation of received signal due to the aural keying A 100-watt transmitter was used to supply the separate carrier on the 125 020 megacycles. The energy was fed into the lower center antenna and the aural side antennas were short-circuited. For these tests, the aural system was not used since it was desired to determine only if intelligible voice could be obtained with this method. If this method of operation proved desirable the aural signals could again be added without difficulty The problem of detection in the receiver for the two-carrier system was given careful consideration Both square-law and linear detection were investigated experimentally and theoretically

Let two carriers of amplitudes E_1 and E_2 and radian frequencies ω_1 and ω_2 be modulated to degrees m_1 and m_2 by radian frequencies p and q, respectively Analysis of square-law detection, given in Appendix IV, shows that a normal amount of second harmonic is present and no components of radian frequencies $(p \pm q)$ are present. If the difference frequency of the two carriers is supersonic, no distortion terms other than second harmonics will be heard in the detector output

Analysis of linear detection indicates that distortion terms of all possible combination frequencies are present.[13] The principal audio distortion terms are of radian frequencies 2p, 2q, $(p \pm q)$, $(2p \pm q)$, $(2q \pm p)$ and $2(p \pm q)$ As brought out in Appendix V, the series used in evaluating the various terms in the frequency spectrum for linear detection converge for a restricted range of values of carrier amplitude ratio K and degrees of modulation m_1 and m_2 only, thus limiting analysis of the problem

Using the equations given in Appendices III and IV, the amplitudes of output voltages after square-law and linear detection were computed for $K = 1/10$, $1/3$, $1/2$, and $m_1 = m_2 = 0\ 5$, and collected in table II.

$K = 1/2$ is somewhat beyond the limiting value of K_{max} for linear detection, as determined from figure 26 It is believed, however, that the computed amplitudes for $K = 1/2$ are still fairly close to the actual values. The results given in table II are plotted in figures 27 to 29, inclusive Figure 29 shows relative amplitudes after square-law and linear detection versus ratio of carrier amplitudes, the ordinates are in terms of the amplitude of the fundamental of modulation frequency $q/2\pi$ of the stronger carrier

Similarly, figure 28 shows the relative amplitudes of the detection products versus K, but the ordinates are in terms of the amplitude of the fundamental of modulation frequency $p/2\pi$ of the weaker carrier. Figure 27 shows a frequency spectrum

---

[13] C B Aiken, "Theory of the Detection of Two Modulated Waves by a Linear Rectifier," Proceedings of the I R.E , pp. 601-629, April 1933.

TABLE II

RELATIVE AMPLITUDES OF OUTPUT VOLTAGES OF DETECTOR

K = Carrier Amplitude Ratio Degrees of Modulation $m_1 = m_2 = 50\%$

SQUARE-LAW DETECTOR

Relative Amplitudes	K = 1/10		K = 1/3		K = 1/2	
	ref to q	ref to p	ref to q	ref. to p	ref to q	ref to p
E_q	100	10,000	100	900	100	400
$\frac{E_{2q}}{E_q}$	12 5	1,250	12.5	113	12 5	50
$\frac{E_p}{E_q}$	1	100	11 1	100	25	100
$\frac{E_{2p}}{E_q}$	0.125	12 5	1 39	12 5	3 13	12 5
$\frac{E_{p \pm q}}{E_q}$	0	0	0	0	0	0

LINEAR DETECTOR

E_q	100	17,300	100	1,450	100	566
$\frac{E_{2q}}{E_q}$	0 09	15 5	1 17	16 9	3 4	19.2
$\frac{E_p}{E_q}$	0.58	100	6 93	100	17.7	100
$\frac{E_{2p}}{E_q}$	0.073	12 6	0 92	13 3	2 6	14 7
$\frac{E_{p \pm q}}{E_q}$	0.149	25 7	1 72	24 8	4.14	23 4

based on table II The length of the lines are approximately proportional to the amplitudes

The following conclusions can be drawn from consideration of the above figures Second harmonic distortion of the modulation of the stronger carrier is considerably less for linear than for square-law detection, however, second harmonic distortion of modulation of the weaker carrier is nearly the same for both types of detectors Second harmonics do not greatly reduce intelligibility of speech or the brilliance of a tone Cross-modulation terms of radian frequencies $(p \pm q)$, etc , reduce the intelligibility of speech and make a tone appear rough. This is especially true if one of

the modulation frequencies is low, for example, 90 or 150 cycles Figure 28 shows that with linear detection a cross-modulation term $(p \pm q)$ of the order of 25 percent of the fundamental amplitude E_p is present and nearly independent of K This and the other cross-modulation terms make speech considerably more difficult to understand with linear detection than with square-law detection

It is worth mentioning that if the weaker carrier is not desired, as for instance in case of an interfering station, linear detection gives less distortion than square-law detection as long as the ratio of carrier amplitudes is substantially smaller than unity.

The theoretical studies were confirmed by actual tests both on the ground and in the air With approximately equal amounts of power contributed by the visual transmitter and the voice transmitter, the relative field at a distance of 200 feet was about 5 to 1 in favor of the visual transmitter This was largely due to the loss in the tie line and the lower height of the voice center antenna. The distortion measurements were made with a wave analyzer in the receiver laboratory of the CAA Experimental Station, which was located about 3200 feet away from the range station Excellent voice quality with very low distortion was obtained when a square-law detector was used. A linear detector produced speech which was understandable but which contained considerable distortion

In making the flight tests, the receiver was arranged to provide both linear and square-law detection; linear detection was used for the visual range indications, and either linear or square-law detection was used to rectify the voice signals The visual indications were normal and no interaction from the voice signals was encountered The quality of the received voice was good when the square-law detector was used When the linear detector was used the voice quality was inferior and was quite difficult to understand under flight conditions.

Because of the numerous extraneous noises encountered while in flight, voice quality for aircraft use must be considerably better than that quality which will give intelligible speech on telephone circuits For this reason the linear detector was not satisfactory for use in aircraft service, although in a quiet laboratory a fair degree of intelligibility could be obtained

These flight tests indicated that satisfactory voice could be obtained, however, the distance range was only about 10 miles due to the excessively low field strength from the voice carrier In order to increase the distance range and to obtain more complete data, the voice transmitter was fed into a separate antenna located at the edge of the counterpoise at a distance of 15 feet from the visual center antenna and one-half wavelength above the counterpoise. The aural sidebands were fed into the lower center loop and lower side loops in the usual manner, and complete simultaneous operation was obtained The flight tests with this range gave a distance range of approximately 22 miles on visual, voice, and aural at 1000 feet altitude. At this time a loop-type receiving antenna was used on the airplane Later information obtained on a V-type receiving antenna indicated that the distance range would have been approximately 36 miles if this type of aircraft receiving antenna had been used during the tests on this range system.

During these tests the two carriers were adjusted to be equal. Ground tests were also made with the aural system inoperative, with the visual system operating normally, and with the voice channel modulated with 1020 cycles using both linear and square-law detection. Under these conditions the distortion terms 870 and 1170 cycles $(p \pm q)$ were about 3 5 percent of 1020 cycles for square-law detection and approximately 20 percent of 1020 cycles for linear detection

Five-Loop Simultaneous Range - System No. 2

The need for developing a visual-aural range with a simultaneous voice facility brought up the question as to what type of antenna configuration and circuit arrangement would be most desirable The previous section describes some tests using a sepa-

rate carrier in which the voice was transmitted from an antenna located about 15 feet away from the center of the visual-aural antenna system Although this operated satisfactorily, it was not considered a desirable arrangement since the voice signal would have a different field pattern in the vertical plane from those of the visual and aural signals

It was also desired to set up a simultaneous range in which the aural and voice signals would consist of double sideband energy which combined with the carrier supplied from the visual system To do this, it was essential that all three signals have the same center of radiation Otherwise, the phase of the sidebands with respect to the carrier would change as the azimuth angle changed with a resultant increase in distortion and possible loss of the aural and voice signals at critical angles

When the program of developing a visual-aural radio range was first initiated, numerous methods were proposed for accomplishing the desired results The system which appeared to be most straightforward was the six-loop system using a tie line to prevent interaction between the two systems Early tests using this antenna arrangement showed that the system had definite possibilities and, accordingly, the first part of the work described in this report centered around this system

Later it became obvious that the problem of making the tie line operate in the desired fashion was not a simple one and another system using five loops which had several advantages was proposed. This system combined the visual and aural energy into one center antenna by means of a radio-frequency bridge of the same type as that used in the mechanical modulator The only disadvantage of this arrangement was the necessity of dissipating a considerable amount of energy in the balancing impedance of the bridge At the time this proposal was made, it was thought that the tie line could be made to operate satisfactorily without any loss in efficiency, so the five-loop system was not tried Later developments showed that it was necessary to dissipate some power in the tie line in order to reduce the high angle lobes; therefore, the question of comparing the respective power efficiencies of the two systems became less of a factor in deciding their relative merits.

When it became evident that a six-loop antenna system was not well suited to a simultaneous range system, it was decided to proceed with the development of a five-loop antenna system which combined all three signals into the center antenna by means of two radio-frequency bridges Thus, a more symmetrical array resulted with a consequent reduction in complexity of the feeding circuits. Figure 30 shows the five-loop antenna system which is spaced one-half wavelength above the counterpoise The spacing of the outer loops was set at 120° for the reasons given in the theoretical discussion

The block diagram of System No 2 is shown in figure 31 As before, single lines on the diagram represent two-wire balance shielded transmission lines The manner in which the visual energy is modulated is exactly the same as in the previous range, with the exception that the carrier output of the upper bridge of the mechanical modulator does not feed the center antenna directly Instead, it connects to r-f bridge No. 3, which combines the visual sidebands, aural and voice subcarrier sidebands, and carrier into the center antenna The bridge is balanced by impedance Z_3, which is equal to the impedance looking into the transmission line feeding the center loop Since the bridge is balanced, no energy from the visual system can appear in either the aural or the voice channel, and vice versa

The aural and voice subcarrier sidebands are combined in r-f bridge No. 4, which in turn feeds r-f bridge No. 3 If it were not necessary to furnish voice, the aural subcarrier sidebands could be fed directly into bridge No 3. However, when voice is supplied, it is necessary to prevent interaction between the aural and the voice channels, in addition to preventing interaction between these two channels and the visual channel Therefore, bridge No 4 is necessary and must be balanced in the same way as bridge No. 3 That is, Z_4 must be equal to the impedance looking into bridge No. 3 so that the voice channel is independent of the aural channel, and vice versa.

As in the original visual-aural range, the side aural loops are fed from the same source that feeds the center loop. Suitable means are used for adjusting the relative amplitude and phase of the side antennas with respect to the center loop Keying of the aural patterns is accomplished by reversal of the line feeding the side antennas

A total of four phasers is necessary to ensure correct phase relationships in the various parts of the system One is used for each pair of side antennas and one is used for each sideband generator, that is, the current in each pair of side antennas must be correctly phased with respect to the current in the center antenna in order to obtain the correct field pattern, while the phase of the sidebands with respect to the carrier must be correctly adjusted in order to obtain minimum distortion The antenna phasing adjustments have already been described and need to be made only when the system is first tuned since the characteristics of the antenna system will remain constant The phase of the sideband generators is dependent on the tuning of the tank circuits, thereby making it necessary to rephase the sidebands when tube replacements are made. Phasing of the sideband generators is accomplished by adjustment of phasers placed between each sideband generator and bridge No. 4, as shown in figure 31 The phaser in the aural sideband circuit is adjusted for minimum 150-cycle response and maximum 1020-cycle aural response. The 150-cycle minimum and 1020-cycle maximum occur at approximately the same phaser position Figure 32 is a graph showing measurements taken in adjusting the phaser The phaser in the voice sideband generator circuit is adjusted in a similar manner

System No. 2 transmits the aural and voice intelligence on subcarriers, as shown in figure 33 The 1020-cycle aural modulation is placed on a 12-kilocycle subcarrier and the voice modulation is placed on a 20-kilocycle subcarrier The main purpose of using two subcarriers was to provide a system which had the maximum degree of freedom With this system it was possible to transmit the entire voice spectrum without eliminating the low frequencies in the visual modulating frequency spectrum or the band around 1020 cycles It also precluded the possibility of the voice being broken up by the higher order harmonics produced by the mechanical modulator Furthermore, it was believed that there would be less possibility of overmodulation in the voice channel producing any effect on either the visual or the aural indications A secondary consideration was the possibility of reducing the weight of the aircraft equipment due to the simpler filters which could be used for separating the 12-kilocycle and 20-kilocycle channels rather than the band pass-band rejection filters which are now necessary for separating the 1020-cycle aural modulation and the voice modulation

Excellent voice reproduction was obtained with little interference from either the aural modulation or the visual modulation A graph of the over-all transmitter and receiver audio response is shown in figure 34 for both the aural range and voice channels. The use of the subcarriers somewhat complicated the receiving circuits and it was subsequently found that no substantial improvement was obtained After the main carrier was rectified and the 90- and 150-cycle modulation frequencies were obtained, it was necessary to separate the subcarriers and detect each one separately. Although the 12-kilocycle and 20-kilocycle detector-amplifier unit was not reduced to its lightest weight, it did not appear that any weight improvement could be made over other systems to be described later.

Subsequent development showed that the same results could be obtained without the necessity of placing the voice and aural course intelligence on subcarriers However, the development of System No 2 showed the practicability of a five-loop system and its advantages over the original six-loop system Also, much valuable experience in regard to the use of subcarriers in aircraft applications was obtained

Five-Loop Simultaneous Range - System No 3

This system used essentially the same r-f circuit as that of system No 2 A block diagram of system No 3 is shown in figure 35, the main difference between this and the previous system being the distribution of frequency components The frequency spectrum is shown in figure 36 The antenna system and radiated field pat-

terns are identical to those of system No 2

Work on this range was started by International Telephone and Radio Laboratory engineers some time after system No 2 had been partially constructed The original intent had been to use the visual-aural system previously described and add the voice facility by using a bridge network to combine the aural and voice energy Considerable time was spent in an effort to make this scheme operate The work may be best summed up by stating that the tie line was finally found to possess disadvantages over the r-f bridge from the standpoint of power efficiency when it is desired to feed a considerable amount of energy to the lower center loop

From the standpoint of using the simplest antenna configuration and having the most straightforward adjustment procedure, the system using five antennas with a bridge in the center antenna circuit is the most desirable one This was adopted and utilized the same equipment which was originally used with the six-loop visual-aural system The only additional pieces of equipment necessary were the sideband generators which supplied 40 watts of voice-modulated energy and the 20-kilocycle subcarrier equipment Since the major difference between this system and system No 2 is the lack of a subcarrier for the aural system, it will not be necessary to describe the radio-frequency circuits. The results obtained with this system were entirely satisfactory and the receiving equipment used was simpler and lighter than that used with system No. 2

Five-Loop Simultaneous Range - System No 4

System No. 4, the block diagram of which is shown in figure 37, is essentially the same as system No 3 except that a subcarrier was not used for voice Instead, voice sidebands were applied directly to the main carrier The frequency spectrum for system No. 4 is shown in figure 38 The equipment used was identical to that of system No 3 The changeover was effected merely by removing the 20-kilocycle subcarrier generator from the circuit and modulating the sideband generator directly with voice

Numerous flight tests were made in which systems Nos 2, 3, and 4 were compared directly Briefly summarized, the flight tests showed that it made little difference whether the aural and voice facilities were placed on subcarriers or whether they were transmitted directly on the carrier Direct comparison between systems Nos 2 and 3 showed that the aural signal had the same quality with either system, and in neither case was there any appreciable amount of keying reaction on the visual or voice circuits Direct comparison between systems Nos. 3 and 4 disclosed no difference in voice quality or intelligibility. In fact, it was quite difficult to distinguish between the three systems when they were properly adjusted. It was observed that the noise level on the voice circuit at the extreme service radius was noticeably higher when subcarrier transmission was used.

Since there was little difference between the results obtained with each of these three systems, it was finally decided to transmit all of the facilities directly on the carrier This simplified the transmitting and receiving equipments due to the elimination of subcarrier equipment and more complicated receiving equipment

The most important feature of systems Nos 1, 2, 3, and 4 is that the visual indications are independent of phase shift and changes in power output which might be caused by heating of tuned circuits, tube aging, etc , that is, the course sharpness, course location, and pattern clearance are not affected by these changes This is due to the fact that the shape of the transmitted patterns is determined only by the physical constants of the transmission lines, bridges, and phasers which appear between the center antenna and the side antennas Any change in radiated carrier power will have little effect on the courses since the receiver operates on automatic gain control and would therefore maintain a constant audio level and, hence, a constant visual course width Phase shift in either of the sideband generators has no effect on the courses, although the relative level and distortion on the voice or aural channel will be affected A change in sideband power output will affect the audio level of either the voice signal or the aural signal, but since all three aural antennas are fed from the same source, the pattern shape and the course sharpness will re-

main constant

These statements have been checked by actual tests which simulated the sort of conditions which might be encountered in practice The power output was reduced in various parts of the system and the phasing of various circuits changed by detuning of the tank circuit without any effect on the location or sharpness of the courses Also, either the voice or aural facility could be turned off without affecting the remaining services. Loss of the visual system will result in the complete loss of all three facilities since the carrier is supplied from the visual transmitter One of the major advantages of this system is that a false indication cannot be given under any circumstances since either the correct signal will be transmitted or no signal will be transmitted.

Five-Loop Simultaneous Range - System No 5

It was previously stated that systems Nos 2, 3, and 4 had an extremely high degree of stability and that the course sharpness and course location are unaffected by normal changes in the transmitting equipment It was also stated that there was a loss of power efficiency in these systems because of the necessity of dissipating a portion of the r-f energy in the balancing impedances of the bridges

The frequency spectrum for system No 5 is identical to that of system No 4 which is shown in figure 38 This system represents a compromise between efficiency and stability In this system, the bridge losses have been reduced to a negligible amount by utilizing class C amplifiers instead of sideband generators Referring to figure 39, r-f bridge No 4 is fed by two class C amplifiers whose outputs are equal to each other and on the same frequency as the main transmitter When no modulation is applied to either of the amplifiers, all of the carrier energy flows to bridge No. 3 None of the carrier energy appears at the side aural antennas because of the crossover in bridge No 4 The side aural antennas also act to balance the bridge and prevent interaction between the two class C amplifiers

Both amplifiers are modulated in phase with voice and the sidebands are fed to bridge No 4 All of the voice sideband energy flows to bridge No 3 and none appears in the side aural antenras

To transmit the aural sidebands, only one of the class C amplifiers is modulated The aural sideband energy is divided in bridge No 4, one-half of the energy being fed to bridge No 3 and the other half of the energy being fed to the side aural antennas In order to obtain the aural courses, a reversing relay is placed in the line to the side aural loops in a manner similar to the arrangement used in other systems. An alternate method of keying is to modulate first one class C amplifier and then the other in accordance with the D-U keying rhythm In this way, the phase of the aural side-band energy in the side antennas with respect to the phase of the aural sideband energy in the center antenna is reversed because of the crossover in bridge No 4

This system is identical to the systems previously described in that one-half of the sideband energy is dissipated in bridge No. 3 However, only a small amount of carrier power is dissipated for the same reason that no energy is lost in bridge No 4, that is, the carrier energy from bridge No 2 and bridge No 4 combine in phase to feed the center antenna Because of the crossover, the carriers will partially cancel at impedance Z_3, resulting in a substantial reduction of power loss When both carrier powers are equal, no voltage will appear across Z_3 and consequently no power will be dissipated Even when the carrier power from bridge No 2 is much greater than that from bridge No 4, the power loss is still quite low For instance, when the power from the main transmitter is twice that of the power supplied by both class C amplifiers, the carrier power lost in Z_3 is less than 3 percent of the total carrier power passing into the center antenna It can thus be seen that a large increase in power efficiency has been obtained with system No 5, since the network efficiency for both the carrier energy and the sideband energy is approximately twice that obtained with the previous systems

It is necessary to dissipate a portion of the energy supplied to the side antennas in order to obtain the current ratio which will produce the desired pattern shape. As discussed in the first section of this report, the most favorable shape of pattern is obtained when the value of K is 2 0 With the arrangement shown in figure 39, the value of K for the visual array would be 1 0 if Z_2 were omitted, while the aural array would have a value of K equal to 1 41 if Z_4 were omitted Since the power in the side loops cannot be varied by adjusting the impedance into which the bridge looks, because of the necessity of keeping the bridge balanced, it was necessary to place dummy loads, Z_2 and Z_4, across the lines feeding the side loops In this way the correct impedance can be presented to the bridge, since after the power is correctly divided by adjusting the dummy load, the transmission line is matched to rebalance the bridge.

Although system No 5 is considerably more efficient than systems Nos 2, 3, and 4, it does not possess the inherent stability of these systems A change in phase or amplitude of either of the class C amplifier outputs or of the main transmitter output of system No 5 will produce a more harmful effect than a similar change of phase or amplitude in the units of the previous systems It will be recalled that tests on the previous systems showed the course indications to be substantially free of phase and amplitude changes

This is not true of system No 5, as can be seen from both theoretical considerations and actual tests For instance, a change in the phase or amplitude of one of the class C amplifiers will allow carrier and voice energy to appear in the side aural antennas due to the fact that bridge No 4 will become unbalanced. Because of the keyer in the line to the side loops, the phase of the carrier and voice energy appearing in the side aural loops will be reversed in accordance with the keying rhythm and, will cause fluctuation of both the carrier and the voice levels Except when the airplane is on the visual course, fluctuation of the carrier level will cause the visual indicator to vary in rhythm with the D-U keying, which is annoying to the pilot Also, the voice transmission will become difficult to understand at some azimuth angles because of the fact that it will be keyed similarly to the aural signals The degrees to which these difficulties impair the operation of the system depends upon the amount of phase or amplitude change Systems Nos 2, 3, and 4 are free from these defects since a failure of the voice or aural facility has no effect on the remaining services

TRANSMITTING EQUIPMENT

Type TUE Transmitter - Non-Simultaneous System and Systems Nos 1, 3, 4, and 5

The type TUE transmitter operated on a frequency of 125 megacycles A type 807 tetrode served as a combination crystal oscillator and quadrupler stage The crystal was ground to oscillate on a frequency of 3906.25 kilocycles. An 807 doubler stage followed, which in turn excited two more doubler stages using 304-B triodes The output of the 125-megacycle doubler was link coupled to a neutralized push-pull amplifier-driver stage which used two 100TH triodes The output of this stage excited the neutralized power-amplifier stage which used two type HK-454-H triodes A tuned output circuit was used to couple the transmitter to the mechanical modulator unit The average carrier power appearing at the transmitter output terminals was approximately 200 watts

Excitation for the sideband generators used in systems Nos 3 and 4 was obtained from the last 304-B doubler stage Excitation for the voice and aural class C amplifiers used in system No 5 was obtained from a link which coupled to the tuned output circuit A diode monitor which used a 6H6 tube was capacitively coupled to the output circuit

Protective grid bias to all stages was supplied by a selenium rectifier power supply. Plate and screen voltages for the oscillator and multiplier stages were supplied by a bridge rectifier using four 5Z3 tubes Plate voltage for the amplifier-driver and power-amplifier stages was supplied by a bridge rectifier using four 866-A tubes

Type TUD Transmitter - Systems Nos 1 and 2

The type TUD transmitter operated on 125 4 megacycles A type 807 tube was used as a fundamental crystal oscillator and frequency quadrupler A crystal frequency of 5225 0 kilocycles was used The crystal stage was followed by an 807 doubler and a neutralized fundamental amplifier which used a type HK-54 tube. This stage was link coupled to a pair of HK-54 tubes which were used as a push-pull tripler The tripler stage was inductively coupled to the neutralized power amplifier which also used a pair of HK-54 tubes An untuned output circuit coupled the output to the mechanical modulator. A 6H6 diode, capacitively coupled to the output circuit served as a monitor The average carrier power output of the transmitter was approximately 150 watts

The same transmitter rack also contained a class B audio amplifier which had originally been used to modulate the power-amplifier stage Since plate modulation of the final amplifier was not used in system No 2, the class B amplifier was disconnected from the final amplifier and used to modulate the 20-kilocycle subcarrier generator which fed the voice sideband generator A pair of type 805 tubes served as the class B audio amplifier These were driven by two type 2A3 tubes which were driven by a 6C5 audio stage

The high-voltage rectifier used a pair of type 872 tubes, and the low-voltage rectifier used a pair of type 866-A tubes Grid bias for all stages was supplied by a 5Z3 rectifier.

Sideband Generator - Non-Simultaneous System

A schematic of the sideband gererator used in the original non-simultaneous development is shown in figure 40 A type 829 tube acted as a balanced modulator and supplied approximately 6 watts of sideband energy The grids of this tube were excited in parallel with r-f energy while audio energy was applied in push-pull Controls were provided to balance the plate current and audio voltage in each section of the tube so that the carrier could be completely balanced out in the plate circuit, leaving only the sideband energy

The 1020-cycle energy was supplied by two type 6G6-G tubes, one as a grid feed back oscillator and the other as an isolation amplifier A type 5V4-G tube supplied plate power for these two tubes and the 829 balanced modulator Another pair of 5V4-G tubes in the same unit supplied 110 volts d c to operate the D-U transmission line reversing relay.

Suppressor Transmitter - Non-Simultaneous System and Systems Nos 1, 3, 4, and 5

The suppressor transmitter which was used with the non-simultaneous range as well as with systems 1, 3, 4, and 5 supplied approximately 40 watts on 124 975 megacycles A type 6N7-G tube was used as a combination oscillator-tripler The fundamental frequency of the crystal was 4628.70 kilocycles A type 6V6 tube acted as a frequency tripler which excited a pair of type 7C5 tubes operating as a push-pull frequency tripler A type 829 tube was used as the final power amplifier which was inductively coupled to the transmission line that fed the antenna The power supply used four type 866-A tubes Two were used to supply the oscillator and multiplier stages and two were used to supply the final amplifier stage

Sideband Generators - System No. 2

A schematic of the sideband generators used in system No 2 is shown in figure 41 A pair of HK-24 tubes was used for each balanced modulator The grids were excited in parallel with r-f energy, and the plates were connected in push-pull No d-c plate voltage was used. The audio voltage was applied to the plates in push-pull and served to generate the sidebands An HK-24 tripler stage was used to excite each sideband generator Direct-current plate power for the tripler stage was supplied by a rectifier using two type 866-A tubes A photograph of the sideband generators is shown in figure 42

Sideband Generator Monitors - System No 2

In order to observe the output wave form of the sideband generators on an oscilloscope, diode type monitors were used to rectify a part of the output These monitor units are located directly above the sideband generator panel Figure 43 shows the schematic diagram of each monitor A type 6H6 tube was used for each rectifier The r-f energy for each tube was obtained by a combination of inductive and capacitive coupling. A high-pass filter was placed in the rectified output of each monitor in order to prevent all components except the subcarrier wave from appearing on the cathode ray screen

Subcarrier Generators - System No. 2

A schematic diagram of the 12-kilocycle subcarrier generator is shown in figure 44 A pair of type 807 tubes operated as a push-pull oscillator at 12,000 cycles and excited a pair of type 805 tubes as a class C push-pull amplifier. This amplifier was modulated at 1020 cycles by a pair of 805 tubes operated as a class B amplifier The modulator tubes were driven by an audio amplifier which was excited by a 1020-cycle audio oscillator

The 20-kilocycle subcarrier generator which is shown schematically in figure 45 used a pair of 807 tubes as a push-pull oscillator to drive a pair of 805 tubes as a class C amplifier The 20-kilocycle output was modulated by voice energy supplied from the class B audio amplifier and speech amplifier in the TUD transmitter

Sideband Generator - Systems Nos 3 and 4

A schematic diagram of the sideband generator used in systems Nos 3 and 4 is shown in figure 46 A novel circuit using two type 829 tubes was utilized Individual grid and tank circuits were used for each tube and the elements of each tube were connected in push-pull The two grid tanks were connected in parallel by a half-wave line, and the two plate tanks were connected in parallel by a half-wave line which had a crossover in it In this way, the carrier was cancelled Either voice modulation or 20-kilocycle subcarrier with upper and lower voice sidebands was applied in push-pull to the paralleled screens in each 829 tube This arrangement produced only sideband energy in the plate tanks. Output energy was obtained by coupling inductively to one of the plate tanks Equal amounts of energy were delivered by each tube due to the half-wave line which tightly coupled the two tank circuits together

Class C Amplifier and Modulating Equipment - System No 5

The voice and aural class C amplifiers used in system No 5 were built on a single chassis in a symmetrical arrangement Figure 47 shows a schematic diagram of this equipment Each amplifier used a single type 829 tube operating in push-pull The output from each stage was inductively coupled to the output phasers and bridge The grid circuits of each tube were untuned, with common coupling to the inductive link which carried the excitation from the main transmitter

Each amplifier stage was modulated by four 6L6 tubes in push-pull-parallel acting as class AB audio amplifiers Two type 6J5 tubes were used in cascade as voltage amplifiers, and one pair of 6J5 tubes was used in push-pull to drive each modulator One audio amplifier was supplied with voice signal only, while the other audio amplifier was supplied with both voice and 1020-cycle energy The two signals were combined in a bridge circuit to prevent interaction between them

The 1020-cycle energy was supplied from the same audio oscillator that was used for the sideband generator of the non-simultaneous range Power for the class AB modulator was supplied by two identical power supplies, each of which used two type 5Z3 tubes

RECEIVING EQUIPMENT

Type RUM Receiver

The receiver used for most of the non-simultaneous tests and for a large part of the simultaneous tests was a Western Electric type RUM receiver This receiver was a type RUK localizer receiver which was modified to include an r-f amplifier and several other improvements [14]

A type W.E 385-A tube was used as an r-f amplifier and its grid circuit was capacitively coupled to the antenna input circuit The plate circuit was inductively coupled to a type 6J7 mixer tube The heterodyne voltage was applied to the screen grid of the mixer A crystal-controlled oscillator operating on a frequency of 9 583 megacycles or 9.617 megacycles and three harmonic multipliers were used to produce the heterodyne voltage Two twin triode type 6N7 tubes served as the crystal oscillator and harmonic multipliers.

The mixer stage coupled into a three-stage, 10-megacycle intermediate-frequency amplifier which used three type 6SK7 tubes. The shape of the intermediate-frequency response curve was such as to provide a band width of approximately 70 kilocycles at 6 decibels attenuation and 275 kilocycles at 60 decibels The diode portion of a type 6SQ7 tube constituted the detector and the delayed avc rectifier. The triode portion of the 6SQ7 tube acted as the first audio amplifier and a type 6J5 tube was used as the second audio amplifier.

In the original receiver which was developed for non-simultaneous operation, no provision was made for voice reception During the simultaneous voice development, a separate amplifier for voice was essential and a twin triode type 12SN7-GT tube was installed in place of the 6J5 tube One triode was used to amplify the visual signal and the other triode was used to amplify the voice and aural range signals Simple resistance-capacity low-pass and high-pass filters were placed in the grid circuits of the visual and voice amplifiers, respectively These filters proved to be very effective in reducing the interaction between the two services The audio-frequency response of the aural channel was attenuated 19 decibels at 100 kilocycles, 3 decibels at 400 cycles, and 7 5 decibels at 4000 cycles from the response obtained at 1000 cycles

When subcarriers were used, it was necessary to install a tuned trap in the plate circuit of the first audio tube and make several minor modifications in the detector circuit in order to increase the response of the circuit at 12 kilocycles and 20 kilocycles A separate unit was used to demodulate the subcarriers in order to obtain the voice and aural signals.

The visual output was coupled to two band-pass filters in parallel, which passed the 90-cycle and 150-cycle modulation frequencies The outputs of the two filters were applied to copper oxide rectifier units which were connected in a balanced bridge circuit A crossed-pointer d-c instrument was operated by the rectified difference of the two voltages.

The receiver was designed to operate from a source of 12 volts The filaments were connected in a combination of series parallel and parallel A vibrator type power supply furnished plate and bias voltage A type 0Z4 tube served as the plate rectifier and a type 6Z Y5-G tube served as the bias rectifier

Type 32A Receiver

The receiver used for some of the non-simultaneous demonstrations and for part

---

[14] See reference 6, page 9.

of the simultaneous tests was a Western Electric type 32A receiver This receiver was specifically designed for airline use and covered the frequency range of 109-111 megacycles for localizer service and the frequency range of 119-133 megacycles for range and traffic control services Remote electrical tuning by means of a motor-driven ganged condenser could be used for 30 spot frequencies in these bands Provision was also made for local manual tuning The essential features of the receiver are shown schematically in figure 48 Figure 49 is a photograph of this receiver.

The balanced antenna circuit was inductively coupled through an electrostatic shield to the first tuned circuit. Three tuned circuits were provided between the antenna circuit and the control grid of the type 6AC7 mixer tube as a band-pass filter to improve the image rejection characteristics The heterodyne oscillator voltage was injected into the control grid of the mixer stage by capacitive coupling The heterodyne oscillator voltage was produced by a variable-frequency oscillator and a harmonic multiplier which used two type 955 tubes The variable-frequency oscillator operated throughout the band of 44 to 49 megacycles In the 109- to 111-megacycle band the second harmonic of the oscillator was used, and in the 119- to 133-megacycle band the third harmonic of the oscillator was used The heterodyne frequency was lower than the signal frequency for reception in the 109- to 111-megacycle band and was higher than the signal frequency during operation in the 119- to 133-megacycle band

Three stages of 13-megacycle intermediate-frequency amplification followed the mixer stage The shape of the intermediate-frequency response curve was such as to provide a band width of approximately 115 kilocycles at 6 decibels attenuation and 395 kilocycles at 60 decibels A type 6AB7 tube was used in the first stage with two type 12SG7 tubes in the other two stages. A 12SQ7 multiple purpose tube served as a diode detector and first audio amplifier This tube also provided delayed amplified avc action Another 12SQ7 tube acted as a noise limiter and codan or carrier-operated noise suppressor To obtain negative voltage for operation of the delayed amplified avc system, a type 12SR7 was used as a bias oscillator and its output was rectified by a diode in the same envelope

The detector output fed voice and aural dual output channels using 12A6 tubes The grids of the visual output tube, which was a 6SN7-GT double triode tube with both sections in parallel, were also connected to the detector output Resistance-capacity low-pass and high-pass filters were placed in the visual and voice channels, respectively The audio-frequency response of the aural channel was attenuated 28 decibels at 100 cycles, 5 decibels at 400 cycles, and 8 5 decibels at 4000 cycles from the response obtained at 1000 cycles The visual band-pass filters and rectifier units were essentially identical to those used in the type RUM receiver

The receiver was designed to operate on either 12 or 24 volts The filament heaters were connected in series-parallel Plate voltage was supplied by either a 12- or a 24-volt dynamotor, the voltage rating of which corresponded to the supply voltage in use.

A function selector switch was arranged to set the sensitivity control, avc time constant, codan, and audio level at the same time it operated the band changing relay

Some of the performance characteristics of the type 32A and the type RUM receivers are shown in figures 50 to 59, inclusive

Subcarrier Amplifier-Detector Unit - System No 2

Since the receivers had no means for demodulating the subcarriers used in system No 2, it was necessary to provide an external unit for this purpose A schematic of this unit is shown in figure 60 and a photograph of it is shown in figure 61 This unit was designed to operate with the RUM receivers

The 12-kilocycle and 20-kilocycle voltages were developed across a trap circuit in the plate circuit of the type 6SQ7 tube in the RUM receiver and fed to the inputs of the 12-kilocycle band-pass filter and the 20-kilocycle high-pass filter

which were connected in parallel

The response of the 12-kilocycle and 20-kilocycle filters is shown in figure 62 The outputs from each of these filters were coupled to type 12SQ7 tubes which operated as triode amplifiers and diode detectors The demodulated voice in the 20-kilocycle crannel and the demodulated 1020-cycle range signals in the 12-kilocycle channel were each amplified by type 12SN7 tubes with both triode sections connected in parallel The output of each channel was fed to the headphones through a matching transformer The over-all output response for the complete transmitting and receiving system when this unit was used is shown in figure 63

Subcarrier Amplifier-Detector Unit - System No 3

A schematic of this unit is shown in figure 64 and a photograph of it is shown in figure 65 The unit was very simple and light in weight This unit was coupled to the 20-kilocycle tuned circuit in the plate of the 6SQ7 in the RUM receiver This unit demodulated the 20-kilocycle subcarrier and used a type 6AG7 tube that acted as a grid leak power detector The output was coupled to the headphones through a matching transformer The audio response curve of the over-all system using this unit is shown in figure 63

Band-Pass Band-Rejection Filter

Systems Nos 1, 4, and 5 used a band-pass, band-rejection filter to separate the voice and range signals The filter used was a standard aircraft filter unit used with the low-frequency ranges The response of this unit is shown in figure 66

TESTS

Ground Measurements of Radiated Patterns

In order to obtain the correct field patterns, it was necessary to make experimental ground measurements The correct current ratio was set up in each group of antennas with the aid of radio-frequency current indicators which clamped on to the antenna elements Phasing between the side antennas and the center antenna was accomplished in the manner described under Theoretical Discussion

When all of the adjustments had been completed, the shapes of the field patterns were determined by taking measurements on the ground at a radius of 200 feet from the antenna system Measurements were made with a portable field intensity meter similar to that used for instrument landing system measurements [15] Figure 67 shows the pattern obtained when only the center loop was driven The pattern deviates from a circular shape by approximately ± 15 percent due to a slight unbalance in the antenna elements and the presence of the other four loop radiators

The pattern obtained when only the side visual loops were excited is shown in figure 68 The resultant bean patterns obtained when all three visual antennas were excited are shown in figure 69 The resultant patterns obtained when the aural antennas were energized are shown in figure 70 The patterns agree fairly well with theory, the biggest discrepancy occurring in the amplitude of the minor lobes This was primarily due to the fact that it was not possible to read the field intensity meter accurately at the low end of the scale

The field patterns shown are those taken with system No. 2 which are representative of all the systems

---

[15] See reference 6, page 9

Distortion Tests

Extensive distortion and cross-modulation tests were conducted on systems Nos 2, 3, 4, and 5 to determine the quality of the signals provided by the aural range and voice channels For these tests the normal 90-150-cycle frequencies were applied to the visual channel, the 1020-cycle tone was applied to the range channel, and a frequency of 1500 cycles was applied to the voice channel A type RUM receiver was installed at the Experimental Station and connected to a loop antenna mounted on the roof of the Experimental Station The receiver installation was identical to that used on aircraft The receiving antenna was located approximately midway between the north aural and the east visual courses in the 150-cycle visual sector and the "D" aural sector The results of these tests are shown in table III System No 5 provided signals with the least distortion The distortion frequencies $p \pm q$ (870, 1170, 1350 and 1650 cycles) were less than 2 9 percent and had an average value of 1.7 percent The distortion terms caused by the 90-cycle frequency were not present because the receiver was located in the 150-cycle sector. The cross-modulation was highest in the range channel where 8 5 percent of 1500 cycles was observed The distortion observed in the other systems was only slightly more than that for system No. 5 The largest amount of distortion was observed in the voice channel of system No 3 where exact phasing of the 20-kilocycle sidebands was not accomplished

With further development, all of these systems could be made to give equivalent performance with respect to the quality of the various signals

Aircraft Antenna Tests

A loop antenna of the type shown in figure 71 was used in the first part of the flight tests During the course of the flight work, another type of antenna was proposed in an effort to decrease the aerodynamic drag. This antenna consisted of a half-wave dipole bent around to form a "V." Figure 72 shows this V antenna mounted on the tail of NC-11 The antenna consisted of two rods 26 2 inches long and mounted with an included angle of 80° The antenna was fed with 90-ohm line tapped out 5 8 inches from the apex

The V antenna possessed several advantages over the loop antenna previously used. Its aerodynamic drag was considerably less than that of the loop while its gain was approximately 3 db higher Because of its smaller size it was possible to mount the V antenna on top of the vertical stabilizer and thus reduce the noise background in the receiver since the antenna was located farther away from the engine ignition system This location improved the signal-to-noise ratio by approximately 3 db

The field pattern of the V antenna is not as circular as that of the loop antenna[16] since it pulls in slightly at the sides, as may be seen from figure 73 The measured pattern was obtained on the ground with a V antenna mounted on a pole one-half wavelength above ground. The calculated pattern was obtained from the equation which was derived in Appendix VI The fact that the pick-up at the sides is not so great as that directly in line with the antenna is considered an advantage since reception is usually in line with the apex of the V

One reason for the increased gain of the V antenna over the loop antenna is its higher radiation resistance. Theoretically, in free space, the two antennas would have almost equal efficiency in the direction of maximum pick-up However, it is much more difficult to build an efficient matching circuit for the loop antenna, since its radiation resistance is only about 10 ohms The radiation resistance of the V antenna is about 37 ohms, so that much less difficulty is encountered in matching it efficiently to the transmission line The location of the V antenna high above the skin of the ship further improved the antenna gain

---

[16]Andrew Alford and A G Kandoian, "Ultra-High-Frequency Loop Antennas," AIEE Transactions, Vol 59, pp 843-848, 1940

TABLE III

MODULATION CONDITIONS AND THE RESULTS OF DISTORTION TESTS ON SYSTEMS NOS 2, 3, 4 AND 5

RANGE NO	MODULATION CONDITIONS	PERCENT MODULATION		
		EACH VISUAL	AURAL	VOICE
2	Voice on 20-kc subcarrier Aural range on-12 kc subcarrier Visual range on main carrier	20.0	14 5	33 0
3	Voice on 20-kc subcarrier Aural range on main carrier Visual range or main carrier	25 0	5 0	13 0
4	Voice on main carrier Aural range on main carrier Visual range on main carrier	25 0	5.0	25 0
5	Voice on main carrier Aural range on main carrier Visual range on main carrier	15 65	5 4	24 0

RANGE NO	PERCENT OF UNDESIRED RESPONSE REFERRED TO THE DESIRED FREQUENCY OF 1020 CYCLES							PERCENT OF UNDESIRED RESPONSE REFERRED TO THE DESIRED FREQUENCY OF 1500 CYCLES							EXTERNAL FILTER (COMBINATION LP-BP-BE)
	% 150	% 870	% 1020	% 1170	% 1350	% 1500	% 1650	% 150	% 870	% 1020	% 1170	% 1350	% 1500	% 1650	
2	1.9	7 4	100.0	5 8	--	--	--	9 7	--	15 8	--	3 5	100 0	4 2	NONE USED
3	202 0	14 9	100 0	10 6	--	--	--	33 3		11 4		17 6	100 0	16 6	WITHOUT
	0 006	6 0	100 0	1 9	--	--	--	None used in voice channel							WITH
4	216 0	15.9	100 0	12 5	8 2	159 0	3 1	136 0	10 0	62 8	7.8	5 1	100 0	1.9	WITHOUT
	0 007	6.3	100.0	2 2	0 3	2 8	0 003	5 2	3 0	0 3	2 4	4.3	100.0	2 0	WITH
5	194.0	4 0	100 0	3 9	16 4	477 0	7 5	40 6	0.08	20 9	0 08	3 4	100 0	1.6	WITHOUT
	0 006	1 6	100 0	0.7	0 6	8 5	0 5	1 5	0 02	0 09	0 02	2.9	100 0	1 7	WITH

Measurements taken in the 150-cycle sector of the visual channel with 1500 cycles applied to the voice channel and 1020 cycles applied to the aural channel

Figure 74 shows the actual patterns of both the loop and the V antennas. These patterns were obtained by flight tests with the aircraft in horizontal flight and at various angles of bank.

Aircraft Installation

Some of the early flight tests on the non-simultaneous system were made in a single-engine airplane, a Waco Model N However, most of the tests were made in a Model 247-D Boeing, NC-11 The interior of NC-11 was modified to provide ample space for mounting several units of equipment to be tested, and a duplicate set of the necessary flight instruments was provided in the cabin These duplicate instruments are all mounted on one panel and are located so that they may be seen by the flight engineer or by any observers who are participating in the flight demonstrations Figure 75 shows the interior of NC-11 as arranged for flight tests on the radio range equipment The duplicate flight instrument panel is mounted in the center of the work bench and contains the crossed-pointer instrument which is connected in parallel with a similar instrument used by the pilot for flying the range system, an altimeter, an airspeed indicator, a gyro compass, a rate of climb indicator, an accelerometer, three marker indicators, and two instruments not required for these tests The Western Electric type 32A receiver is mounted on a shelf directly under the bench at the left side of the photograph. The type RUM receiver is mounted at the same level and is shown in approximately the center of the photograph The auxiliary detector-amplifier and filter units are mounted to the right of the marker receiver which is located adjacent to the type RUM receiver The Esterline-Angus recorders and the d-c amplifier are mounted directly below the 32A receiver, and a gyro recording device is located directly below the RUM receiver The controls for the 32A receiver are shown to the left of the door to the cockpit Figure 76 shows the crossed-pointer instruments mounted in the cockpit The lower section of the instrument face is colored blue and yellow with the dividing line at the center of the instrument These colors indicate whether the airplane is located north or south of the range course In this installation the airplane was located north of the course when the vertical needle of the indicator pointed to the blue side, and south of the course when the indicator pointed to the yellow side In flight, the pilot navigates to keep the vertical needle centered along the vertical dots on the face of the instrument The aural range is used in the same manner as the present low-frequency ranges except that D and U are used instead of N and A as interlocking signals With the combination of the aural and the visual signals, the pilot is able to determine immediately in which quadrant of the range he is flying For example, if he heard the letter D from the aural system and the visual indicator pointed at the blue sector of the instrument, the airplane would be located northeast of the range station Similarly, the combinations U and blue indicate northwest, U and yellow indicate southwest, and D and yellow indicate southeast

Figure 77 is a block diagram showing the receiving installation in NC-11 that was used for the greater part of all flight tests on all of the systems The tuning box for transferring from dual to single conductor transmission line was necessary because of the fact that the type RUM receiver was constructed with a single conductor unbalanced input circuit When the type 32A receiver was used, the tuning box was eliminated and the dual line connected directly to the 32A balanced input circuit.

Both visual and aural recordings were made simultaneously during all flight tests Two Esterline-Angus Model AW, 0-5 milliampere, graphic recorders were used The General Radio type 715AE d-c amplifier was used to provide sufficient amplification of the direct current in the meter circuit so that full-scale recordings would equal approximately full-scale indications of the crossed-pointer instruments For these tests the recorder was adjusted so that zero signal would indicate on the center of the recorder chart, thereby making it possible to record right and left indications The d-c amplifier was balanced to indicate at the center of the chart when the airplane was on course and equal 90- and 150-cycle frequencies were obtained All recordings of the visual system were calibrated to show the magnitude of amplification This calibration was accomplished by marking the record when the vertical needle of the crossed-pointer instrument was deflected to the wing tip of the miniature airplane, three dots and four dots in either direction Figure 76 shows the miniature airplane and dots on the face of the instrument The distance from the center of the scale to the wing tip of the

miniature airplane is equal to the space between two dots Therefore, the first and second dots beyond the miniature airplane were considered three dots and four dots, respectively Visual course width was measured in terms of a pointer deflection of four dots right to four dots left, three dots to three dots and wing tip to wing tip

An amplifier was placed in the output of the aural channel of the receiving equipment to provide sufficient amplification to make the aural recorder indicate at least one-third full-scale amplitude With this degree of amplification course characters (D or U) may be recorded near the course when they can no longer be distinguished in the phones During cross-course tests on the aural system, the recording was marked where the last character was heard going into the course and the first character heard coming out of the course. The distance between these marks was used to compute the course width

Flight tests

The results of flight tests on all of the radio range systems were substantially the same and typical recordings of various systems are included

One of the first flight tests made on each system consisted of circling the station at a 2-mile radius recording both the visual and the aural signals These records show the general shape of the radiated patterns, the amount of clearance and the quality of the aural and visual courses Actual flight recordings for this test are shown in figure 78 The effect of minor lobes is clearly shown in this figure in the recording of the aural signal where the minimum signal midway between each aural and visual course does not reach zero on the chart This provides an indication of clearance The clearance shown in figure 78, however, is more than ample A slight indication of minor lobes is shown on the visual recording where there is a tendency for less than maximum signal near the south aural course Clearance of the visual signal is considered ample when the vertical pointer of the instrument does not indicate less than full scale at intermediate points between the courses System No 2 provided field patterns that had much more clearance than that for system No 5 This is shown in figure 79 In this figure the gain of the d-c amplifier was reduced so that the recorded visual signal would remain within the chart area and provide a means of determining if there was any tendency for the indicator to return at off-course points No noticeable tendency can be observed on the record. It will also be noted that the minimum of the aural signal never deviated from zero at off-course points This indicates that the minor lobes were negligible in system No 2 Since the antenna spacing and current ratio for systems Nos 2 and 5 were identical, the difference between the recorded signals of the two systems could have been made negligible by further adjustment of the antenna system for system No. 5

Flight recordings of the visual signal of system No 5 were made while crossing each visual course at right angles and are shown in figure 80 The west course is slightly worse than the east course with respect to roughness of the recorded signal This roughness, however, is barely noticeable on the cross-pointer instrument because of the relatively low amplitude Both courses were considered extremely good and easy to fly on course Before these flight recordings were made it was necessary to adjust the 90-150-cycle filter input voltage in the receiver until the desired course width was obtained It is possible to vary the resulting course width over a very wide range merely by varying the filter input voltage Early flight tests indicated that courses having 20° of total width from four dots to four dots on the visual indicator provided optimum results for airway flying since the courses were sufficiently accurate and easy to fly During these early tests it was found that the filter input potential should be 25 volts to provide 20° courses. This potential was maintained during all of the final flight tests for all systems

During the demonstration of the non-simultaneous system to the Air Line Pilots Association, some flight tests were conducted to determine visual course width at considerably higher altitudes than those used for the greater part of the tests Flight tests were made up to 17,000 feet above the station The results of these tests are shown in figure 81 The course broadened appreciably below an altitude of 3000 feet above the ground at a distance of 17 miles due to rapidly decreasing signal These

tests were made using the loop-type receiving antenna Above an altitude of 3000 feet the course broadened approximately 38 percent at 12,000 feet Later tests on simultaneous system No 5 indicated an increase in width of approximately 10 percent from 3000 to 12,000 feet This conflicts with the earlier Air Line Pilots Association tests and may be due to the different transmitting antenna systems The non-simultaneous system used two center antennas and system No 5 used one antenna

Copies of cross-course recordings made on the north and south aural courses are shown in figure 82 Courses having a width of approximately 1° were obtained These courses are very smooth and easy to fly No multiple courses or tendencies toward multiple courses were observed aurally or noted on the recording Flight tests on some of the early ultra-high-frequency ranges indicated "pushing" effects when flying across the course and when circling near the course This pushing effect was evidenced by apparent displacement of the course for different directions of flight With this effect it was quite difficult to locate the true course and maintain flight on course Bracketing of the course was particularly difficult

When the non-simultaneous range was first installed, pushing was observed on the aural courses and not on the visual courses The antennas which produced the visual course were one-half wavelength above the counterpoise, and the antennas which produced the aural course were three-eights of a wavelength above the counterpoise When the aural antennas were placed one-half wavelength above the counterpoise, pushing effects disappeared It is probable that the pushing was caused by excessive currents flowing in the counterpoise which radiated vertically polarized waves

No pushing was observed when the V or loop antenna was used in level flight on any of the simultaneous systems tested However, a slight amount of course displacement was observed when circling close to the course in a 30° bank using the loop antenna This effect is probably due to the shielding effect of the wing on the direct signal and not to the type of antenna used

Figure 83 shows copies of flight recordings taken while flying away from the station on both the west visual and the south aural courses These records indicate the ease with which the pilot was able to follow the visual and aural courses since the visual record barely deviated from zero-center on the chart and the aural record shows very little trace of off-course characters

Several tests were made on the cone area over the station at altitudes from 1000 to 12,000 feet with and without the suppressor system energized Figure 84 shows samples of recordings taken at an altitude of 3000 feet The cone area without the suppressor system operating is described as that area above the station where abnormal movement of the visual indicator and abnormal fluctuations in the intensity of the aural signal are observed As indicated on the recordings, the suppressor acts to stabilize the visual indicator and provides a definite aural cone-of-silence over the station The results of the cone area tests are shown graphically in figure 85 The area of abnormal fluctuation of the meter pointer on the visual courses without the suppressor was identical to that of the zero signal area with the suppressor operating The width of the area of abnormal fluctuations in signal intensity on the aural courses without the suppressor is the same as the width of the zero signal area with the suppressor The width of the cone area of the aural signal along the visual courses with the suppressor operating is expressed in terms of zero signal and 10 db down from the normal signal on course The cone-of-silence is considerably larger than the area of abnormal fluctuation in signal intensity without the suppressor Similarly, the cone area of the visual signal along the aural courses with the suppressor operating is expressed in terms of zero signal and three dots to three dots Both cone areas are considerably wider than the cone of abnormal meter fluctuation without the suppressor

The results of the flight tests made to determine course widths and cone widths for all systems are shown in table IV Visual course widths are given in terms of four dots to four dots, three dots to three dots, and wing tip to wing tip, while the cone areas are shown with and without the suppressor system operating Cone areas are shown for both 3000 and 12,000 feet above the station when the suppressor is energized Course-width data for system No 5 have been applied to the map in figure 86 The

miniature airplane and dots have been included to show the relative areas covered in actual flight on the visual courses When flying the visual courses, it is easily possible to keep the visual indicator within the center portion of the miniature airplane with a resulting apparent course width of approximately 1 5° The width of the aural courses is approximately 1° It is possible to fly these courses with an accuracy of plus or minus 1°.

During the demonstration of the non-simultaneous system to members of the Air Line Pilots Association, some tests were also made to determine cone width as well as course width at various altitudes. Figure 87 shows the visual courses and cone width measured during these tests at an altitude of 12,000 feet above the station. At any point within the area of the curve the visual pointer will not indicate more than three dots on the instrument. The size of the cone area is determined by the relative power of the suppressor system compared to that of the range antenna system and is considered to be excessively large in this case A similar curve is shown in figure 88 for system No. 5 where the cone area for three dots deflection has been considerably reduced to provide more accuracy in determining position and still maintain ease of flight over the station The variation of course width with altitude has also been considerably reduced

Tests were conducted on all systems to determine the distance range at an altitude of 1000 feet above the station Some of the tests were made with both a loop and a V receiving antenna The results of these tests are shown in table V In this table the relative carrier powers and percentages of modulation have been included to assist in judging the merit of the various systems System No 5 provided the best coverage due primarily to the increased carrier power and the gain acquired through the use of the V antenna With this system, a distance range of 48 miles was obtained where optical line of sight is 45.7 miles The same distance range was obtained with all services of a given simultaneous system

During the tests made to determine the distance range of the various systems, recordings were also made of the receiver avc current in order to determine the vertical field pattern of the transmitting antenna system. The data obtained from the recording for system No 5 are shown in figure 89 The avc current was then transposed to relative field intensity in microvolts by means of a calibration curve for the receiver of avc current versus input in microvolts Figure 90 shows the vertical field pattern obtained from these data Without a counterpoise and assuming perfect reflection, a total of nine maxima should occur at 0 04, 0 11, 0 17, 0.23, 0 31, 0 43, 0.63, 1 08 and 3 28 miles from the station at an altitude of 1000 feet Similarly, a total of eight minima should occur at 0 08, 0 14, 0 20, 0 27, 0 36, 0 51, 0 80 and 1.63 miles from the station at an altitude of 1000 feet However, the counterpoise effectively eliminates all but the last two maxima at 1 08 and 3 28 miles, as well as all but the last minima at 1 63 miles Partial elimination of the minima at 0 80 miles is also accomplished

Avc current curves such as that shown in figure 89 also provide an effective means of determining the distance range In the case of the simultaneous systems where comparatively low percentages of modulation are used, the limit of usability of the range system occurs at the point where the avc current reaches its maximum value This point occurs at a distance of 48 miles from the station for system No 5 and coincides exactly with the distance range determined by observation of the aural and the visual signals When the percentage modulation is increased, however, the limit of usability of the system occurs beyond the point where the avc curve flattens off

CONCLUSIONS

As a result of this development, the following conclusions are drawn

1 An ultra-high-frequency two-course visual radio range with sector identification has been developed The Radio Technical Commission for Aeronautics, the Air Line Pilots Association, and other groups of pilots have thoroughly tested this type of range and have unanimously preferred it to the four-course aural range This selection was brought about by the simplified system of navigation which continuously

TABLE IV

COURSE AND CONE WIDTHS

COURSE WIDTHS	NON-SIMULTANEOUS SYSTEM AND SYSTEMS NOS 3, 4, 5	SYSTEM NO. 2
WIDTH OF VISUAL COURSES AT 3,000 FEET (4 DOTS TO 4 DOTS)	17 7°	21 1°
WIDTH OF VISUAL COURSES AT 3,000 FEET (3 DOTS TO 3 DOTS)	12.3°	13 6°
WIDTH OF VISUAL COURSES AT 3,000 FEET (WING TIP TO WING TIP)	7.2°	7 6°
FILTER VOLTS FOR VISUAL COURSE MEASUREMENTS WITH TYPE RUM RECEIVER.	25 VOLTS	25 VOLTS
WIDTH OF AURAL COURSES AT 3,000 FEET	0 9°	1 1°
WIDTH OF AURAL COURSES AT 12,000 FEET	1 0°	
WIDTH OF CONE AREA WITHOUT SUPPRESSOR		
VISUAL CONE ALONG VISUAL COURSES AT 3,000 FEET	4,000 FEET	3,560 FEET
VISUAL CONE ALONG AURAL COURSES AT 3,000 FEET	0 FEET	1,400 FEET
AURAL CONE ALONG AURAL COURSES AT 3,000 FEET	2,160 FEET	3,360 FEET
AURAL CONE ALONG VISUAL COURSES AT 3,000 FEET	1,140 FEET	2,340 FEET
WIDTH OF CONE OF SILENCE WITH SUPPRESSOR		
VISUAL CONE ALONG VISUAL COURSES AT 3,000 FEET	4,000 FEET	
VISUAL CONE ALONG AURAL COURSES AT 3,000 FEET	1,700 FEET	
AURAL CONE ALONG AURAL COURSES AT 3,000 FEET	2,200 FEET	
AURAL CONE ALONG VISUAL COURSES AT 3,000 FEET	3,200 FEET	
VISUAL CONE ALONG VISUAL COURSES AT 12,000 FEET	20,900 FEET	
VISUAL CONE ALONG AURAL COURSES AT 12,000 FEET	7,300 FEET	
AURAL CONE ALONG AURAL COURSES AT 12,000 FEET	8,500 FEET	
AURAL CONE ALONG VISUAL COURSES AT 12,000 FEET.	12,600 FEET	

TABLE V

DISTANCE RANGE OF THE VARIOUS SYSTEMS

SYSTEM NO.	CARRIER POWER IN CENTER ANTENNA	MODULATION ON COURSE IN PERCENT			DISTANCE RANGE IN MILES AT AN ALTITUDE OF 1000 FEET	
		AURAL	VISUAL	VOICE	LOOP ANTENNA	V ANTENNA
NON-SIMULTANEOUS	150	3	60	—	46	—
1	150	2	40	33	22	—
2	75	14.5	40	33	21	34
3	90	5.0	50	13	24	38
4	90	5.0	50	25	25	39
5	240	5 4	31	24	—	48

and positively identifies each of the four quadrants and also by the use of visual indication for flying the airways. As a result of this work, it has been decided to install facilities using these basic principles on a universal basis throughout the Federal Airways

2. The simultaneous voice feature has been added to this type of range to provide weather information and airway traffic control without sacrificing any of the basic features of the original system.

3. A simplified transmitting antenna system has been developed, and several satisfactory methods of providing simultaneous voice have been tested. Systems Nos 1, 2, 3 and 4 provide the ultimate in stability at a large sacrifice in efficiency, whereas system No 5 provides a sufficient degree of stability at a very much higher over-all efficiency.

4. Numerous tests with subcarrier modulation have shown that it is satisfactory for aircraft use although it requires additional transmitting and receiving equipment. If it becomes necessary to add another voice channel or communication chan nel to the radio range facility in the future, subcarrier modulation offers a satisfactory solution to this problem.

5 The optimum shape of visual and aural patterns has been determined theoretically and confirmed by tests.

6 The optimum visual course indicator sharpness for airway flying was found to be full-scale deflection (35° pointer deflection) for 10° deviation from the center of the course.

7. During the course of this development, an improved u-h-f aircraft receiving antenna was used which is known as the V antenna. This antenna has several advantages over the-loop antenna previously used in that it has a greater pickup, less aerodynamic drag, and better broad-band characteristics. Furthermore, it was possible to locate the antenna on the top of the vertical stabilizer, which permitted excellent signal pickup and simultaneously reduced the ignition interference

APPENDIX I

Tuning of Antennas for Non-Parasitic Operation

The length of line θ_3 which will prevent parasitic current can readily be calculated by considering the equivalent circuit. To simplify matters, the case of a half-wave dipole will be assumed Figure 91A shows the schematic of the antenna as it appears when acting parasitically. The reason for the virtual short at the end of θ_3 is explained in the text.

The antenna may be replaced by a generator and impedance, as shown in figure 91B, the induced voltage being equal to the product of the current in the exciting antenna by the mutual impedance, and the generator impedance being equal to the self-impedance of the antenna. The circuit of figure 91B may be further simplified to that of figure 91C where X_T is the equivalent reactance of the transmission lines, θ_1, θ_2, and θ_3. The parasitic current is then given by:

$$I_p = \frac{-I_o \ Z_M}{Z_S + X_T}$$

In order for the parasitic current to be zero, either the numerator must be zero or the denominator must approach infinity. The first condition can be obtained only by reducing the mutual impedance to zero, which means that the spacing between the two antennas must be made very great This is obviously an impossible condition, so the denominator must be made very large. Since θ_3 is the only quantity which can be varied, its length must be so adjusted that the impedance which the center of the antenna looks into is very large. This impedance consists of two shorted transmission line sections in parallel connected through another length of transmission line. If we let X_2 and X_3 be the reactance of lines θ_2 and θ_3, respectively, then the reactance reflected into the center of the antenna is

$$X_T = Z_o \left[\frac{\frac{X_2 \ X_3}{X_2 + X_3} + j Z_o \tan \theta_1}{Z_o + j \frac{X_2 \ X_3}{X_2 + X_3} \tan \theta_1} \right]$$

In order for the above expression to become infinite, the denominator must become equal to zero

$$Z_o + j \frac{X_2 \ X_3}{X_2 + X_3} \tan \theta_1 = 0$$

Substituting $X_2 = j \ Z_o \tan \theta_2$

$$X_3 = j \ Z_o \tan \theta_3$$

and simplifying, we obtain

$$\tan \theta_2 + \tan \theta_3 - \tan \theta_1 \tan \theta_2 \tan \theta_3 = 0$$

solving for $\tan \theta_3$

$$\tan \theta_3 = \frac{\tan \theta_2}{\tan \theta_1 \tan \theta_2 - 1}$$

The above result is true only for half-wave radiators but will give the order of magnitude and direction of variation for other antennas For the antennas actually used in this development, θ_3 had a value which was very close to 180°

APPENDIX II

Optimum Design for Radio-Frequency Bridges

Several radio-frequency bridges, constructed of transmission line elements, are used in all of the ranges described in this report Although these bridges will perform their function when they are constructed with elements of any arbitrary length, it is convenient if the bridges introduce no mismatch when connected into the associated circuits.

Referring to figure 92A, the bridge is used to combine two voltages of the same frequency into a single antenna. When power is fed in at points A A', it is desired that no voltage appear at points C C' In order to obtain this condition, the bridge elements should all be of the same length and the impedance at D D' should equal that at B B' Assuming that the bridge elements are constructed of the same transmission line as that used in the rest of the system, it is desired that the impedance looking into A A' be Z_o when points B B' look into the characteristic impedance Z_o.

To meet this condition, the impedance of each half of the bridge should be equal to 2 Z_o

$$Z_{A\ A'} - B\ B' - C\ C' = Z_{A\ A'} - D\ D' - C\ C' = 2\ Z_o$$

Thus, when the two halves of the bridge are connected, the impedance at A A' will equal Z_o The length, θ, of each element can be solved for as follows

When voltage is applied at A A'

$$E_{C\ C'} = 0 \text{ (assuming the bridge is balanced)}$$
$$\text{then } Z_{C\ C'} = 0$$
$$\text{and}$$
$$Z_{BB'-CC'} = j\ Z_o \tan\theta$$

The impedance at $Z_{BB'}$ consists of two parallel impedances, the antenna load, Z_o, and a shorted transmission line of length, θ.

$$Z_{BB'} = \frac{(Z_o)\ (j\ Z_o \tan\theta)}{Z_o + j\ Z_o \tan\theta}$$

Rationalizing,

$$Z_{BB'} = \frac{j\ Z_o \tan\theta + Z_o \tan^2\theta}{1 + \tan^2\theta}$$

Referring to figure 92B, it can be seen that $Z_{BB'}$ is the receiving end impedance of bridge element A A' - B B' The sending end impedance can be found from the relation

$$Z_s = Z_o \left[\frac{Z_r + j\ Z_o \tan\theta}{Z_o + j\ Z_r \tan\theta}\right]$$

Where Z_s is the sending end impedance and Z_r is the receiving end impedance, Z_s is then set equal to 2 Z_o, Z_r is set equal to $Z_{BB'}$, and the equation is solved for θ.

$$2\ Z_o = Z_s = Z_o \left[\frac{\dfrac{j\ Z_o \tan\theta + Z_o \tan^2\theta}{1 + \tan^2\theta} + j\ Z_o \tan\theta}{Z_o + j \left(\dfrac{j\ Z_o \tan\theta + Z_o \tan^2\theta}{1 + \tan^2\theta}\right)(\tan\theta)}\right]$$

$$Z=\frac{j\,Z_o \tan\theta + Z_o \tan^2\theta + (j\,Z_o \tan\theta)\,(1+\tan^2\theta)}{Z_o + Z_o \tan^2\theta + (j \tan\theta)\,(j\,Z_o \tan\theta + Z_o \tan^2\theta)}$$

Cross multiplying and reducing

$$2 + j \tan^3\theta = j\,2 \tan\theta + \tan^2\theta$$

equating the real terms

$$2 = \tan^2\theta$$

$$\theta = \tan^{-1}\sqrt{2} = 54.7^\circ \qquad \theta = \beta L$$

$$L = 0.152\,\lambda \qquad \beta = \frac{2\pi}{\lambda}$$

APPENDIX III

The Effect of Phase Shift Between Carrier and Sidebands of an Amplitude-Modulated Wave on the Quality of Received Signals

The purpose of this appendix is to analyze the effect of phase shift between carrier and sidebands of an amplitude-modulated wave on the quality of the received signals, using square-law and linear detection. The treatment given below is not concerned with phase modulation whereby the phase of the modulation frequency is varied harmonically.

(1) Square-Law Detection

Let a carrier of frequency $\omega/2\pi$ be modulated by two frequencies $p/2\pi$ and $q/2\pi$. The instantaneous voltage e is

$$e = E(1 + m_1 \cos pt + m_2 \cos qt) \cos \omega t \tag{1}$$

where E = carrier amplitude

m_1 = modulation factor for frequency $p/2\pi$

m_2 = modulation factor for frequency $q/2\pi$

Introducing a phase shift ϕ between carrier and sidebands in equation (1) gives

$$e = E\left[\cos \omega t + (m_1 \cos pt + m_2 \cos qt) \cos(\omega t + \phi)\right] \tag{2}$$

$$e = E\left[\cos \omega t + \frac{m_1}{2}\cos\left\{(\omega \pm p)\,t + \phi\right\} + \frac{m_2}{2}\cos\left\{(\omega \pm q)\,t + \phi\right\}\right] \tag{3}$$

Assuming the detector characteristic

$$i = a_o + a_1 e + a_2 e^2 \tag{4}$$

and neglecting constant terms and terms involving the carrier frequency, we find

$$i = a_2 E^2\left[\frac{m_1}{2}\cos(pt \pm \phi) + \frac{m_2}{2}\cos(qt \pm \phi) + \frac{m_1 m_2}{2}\cos(p \pm q)\,t + \frac{m_1^2}{4}\cos 2pt + \frac{m_2^2}{4}\cos 2qt\right] \tag{5}$$

By a further transformation, the first two members in the parentheses of equation (5) are changed giving

$$i = a_2 E^2 \left[\begin{array}{l} m_1 \cos pt \cos \phi + m_2 \cos qt \cos \phi \\ + \frac{1}{4} \left\{ 2m_1 m_2 \cos (p \pm q)\ t + m_1^2 \cos 2pt + m_2^2 \cos 2qt \right\} \end{array} \right] \qquad (6)$$

Consideration of equation (6) shows that the amplitude of the desired terms (of radian frequencies p and q) varies with the cosine of the phase shift angle ϕ. The distortion terms $(p \pm q)$, 2p, 2q are not affected by the phase shift. Therefore, with increasing phase shift, the relative amount of distortion increases. For $\phi = \pi/2$ the desired terms disappear.

(2) Linear Detection

Starting from equation (2) and calling

$$A = m_1 \cos pt + m_2 \cos qt \qquad (7)$$

we obtain

$$e = E \left[\cos \omega t + A \cos (\omega t + \phi) \right] \qquad (8)$$

The problem of linear detection is to find the envelope of the carrier in terms of the component frequencies.

The expression for the carrier envelope is that part of the voltage equation which remains after factoring out the carrier frequency

$$e = E \left[1 + A^2 + 2A \cos \phi \right]^{\frac{1}{2}} \cos (\omega t + \psi) \qquad (9)$$

where $\tan \psi = \frac{A \sin \phi}{1 + A \cos \phi}$ (see figure 93) (10)

Binomial expansion of the form $(1 + X)^{\frac{1}{2}}$ gives

$$(1 + X)^{\frac{1}{2}} = 1 + \frac{1}{2}X - \frac{1}{8}X^2 + \frac{1}{16}X^3 - \qquad (11)$$

$$\text{let } X = A^2 + 2A \cos \phi \qquad (12)$$

From equation (9) we have

$$(1 + A^2 + 2A \cos \phi)^{\frac{1}{2}} = \left[1 + \frac{1}{2}(A^2 + 2A \cos \phi) \right. \qquad (13)$$

$$\left. - \frac{1}{8}(A^4 + 4A^2 \cos^2 \phi + 4A^3 \cos \phi) + \right]$$

$$= 1 + \frac{A^2}{2} + A \cos \phi - \frac{A^4}{8} - \frac{A^2}{2} \cos^2 \phi - \frac{A^3}{2} \cos \phi +$$

$$= 1 + A \cos \phi + \frac{A^2}{2} \sin^2 \phi \underbrace{- \frac{A^3}{2} \cos \phi - \frac{A^4}{8} +}_{\text{neglect}}$$

Entering equation (7) into (13) gives for the envelope voltage e'

$$\frac{e'}{E} = \left[1 + (m_1 \cos pt + m_2 \cos qt) \cos \phi \right. \qquad (14)$$

$$\left. + \frac{1}{2} \sin^2 \phi \, (m_1^2 \cos^2 pt + m_2^2 \cos^2 qt + 2 m_1 m_2 \cos pt \cos qt) \right]$$

which upon transformation gives the final result

$$e' = E\left[\begin{array}{l} 1 + \frac{1}{4}\sin^2\phi\ (m_1^2 + m_2^2) \\ + \cos\phi\ (m_1 \cos pt + m_2 \cos qt) \\ + \frac{1}{4}\sin^2\phi\ (m_1^2 \cos 2pt + m_2^2 \cos 2qt \\ + \frac{1}{2} m_1 m_2 \sin^2\phi \cos (p \pm q)\, t \end{array}\right] \qquad (15)$$

The rectified current i is proportional to the envelope voltage e', the proportionality constant "a" being equal to the slope of the detector characteristic

$$i = a\, e' \qquad (16)$$

It will be observed that all the frequencies shown in equation (15) depend in their amplitude on the phase shift angle ϕ. For zero phase shift, there is no distortion present, but with increasing ϕ the amplitude of the distortion terms increases proportionally to $\sin^2\phi$, whereas the amplitude of the desired frequencies decreases proportionally to $\cos\phi$, as in the case of square-law detection.

At this point, it is well to examine the limits within which the theory as applied to the case of linear detection holds. From equations (7) and (8) there follows that

$$A < 1$$

$$m_1 + m_2 < 1 \qquad (17)$$

This however is not a sufficient restriction. The series given in equation (11) converges for $X < 1$ only. By equation (12) we have after introducing equation (7)

$$1 > A^2 + 2A\cos\phi = m_1^2 \cos^2 pt + m_2^2 \cos^2 qt + 2m_1 m_2 \cos pt \cos qt$$

$$+ 2\cos\phi\,(m_1 \cos pt + m_2 \cos qt)$$

Letting $\cos pt = 1 = \cos qt$ gives

$$(m_1 + m_2) + 2(m_1 + m_2)\cos\phi < 1 \qquad (18)$$

For $m_1 = m_2 = 0.2$ the inequality (18) is fulfilled for any value of ϕ. For small degrees of modulation, the theory holds for any phase shifts. However, it should be remembered that distortion terms involving harmonics higher than the second, and combination frequencies thereof, have been dropped by neglecting powers higher than A^2 in equation (13).

(3) Conclusions Applied to Double Modulation

To avoid distortion of the subcarrier frequencies and their sidebands, phase shifts between carriers and sidebands must be avoided. This is done by providing phasers at a suitable place between carrier and sideband generators. Also, voice sidebands and the carrier should be radiated from the center antenna only.

A good check on correct phasing suggests itself by inspection of equation (15). The terms of radian frequencies $(p \pm q)$, $2p$, $2q$, should disappear after the first linear detection; p and q designate subcarriers and their sideband frequencies.

APPENDIX IV

Square-Law Detection of Two Amplitude-Modulated Carriers

Let carrier amplitudes be E_1 and E_2 modulated m_1 and m_2 percent by radian frequencies p and q, respectively. The carriers have radian frequencies ω_1 and ω_2. Let the detector characteristic curve be

$$i = a_o + a_1 e + a_2 e^2 \tag{1}$$

The voltage impressed across the detector is

$$\begin{aligned} e &= E_1 (1 + m_1 \cos pt) \cos \omega_1 t + E_2 (1 + m_2 \cos qt) \cos \omega_2 t \\ &= E_1 \cos \omega_1 t + \frac{m_1}{2} \cos (\omega_1 - p) t + \frac{m_1}{2} \cos (\omega_1 + p) t \\ &+ E_2 \cos \omega_2 t + \frac{m_2}{2} \cos (\omega_2 - q) t + \frac{m_2}{2} \cos (\omega_2 + q) t \end{aligned} \tag{2}$$

Introducing equation (2) into (1) and collecting audio terms and terms involving only

$$(\omega_1 - \omega_2) = u \tag{3}$$

we obtain, using the transformation

$$2 \cos A \cos B = \cos (A + B) + \cos (A - B) \tag{4}$$

$$\frac{i}{a_2} = \left[\begin{array}{l} m_1 E_1^2 \cos pt + m_2 E_2^2 \cos qt \\ \quad + \left(\frac{m_1 E_1}{2}\right)^2 \cos 2pt + \left(\frac{m_2 E_2}{2}\right)^2 \cos 2qt \\ \quad + E_1 E_2 \left[\cos ut + \frac{m_1}{2} \cos (u \pm p)t + \frac{m_2}{2} \cos (u \pm q)t\right] \\ \quad + E_1 E_2 \frac{m_1 m_2}{4} \left[\cos (u - p \pm q)t + \cos (u + p \pm q)t\right] \end{array} \right] \tag{5}$$

Equation (5) was used to compute the numerical values of amplitudes given in table II. It is worth noting that if the two carriers are not modulated a distortionless heterodyne signal of frequency $\frac{u}{2\pi}$ is obtained with square-law detection.

APPENDIX V

Linear Detection of Two Amplitude-Modulated Carriers

Analysis of linear detection involves summation of infinite series which are functions of the degrees of modulation and the ratio of the carrier amplitudes. Using the same symbols as for square-law detection, the formulas are applicable as long as

$$K = \frac{E_1}{E_2} < \frac{1 - m_2}{1 + m_1} < 1 \tag{1}$$

Expression (1) states that the minimum of the r-f voltage envelope of the stronger carrier (E_2) must be greater than the maximum of the r-f voltage envelope of the weaker carrier (E_1). To facilitate selection of values of K, m_1 and m_2 for which the theory is applicable, expression (1) is rewritten as an equation

$$K_{max} = - \frac{1}{1 + m_1} m_2 + \frac{1}{1 + m_1} \tag{2}$$

Equation (2) represents a family of straight lines with K_{max} plotted as ordinate, m_2 as abscissa, and with m_1 as parameter (figure 29)

For convenience, the equations for computing E_p, E_q, E_{2p}, E_{2q} as given in Aiken's paper,[17] are reproduced below, and numerical results are shown in table II

$$\pi \frac{E_q}{E_2} = m_2 + \frac{K^2}{8} G_{20} a_{11} + \frac{K^4}{128} G_{40} a_{31} + \frac{K^6}{512} G_{60} a_{51} + \cdots \tag{3}$$

where $K = \frac{E_1}{E_2} < 1$

$$G_{20} = 2 + m_1^2$$

$$G_{40} = 2 + 6 m_1^2 + \frac{3}{4} m_1^4$$

$$G_{60} = 2 + 15 m_1^2 + \frac{45}{4} m_1^4 + \frac{5}{8} m_1^6$$

$$a_{11} = - \frac{2m_2}{\sqrt{1 - m_2^2}\left[1 + \sqrt{1 - m_2^2}\right]}$$

$$a_{31} = - \frac{3m_2}{(1 - m_2^2)^{5/2}}$$

$$a_{51} = - \frac{5m_2 (1 + \frac{3}{4} m_2^2)}{(1 - m_2^2)^{9/2}}$$

$$\pi \frac{E_p}{E_2} = \left(\frac{K^2}{8}\right) G_{21} a_{10} + \left(\frac{K^4}{128}\right) G_{41} a_{30} + \left(\frac{K^6}{512}\right) G_{61} a_{50} + \cdots \tag{4}$$

where

$$a_{10} = \frac{2}{(1 - m_2^2)^{\frac{1}{2}}}$$

$$a_{30} = \frac{(2 + m_2^2)}{(1 - m_2^2)^{5/2}}$$

$$a_{50} = \frac{2 (1 + 3m_2^2 + \frac{3}{8} m_2^4)}{(1 - m_2^2)^{9/2}}$$

$$G_{21} = 2 m_1$$

$$G_{41} = 4 m_1 (1 + \frac{3}{4} m_1^2)$$

$$G_{61} = 6 m_1 (1 + \frac{5}{2} m_1^2 + \frac{5}{8} m_1^4)$$

---

[17] See reference 13, page 22.

$$\pi \frac{E_{2q}}{E_2} = \left(\frac{K^2}{8}\right) G_{20}\, a_{12} + \left(\frac{K^4}{128}\right) G_{40}\, a_{32} + \left(\frac{K^6}{512}\right) G_{60}\, a_{52} + \qquad (5)$$

$$a_{12} = \frac{2m_2^{\,2}}{\sqrt{1 - m_2^{\,2}}\left[1 + \sqrt{1 - m_2^{\,2}}\right]^2}$$

$$a_{32} = \frac{3m_2^{\,2}}{(1 - m_2^{\,2})^{5/2}}$$

$$a_{52} = \frac{5}{2}\left[\frac{m_2^{\,2}\left(3 + \frac{m_2^{\,2}}{2}\right)}{(1 - m_2^{\,2})^{9/2}}\right]$$

$$G_{20} = 2 + m_1^{\,2}$$

$$G_{40} = 2 + 6\, m_1^{\,2} + \frac{3}{4} m_1^{\,4}$$

$$G_{60} = 2 + 15\, m_1^{\,2} + \frac{45}{4} m_1^{\,4} + \frac{5}{8} m_1^{\,6}$$

$$\pi \frac{E_{2p}}{E_2} = \left(\frac{K^2}{8}\right) G_{22}\, a_{10} + \left(\frac{K^4}{128}\right) G_{42}\, a_{30} + \left(\frac{K^6}{512}\right) G_{62}\, a_{50} + \quad .. \qquad (6)$$

$$G_{22} = \frac{m_1^{\,2}}{2}$$

$$G_{42} = m_1^{\,2}\left(3 + \frac{m_1^{\,2}}{2}\right)$$

$$G_{62} = \frac{15}{2} m_1^{\,2}\left(1 + m_1^{\,2} + \frac{m_1^{\,4}}{16}\right)$$

$$a_{10} = \frac{2}{(1 - m_2^{\,2})^{\frac{1}{2}}}$$

$$a_{30} = \frac{(2 + m_2^{\,2})}{(1 - m_2^{\,2})^{5/2}}$$

$$a_{50} = \frac{2\,(1 + 3\, m_2^{\,2} + \frac{3}{8}\, m_2^{\,4})}{(1 - m_2^{\,2})^{9/2}}$$

The expressions for the terms of radian frequencies ($p \pm q$) were taken from Vilbig.[18]

$$\frac{E_{p \pm q}}{E_2} = \frac{m_1 \frac{K^2}{4} \quad (m_2 + \frac{3}{4} m_2^3) + \qquad\qquad (7)}{m_2 \left[1 - \frac{K^2}{4} \left(1 + \frac{m_1^2}{2}\right) S_1 + \frac{K^4}{64} S_2 S_3\right]}$$

where

$$S_1 = 1 + \frac{3}{4} m_2^2 + \frac{5}{8} m_2^4 + \frac{35}{64} m_2^6 + \quad .$$

$$S_2 = 1 + 3 m_1^2 + \frac{3}{8} m_1^4$$

$$S_3 = 3 \left(1 + \frac{5}{2} m_2^2 + \frac{35}{8} m_2^4 + \frac{105}{16} m_2^6 + \quad \right)$$

APPENDIX VI

The case of a quarter-wave V antenna is calculated for the field intensity distribution in both the horizontal and the vertical planes In this analysis, a sinusoidal distribution of current is assumed The total field from the antenna is found by integrating the field from a series of differential lengths of antenna and considering the fact that both the magnitude and the space phase of the field due to the current flowing in the differential dipole vary as the total field is integrated over the length of the antenna

Referring to figure 94, the magnetic field from $d\ell_1$, and $d\ell_2$ at a great distance is given by the expressions

$$dH_1 = \frac{0\ 2\pi}{\lambda\ r_o} I\ d\ell_1 \sin \phi \cos \omega \left(t - \frac{r_1}{c}\right)$$

$$dH_2 = \frac{0\ 2\pi}{\lambda\ r_o} I\ d\ell_2 \sin \gamma \cos \omega \left(t - \frac{r_2}{c}\right)$$

The expression for the current is

$$I = I_o \cos \left(\frac{2\pi \ell}{\lambda}\right)$$

also

$$r_1 = r_o - \ell \cos \phi \qquad\qquad r_2 = r_o - \ell \cos \gamma$$

$$dH_1 = \frac{0\ 2\pi}{\lambda\ r_o} I_o \cos \left(\frac{2\pi \ell}{\lambda}\right) d\ell \sin \phi \cos \omega \left(t - \frac{r_o - \ell \cos \phi}{c}\right)$$

$$dH_2 = \frac{0\ 2\pi}{\lambda\ r_o} I_o \cos \left(\frac{2\pi \ell}{\lambda}\right) d\ell \sin \gamma \cos \omega \left(t - \frac{r_o - \ell \cos \gamma}{c}\right)$$

Expanding

$$dH_1 = \frac{0\ 2\pi}{\lambda\ r_o} I_o \cos \left(\frac{2\pi \ell}{\lambda}\right) d\ell \sin \phi \left[\cos \omega \left(t - \frac{r_o}{c}\right) \cos \left(\frac{\omega \ell \cos \phi}{c}\right)\right.$$

$$\left. - \sin \omega \left(t - \frac{r_o}{c}\right) \sin \left(\frac{\omega \ell \cos \phi}{c}\right)\right]$$

---

[18] F Vilbig, "Lehrbuch der Hockfrequenztechnik," Leipzig, 1939

$$dH_2 = \frac{0\ 2\pi}{\lambda\ r_o} I_o \cos\left(\frac{2\pi\ell}{\lambda}\right) d\ell \sin\gamma \left[\cos\omega\left(t - \frac{r_o}{c}\right)\cos\left(\frac{\omega\ell\cos\gamma}{c}\right) - \sin\omega\left(t - \frac{r_o}{c}\right)\sin\left(\frac{\omega\ell\cos\gamma}{c}\right)\right]$$

The total field is

$$dH = dH_1 + dH_2$$

$$dH = \frac{0\ 2\pi}{\lambda\ r_o} I_o\, d\ell \left\{\left[\cos\omega\left(t - \frac{r_o}{c}\right)\sin\phi\right]\left[\cos\left(\frac{\omega\ell\cos\phi}{c}\right)\cos\left(\frac{2\pi\ell}{\lambda}\right)\right]\right.$$

$$- \left[\sin\omega\left(t - \frac{r_o}{c}\right)\sin\phi\right]\left[\sin\left(\frac{\omega\ell\cos\phi}{c}\right)\cos\left(\frac{2\pi\ell}{\lambda}\right)\right]$$

$$+ \left[\cos\omega\left(t - \frac{r_o}{c}\right)\sin\gamma\right]\left[\cos\left(\frac{\omega\ell\cos\gamma}{c}\right)\cos\left(\frac{2\pi\ell}{\lambda}\right)\right]$$

$$\left. - \left[\sin\omega\left(t - \frac{r_o}{c}\right)\sin\gamma\right]\left[\sin\left(\frac{\omega\ell\cos\gamma}{c}\right)\cos\left(\frac{2\pi\ell}{\lambda}\right)\right]\right\}$$

The total field at any point can be found by integrating the above expression from the apex to the end of the antenna, that is, from 0 to $\lambda/4$. The expression could be used to determine the field from a V antenna any length L by changing the limits of integration from 0 to L and changing the term $\cos\left(\frac{2\pi\ell}{\lambda}\right)$ to $\sin\frac{2\pi(L-\ell)}{\lambda}$

However, the primary interest is the case where the elements are one-quarter wave long since a longer structure would be difficult to place on an airplane, in addition to the fact that nulls would appear in the field pattern

$$H = \frac{0.2\pi}{\lambda\ r_o} I_o \left\{\left[\cos\omega\left(t - \frac{r_o}{c}\right)\sin\phi\right]\int_0^{\lambda/4}\cos\left(\frac{2\pi\ell\cos\phi}{\lambda}\right)\cos\left(\frac{2\pi\ell}{\lambda}\right) d\ell\right.$$

$$- \left[\sin\omega\left(t - \frac{r_o}{c}\right)\sin\phi\right]\int_0^{\lambda/4}\sin\left(\frac{2\pi\ell\cos\phi}{\lambda}\right)\cos\left(\frac{2\pi\ell}{\lambda}\right) d\ell$$

$$+ \left[\cos\omega\left(t - \frac{r_o}{c}\right)\sin\gamma\right]\int_0^{\lambda/4}\cos\left(\frac{2\pi\ell\cos\gamma}{\lambda}\right)\cos\left(\frac{2\pi\ell}{\lambda}\right) d\ell$$

$$\left. - \left[\sin\omega\left(t - \frac{r_o}{c}\right)\sin\gamma\right]\int_0^{\lambda/4}\sin\left(\frac{2\pi\ell\cos\gamma}{\lambda}\right)\cos\left(\frac{2\pi\ell}{\lambda}\right) d\ell\right\}$$

Evaluating the integrals and substituting the limits, we obtain

$$H = \frac{I_o}{10 r_o}\left\{\left[\cos\omega\left(t - \frac{r_o}{c}\right)\sin\phi\right]\left[\frac{\cos\left\{\frac{\pi}{2}(\cos\phi)\right\}}{\sin^2\phi}\right]\right.$$

$$+ \left[\cos\omega\left(t - \frac{r_o}{c}\right)\sin\gamma\right]\left[\frac{\cos\left\{\frac{\pi}{2}(\cos\gamma)\right\}}{\sin^2\gamma}\right]$$

$$\left. - \left[\sin\omega\left(t - \frac{r_o}{c}\right)\sin\phi\right]\left[\frac{\sin\left\{\frac{\pi}{2}(\cos\phi)\right\} - \cos\phi}{\sin^2\phi}\right]\right.$$

$$- \left[\sin \omega \left(t - \frac{r_o}{c}\right) \sin \gamma\right] \left[\frac{\sin\left\{\frac{\pi}{2} (\cos \gamma)\right\} - \cos \gamma}{\sin^2 \gamma}\right]\Bigg\}$$

The electric field intensity then becomes

$$E = \frac{30 I_o}{r_o} \Bigg\{ \left[\cos \omega \left(t - \frac{r_o}{c}\right)\right] \left[\frac{\cos\left\{\frac{\pi}{2} (\cos \phi)\right\}}{\sin \phi} + \frac{\cos\left\{\frac{\pi}{2} (\cos \gamma)\right\}}{\sin \gamma}\right]$$

$$- \left[\sin \omega \left(t - \frac{r_o}{c}\right)\right] \left[\frac{\sin\left\{\frac{\pi}{2} (\cos \phi)\right\} - \cos \varphi}{\sin \phi} + \frac{\sin\left\{\frac{\pi}{2} (\cos \gamma)\right\} - \cos \gamma}{\sin \gamma}\right]\Bigg\}$$

In the plane of the antenna, it can be seen from the geometry of figure 94 that

$$\phi = \Phi - \theta \qquad \gamma = \Phi + \theta$$

These values could be substituted in the expression for E to compute the horizontal field distribution However, since ϕ and γ have been made general angles, it will be possible to obtain the expression for E in terms of the elevation angle α as well as in terms of the azimuth angle θ and the antenna angle Φ In polar coordinates, then,

$$\cos \phi = \cos \alpha \cos (\Phi - \theta)$$

$$\sin \phi = \sqrt{1 - \cos^2 \phi}$$

$$= \sqrt{1 - \cos^2 \alpha \cos^2 (\Phi - \theta)}$$

Similarly,

$$\cos \gamma = \cos \alpha \cos (\Phi + \theta)$$

$$\sin \gamma = \sqrt{1 - \cos^2 \alpha \cos^2 (\Phi + \theta)}$$

Then, for any azimuth angle θ and any elevation angle α

$$E = \frac{30 I_o}{r_o} \Bigg\{ \left[\cos \omega \left(t - \frac{r_o}{c}\right)\right] \left[\frac{\cos\left(\frac{\pi}{2} \cos \alpha \cos (\Phi - \theta)\right)}{\sqrt{1 - \cos^2 \alpha \cos^2 (\phi - \theta)}} + \frac{\cos\left(\frac{\pi}{2} \cos \alpha \cos (\Phi + \theta)\right)}{\sqrt{1 - \cos^2 \alpha \cos^2 (\phi + \theta)}}\right]$$

$$- \left[\sin \omega \left(t - \frac{r_o}{c}\right)\right] \left[\frac{\sin\left(\frac{\pi}{2} \cos \alpha \cos (\Phi - \theta)\right) - \cos \alpha \cos (\Phi - \theta)}{\sqrt{1 - \cos^2 \alpha \cos^2 (\Phi - \theta)}}\right.$$

$$\left. + \frac{\sin\left(\frac{\pi}{2} \cos \alpha \cos (\Phi - \theta)\right) - \cos \alpha \cos (\Phi + \theta)}{\sqrt{1 - \cos^2 \alpha \cos^2 (\Phi + \theta)}}\right]\Bigg\}$$

This expression consists of two waves in time quadrature to each other The absolute amplitude can be found by taking the square root of the sum of the squares

$$E = \frac{30I_o}{r_o}\left\{\left[\frac{\cos\left(\frac{\pi}{2}\cos\alpha\cos\ (\phi-\theta)\right)}{\sqrt{1-\cos^2\alpha\cos^2\ (\phi-\theta)}} + \frac{\cos\left(\frac{\pi}{2}\cos\alpha\cos\ (\phi+\theta)\right)}{\sqrt{1-\cos^2\alpha\cos^2\ (\phi+\theta)}}\right]^2\right.$$

$$+\left[\frac{\sin\left(\frac{\pi}{2}\cos\alpha\cos\ (\phi-\theta)\right) - \cos\alpha\cos\ (\phi-\theta)}{\sqrt{1-\cos^2\alpha\cos^2\ (\phi-\theta)}}\right.$$

$$\left.\left.+\frac{\sin\left(\frac{\pi}{2}\cos\alpha\cos\ (\phi+\theta)\right) - \cos\alpha\cos\ (\phi+\theta)}{\sqrt{1-\cos^2\alpha\cos^2\ (\phi+\theta)}}\right]^2\right\}^{\frac{1}{2}}$$

In the plane of the antenna or $\alpha = 0$

$$E = \frac{30I_o}{r_o}\left\{\left[\frac{\cos\left(\frac{\pi}{2}\cos\ (\phi-\theta)\right)}{\sin\ (\phi-\theta)} + \frac{\cos\left(\frac{\pi}{2}\cos\ (\phi+\theta)\right)}{\sin\ (\phi+\theta)}\right]^2\right.$$

$$\left.+\left[\frac{\sin\left(\frac{\pi}{2}\cos\ (\phi-\theta)\right) - \cos\ (\phi-\theta)}{\sin\ (\phi-\theta)} + \frac{\sin\left(\frac{\pi}{2}\cos\ (\phi+\theta)\right) - \cos\ (\phi+\theta)}{\sin\ (\phi+\theta)}\right]^2\right\}^{\frac{1}{2}}$$

In the vertical plane when $\theta = 0$

$$E = \frac{30I_o}{r_o}\left\{\left[\frac{\cos\left(\frac{\pi}{2}\cos\alpha\cos\phi\right)}{\sqrt{1-\cos^2\alpha\cos^2\phi}} + \frac{\cos\left(\frac{\pi}{2}\cos\alpha\cos\phi\right)}{\sqrt{1-\cos^2\alpha\cos^2\phi}}\right]^2\right.$$

$$\left.+\left[\frac{\sin\left(\frac{\pi}{2}\cos\alpha\cos\phi\right) - \cos\alpha\cos\phi}{\sqrt{1-\cos^2\alpha\cos^2\phi}} + \frac{\sin\left(\frac{\pi}{2}\cos\alpha\cos\phi\right) - \cos\alpha\cos\phi}{\sqrt{1-\cos^2\alpha\cos^2\phi}}\right]^2\right\}^{\frac{1}{2}}$$

$$E = \frac{30I_o}{r_o}\left\{\frac{4\cos^2\left(\frac{\pi}{2}\cos\alpha\cos\phi\right) + \left[2\sin\left(\frac{\pi}{2}\cos\alpha\cos\phi\right) - 2\cos\alpha\cos\phi\right]^2}{1-\cos^2\alpha\cos^2\phi}\right\}^{\frac{1}{2}}$$

$$E = \frac{60I_o}{r_o}\left\{\frac{\cos^2\alpha\cos^2\phi - 2\cos\alpha\cos\phi\ \sin\left(\frac{\pi}{2}\cos\alpha\cos\phi\right) + 1}{1-\cos^2\alpha\cos^2\phi}\right\}^{\frac{1}{2}}$$

These equations can be checked by taking the limiting case of a half-wave dipole or $2\phi = 180°$.

Then the expression for $\alpha = 0$ becomes

$$E = \frac{60I_o}{r_o}\left[\frac{\cos\left(\frac{\pi}{2}\sin\theta\right)}{\cos\theta}\right]$$

The expression for $\theta = 0$ becomes

$$E = \frac{60I_o}{r_o}$$

These relations indicate a toroid with the antenna as the axis of a revolution, the expressions for which check those in the published literature

In order to compute the gain of a V antenna with respect to a half-wave dipole, it is necessary to know the radiation resistance of the V antenna This calculation involves integrating the power flow $\left(\frac{c}{8\pi} E^2 \ dA\right)$ over the surface of a sphere around the antenna, in addition to which the mutual power must be calculated. The solution becomes extremely laborious and has to be computed by numerical integration However, the radiation resistance can be found quite simply by experimental methods This has been done for antennas of various apex angles and lengths, and for a resonant quarter-wave V with an apex angle of 80° the radiation resistance has been found to be approximately 33 ohms. Using this figure to calculate the relative field with respect to a half-wave dipole, assuming the same power in each antenna, the field of the V antenna was found to be 0 8 db below that of the dipole.

Patterns have been calculated in both the horizontal and the vertical planes for an antenna with an apex angle of 80° and are shown in figures 95 and 96

FIGURE INDEX

Figure Page

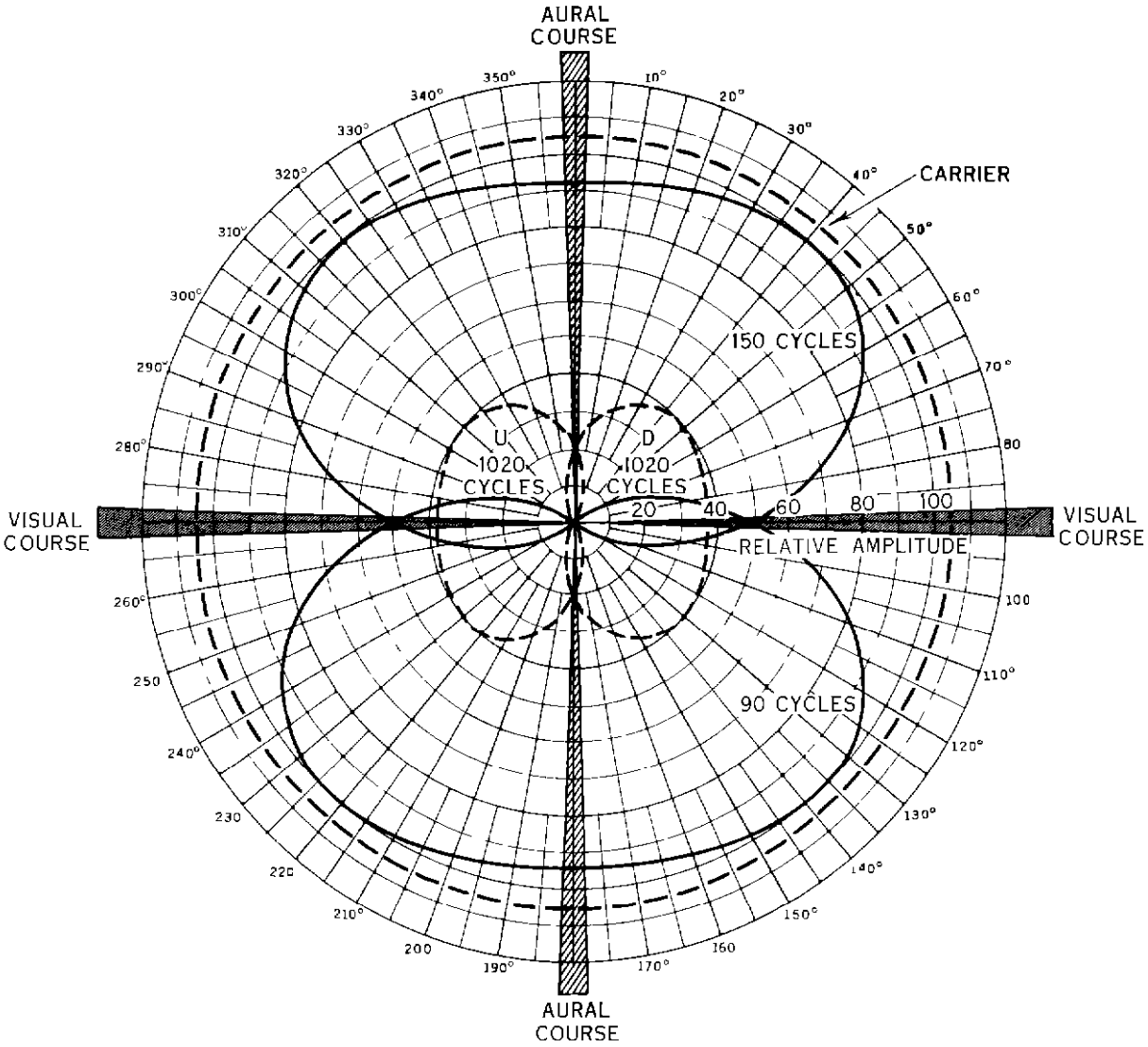

Figure 1 Basic Patterns of the Two-Course Visual Range with Sector Identification

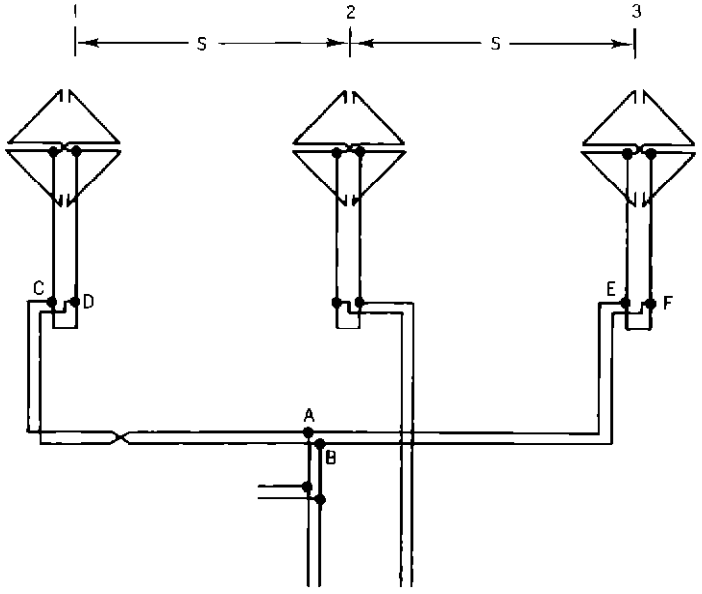

Figure 2 Basic Three-Loop Array for the Two Course Visual Range

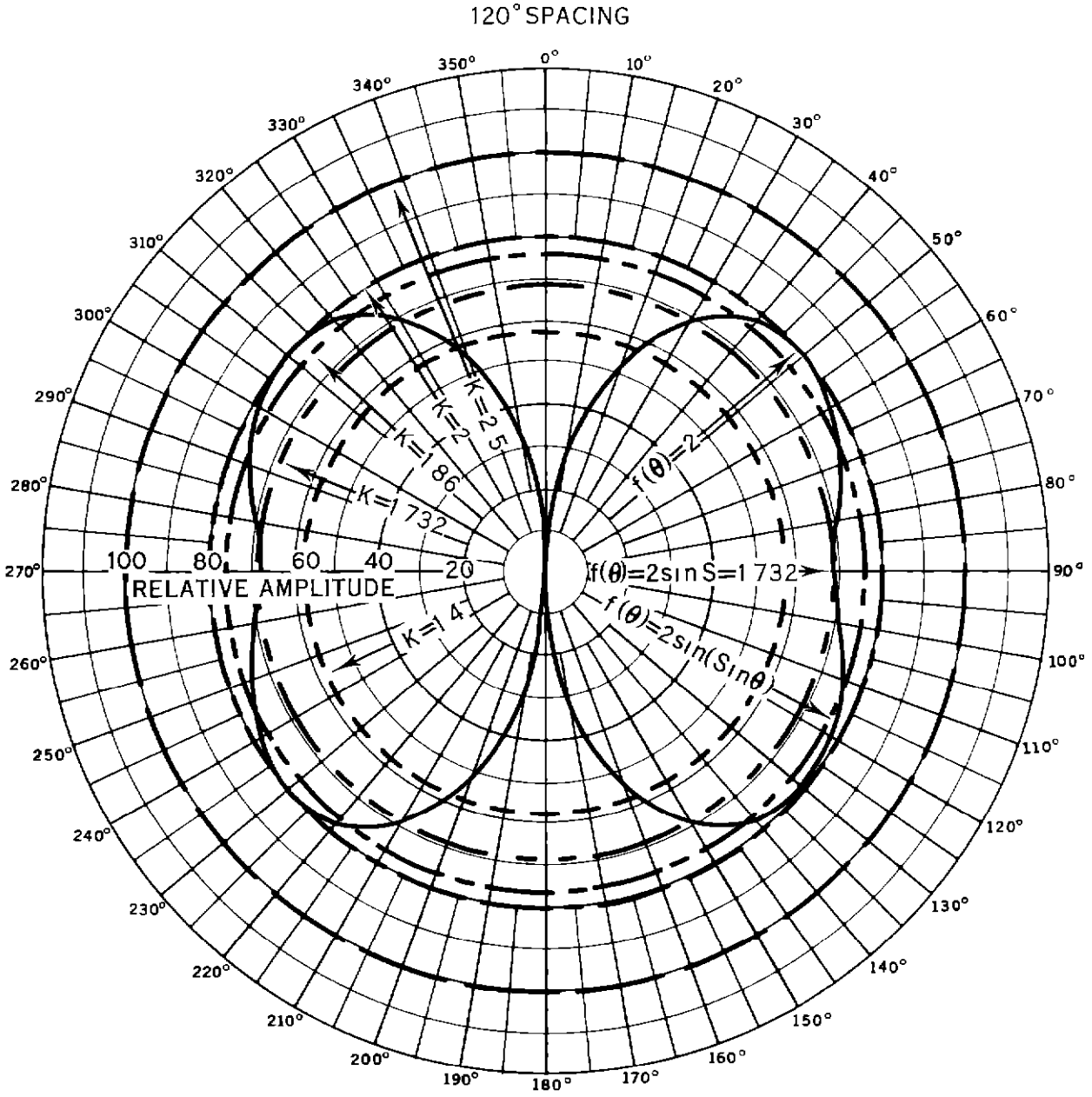

FIVE CENTER LOOP PATTERNS
FOR VARIOUS VALUES OF K

CLOVER LEAF PATTERN
$f(\theta)=2\sin(S\sin\theta)$

Figure 3 Relative Size of the Cloverleaf Pattern and the Circular Pattern for Various Values of Current Ratios

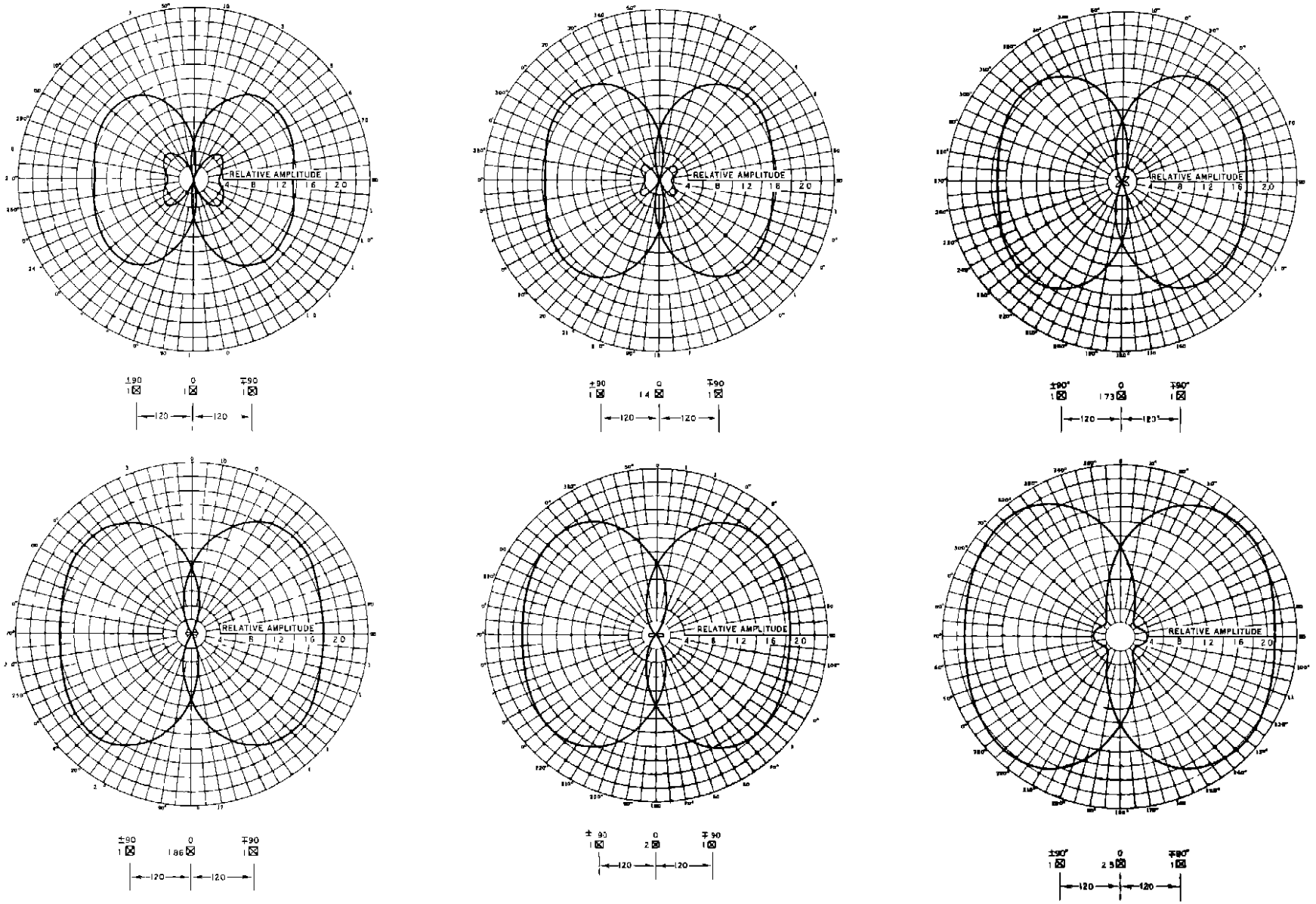

Figure 4 The Effect of Current Ratios on the Bean Patterns

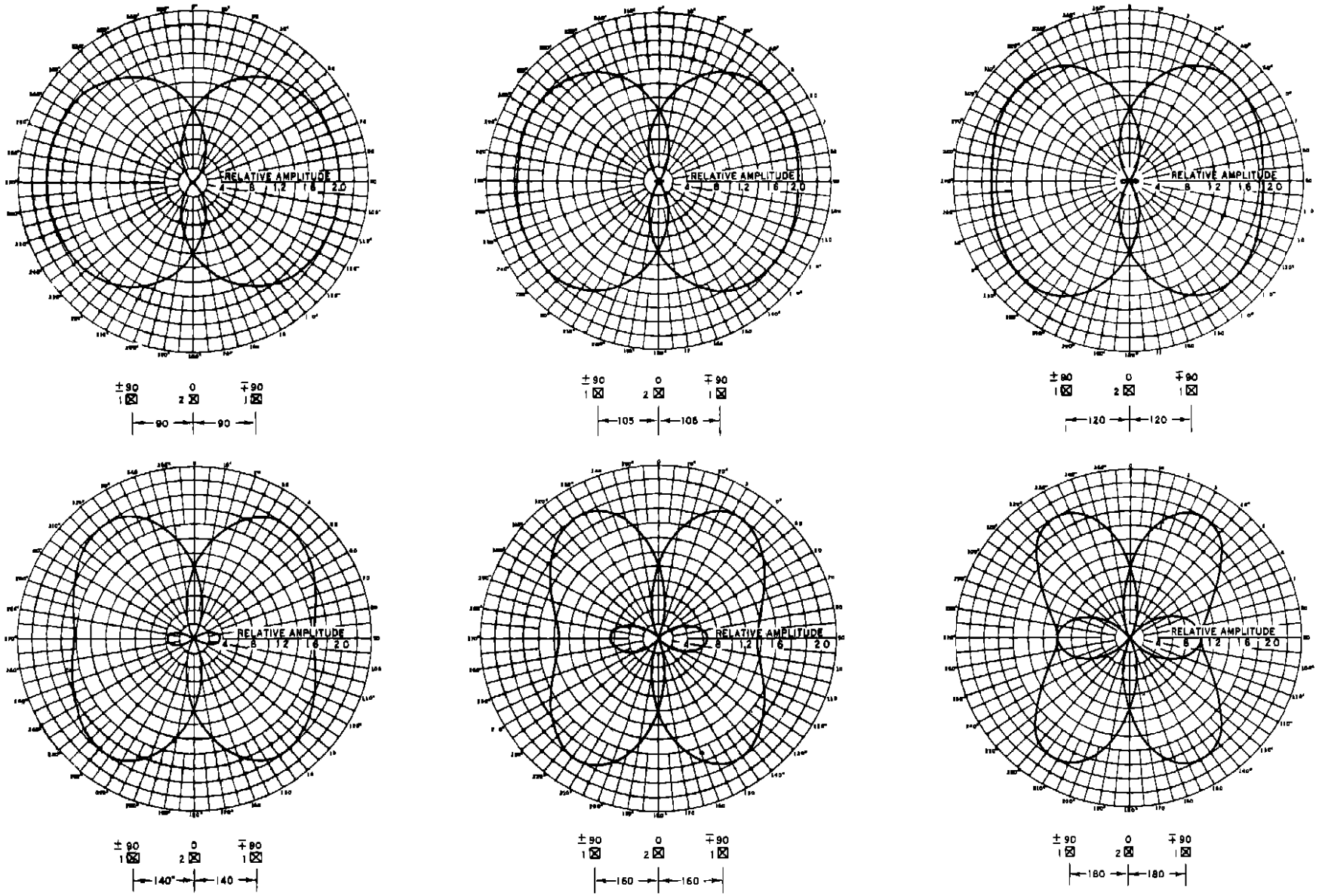

Figure 5 The Effect of Antenna Spacing on the Bean Patterns

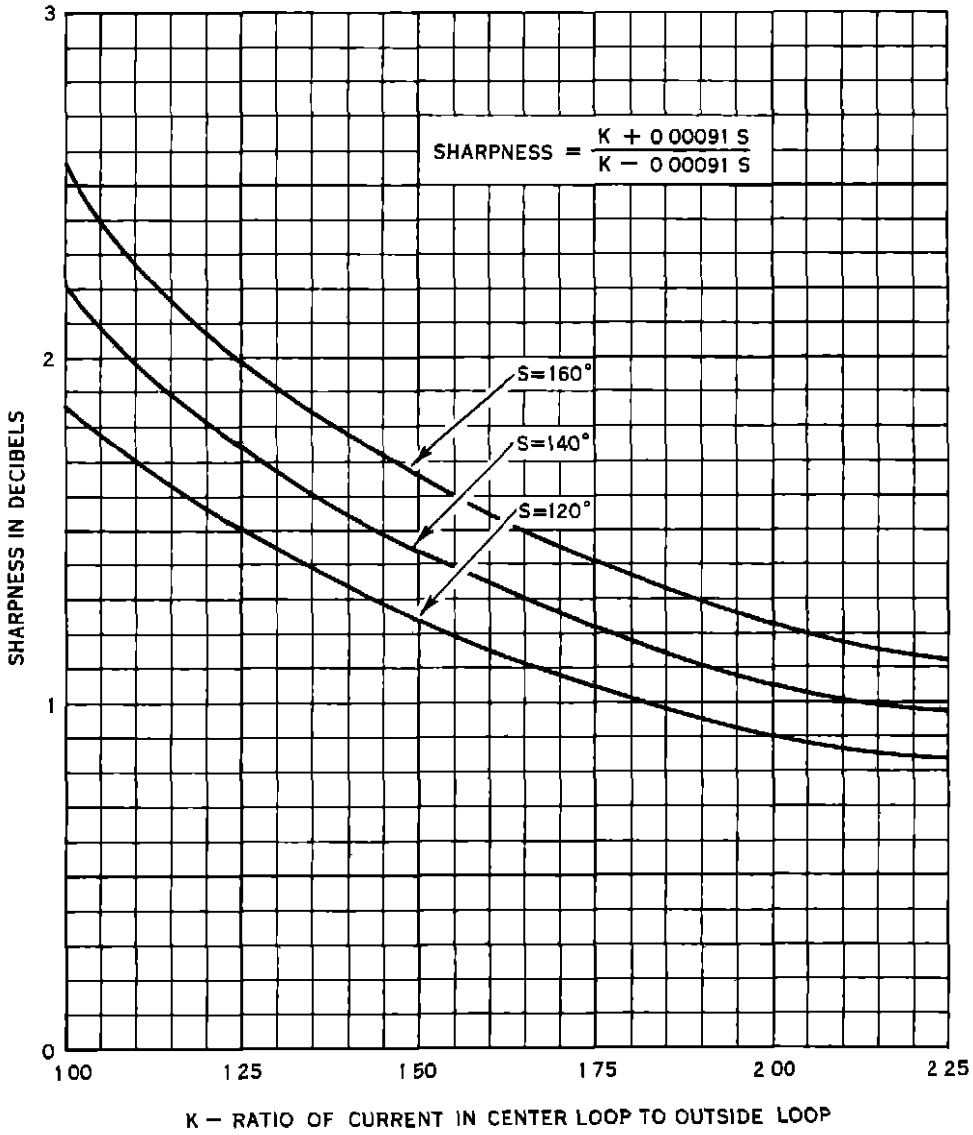

Figure 6 Variation of Course Sharpness versus Current Ratio for Different Antenna Spacings

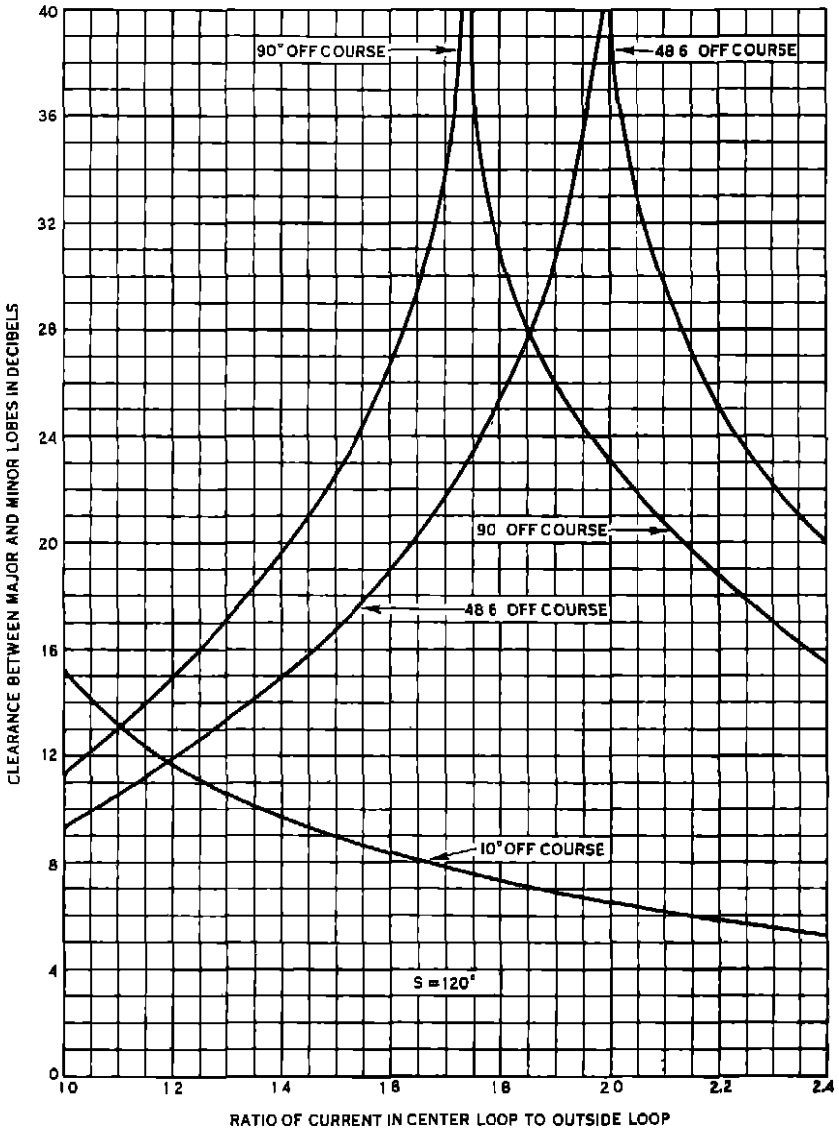

Figure 7 Pattern Clearance versus Current Ratio for 10°, 48 6°, and 90° Off Course

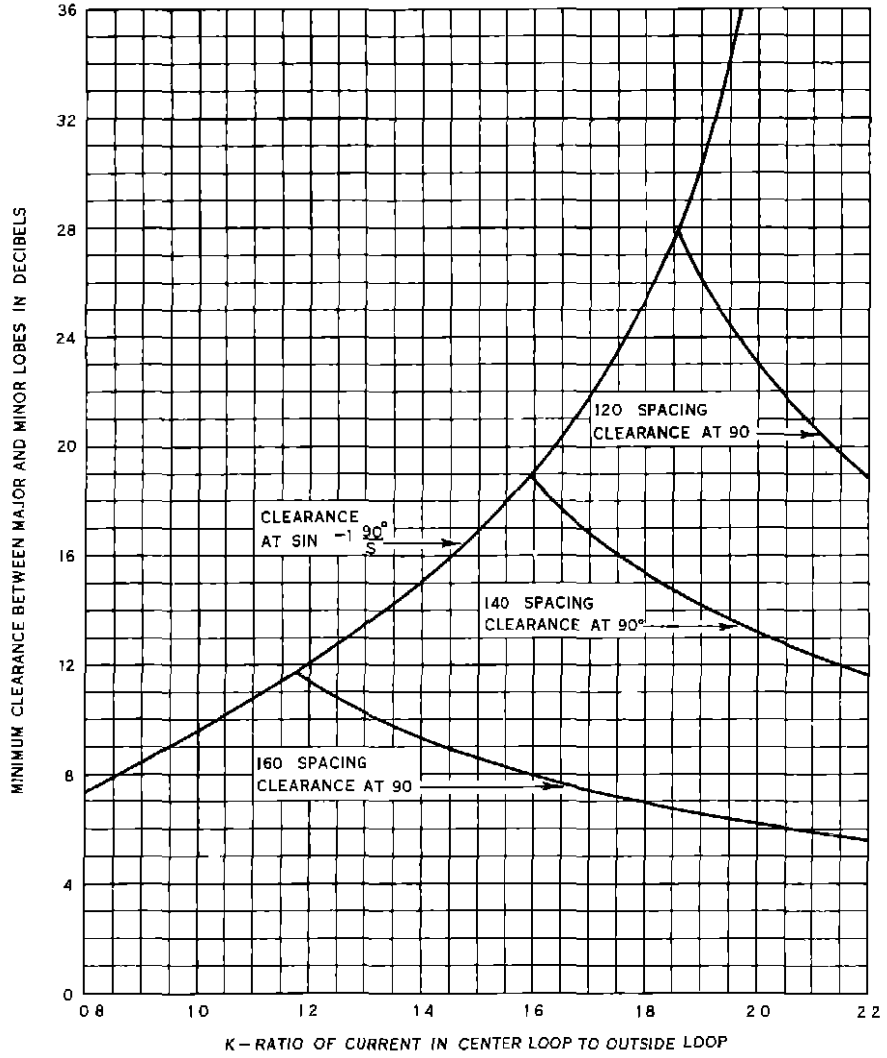

Figure 8 Minimum Pattern Clearance versus Current Ratio for Various Spacings

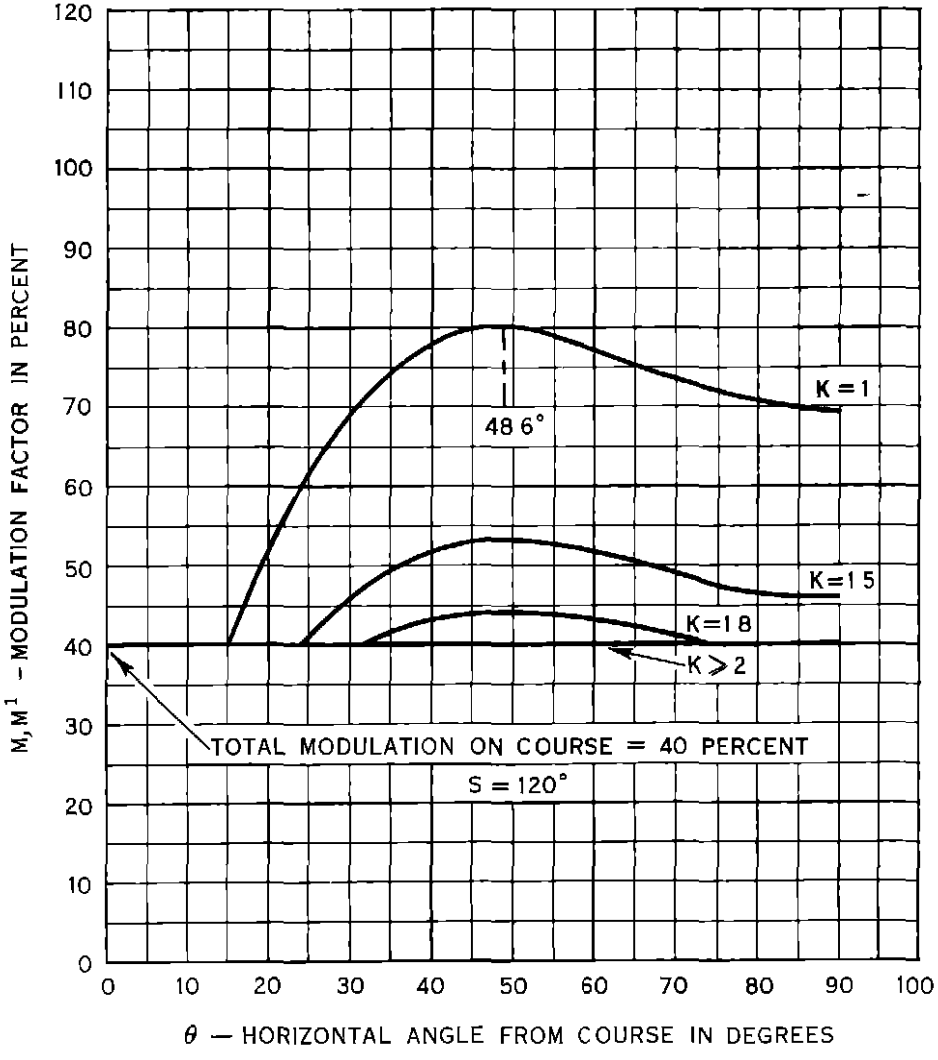

Figure 9 Percentage Modulation versus Azimuth Angle for Several Current Ratios

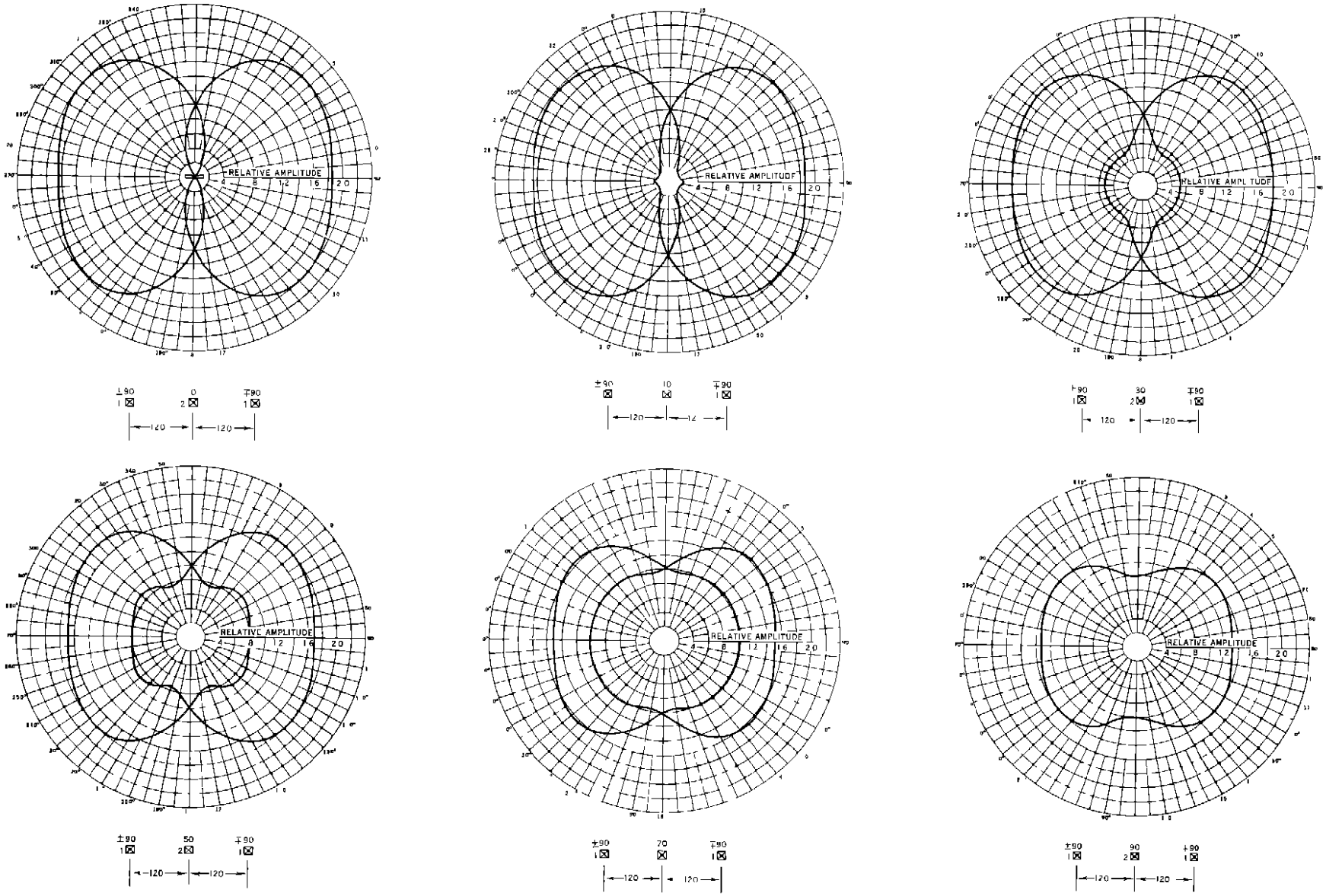

Figure 10 The Effect of Phase on the Bean Patterns

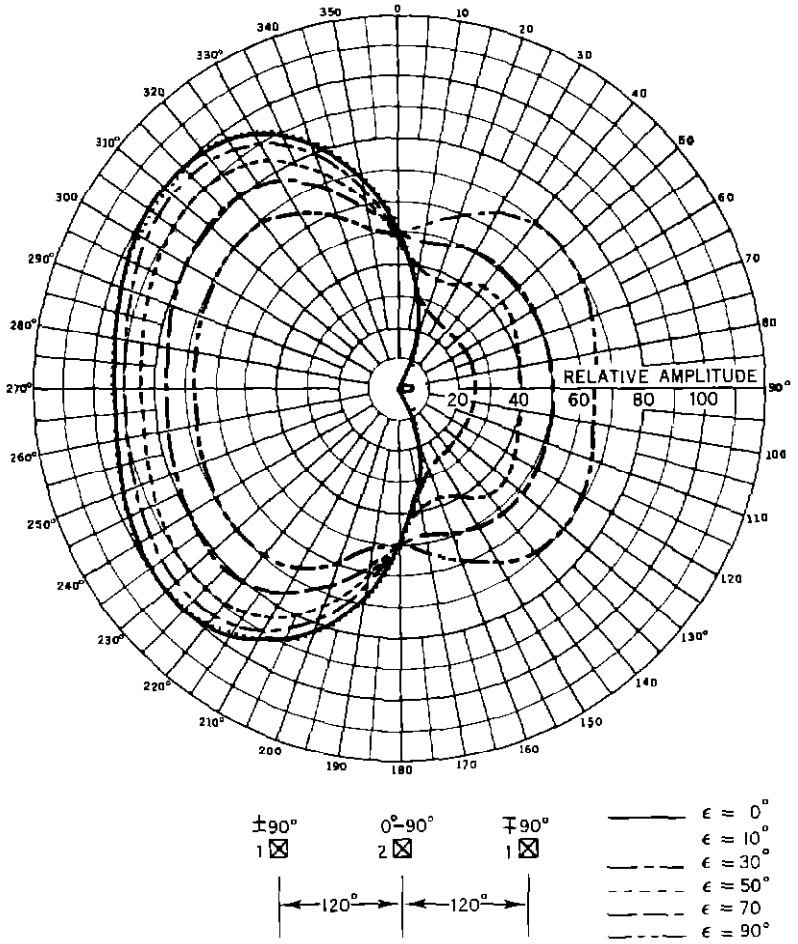

Figure 11 The Effect of Phase on the Bean Patterns Shown on One Graph

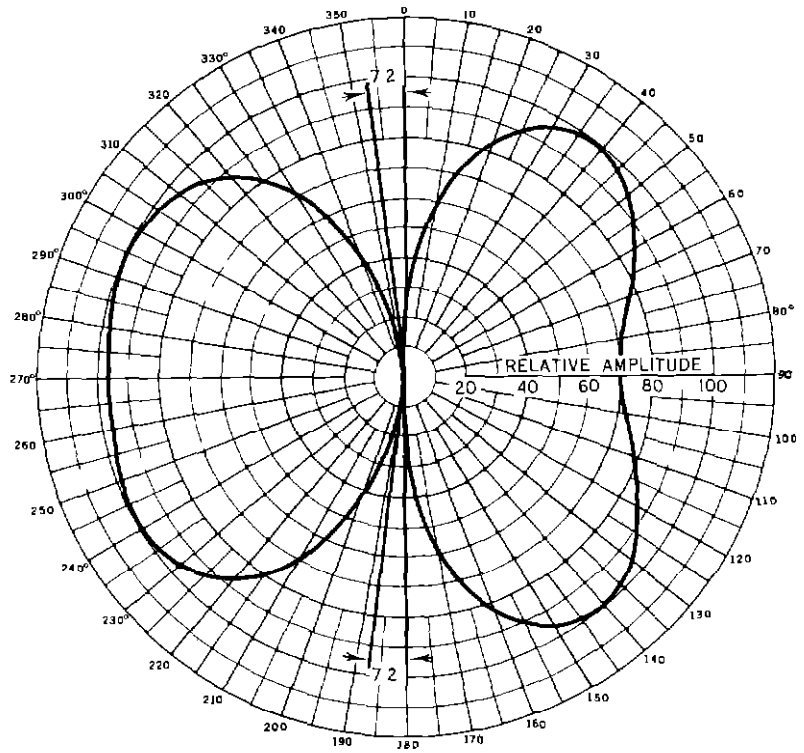

Figure 12 Cloverleaf Pattern for S = 120° and δ = 150°

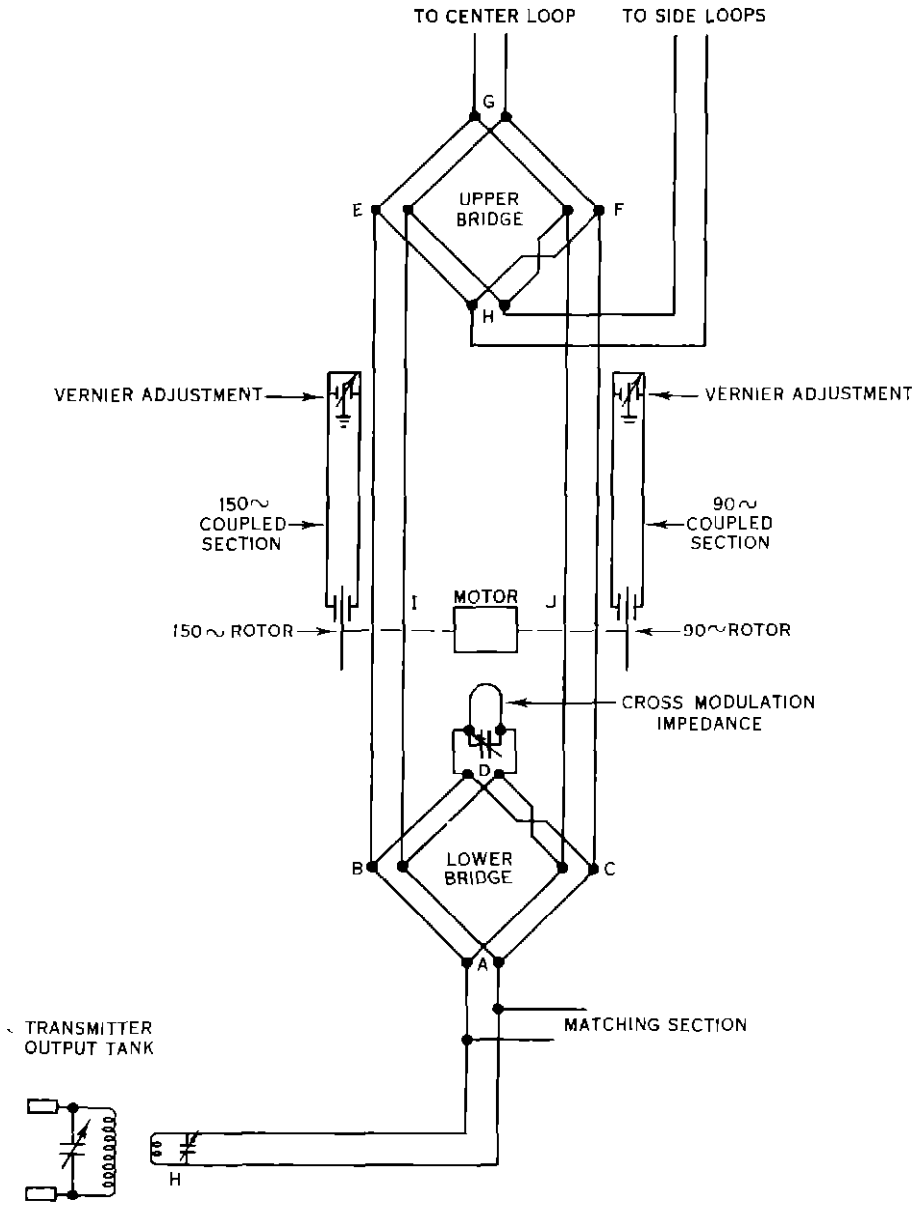

Figure 13 Schematic Diagram of Mechanical Modulator

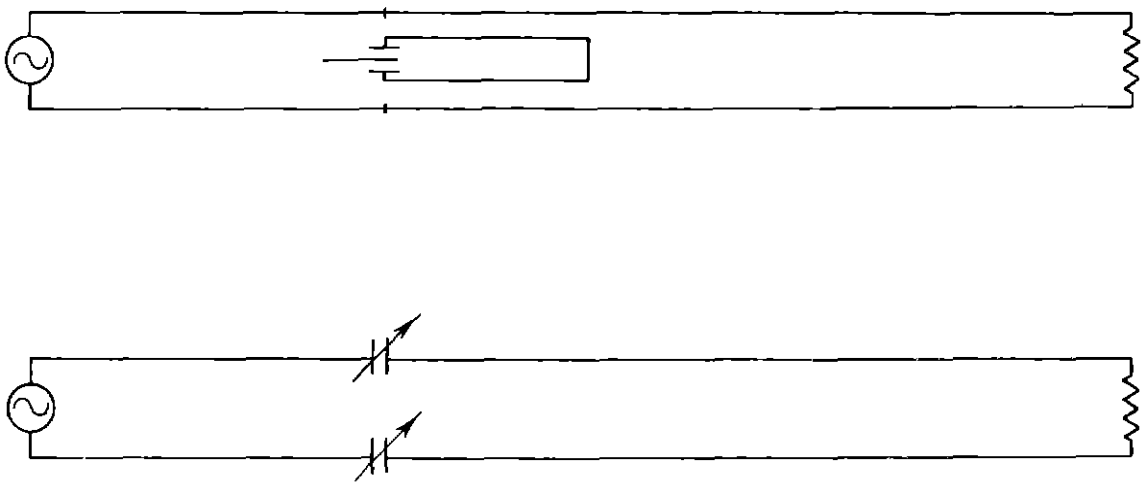

Figure 14 Equivalent Circuit of One Modulator Channel

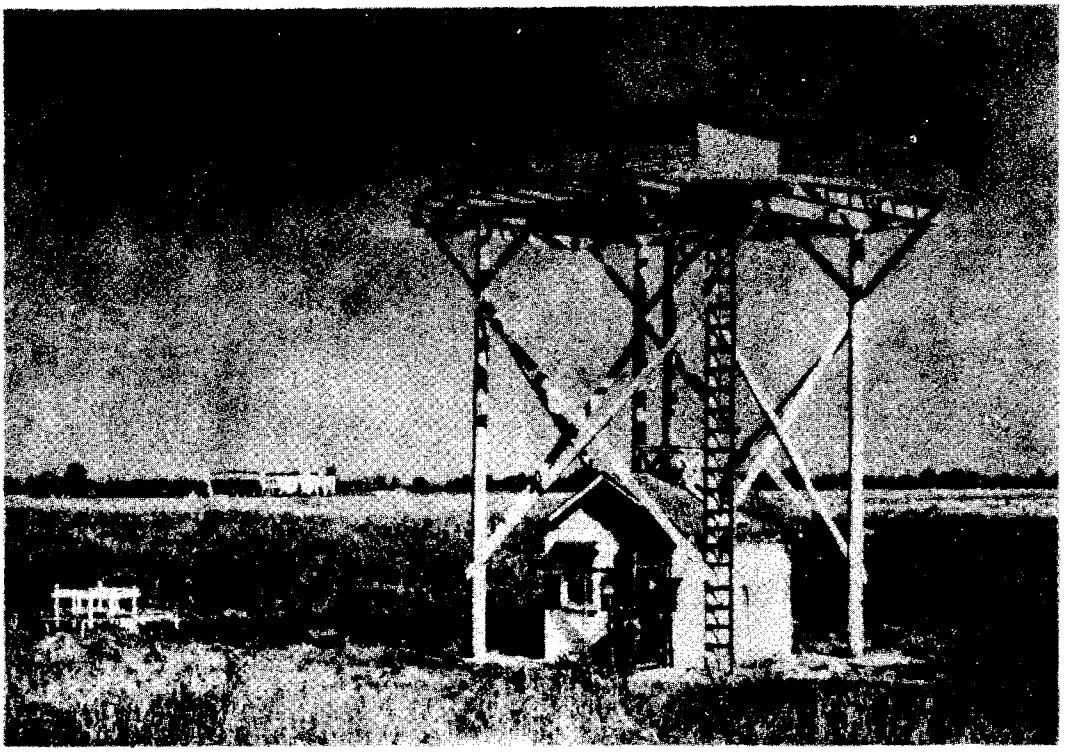

Figure 15. Thirty-foot Tower and Counterpoise with the Suppressor Array Located to the Left of the Building.

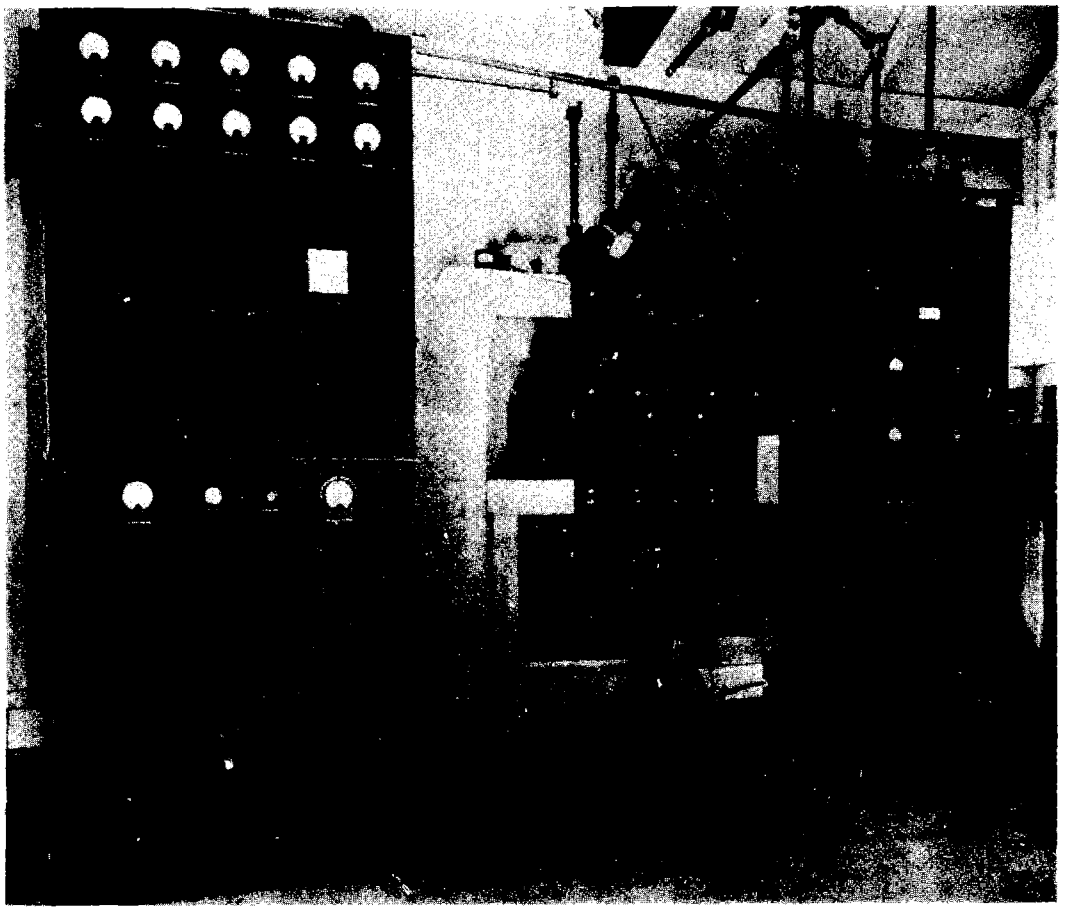

Figure 16. Transmitting Equipment for the Visual-Aural Range.

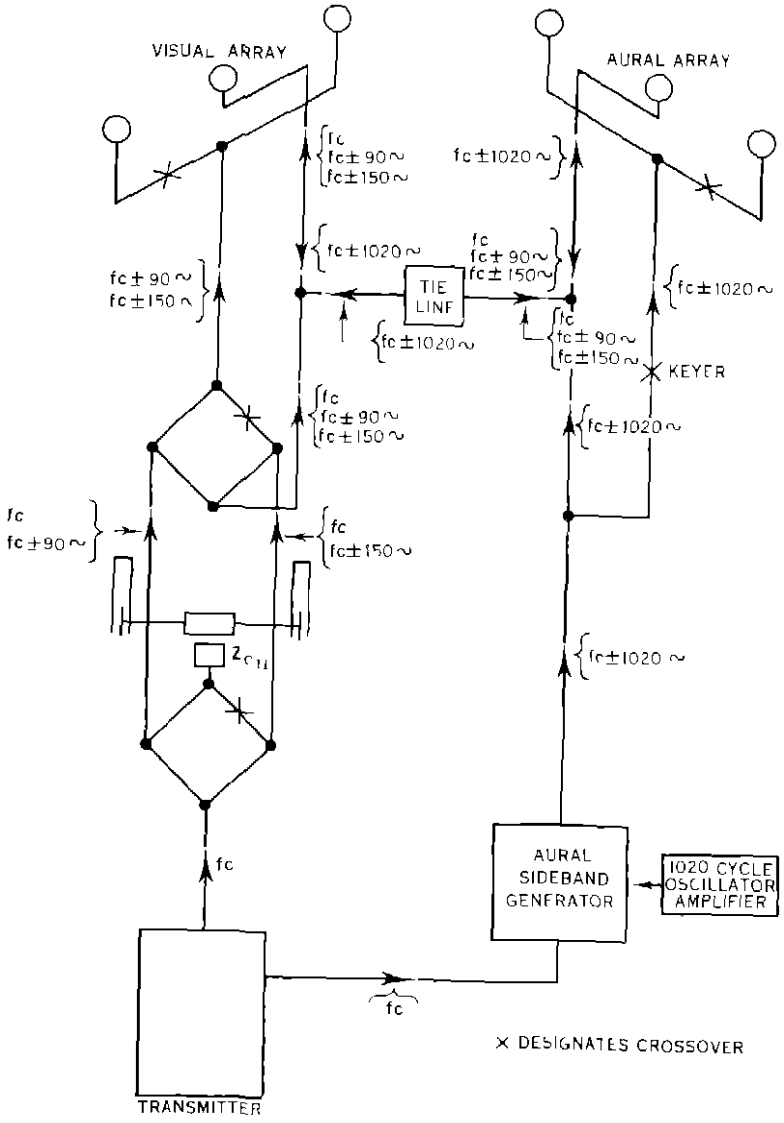

Figure 17 Block Diagram of the Two-Course Visual Range with Sector Identification

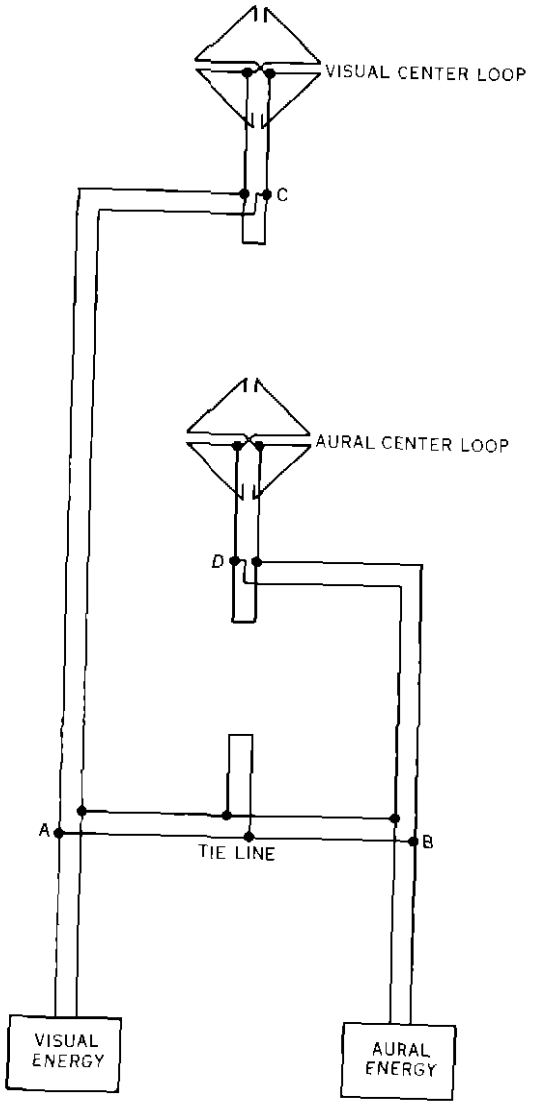

Figure 18 Schematic of the Non Dissipative Tie Line Connected to the Visual and Aural Center Loops

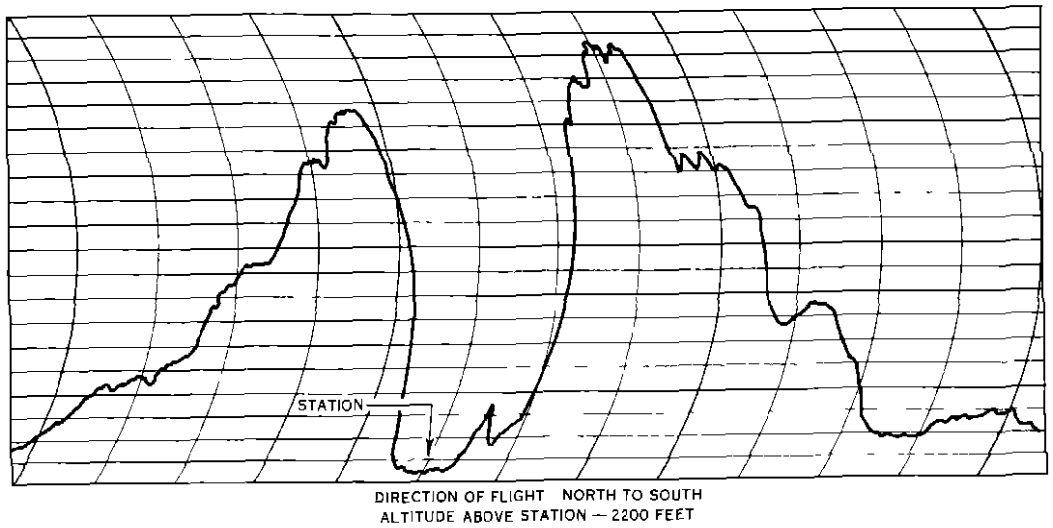

Figure 19A Flight Recording of the Vertical Field Pattern of the Side Visual Antennas

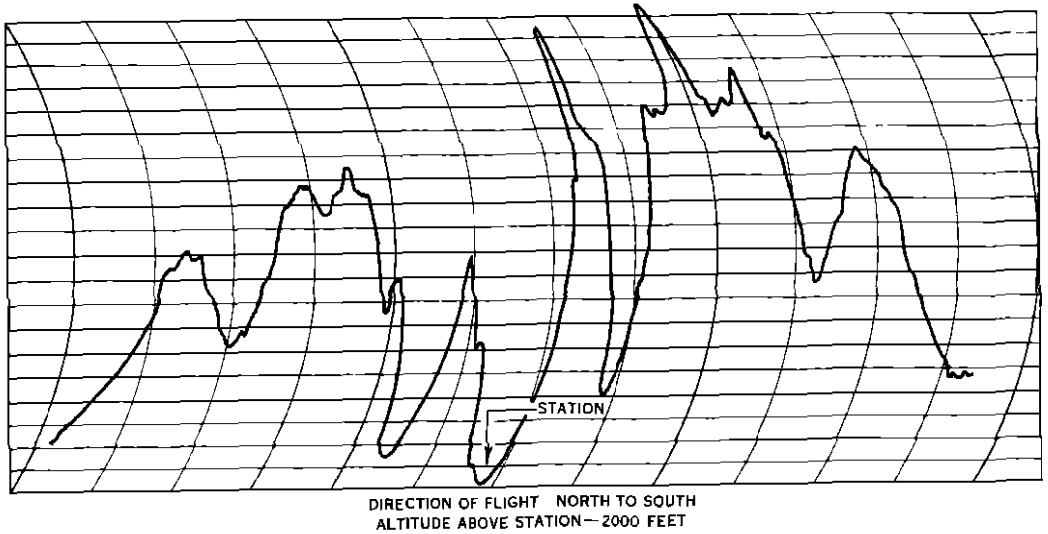

Figure 19B Flight Recording of the Vertical Field Pattern Produced when the Center Visual Antenna was Energized Variations in Field Pattern are Due to Parasitic Current in the Lower Center Antenna

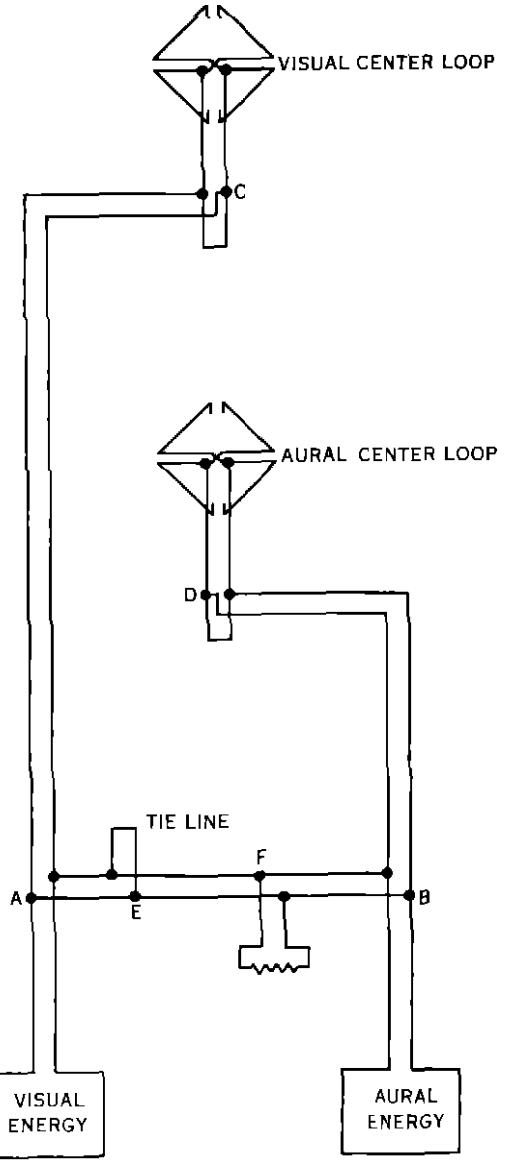

Figure 20 Schematic Diagram of the Dissipative Tie Line Connected to the Visual and Aural Center Loops

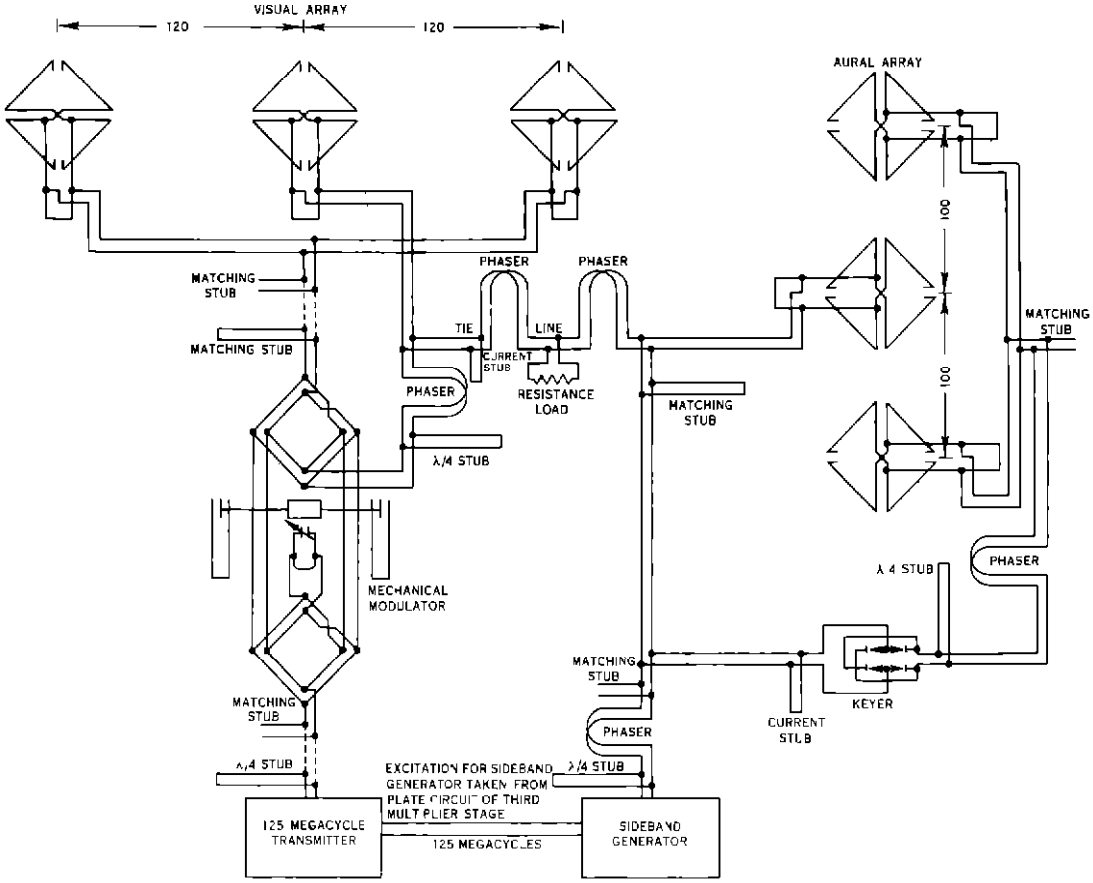

Figure 21 Schematic Diagram of the Two Course Visual-Aural Range

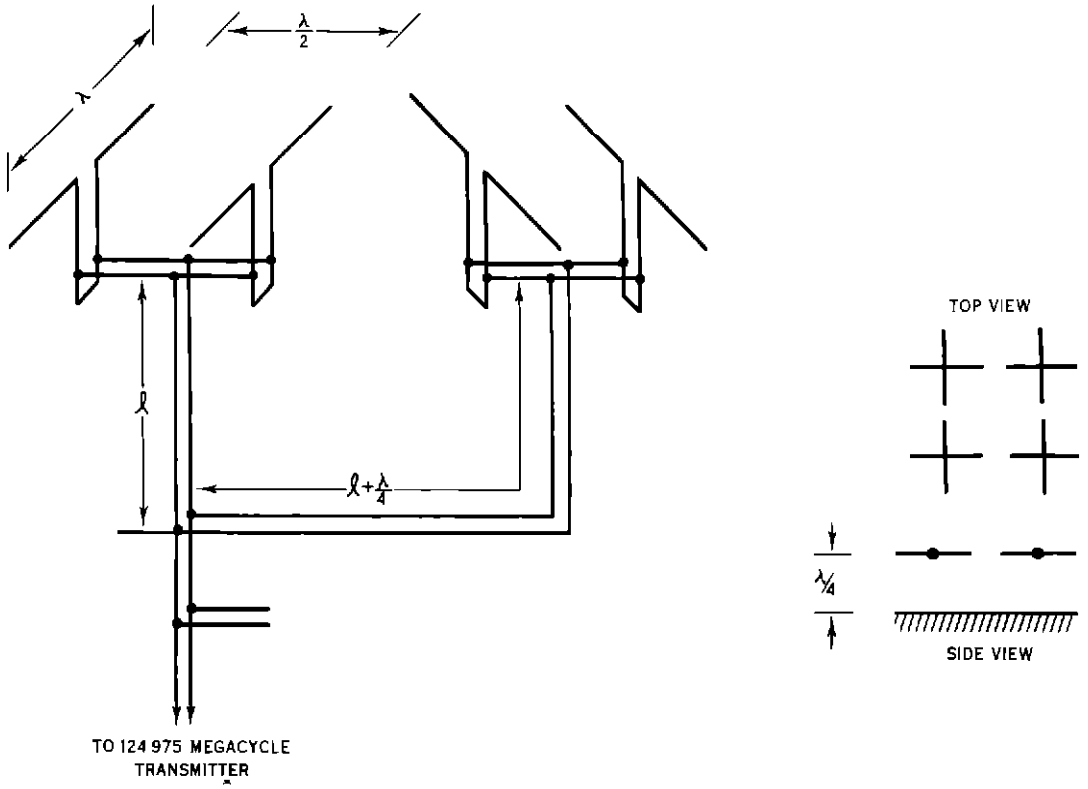

Figure 22 Schematic Diagram of the Suppressor Antenna Array

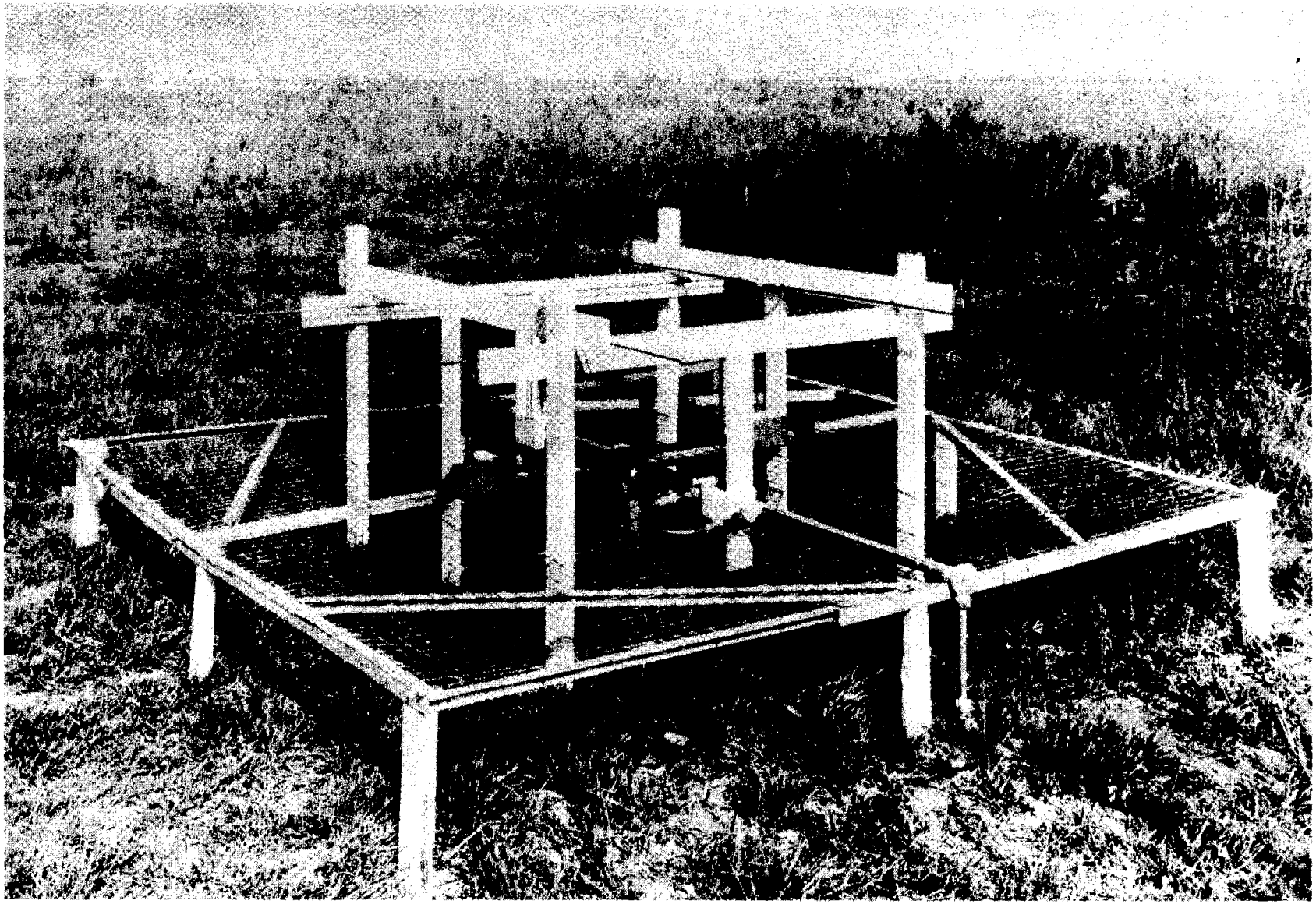

Figure 23. The Suppressor Antenna Array and Counterpoise.

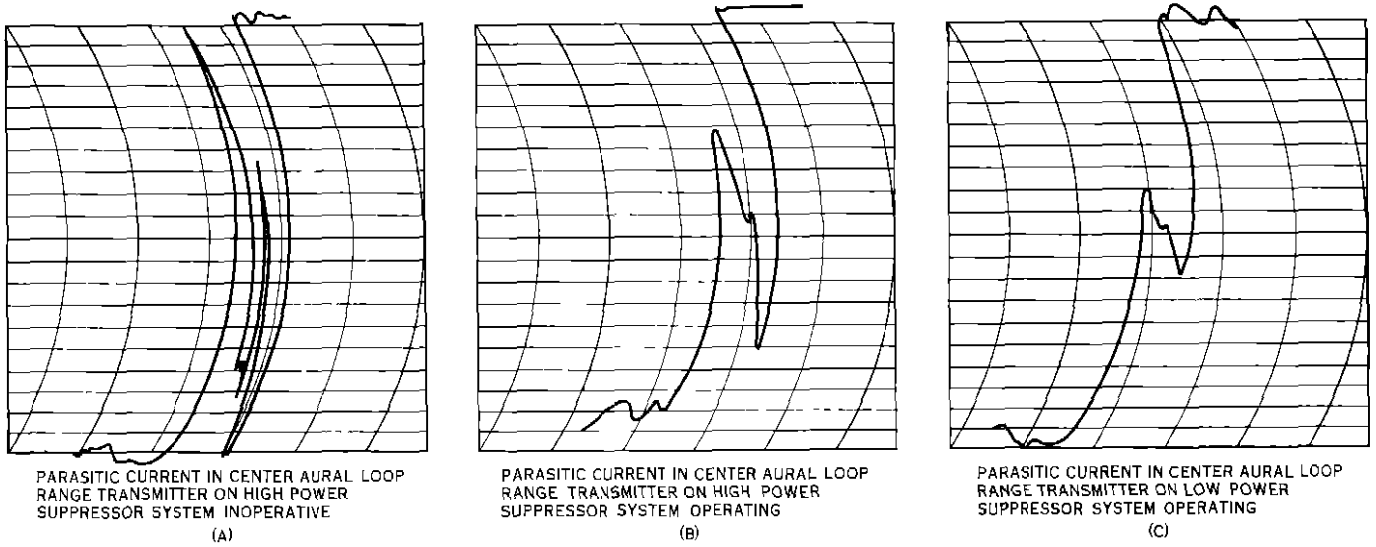

Figure 24 Flight Recordings Showing the Effect of the Suppressor System on the Cone of Silence with Parasitic Current in the Center Aural Antenna

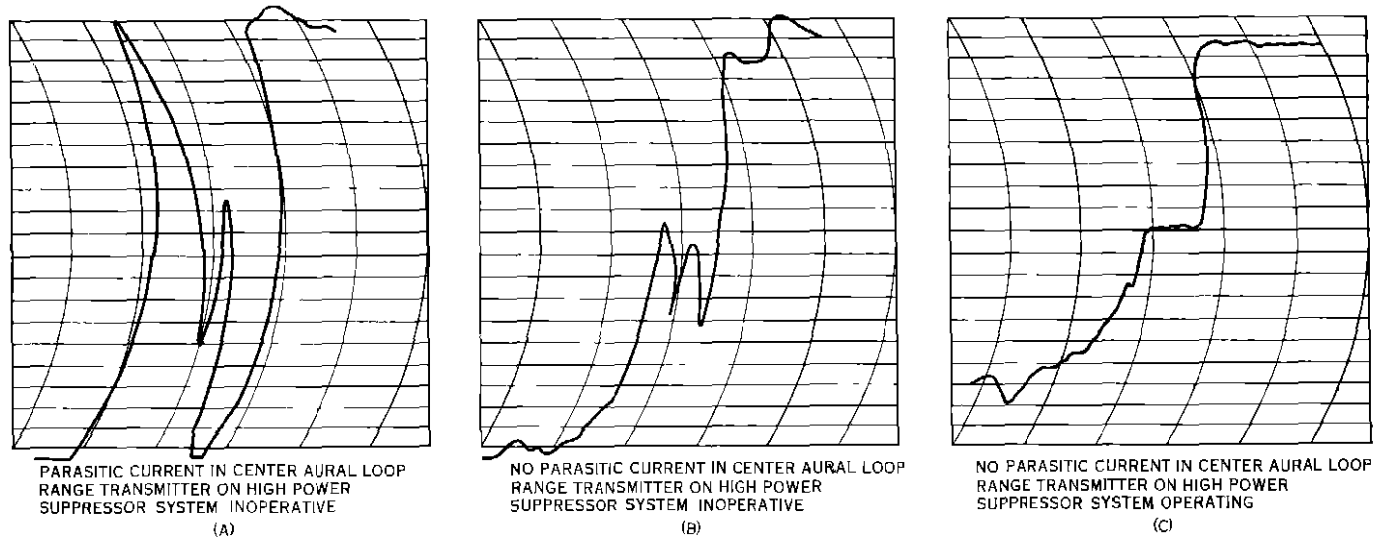

Figure 25 Flight Recordings Showing the Effect on the Cone-of-Silence when Parasitic Current in the Center Aural Antenna is Removed and when the Suppressor System is also Operated

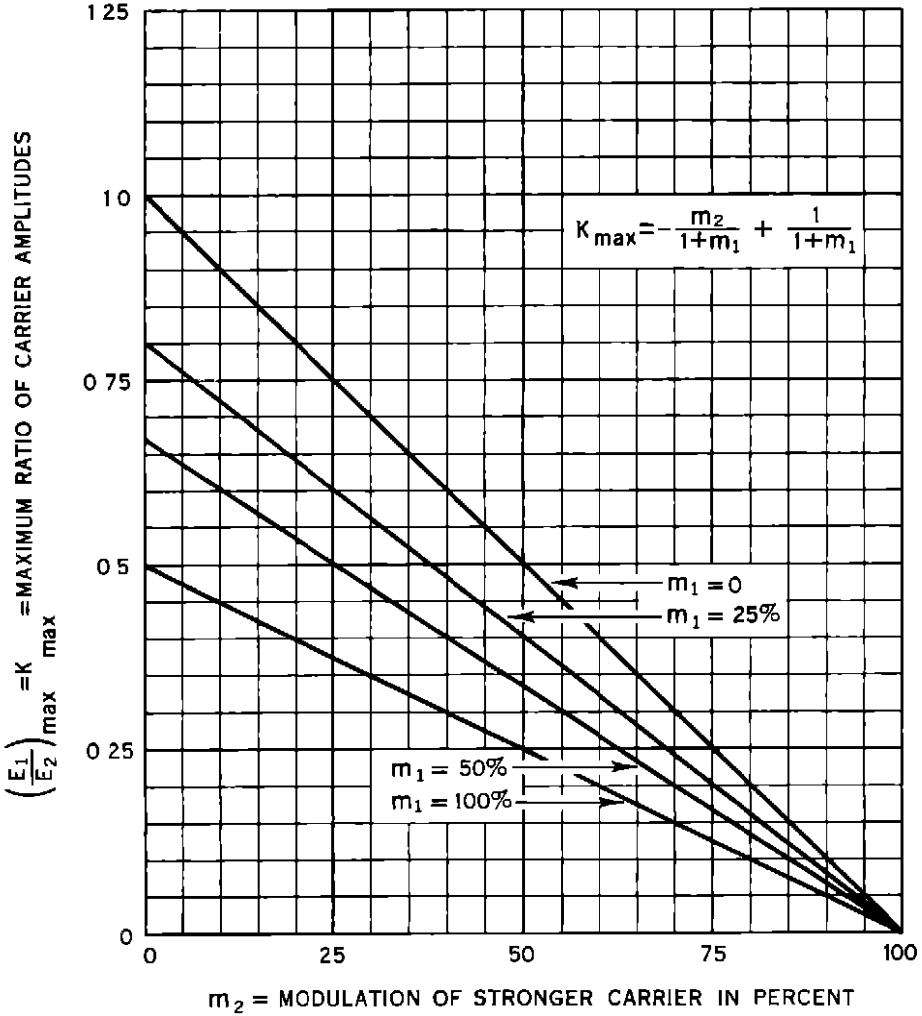

Figure 26 Detection of Two Modulated Carriers with Linear Detection Range of Applicability of Aiken's Theory

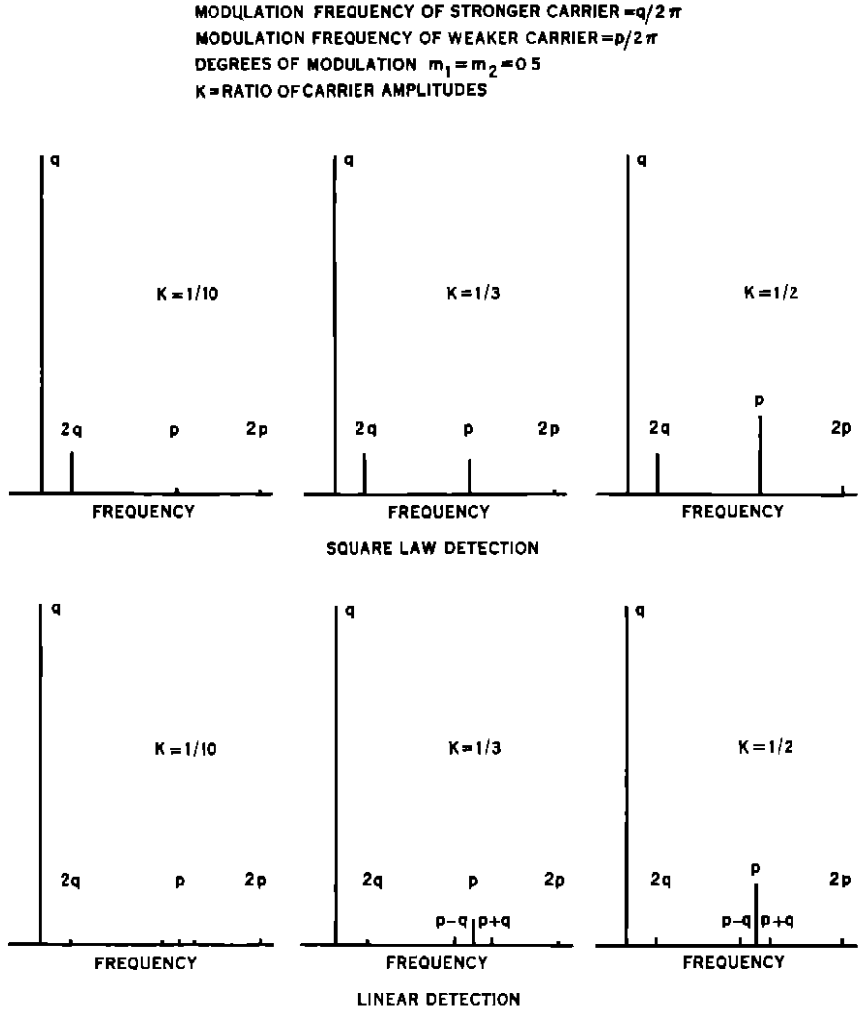

Figure 27 Frequency Spectrum after Square Law and Linear Detection of Two Amplitude Modulated Carriers

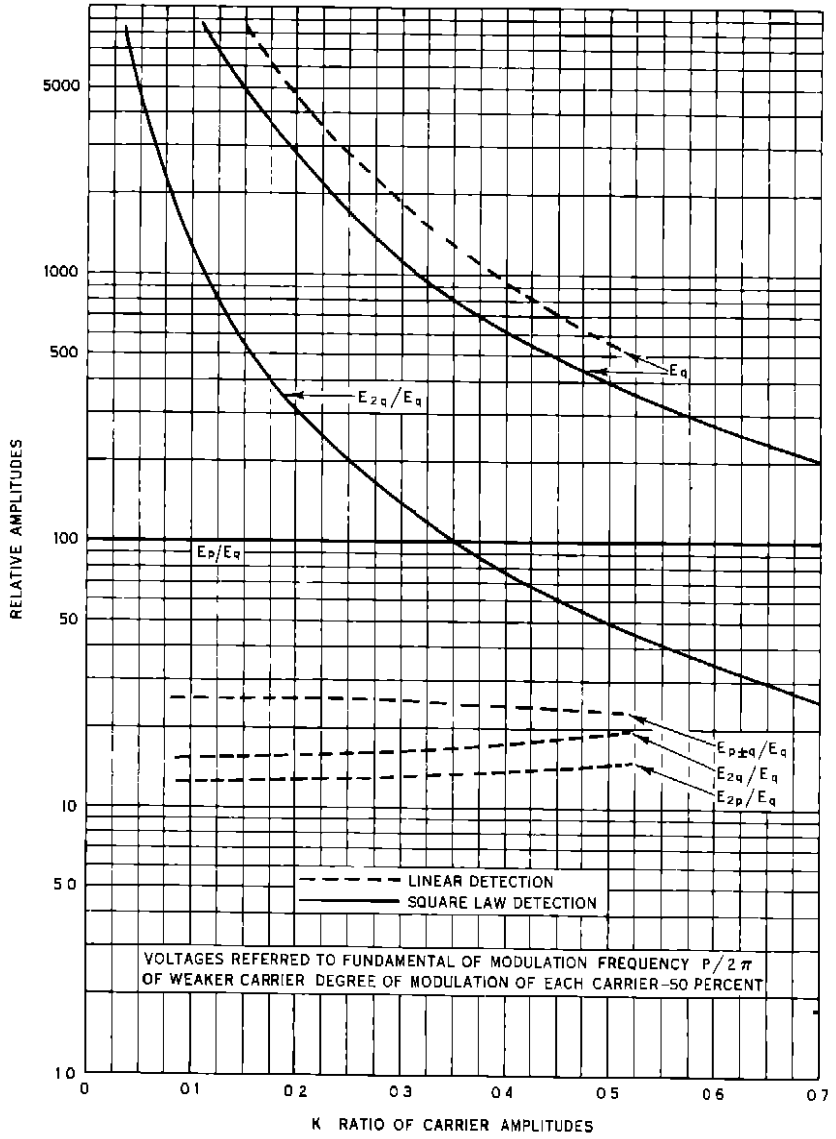

Figure 28 Detection of Two Modulated Carriers Distortion versus Ratio of Carrier Amplitudes Referred to Fundamental Modulation Frequency of the Weaker Carrier

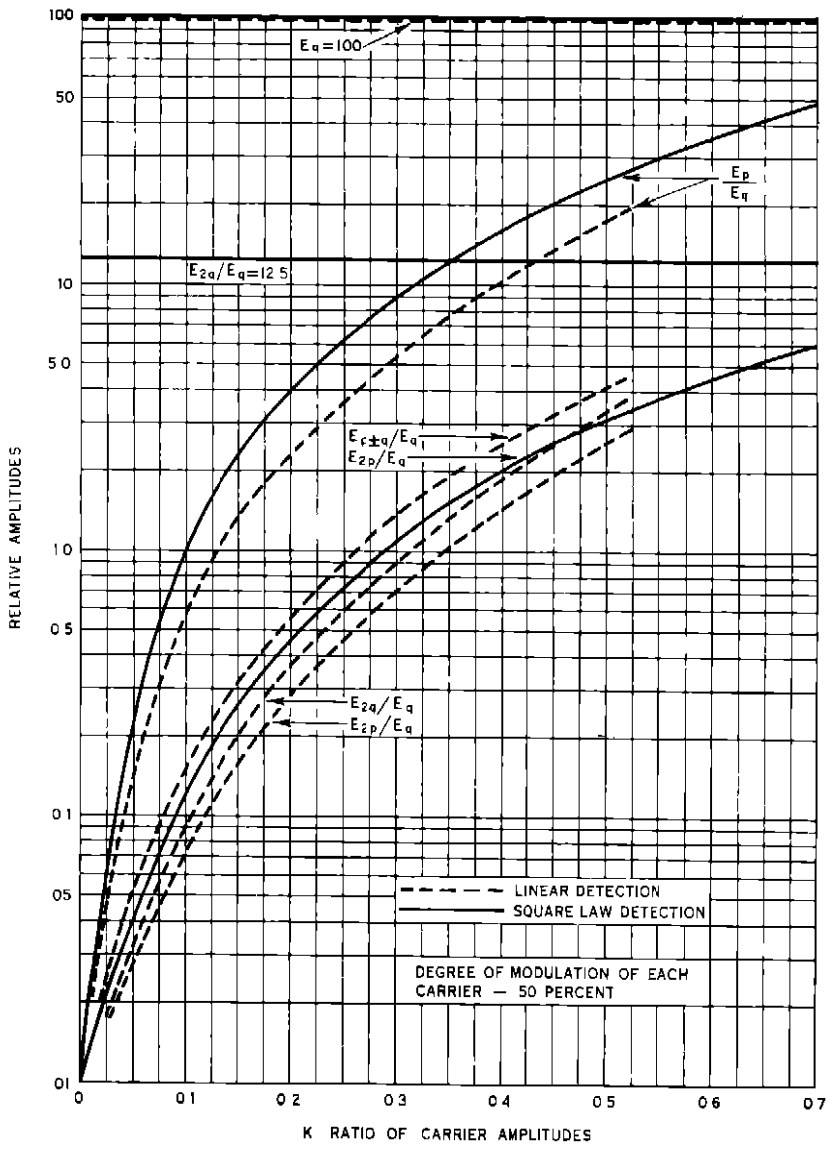

Figure 29 Detection of Two Modulated Carriers Distortion versus Ratio of Carrier Amplitudes, Referred to Fundamental Modulation Frequency $q/2\pi$ of the Stronger Carrier

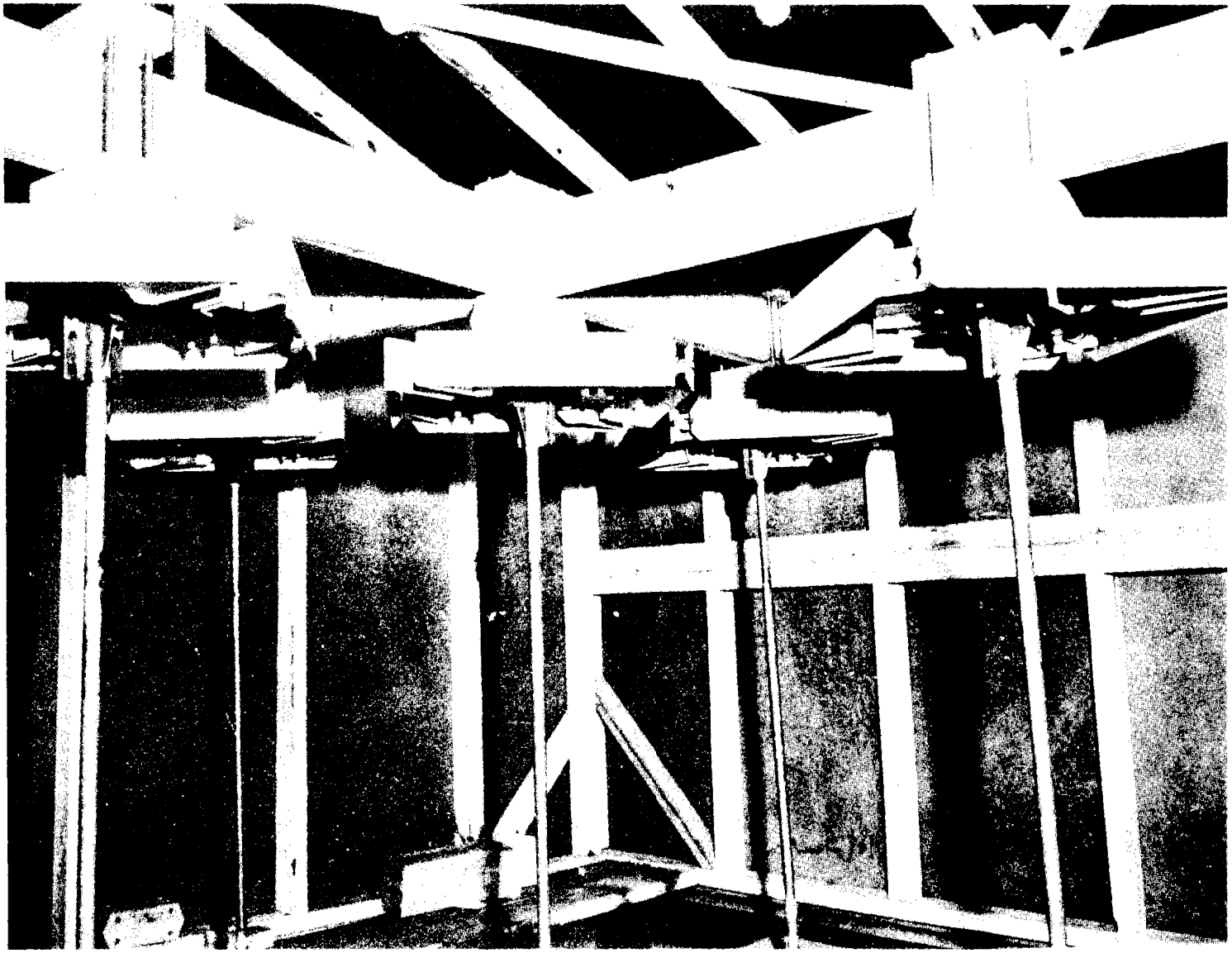

Figure 30. Antenna Array Used in System No. 2 Visual-Aural Range with Simultaneous Voice.

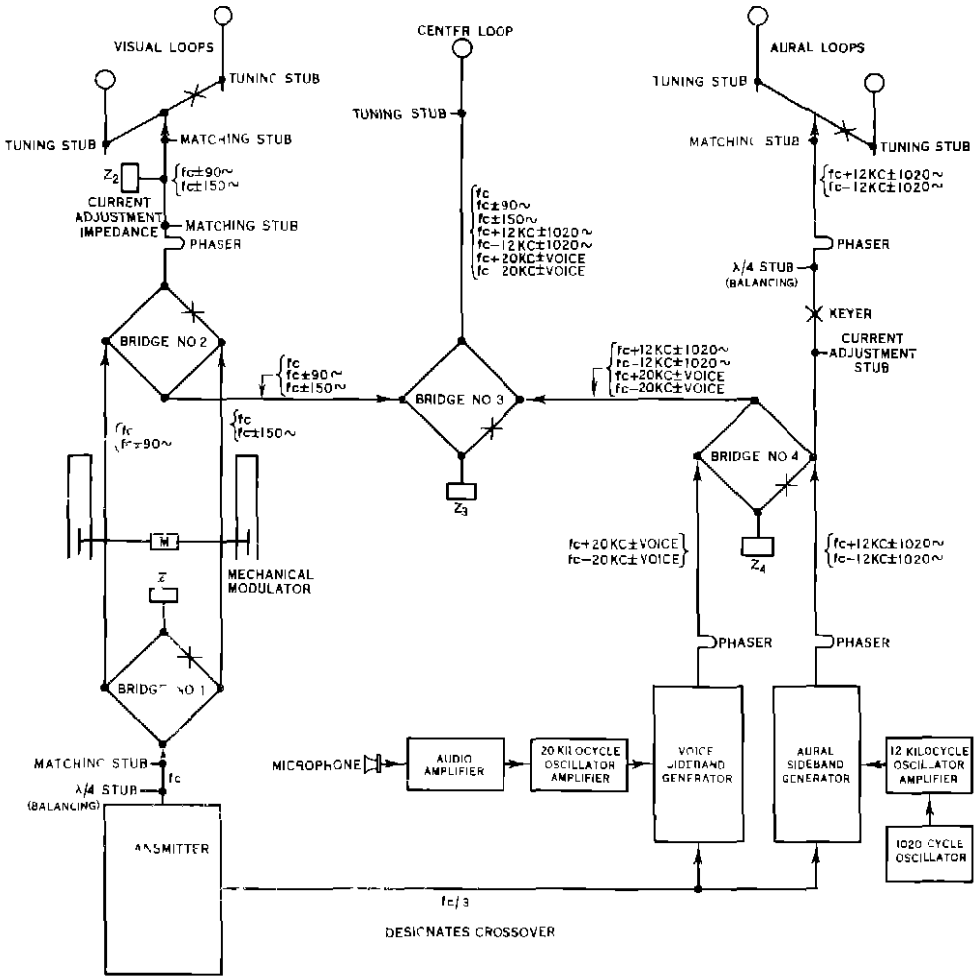

Figure 2 Block Diagram of System No 2

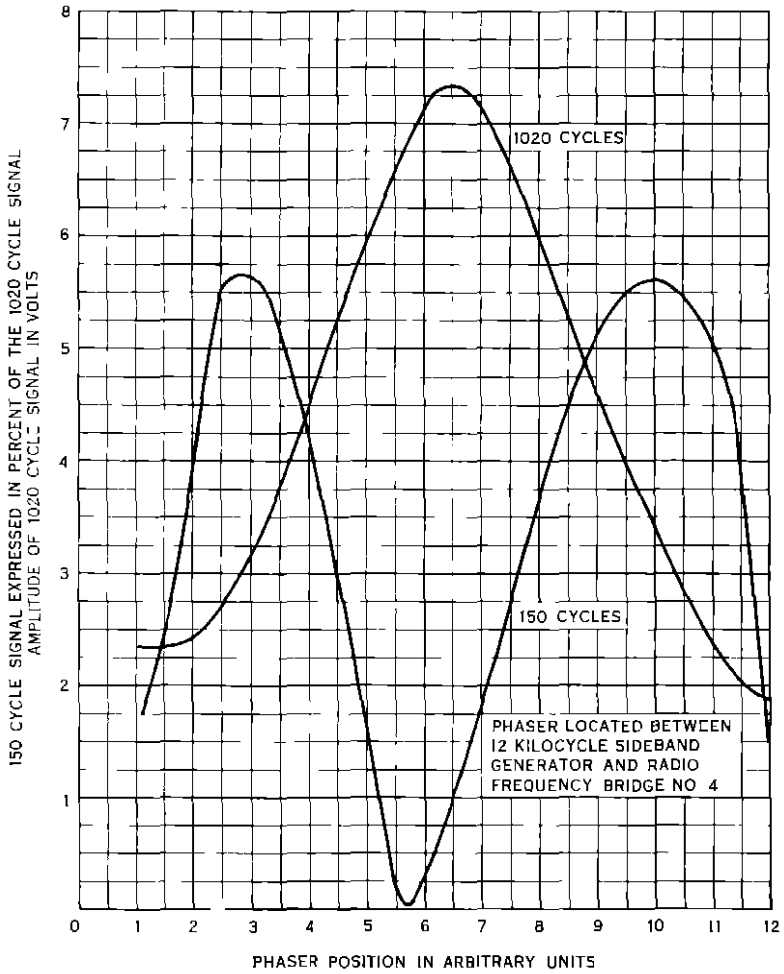

Figure 32 1020 Cycle Output Volts, and 150 Cycle Output in Percent of 1020 Cycle Signal, versus Phaser Position Measurements Made at Output of 12 Kilocycle Detector Amplifier in the Receiving Equipment

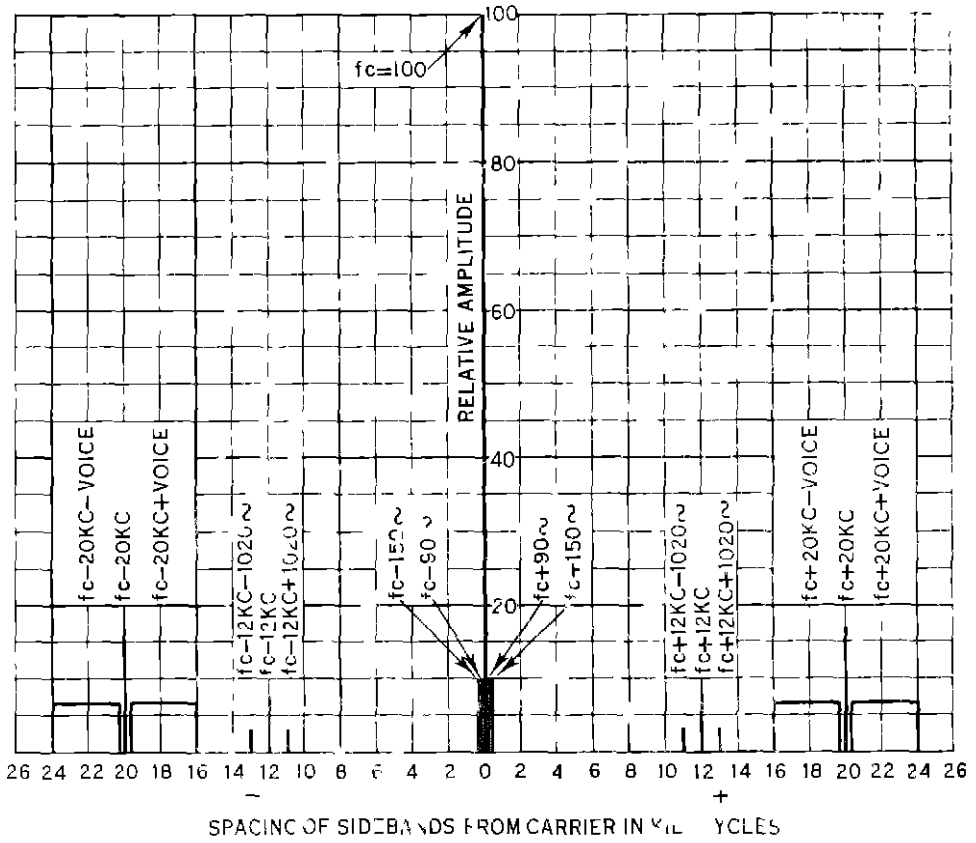

Figure 33 Frequency Spectrum of System No 2

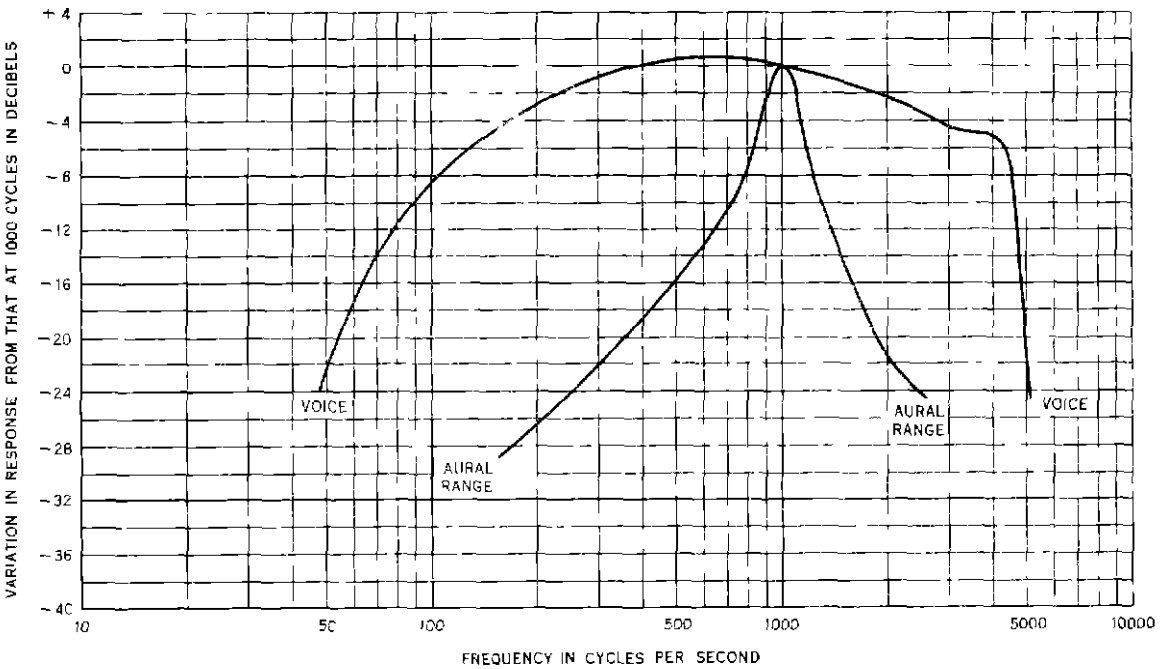

Figure 34 Over-all Transmitter and Receiver Audio Response for Both Voice and Aural Channels of System No 2

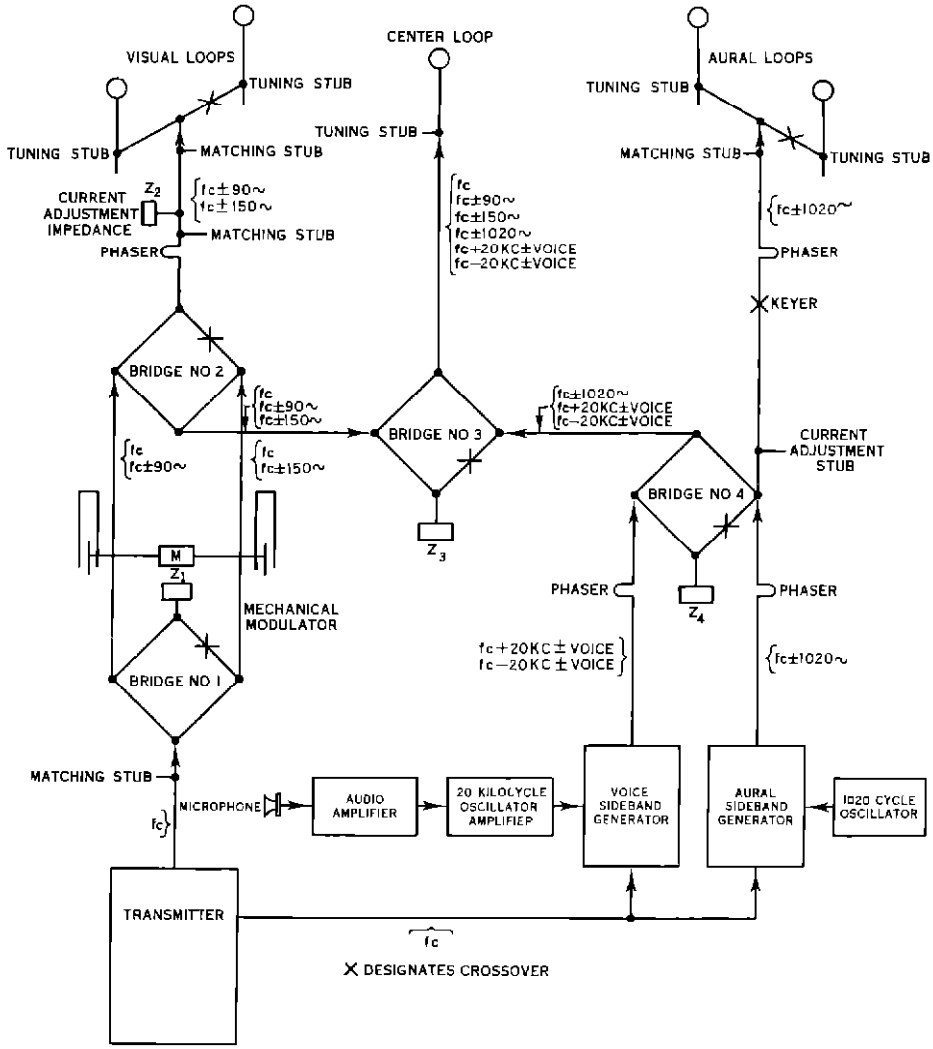

Figure 35 Block Diagram of System No 3

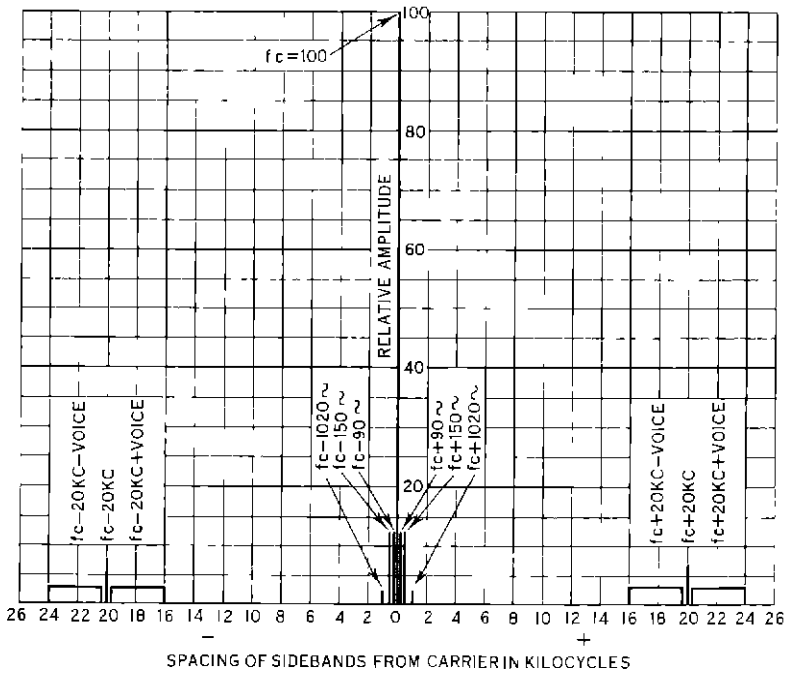

Figure 36 Frequency Spectrum of System No 3

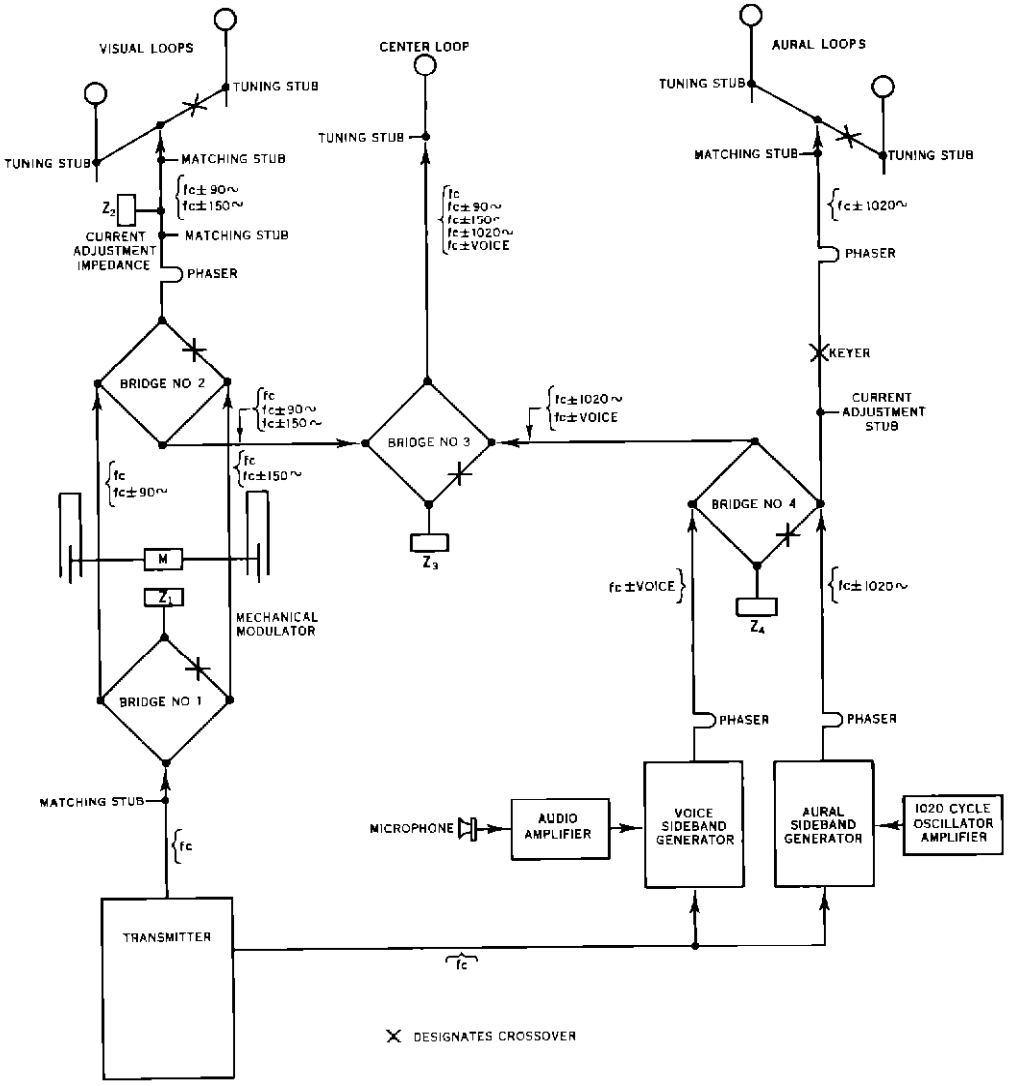

Figure 37 Block Diagram of System No 4

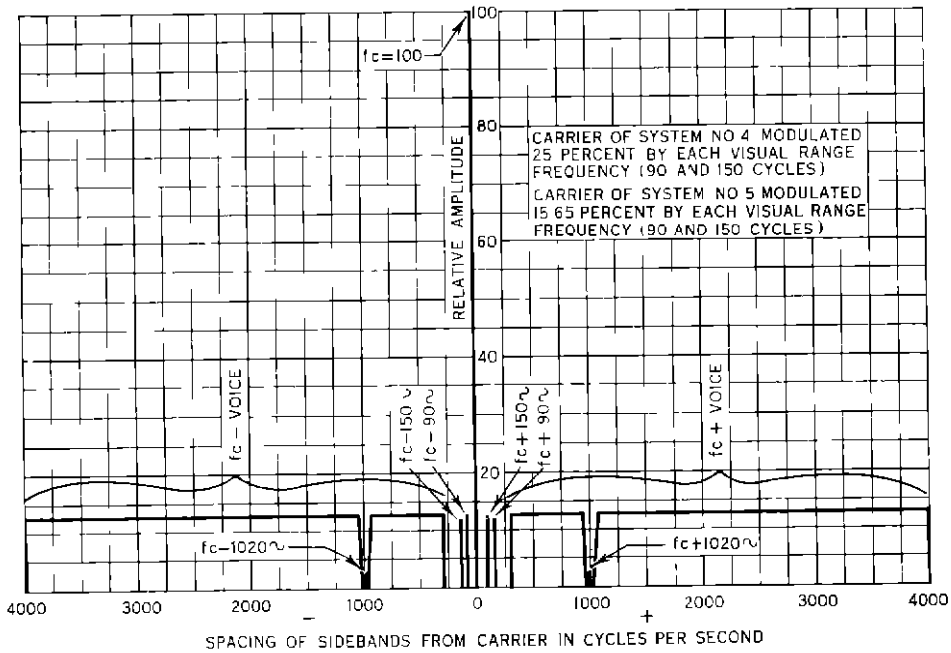

Figure 38 Frequency Spectrum of System No 4

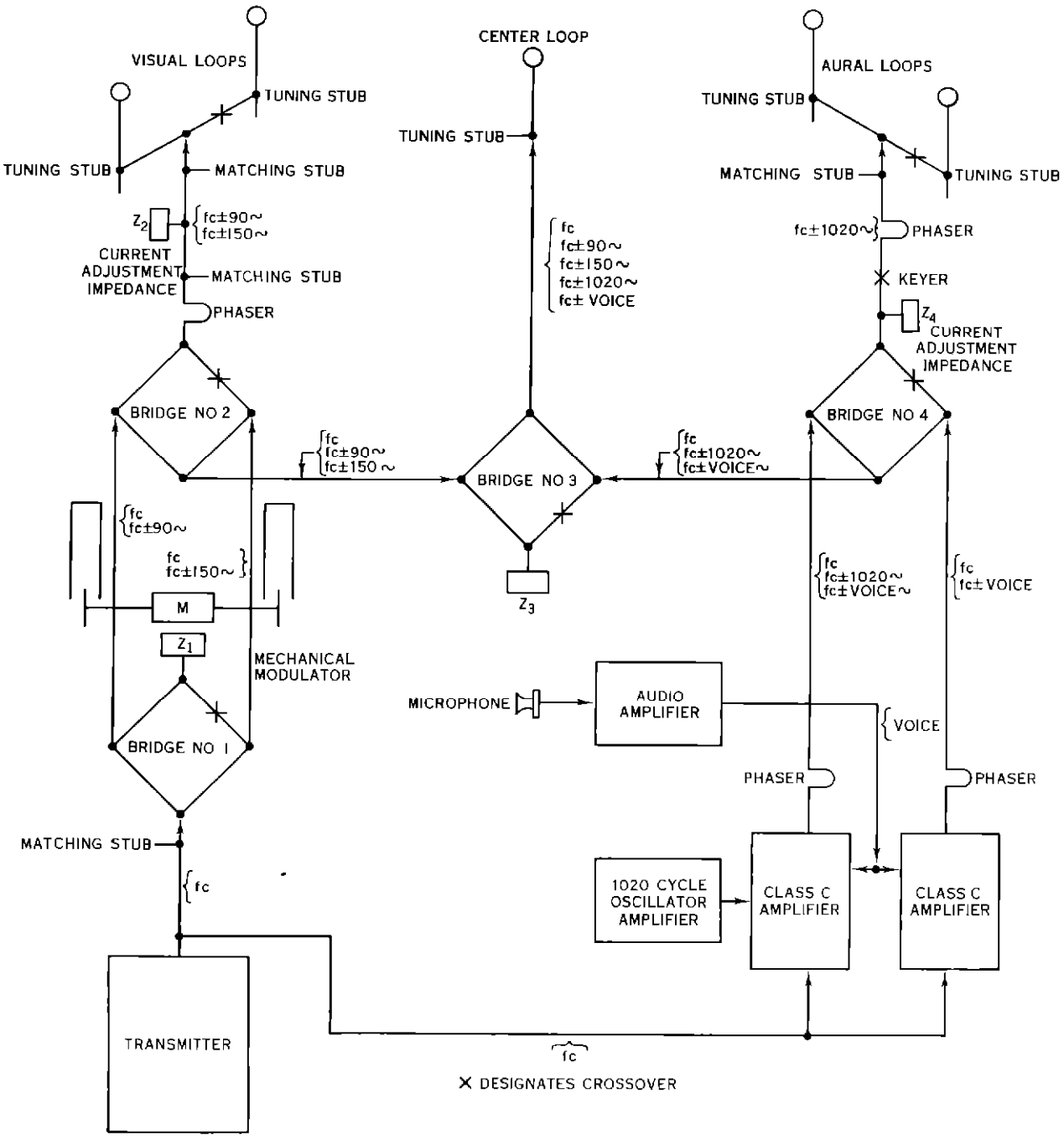

Figure 39 Block Diagram of System No 5

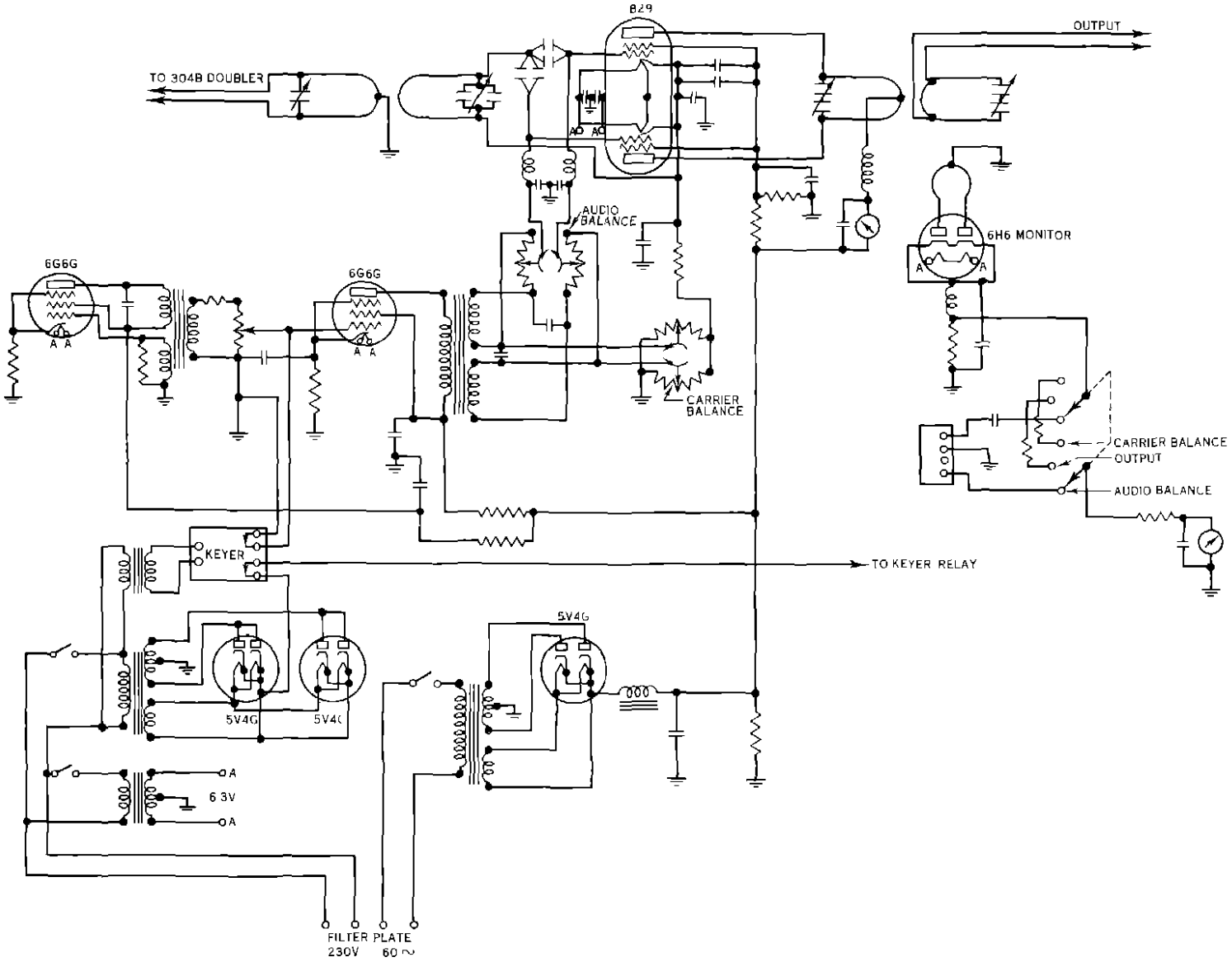

Figure 40 Schematic Diagram of the Sideband Generator Used in the Non-Simultaneous System

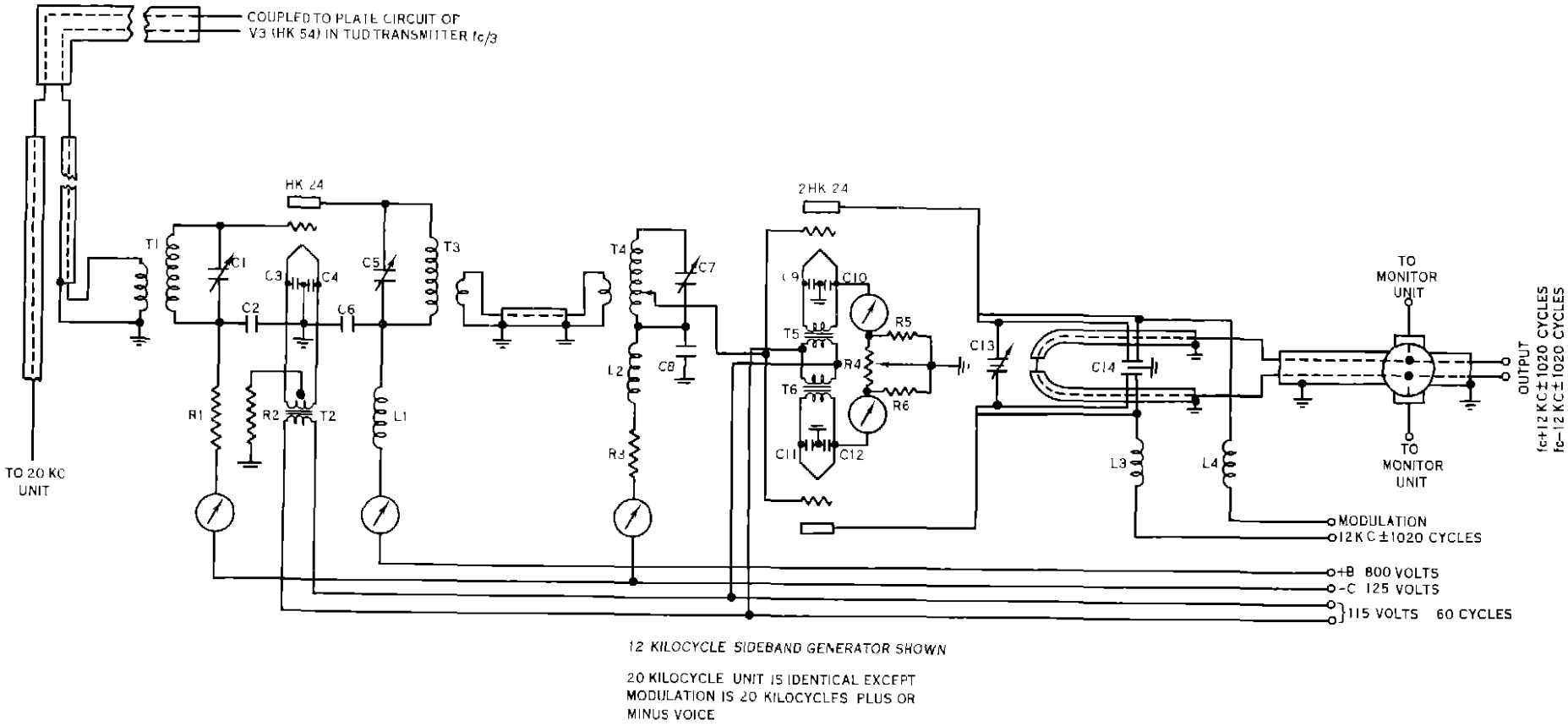

Figure 41 Schematic Diagram of the Sideband Generators for System No 2

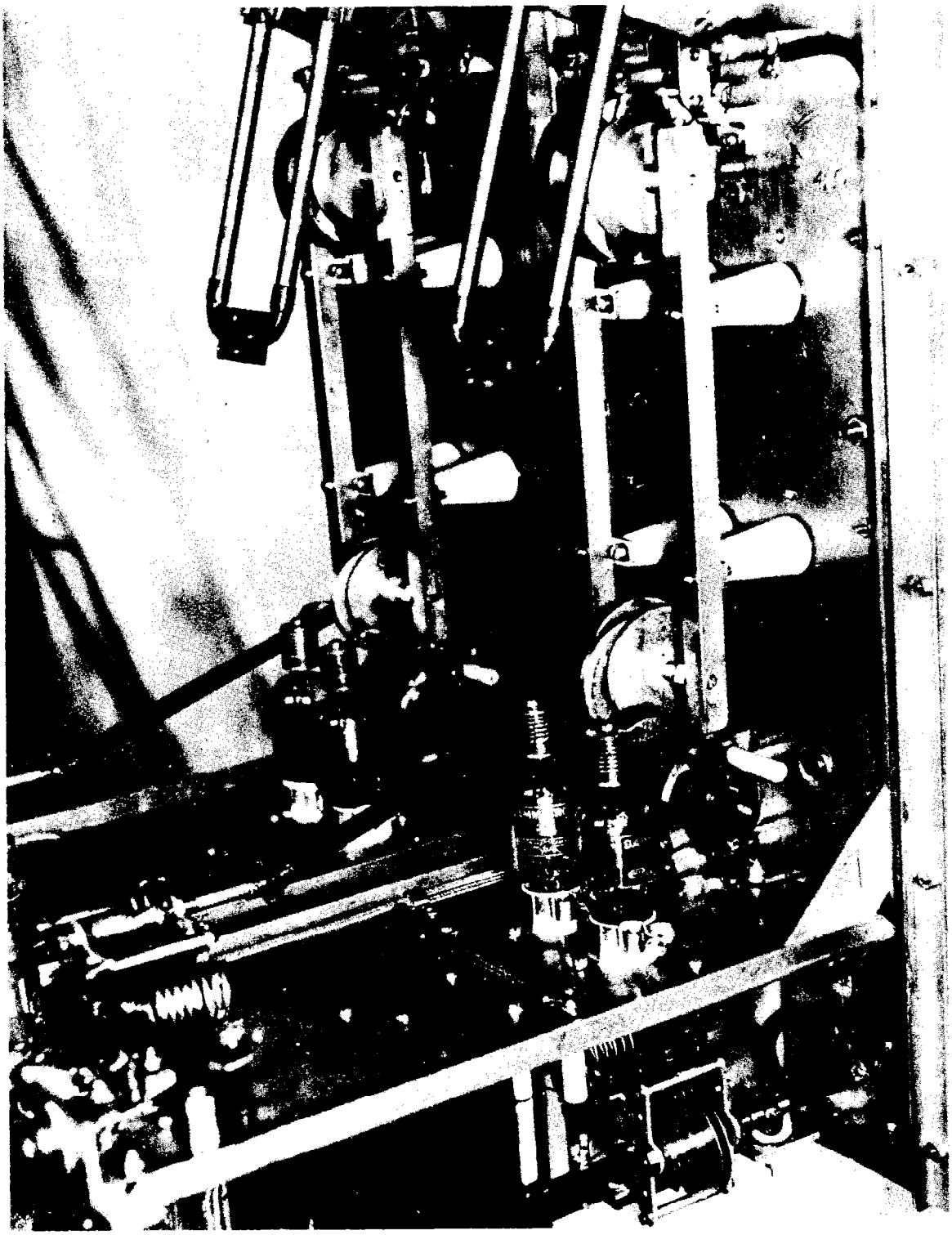

Figure 42. Closeup of the Sideband Generator Tank Circuits for System No. 2.

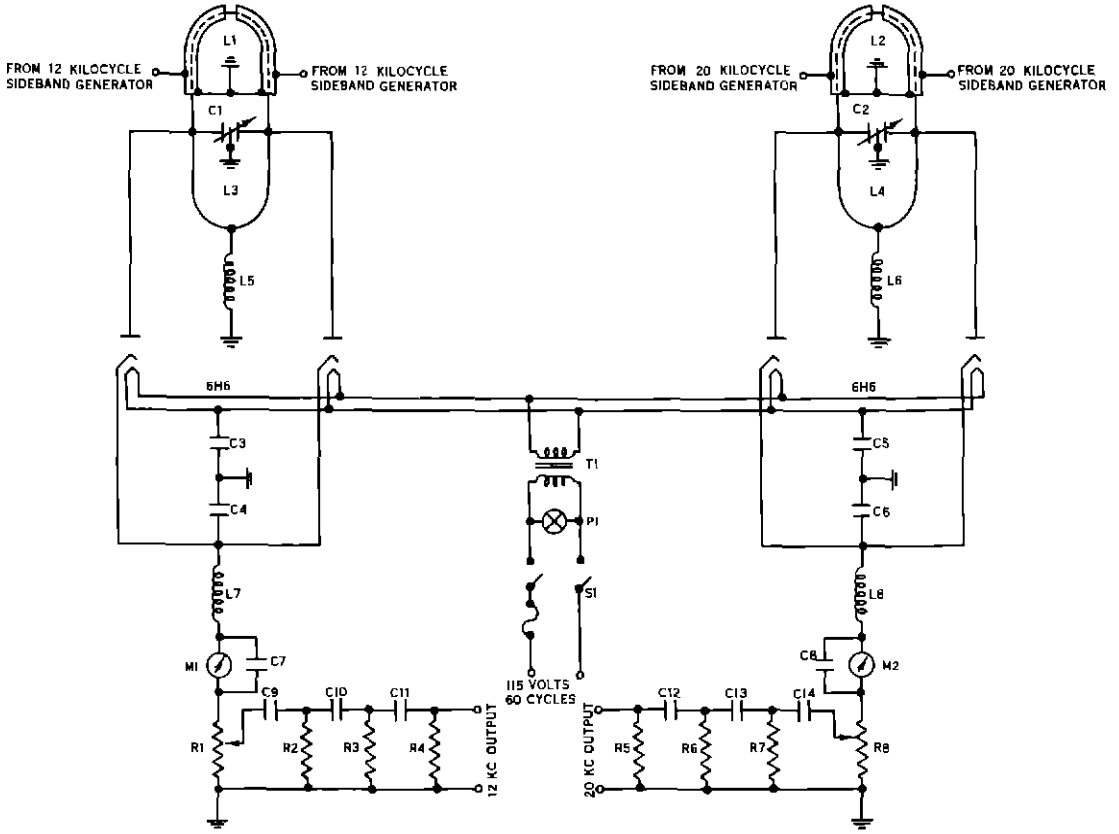

Figure 43 Schematic Diagram of the Sideband Generator Monitors for System No 2

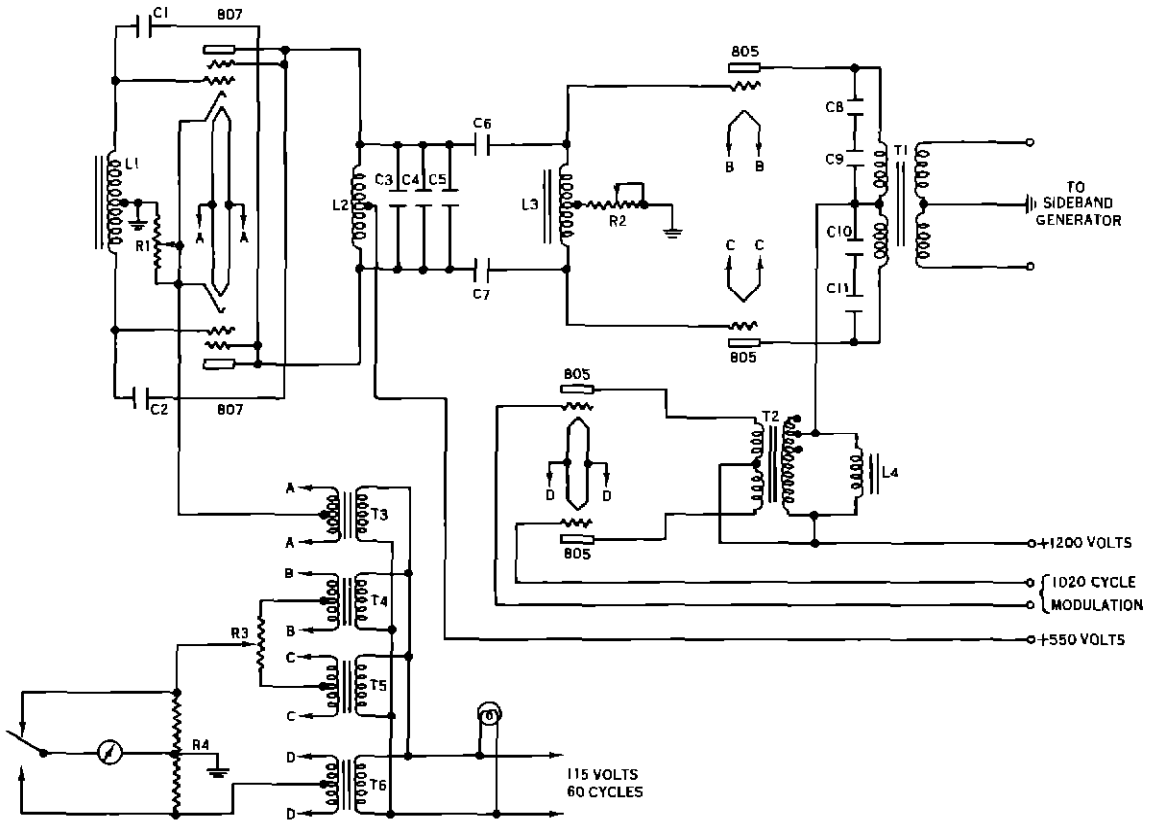

Figure 44 Schematic Diagram of the 12-Kilocycle Subcarrier Generator for System No 2

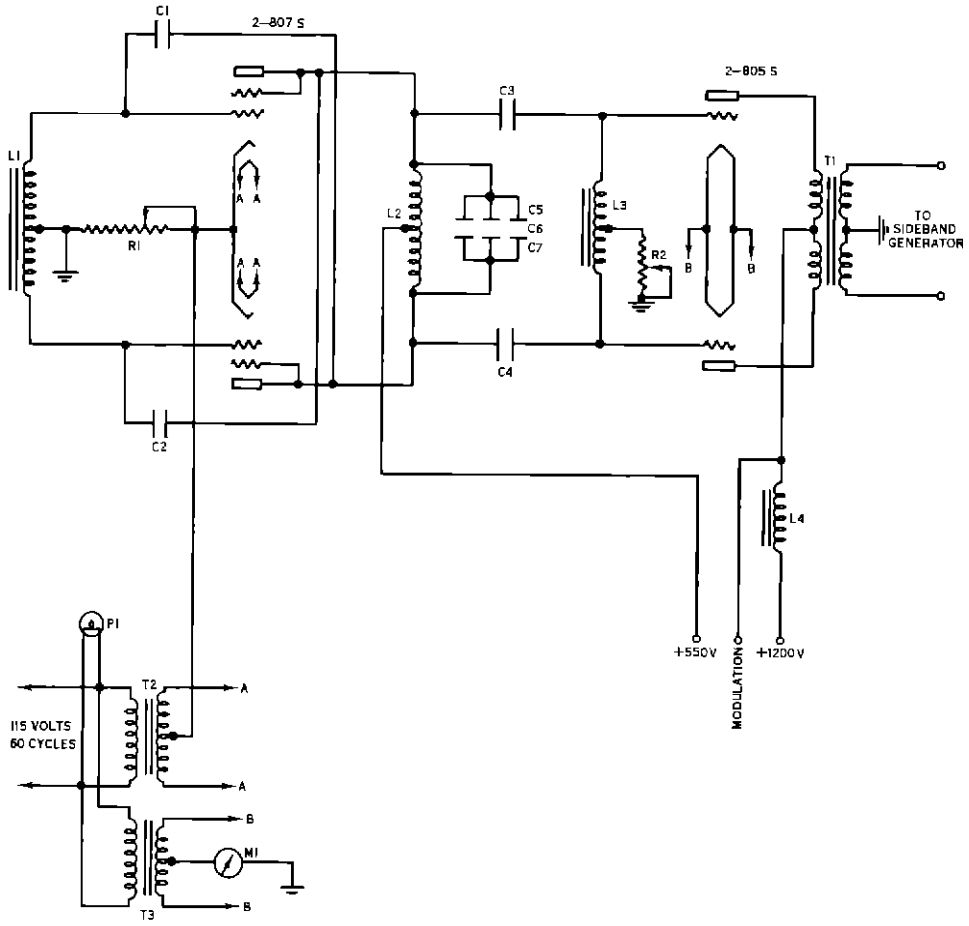

Figure 45 Schematic Diagram of the 20 Kilocycle Subcarrier Generator for System No 2

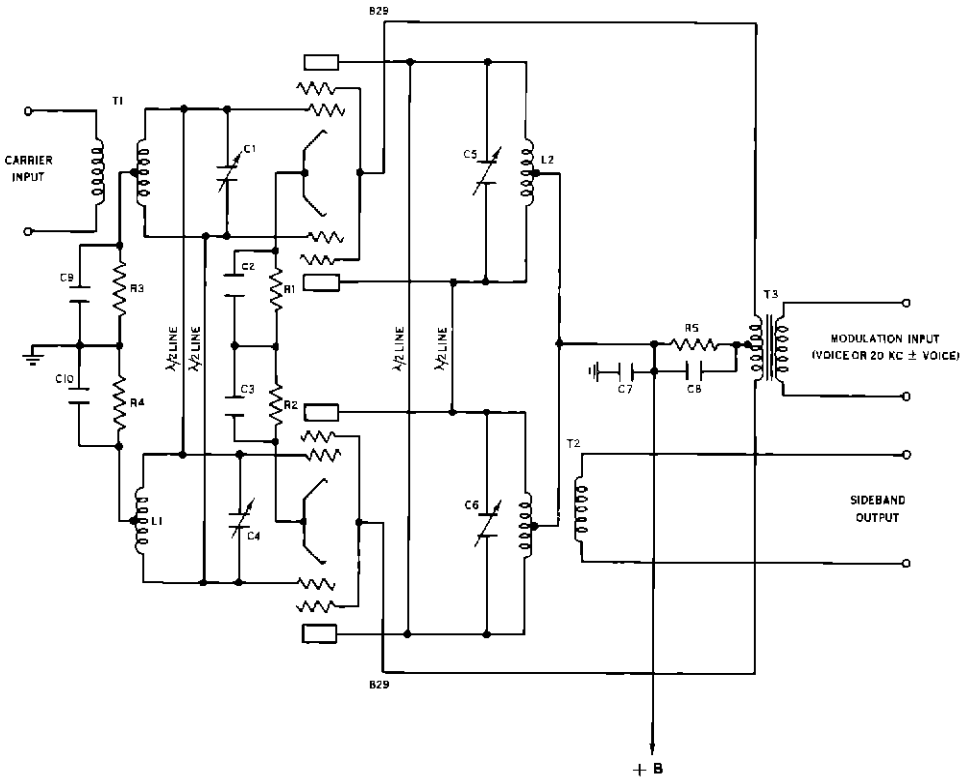

Figure 46 Schematic Diagram of the Sideband Generator for Systems Nos 3 and 4

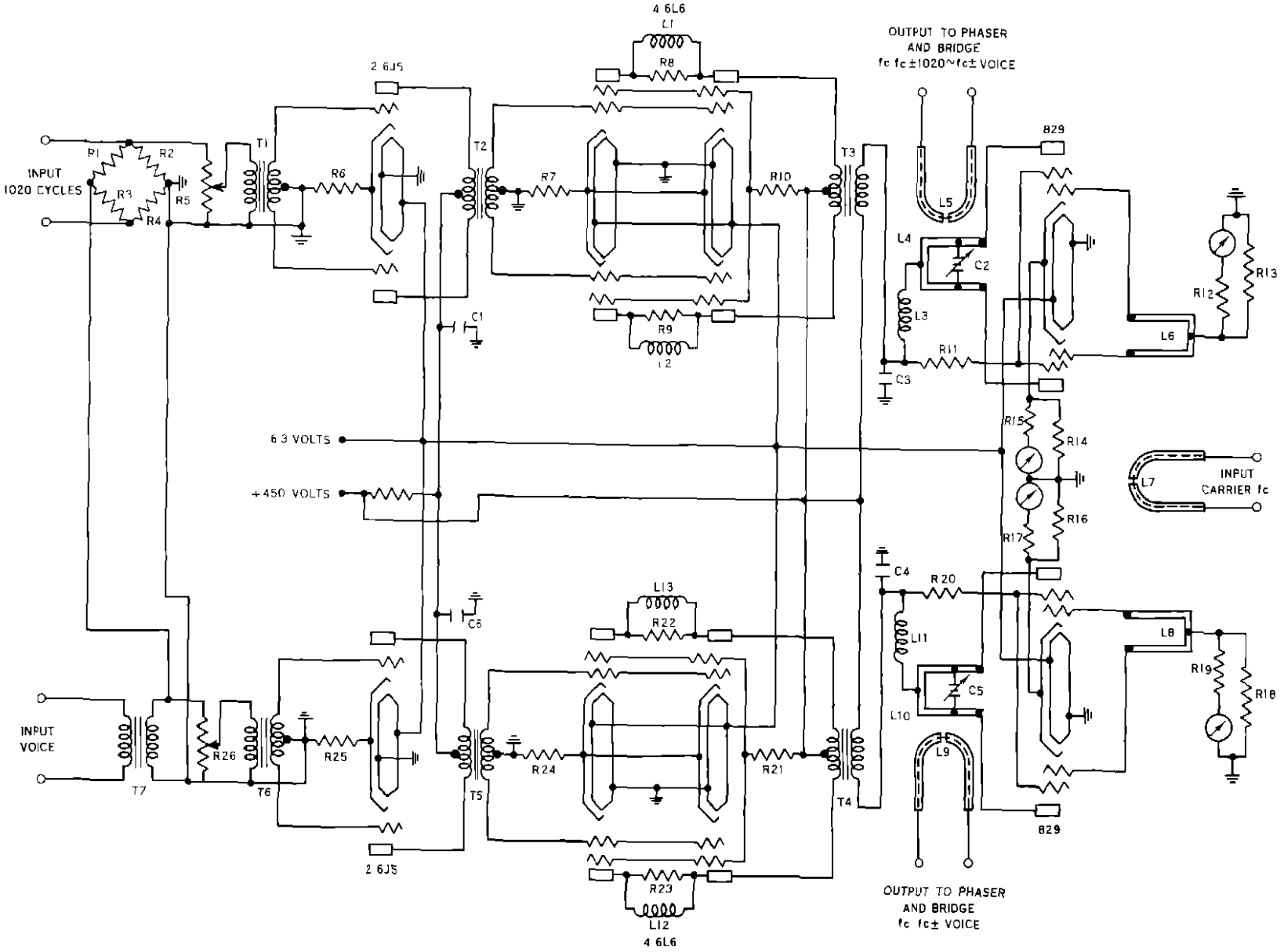

Figure 47 Schematic Diagram of the Class C Amplifiers and Modulating Equipment for System No 5

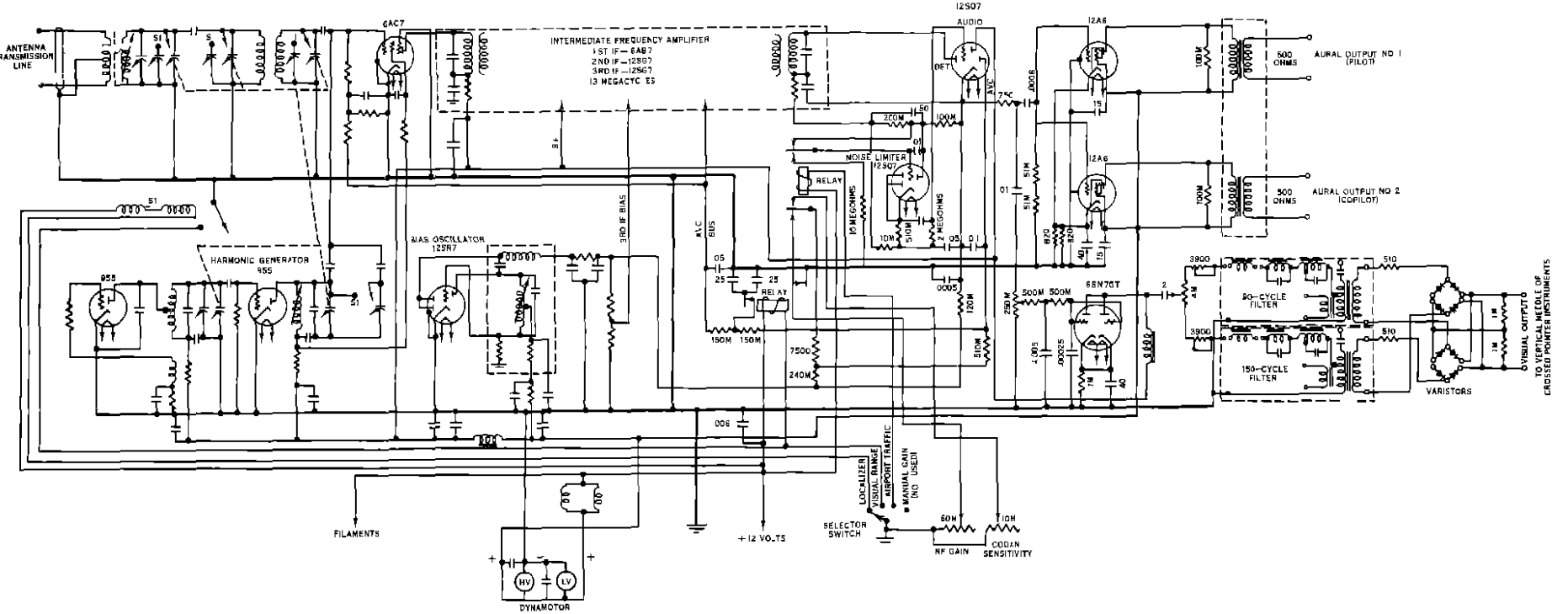

Figure 48 Schematic Diagram of the Type 32A Receiver

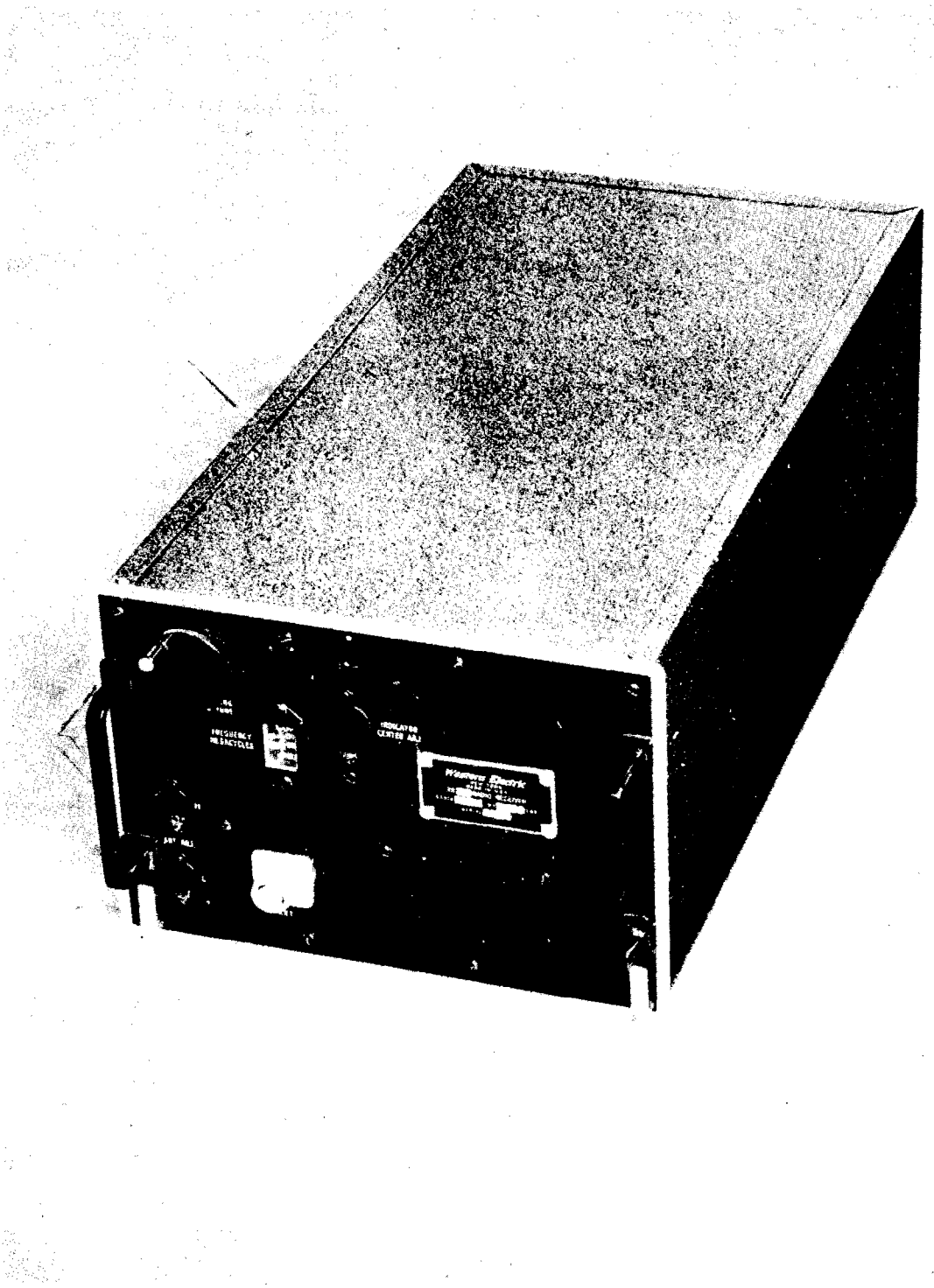

Figure 49. Front View of the Type 32A Receiver.

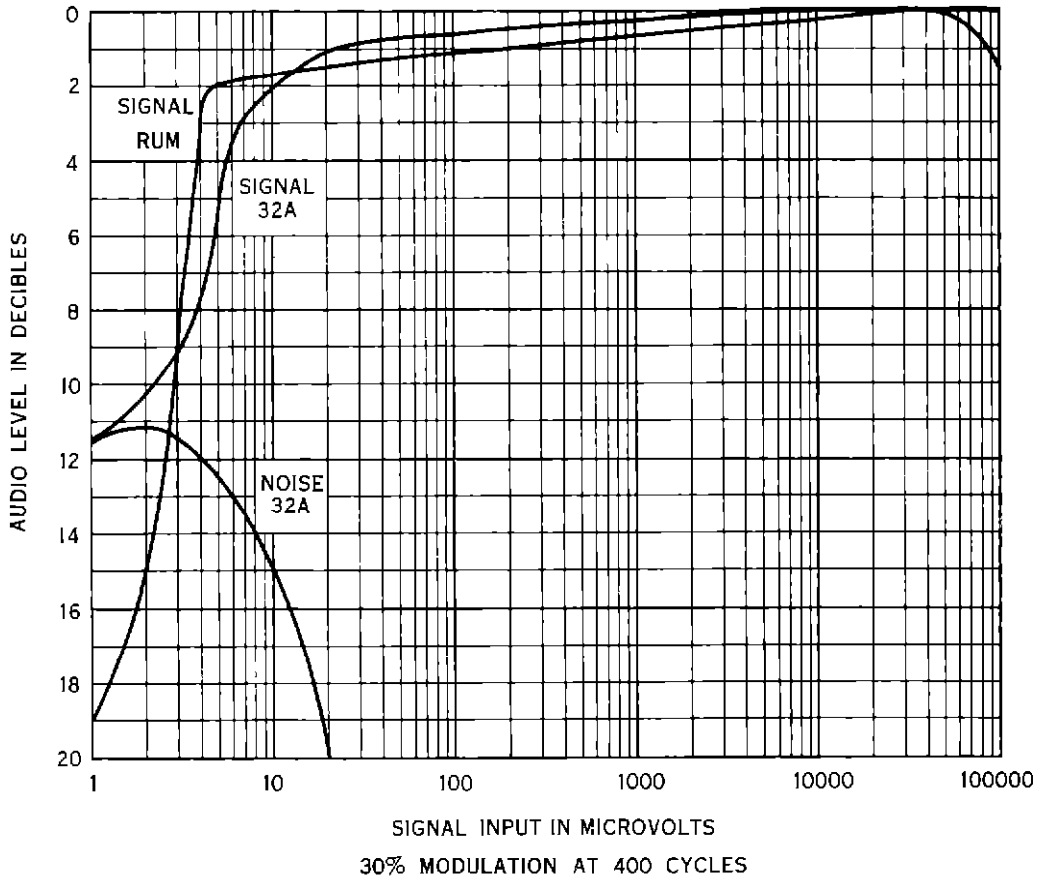

Figure 50 Automatic Volume Control Characteristics for the Type RUM and 32A Receivers

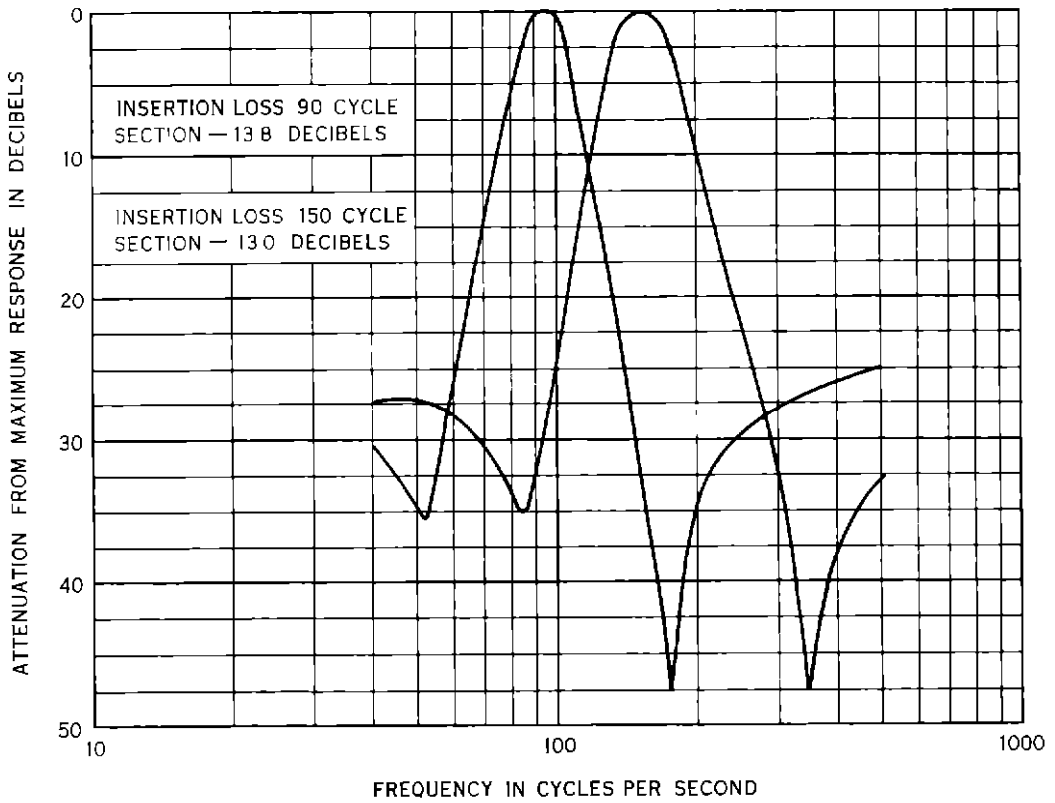

Figure 51 Response of the 90-Cycle and 150-Cycle Audio Filters Used in Both Types of Receivers

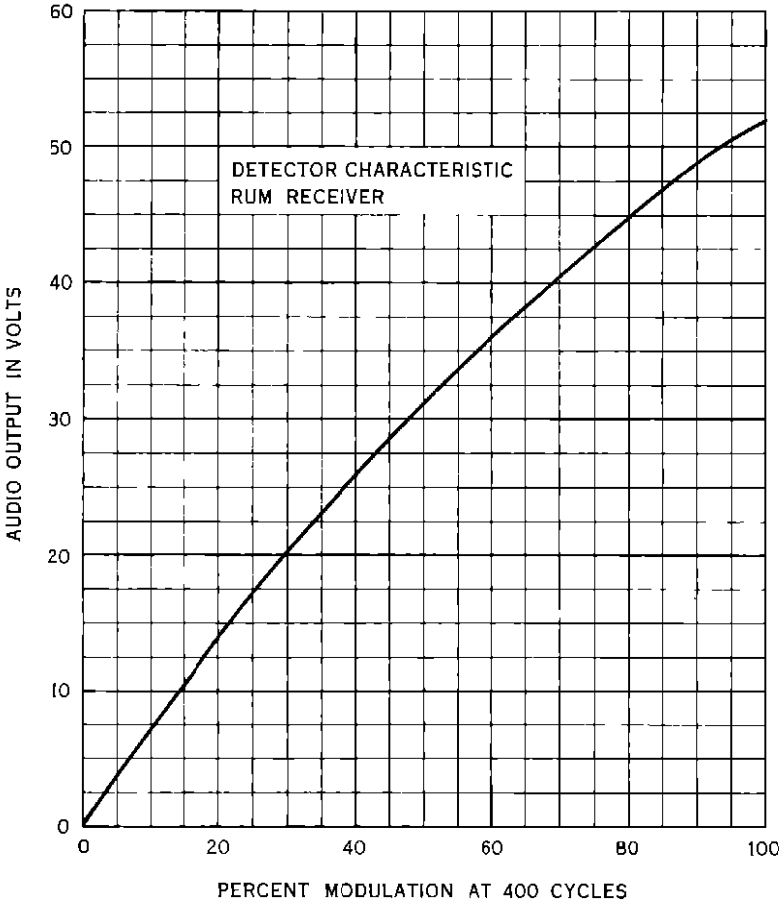

Figure 52 Characteristic of Second Detector Used in the Type RUM Receiver

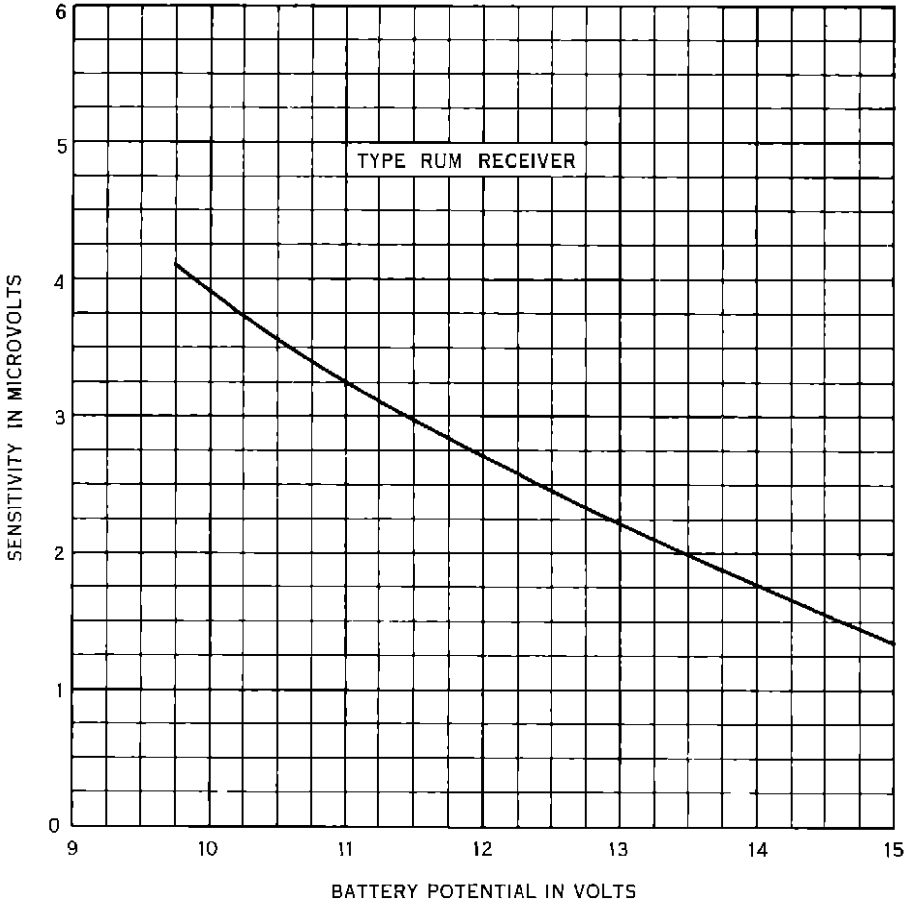

Figure 53 Absolute Sensitivity versus Battery Voltage for the Type RUM Receiver

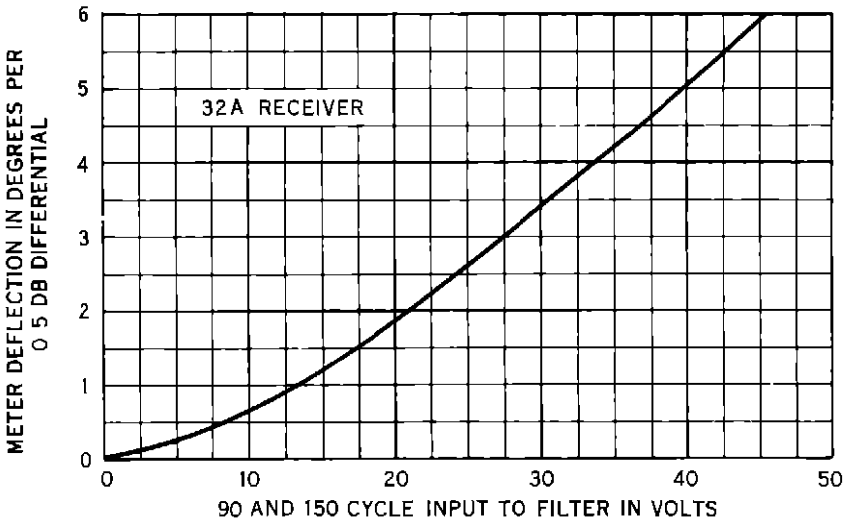

Figure 54 Change in Meter Deflection versus Filter Input Voltage for the Type 32A Receiver

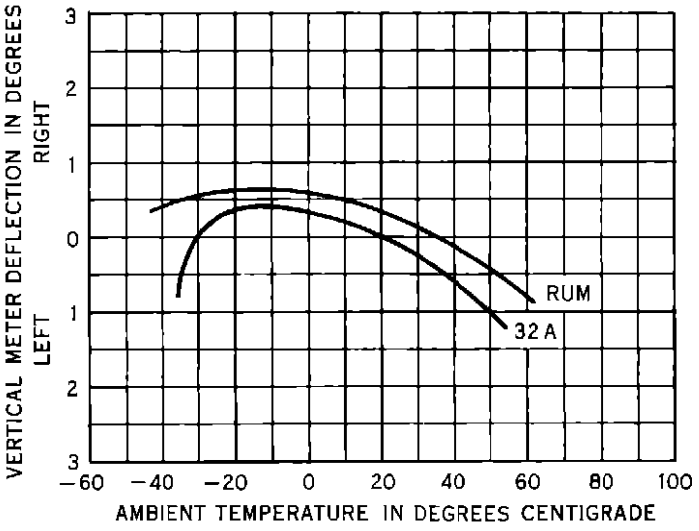

Figure 55 Change in Meter Deflection versus Ambient Temperature for the Type RUM and 32A Receivers

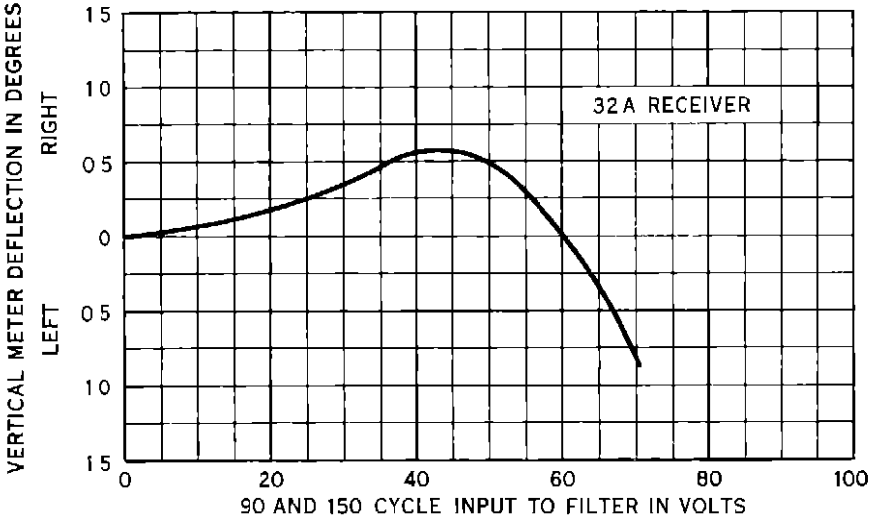

Figure 56 Change in Meter Deflection versus Filter Input Voltage for the Type 32A Receiver

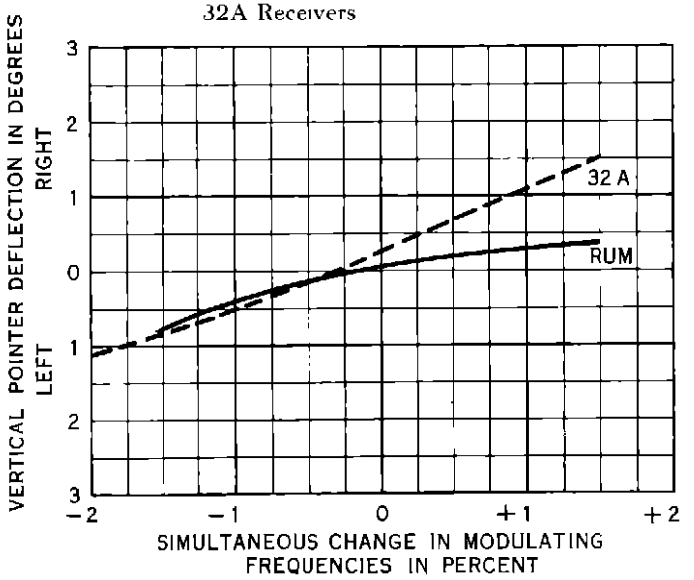

Figure 57 Change in Meter Deflection versus Simultaneous Change in Modulating Frequencies for the Type RUM and 32A Receivers

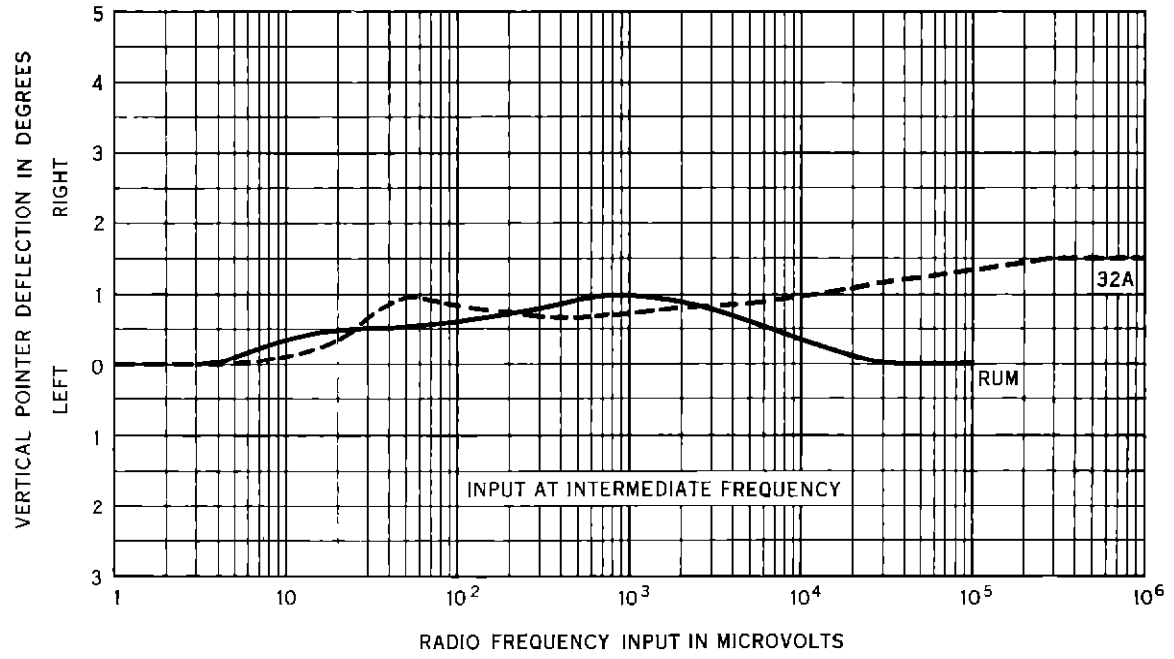

Figure 58 Change in Meter Deflection versus i-f Radio Frequency Input for the Type RUM and 32A Receivers

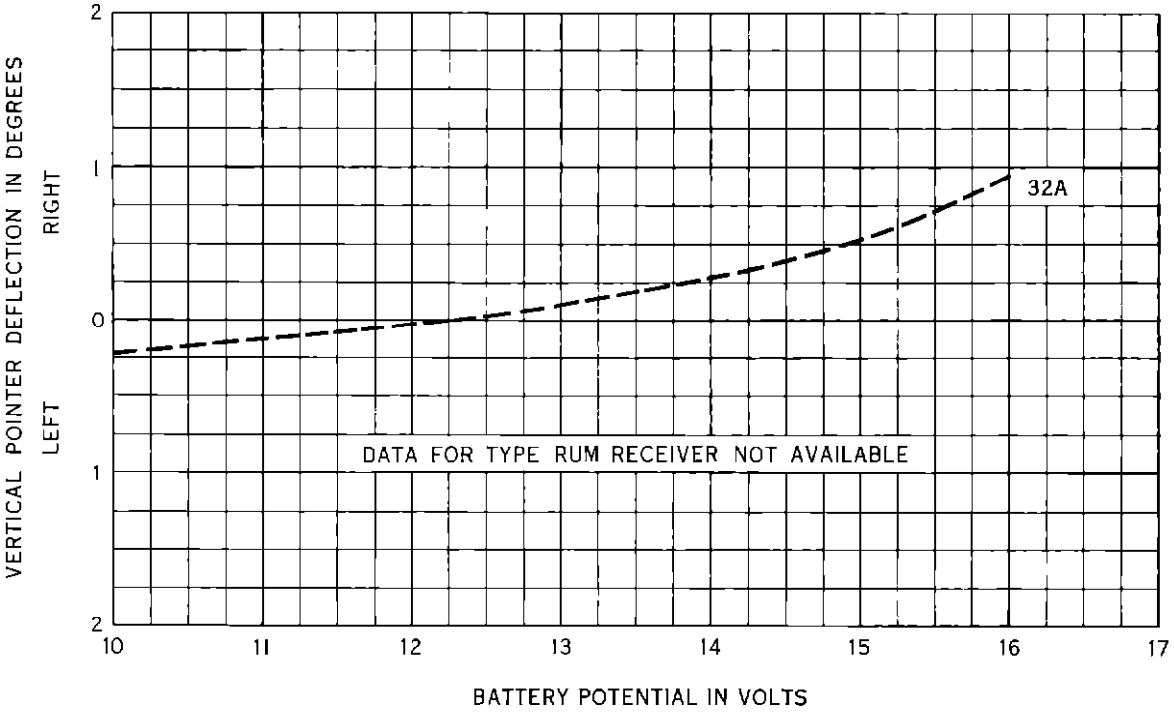

Figure 59 Change in Meter Deflection versus Battery Voltage for the Type 32A Receiver

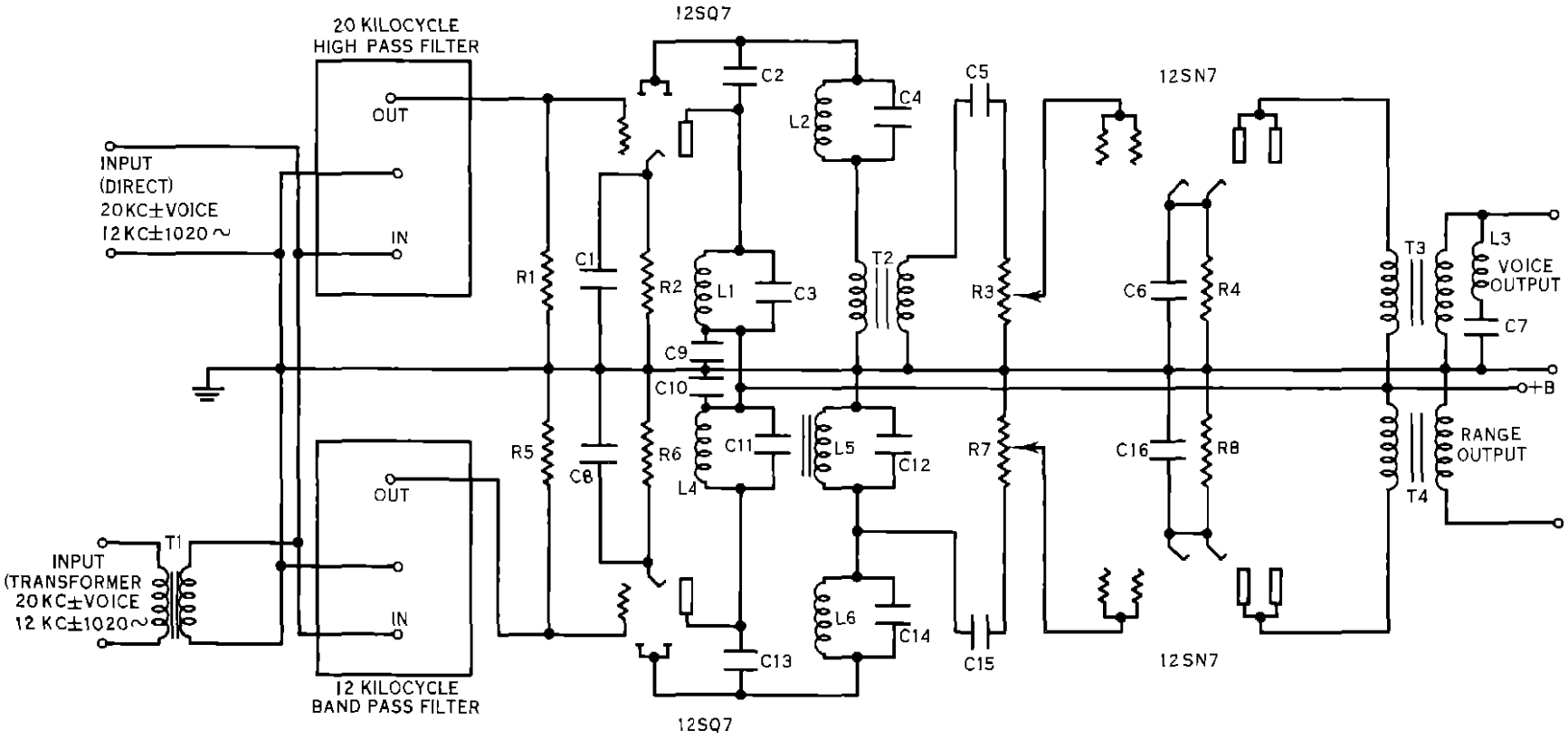

Figure 60 Schematic Diagram of the Subcarrier Amplifier Detector Unit for System No 2

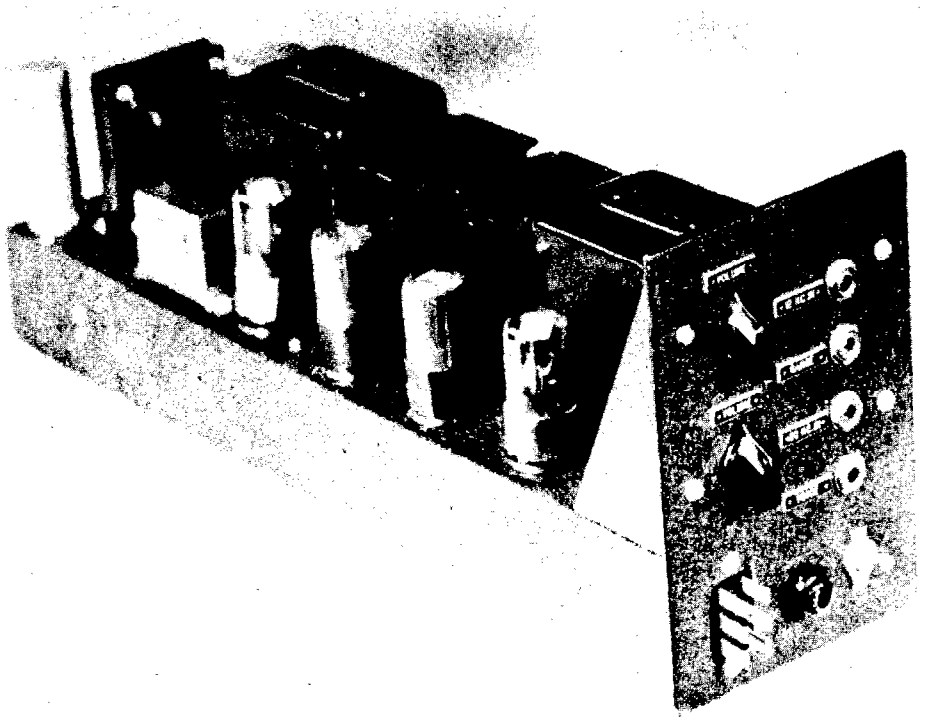

Figure 61. View of the Subcarrier Amplifier-Detector Unit for System No. 2.

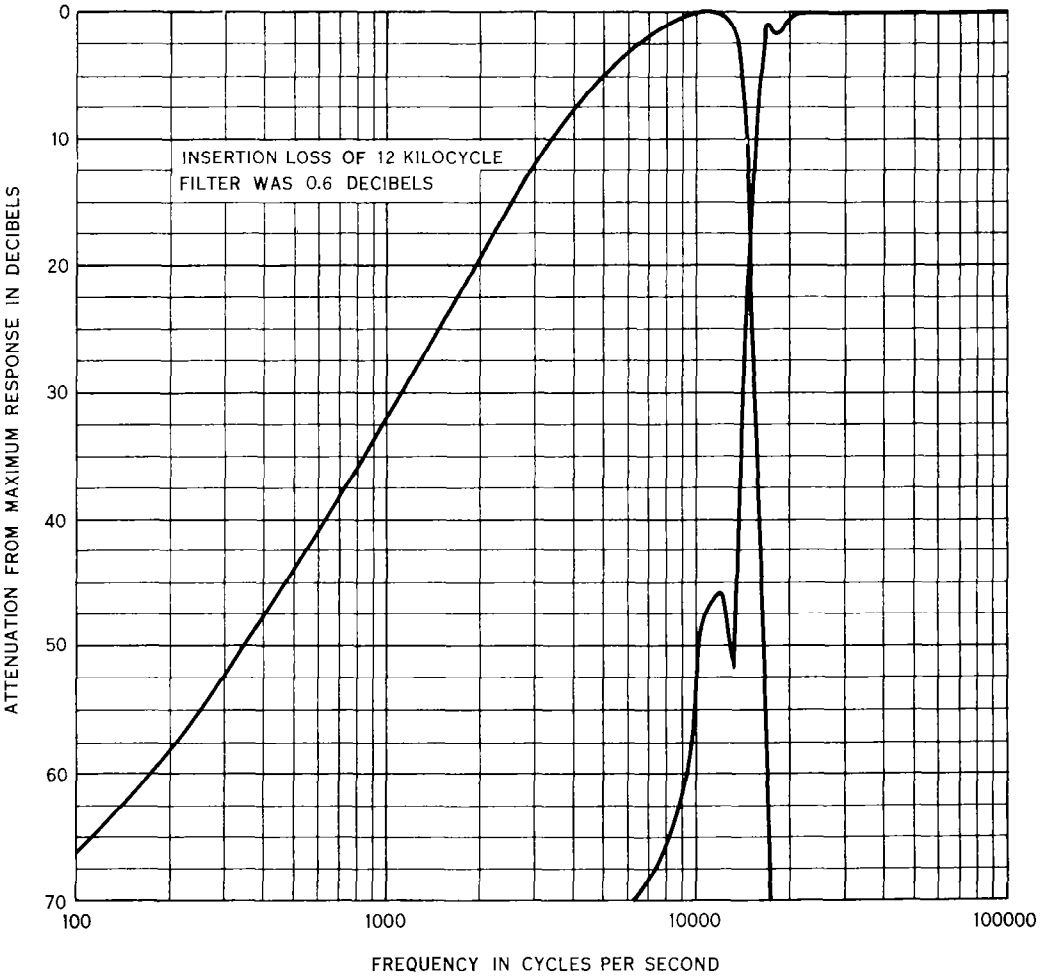

Figure 62. Response of the 12-Kilocycle and 20-Kilocycle Filters.

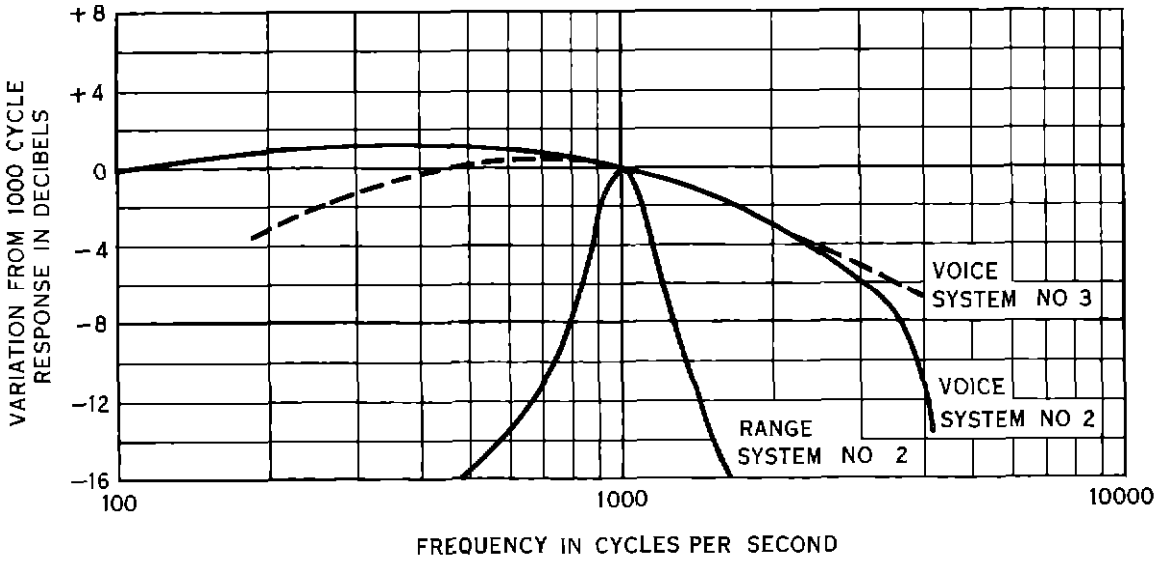

Figure 63 Over-all Output Response of the Subcarrier Amplifier-Detector Unit for System No 2

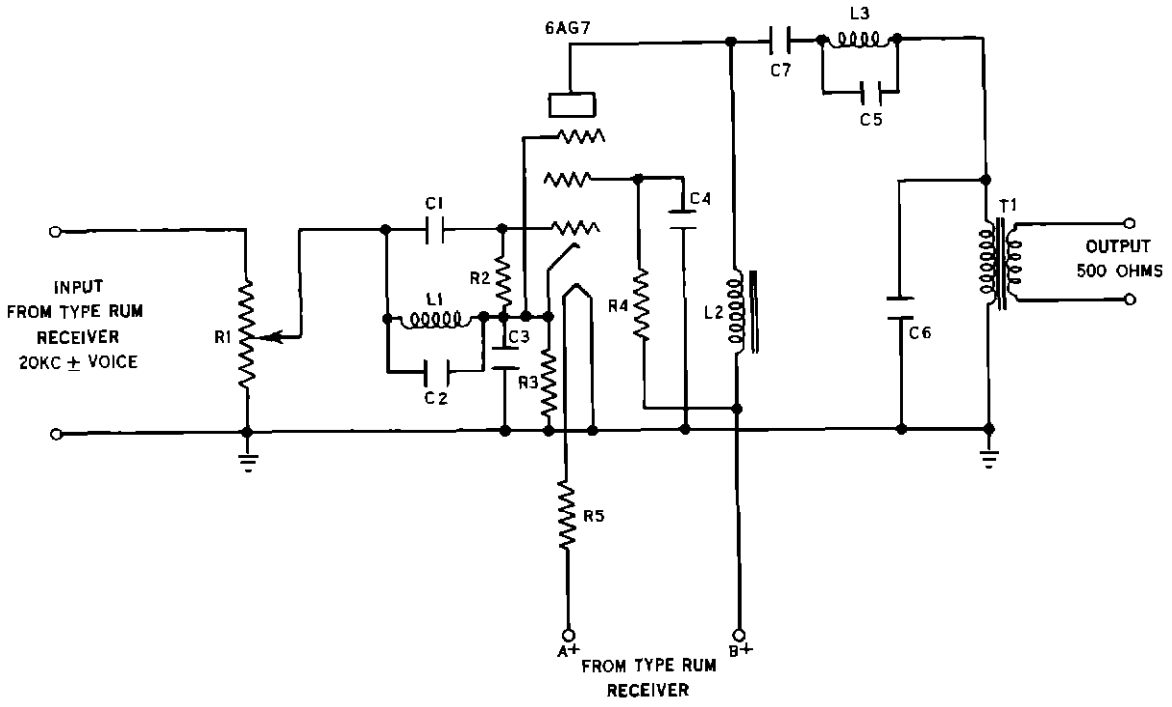

Figure 64 Schematic Diagram of the Subcarrier Amplifier-Detector Unit for System No 3

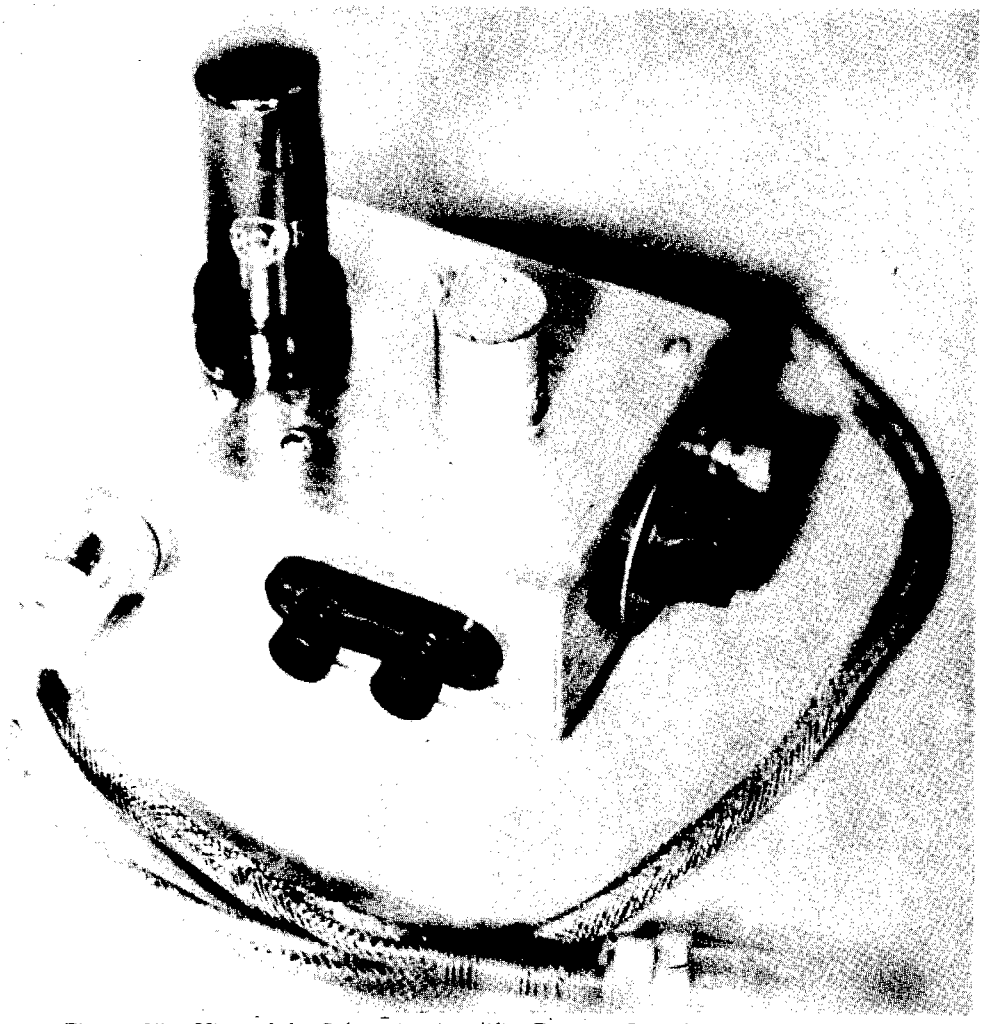

Figure 65. View of the Subcarrier Amplifier-Detector Unit for System No. 3.

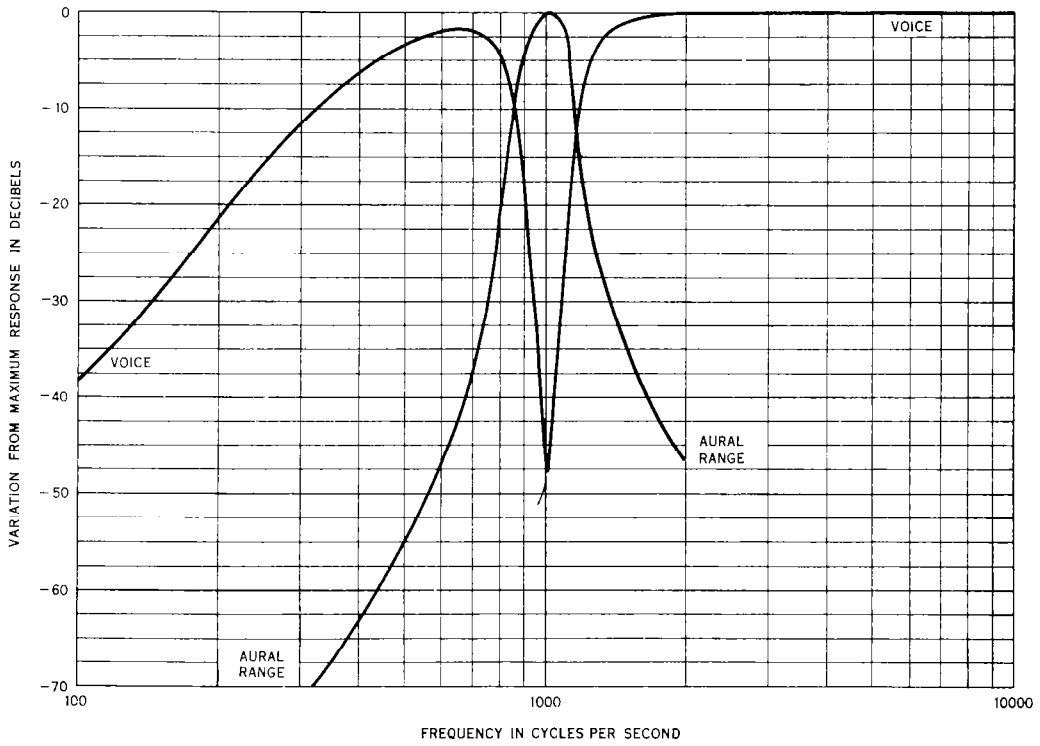

Figure 66. Response of the 1020-cycle Band-Pass Band-Rejection Filter.

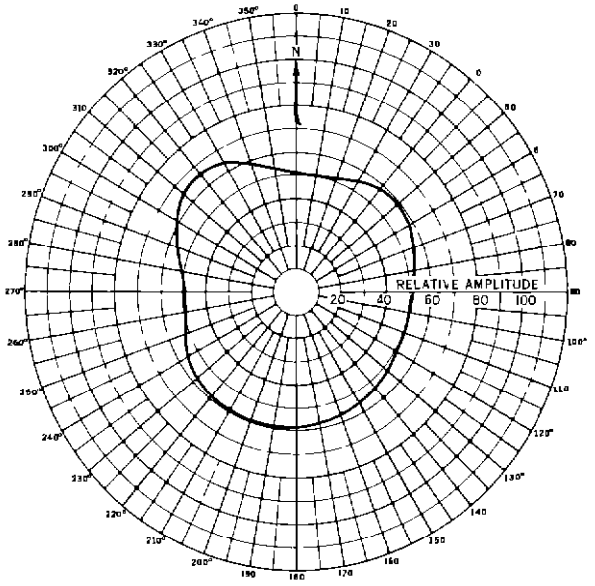

Figure 67 Measured Pattern When Only the Center Loop was Driven in System No 2

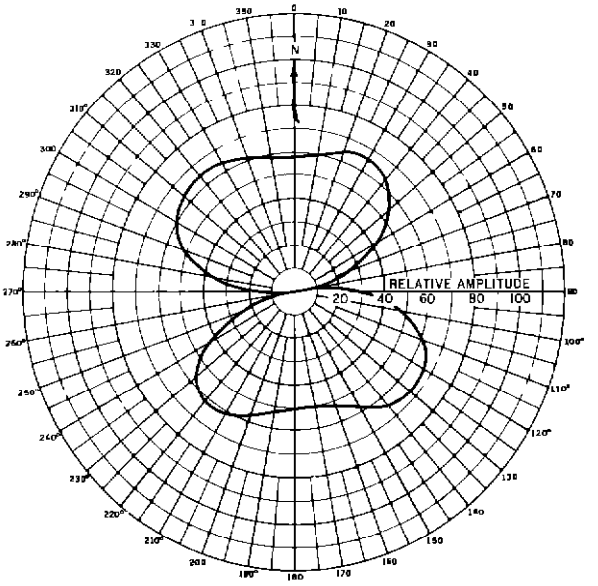

Figure 68 Measured Pattern When Only the Side Visual Antennas Were Driven in System No 2

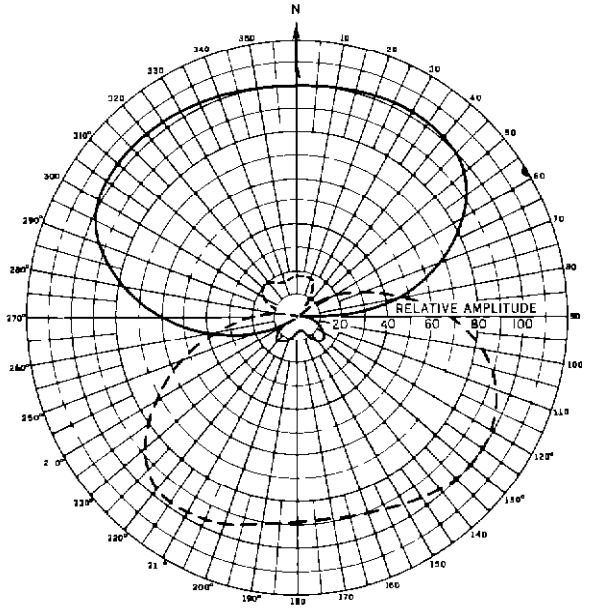

Figure 69 Measured Patterns When all Three Visual Antennas Were Driven in System No 2

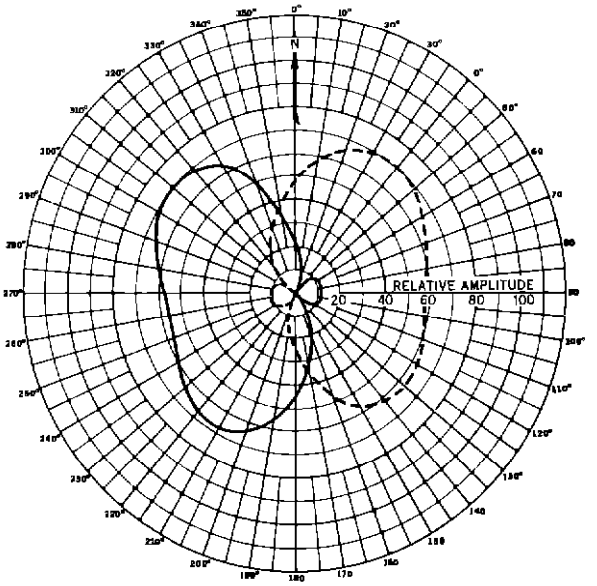

Figure 70 Measured Patterns When all Three Aural Antennas Were Driven in System No 2

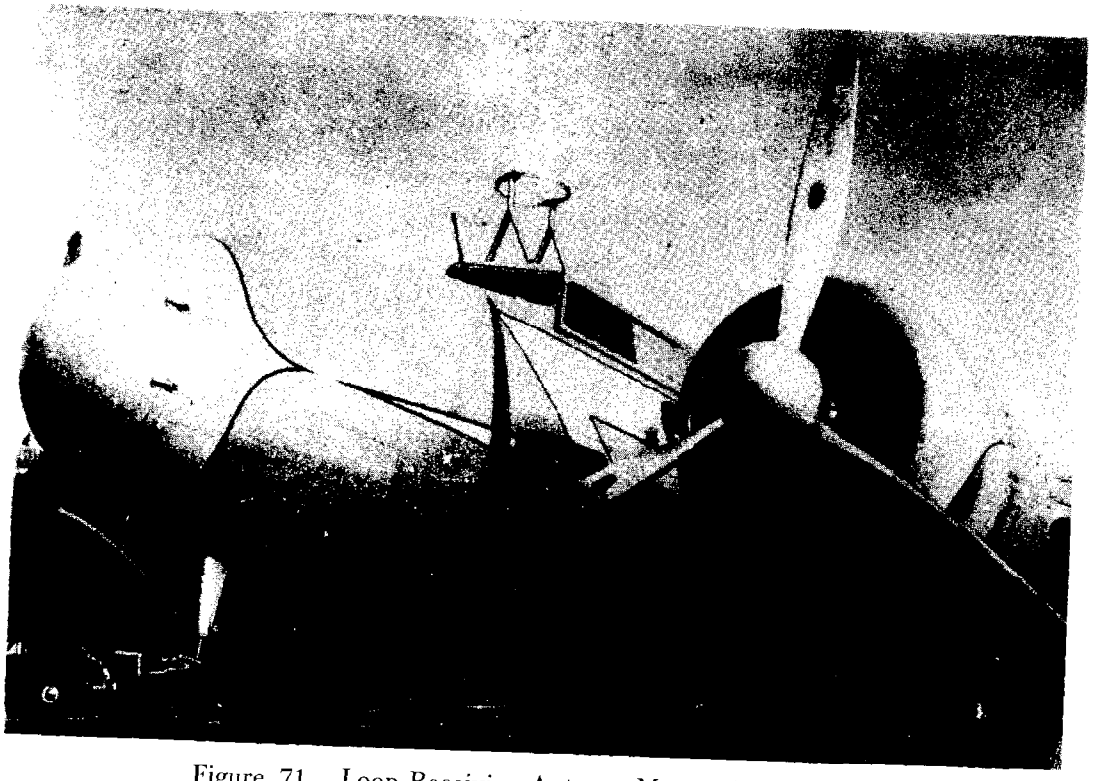

Figure 71. Loop Receiving Antenna Mounted on NC-11.

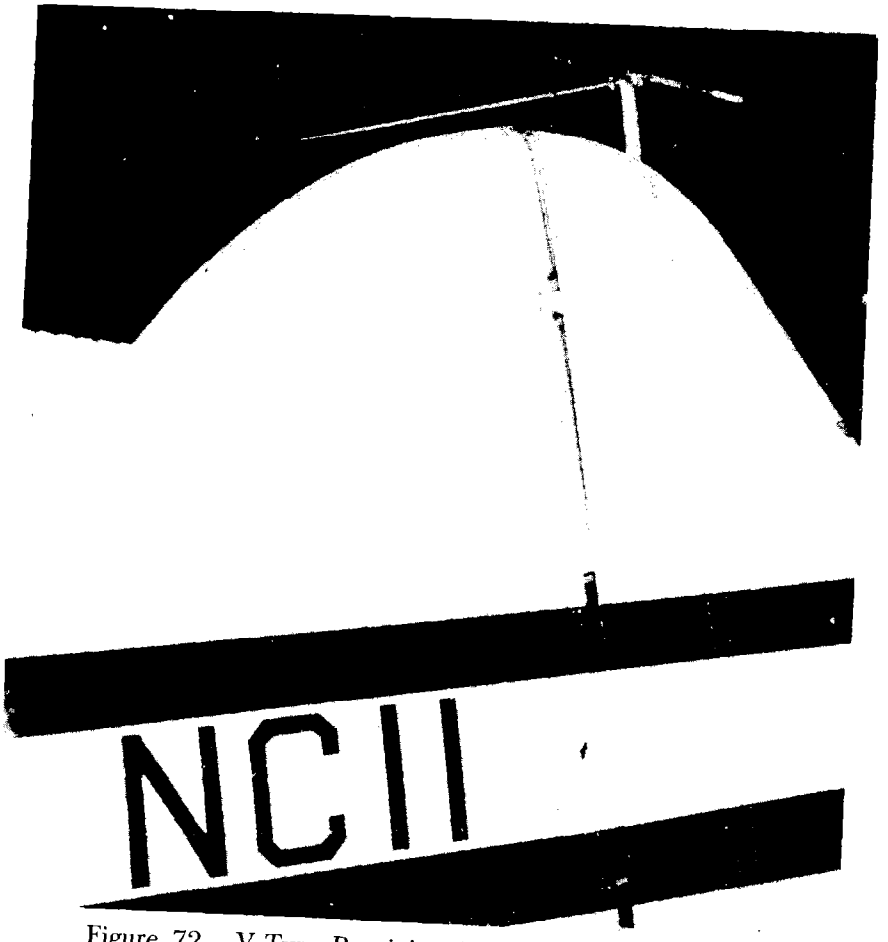

Figure 72. V Type Receiving Antenna Mounted on the Vertical Stabilizer of NC-11.

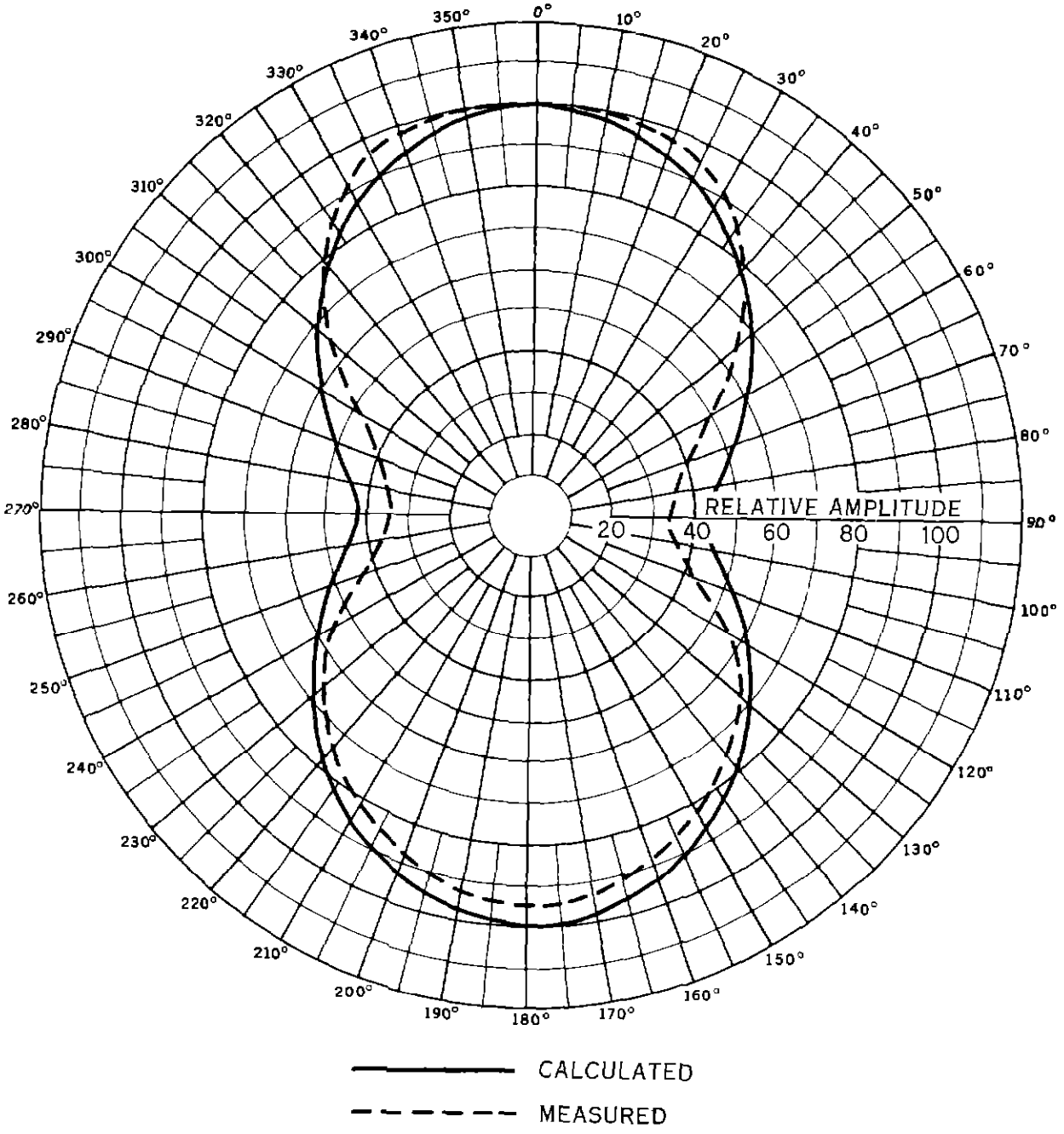

Figure 73 Calculated and Measured Horizontal Field Patterns for the V Type Receiving Antenna

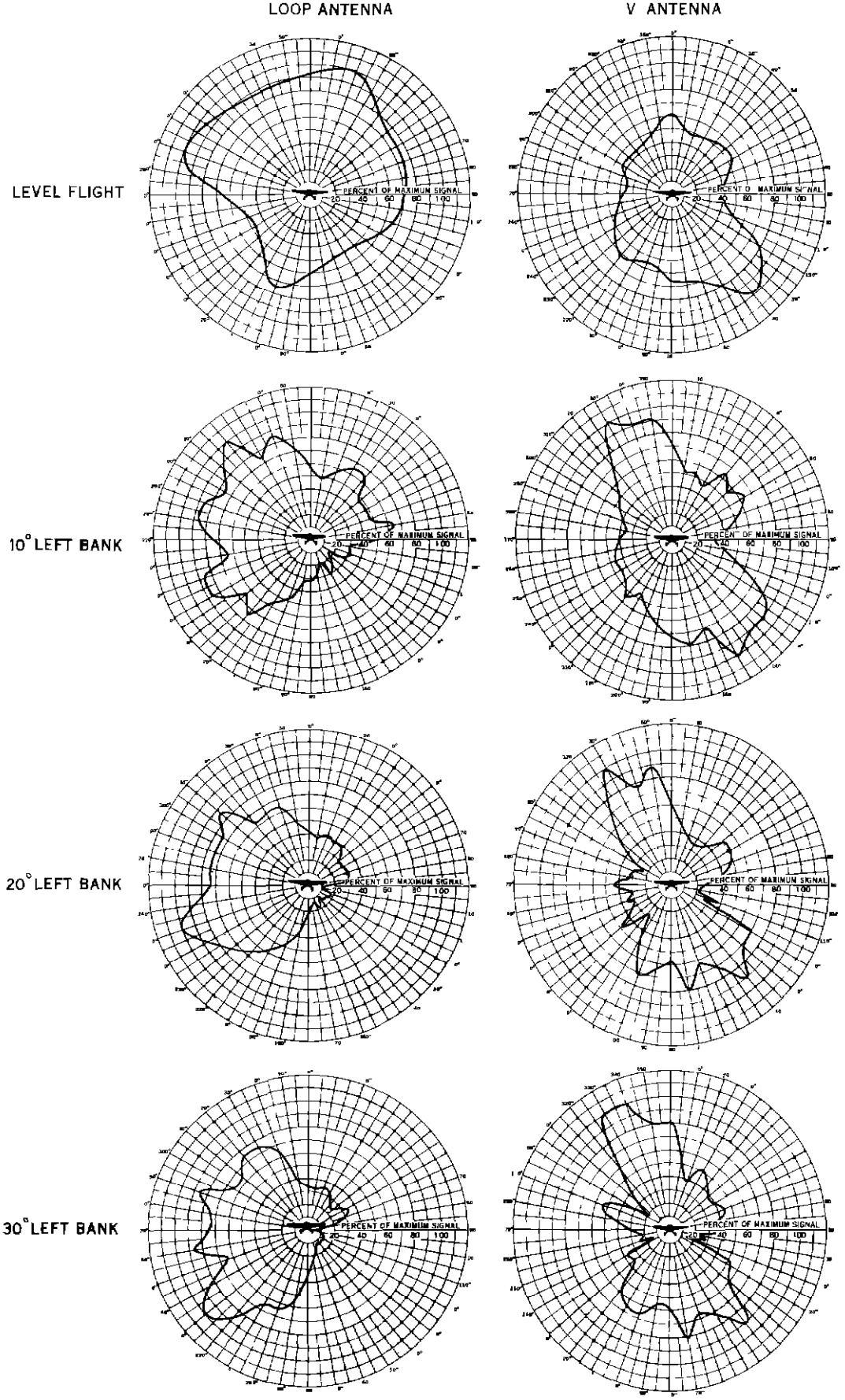

Figure 74 Horizontal Field Patterns of the Loop Antenna and the V Antenna for Level Flight and for Various Degrees of Bank

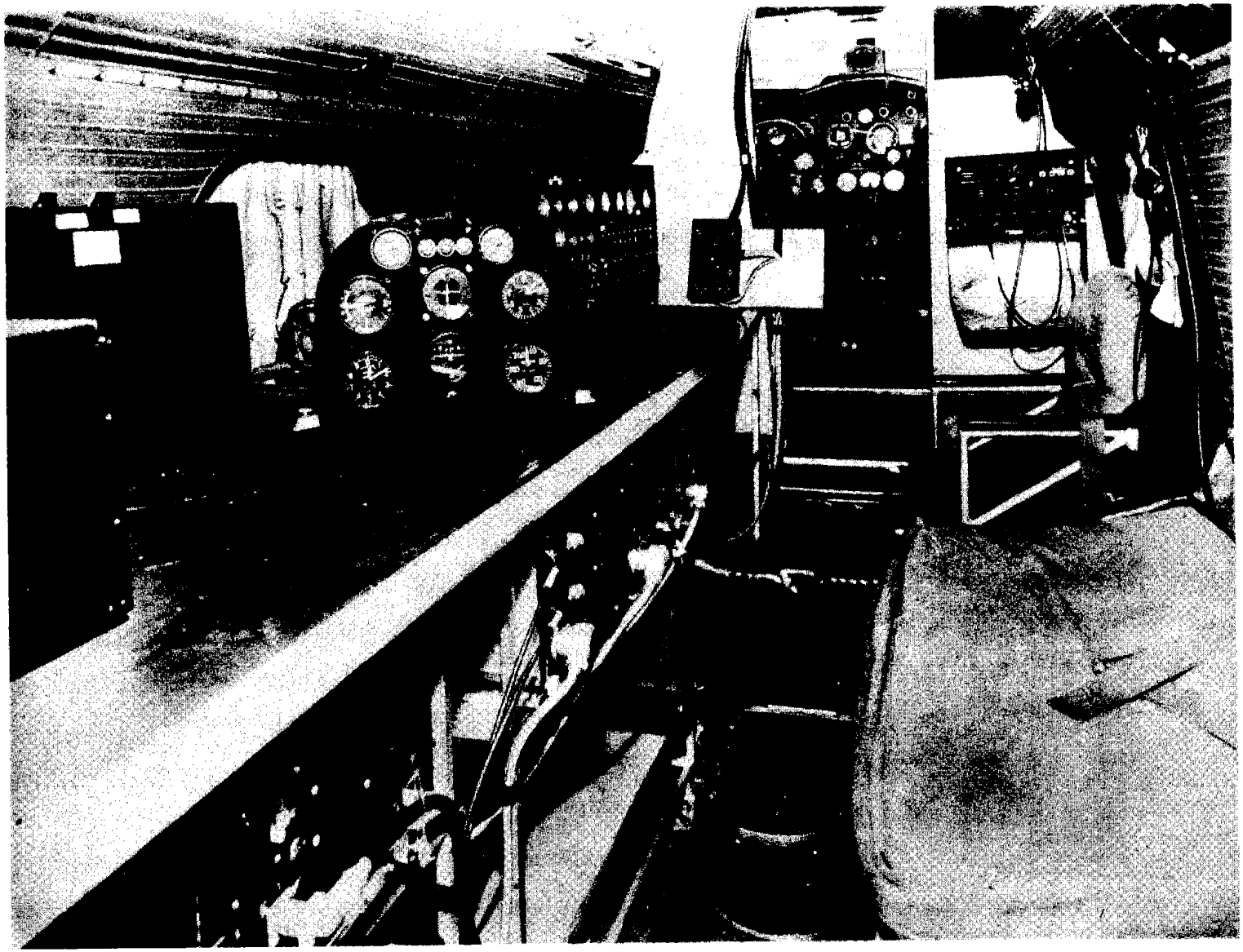

Figure 75. Installation of Receiving Equipment and Special Test Apparatus in the Cabin of NC-11.

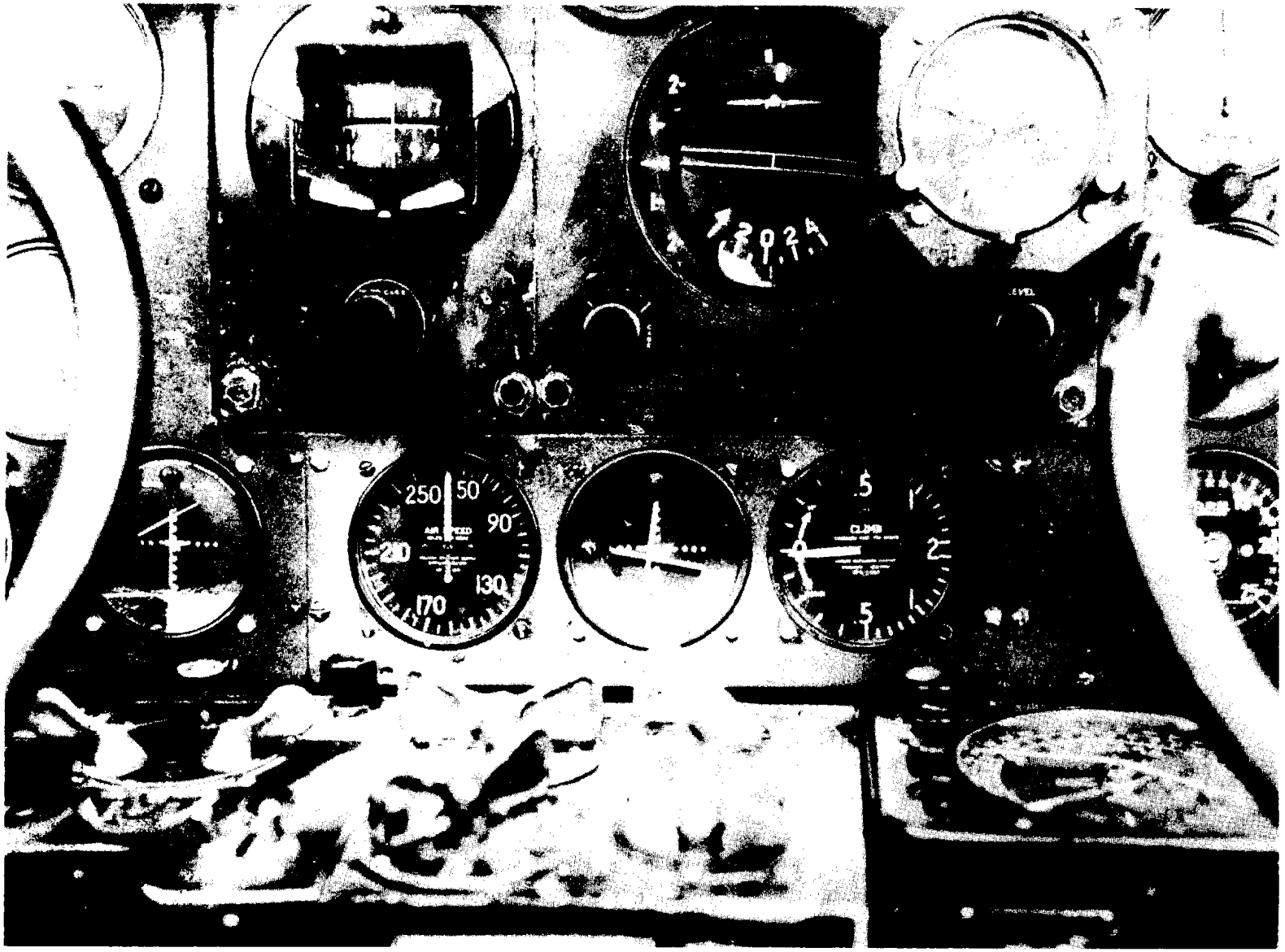

Figure 76. Instrument Panel of NC-11 Showing the Installation of Crossed-Pointer Instruments.

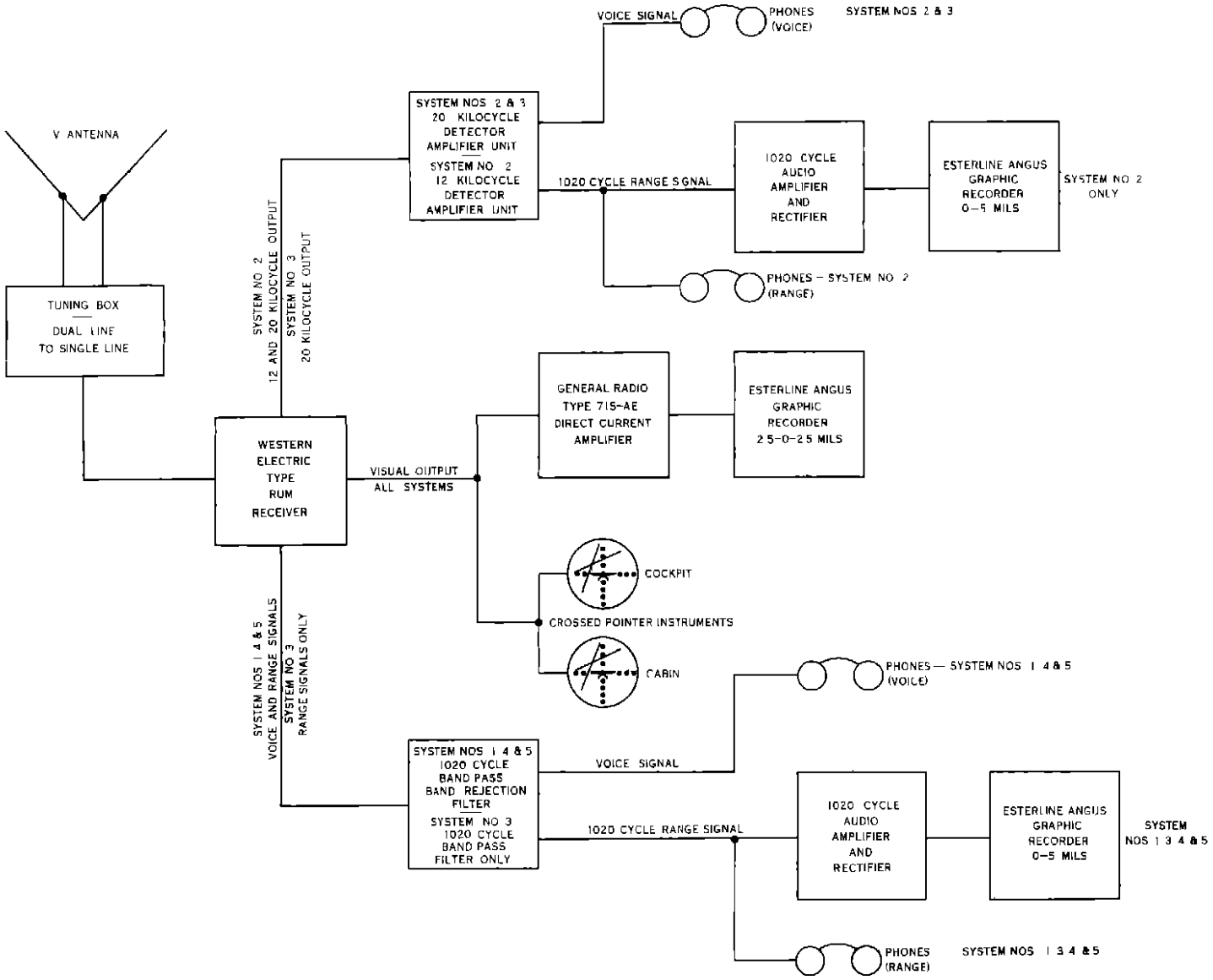

Figure 77 Block Diagram of the Receiving Installation for all Systems

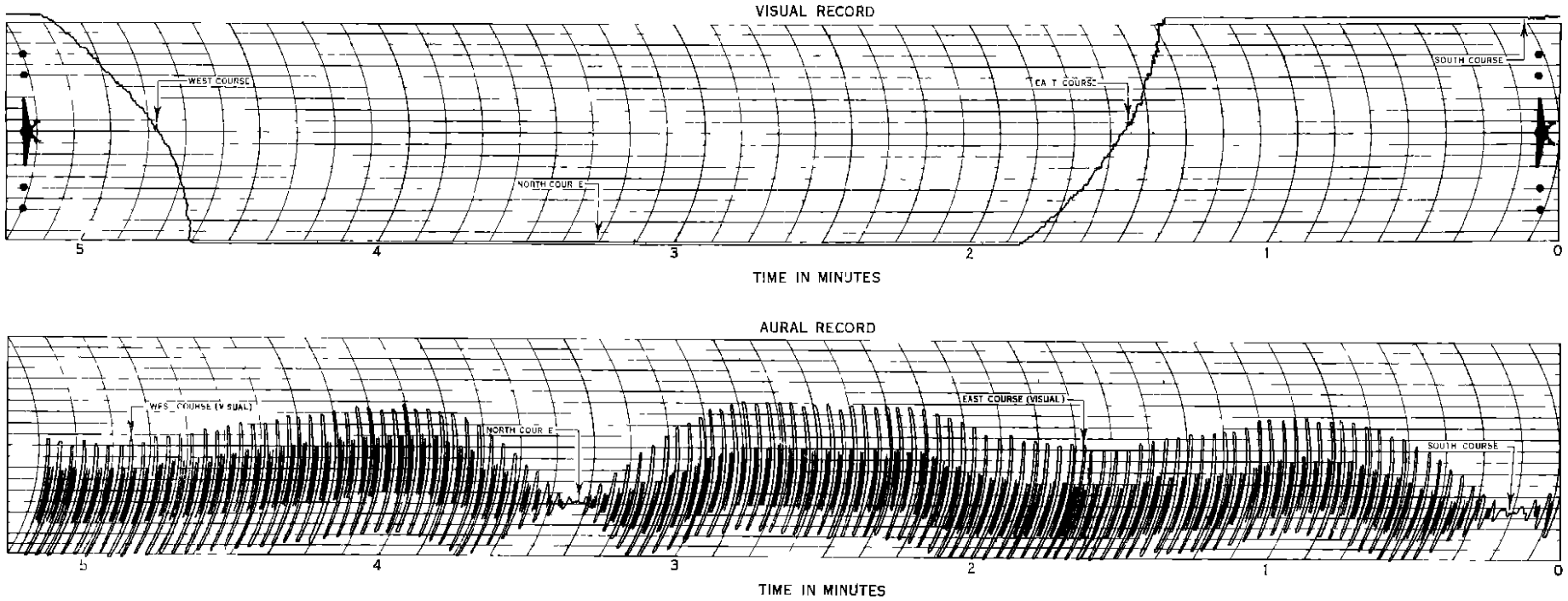

Figure 78 Flight Recordings of Both the Visual and Aural Signals of System No 5 Made While Circling the Station at a Radius of 2 Miles

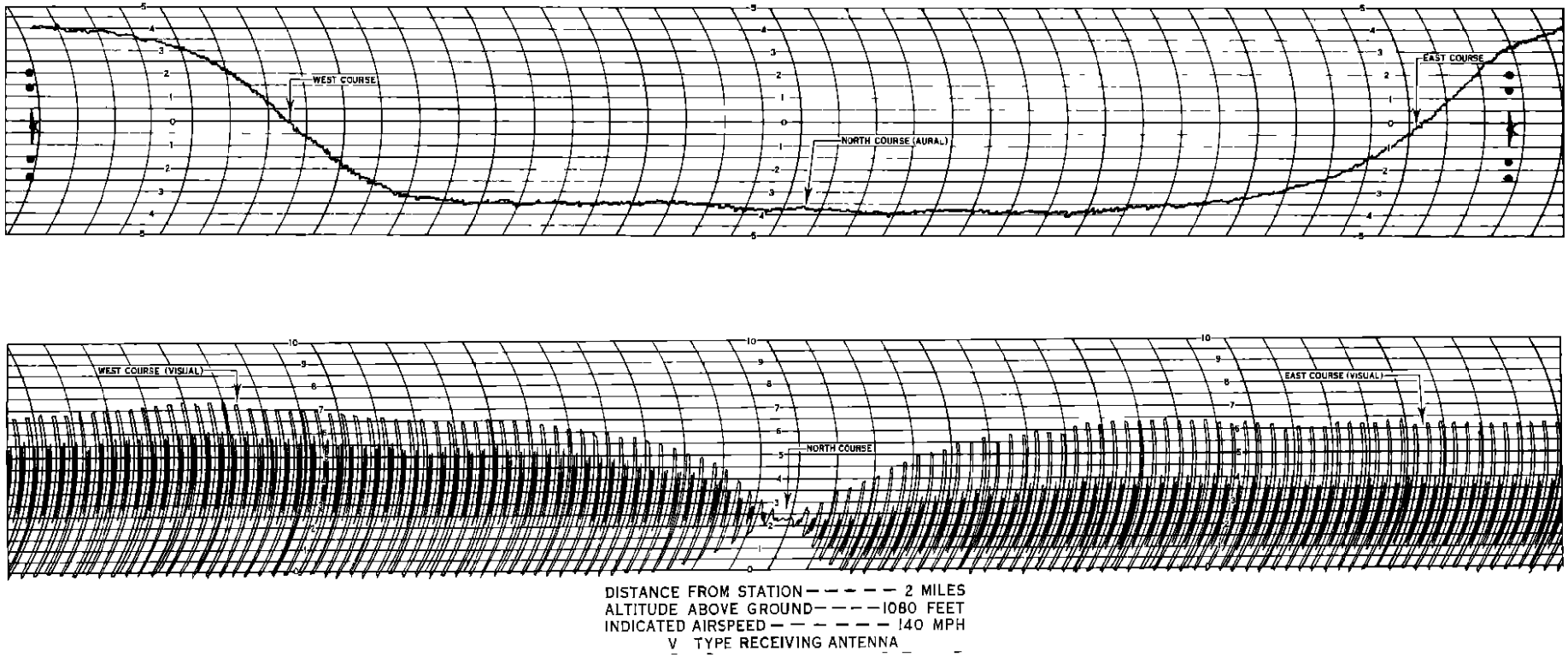

Figure 79 Flight Recordings of Both the Visual and Aural Signals of System No 2 Made While Circling the Station at a Radius of 2 Miles

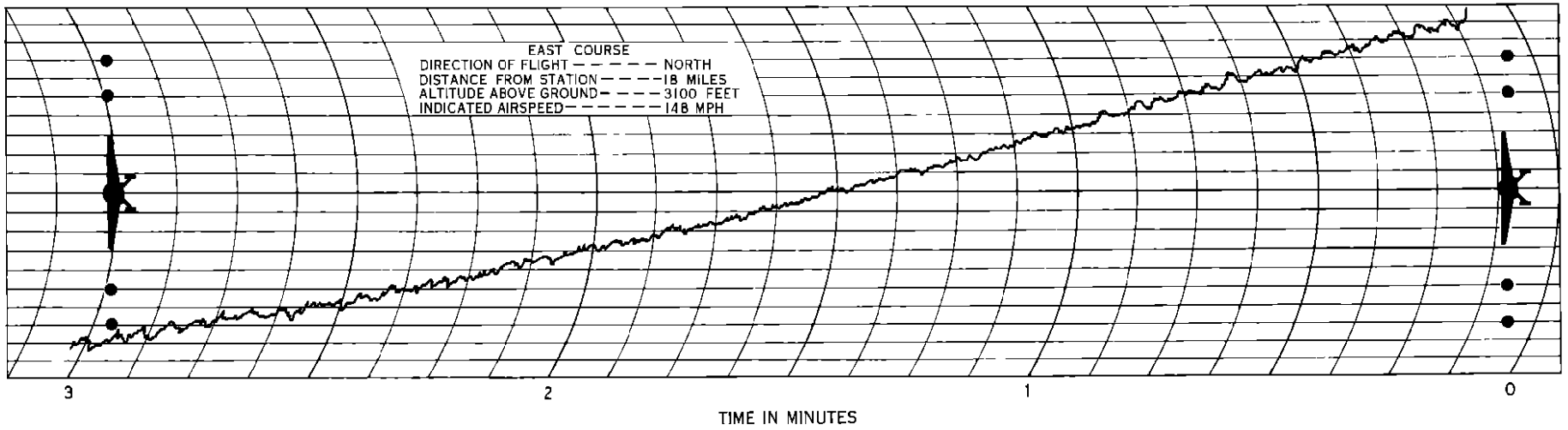

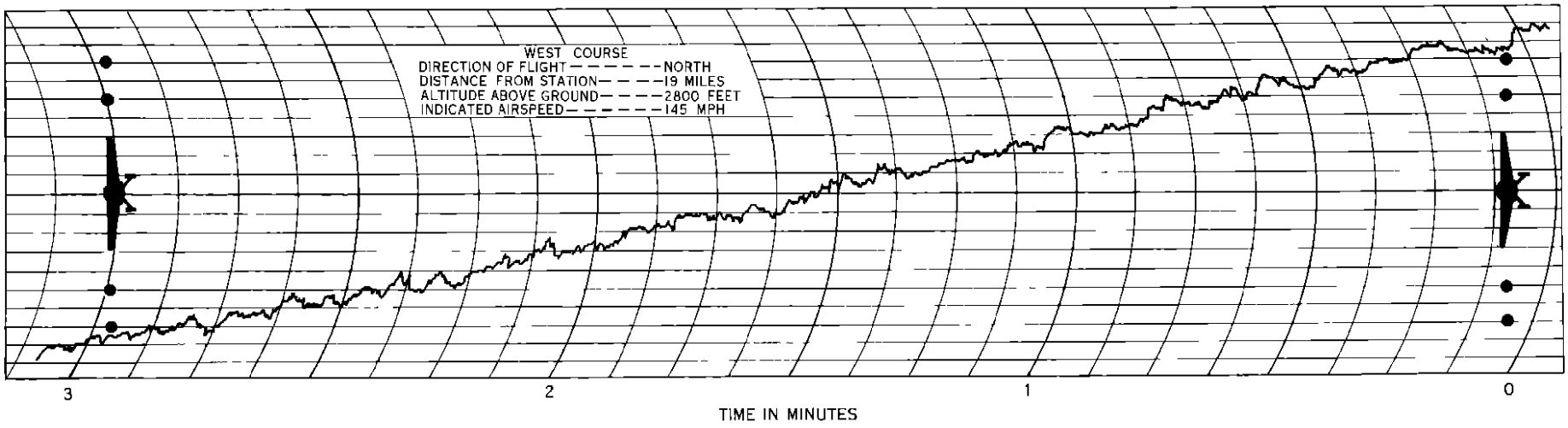

Figure 80 Cross-Course Flight Recordings of the East and West Visual Course of System No 5

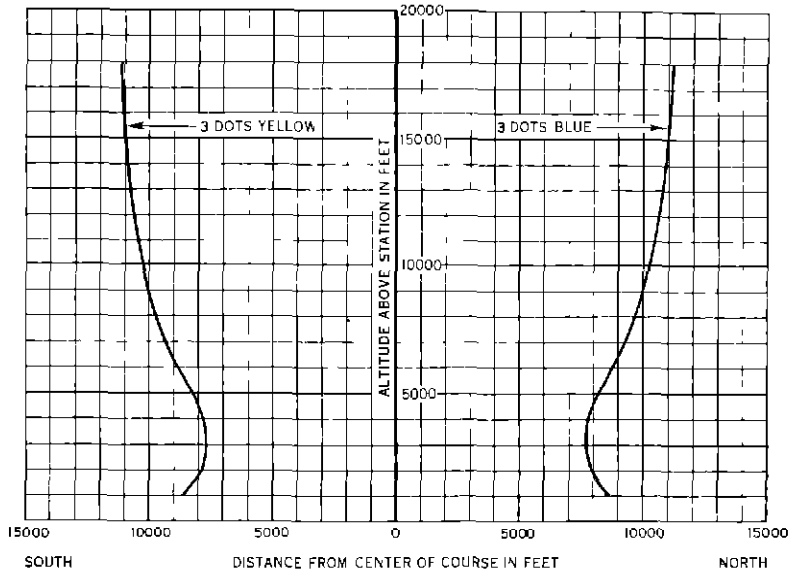

Figure 81 Variation of Course With Altitude for the Non-Simultaneous System

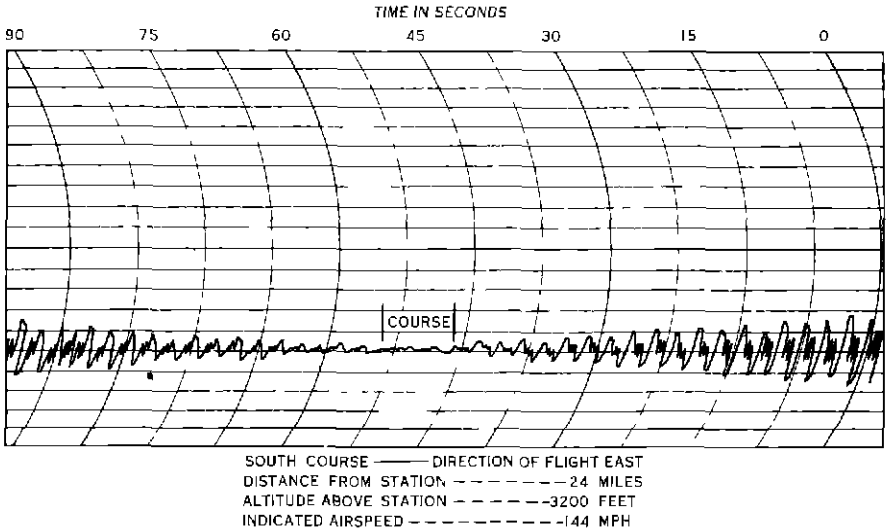

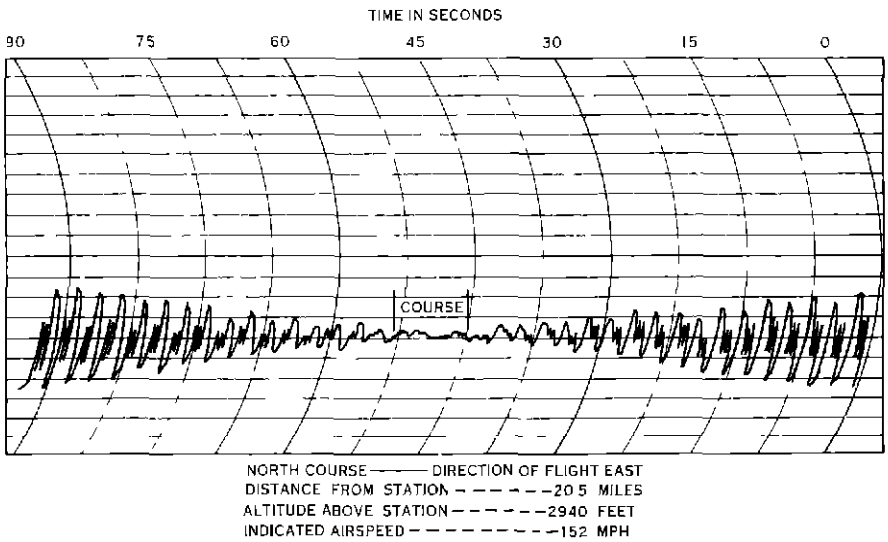

Figure 82 Cross Course Flight Recordings of the North and South Aural Courses of System No 5

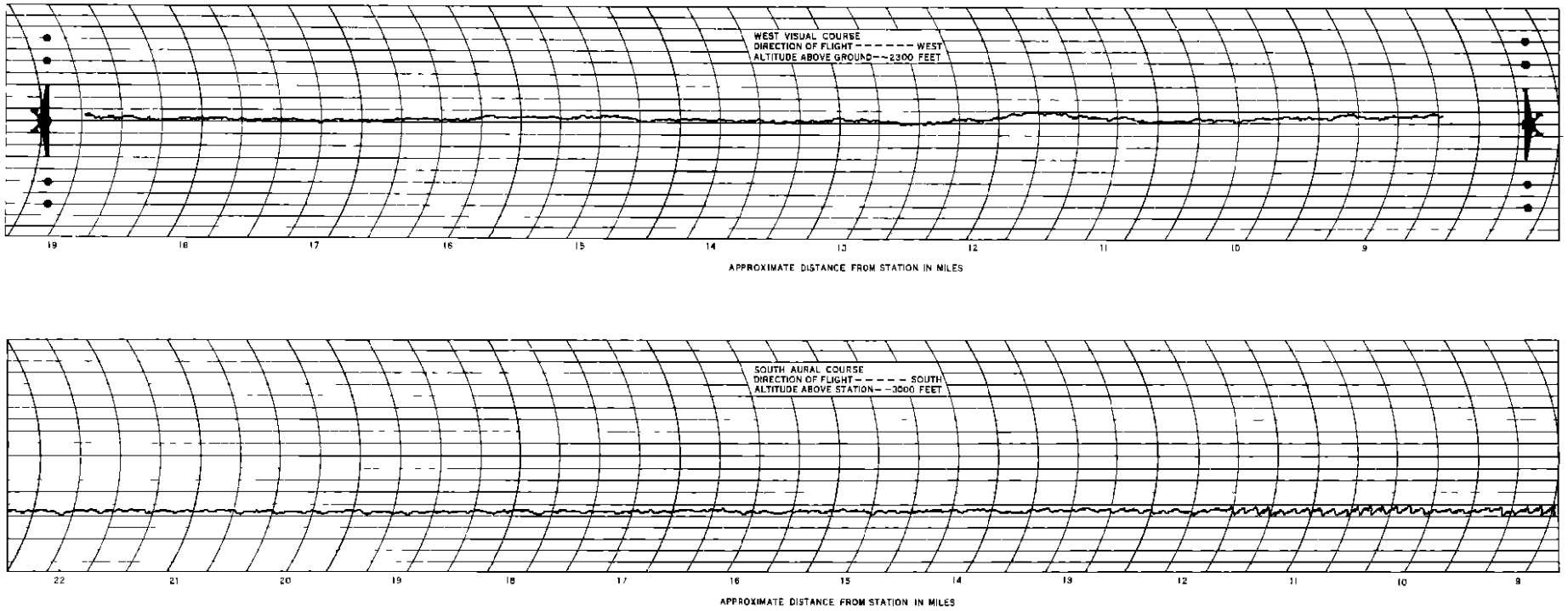

Figure 83 Flight Recordings Made While Flying On-Course on Both a Visual and an Aural Course of System No 5

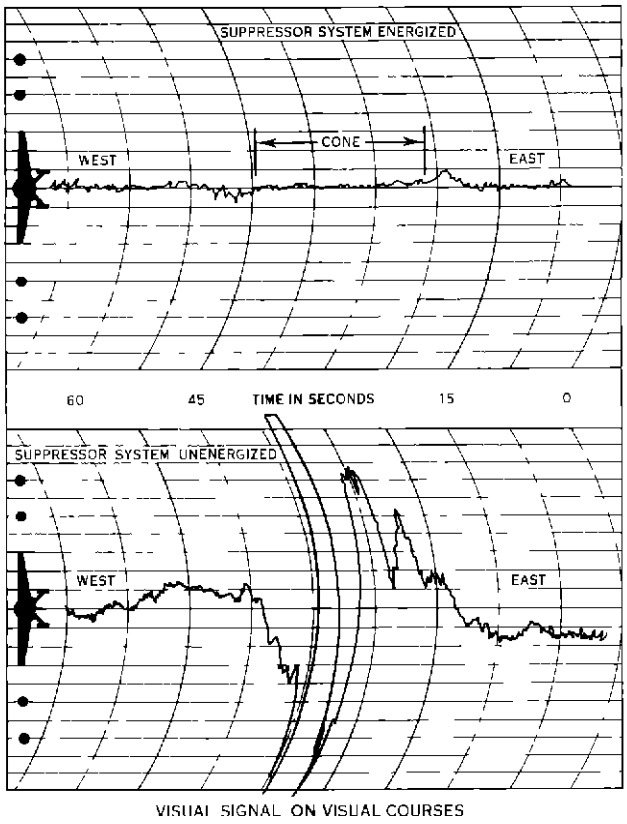

VISUAL SIGNAL ON VISUAL COURSES

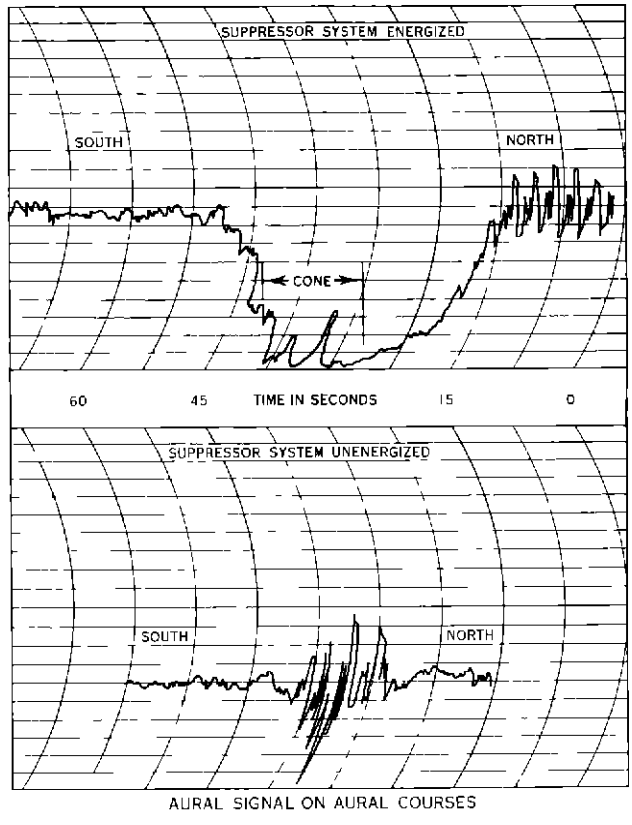

AURAL SIGNAL ON AURAL COURSES

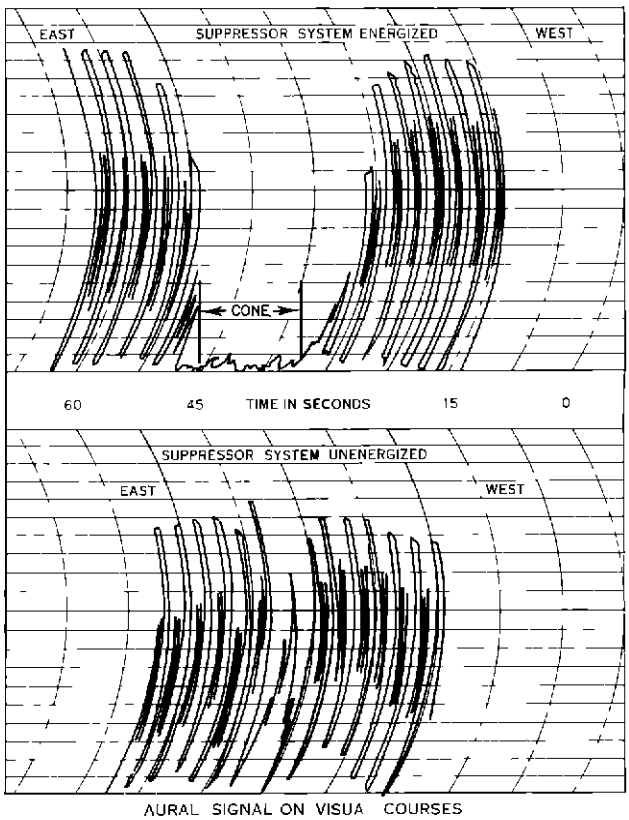

AURAL SIGNAL ON VISUA COURSES

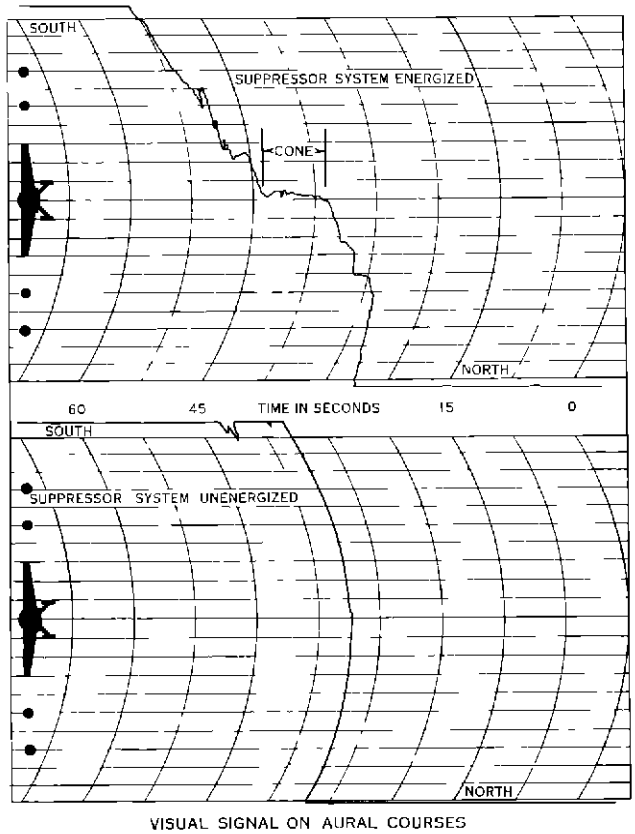

VISUAL SIGNAL ON AURAL COURSES

INDICATED AIRSPEED – 145 MILES PER HOUR

Figure 84 Flight Recordings of Both the Visual and Aural Signals at an Altitude of 3000 feet in the Cone Area of System No 5

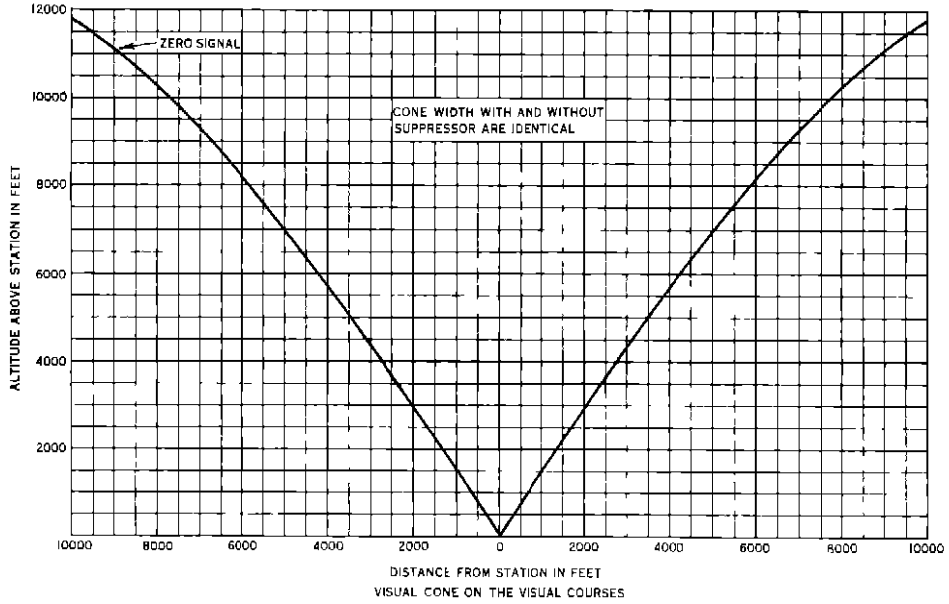

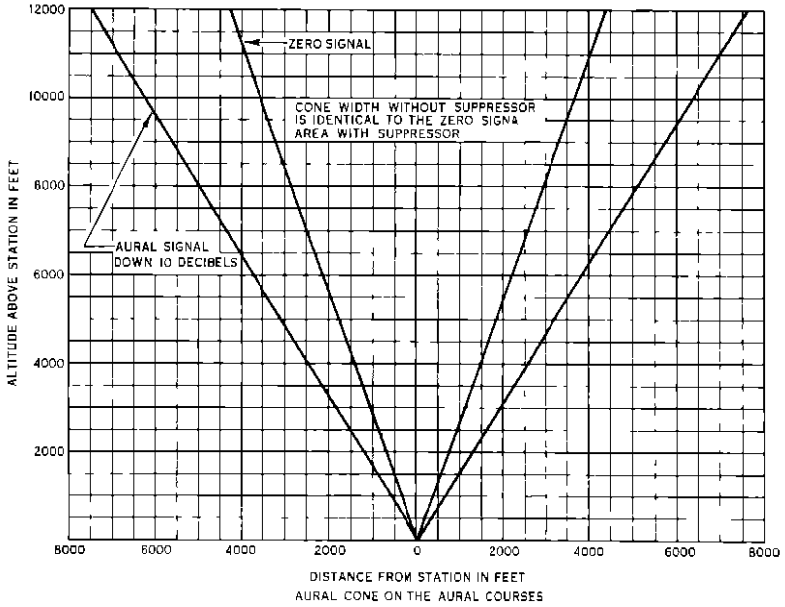

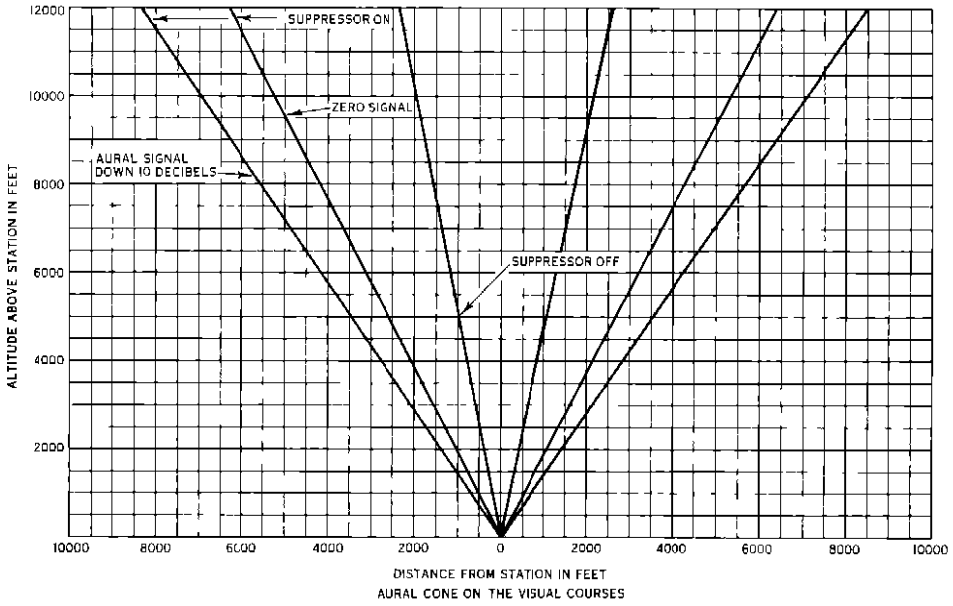

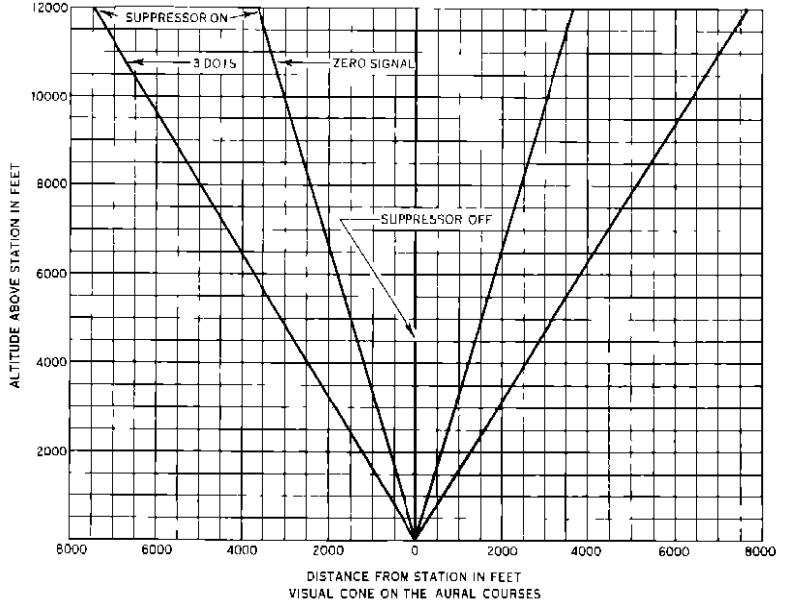

Figure 85 Variation of Visual and Aural Cone Areas with Altitude for System No 5

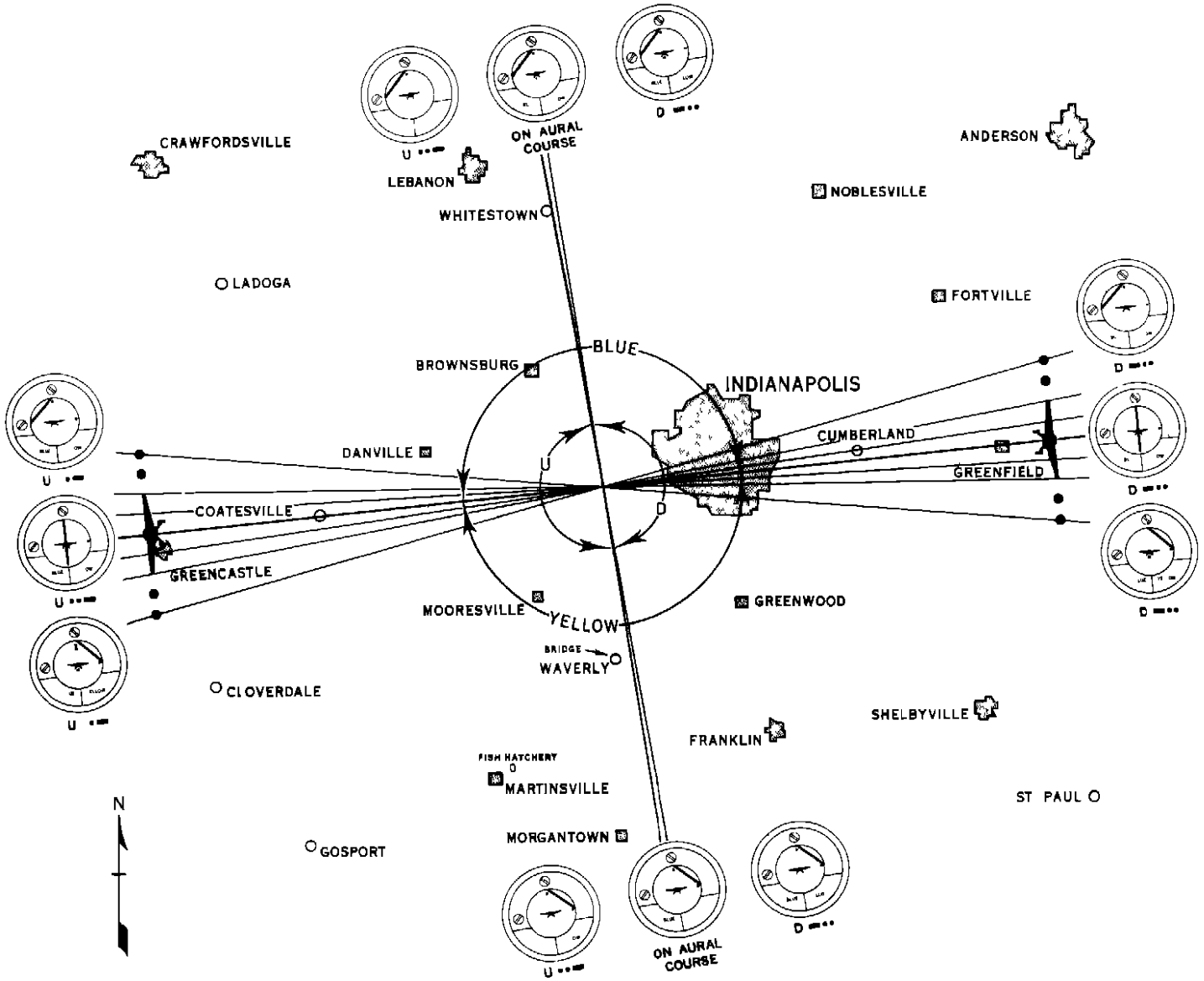

Figure 86 Map Showing the Location and Relative Size of the Visual and Aural Courses of System No 5

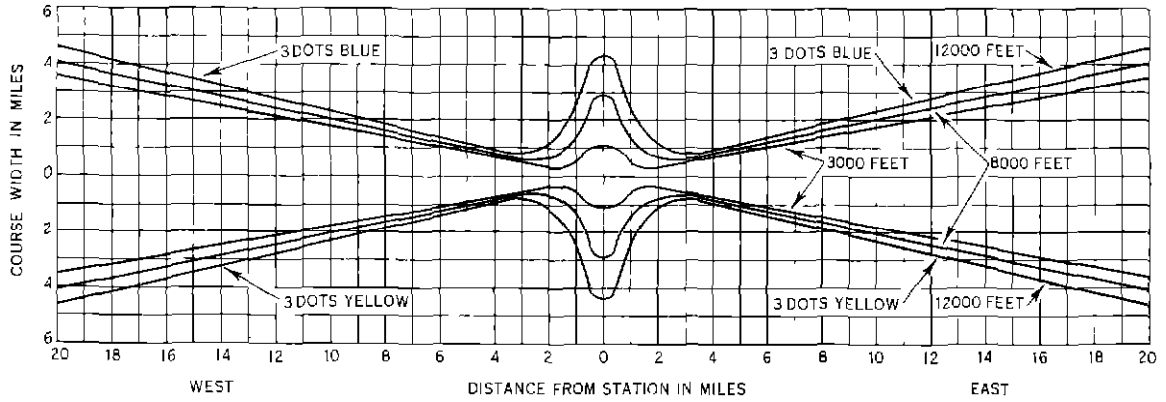

Figure 87 Variation of Visual Course Width and Cone Width with Altitude for the Non-Simultaneous System

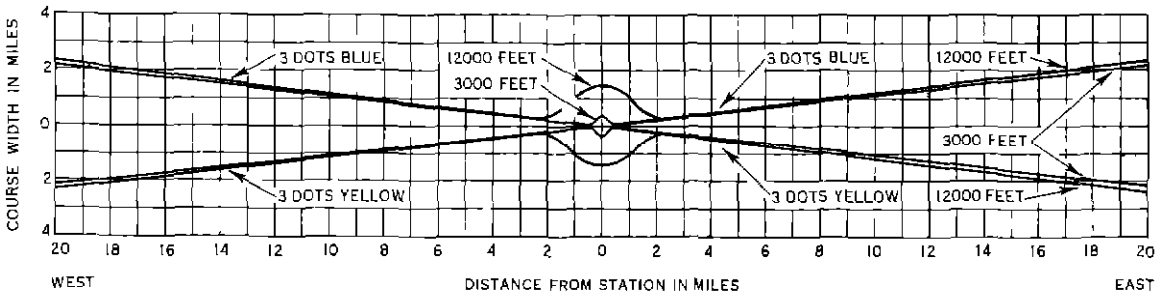

Figure 88 Variation of Visual Course Width and Cone Width with Altitude for System No 5

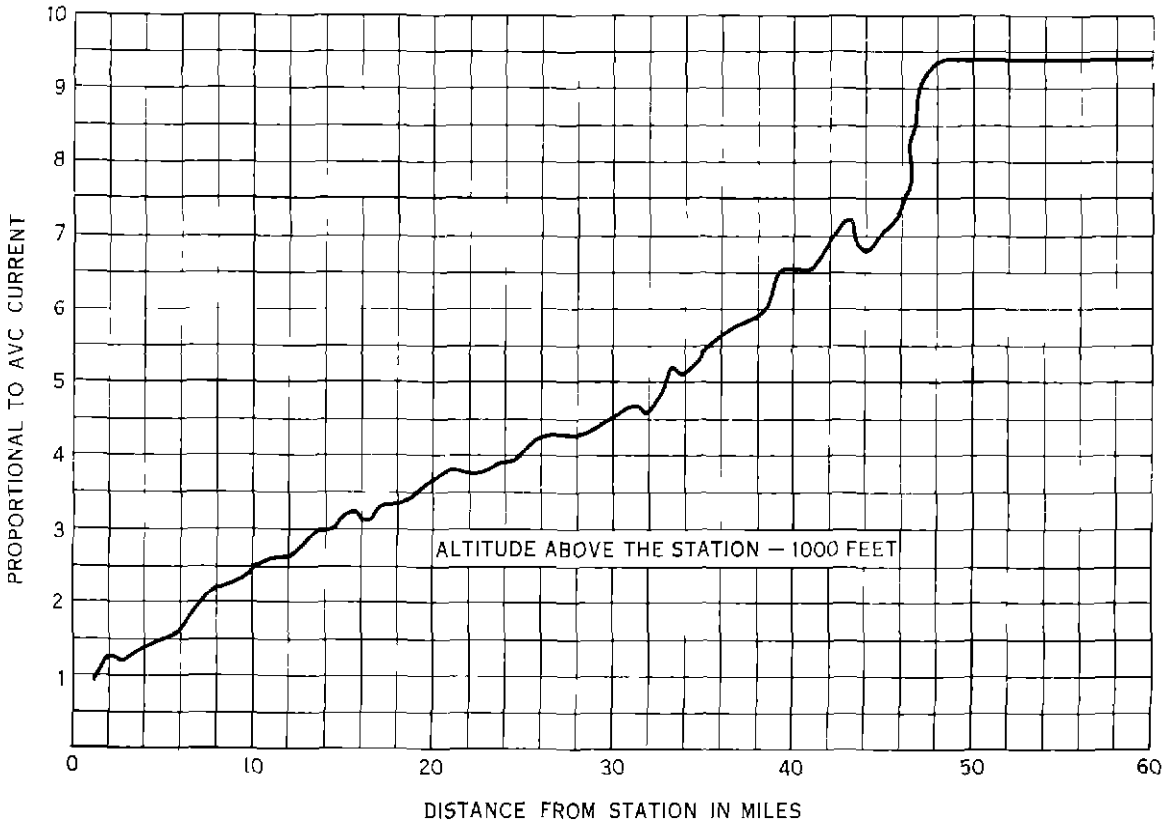

Figure 89 Variation of AVC Current with Distance at an Altitude of 1000 feet for System No 5

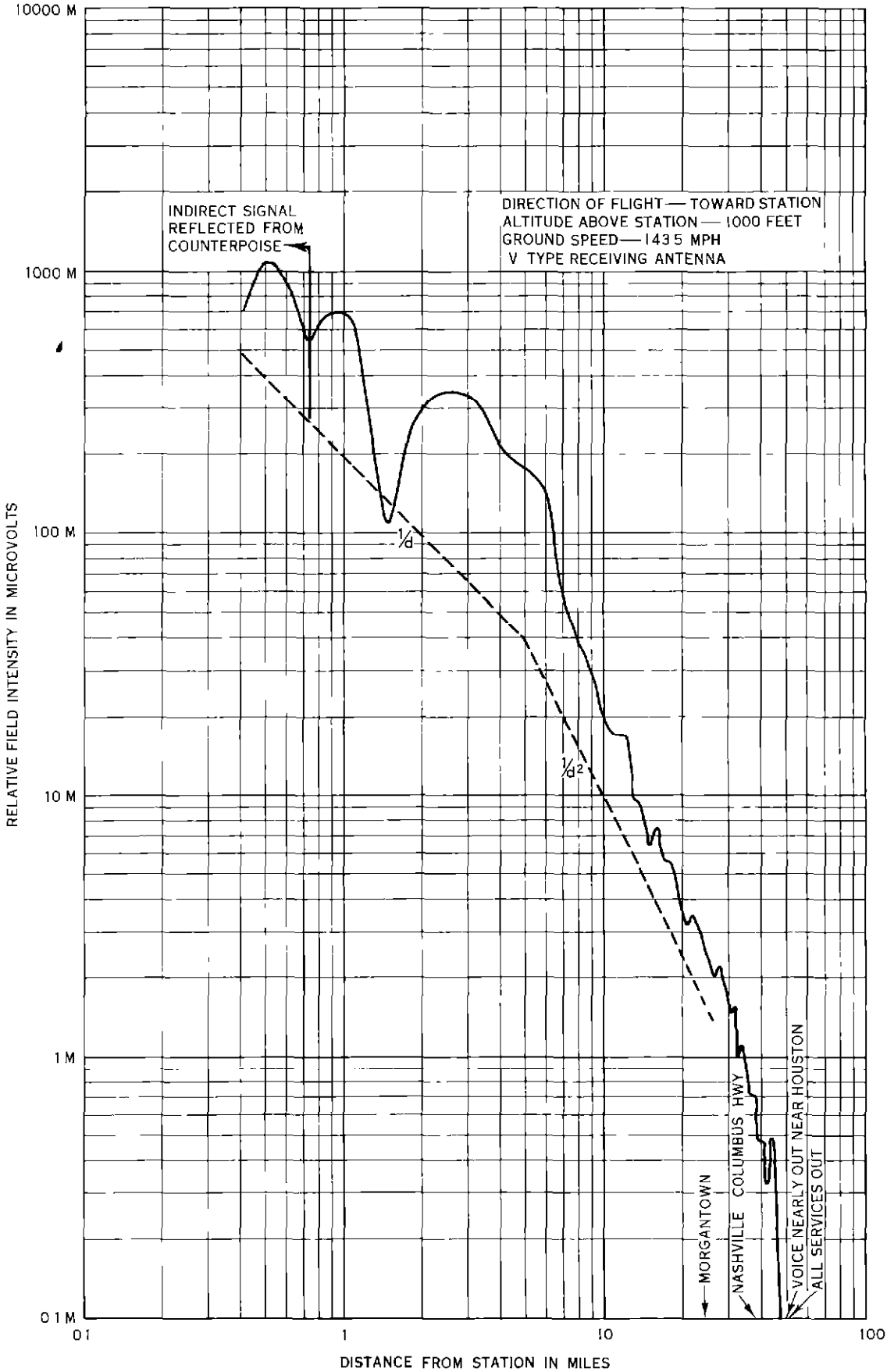

Figure 90 Vertical Field Pattern of System No 5

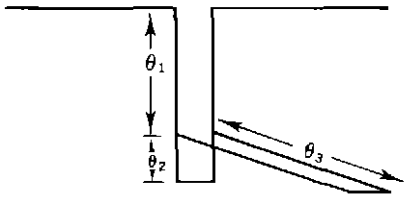

Figure 91A Schematic Diagram of Half Wave Antenna when Operating Parasitically

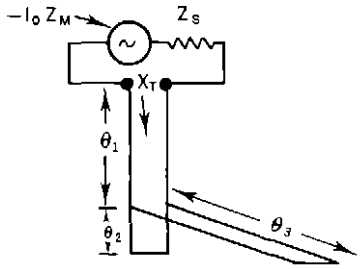

Figure 91B Equivalent Circuit of Parasitic Antenna

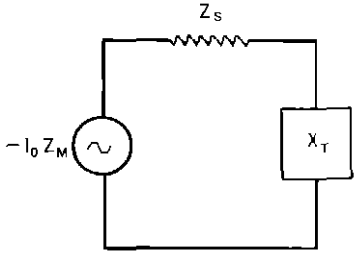

Figure 91C Simplification of Equivalent Circuit of Parasitic Antenna

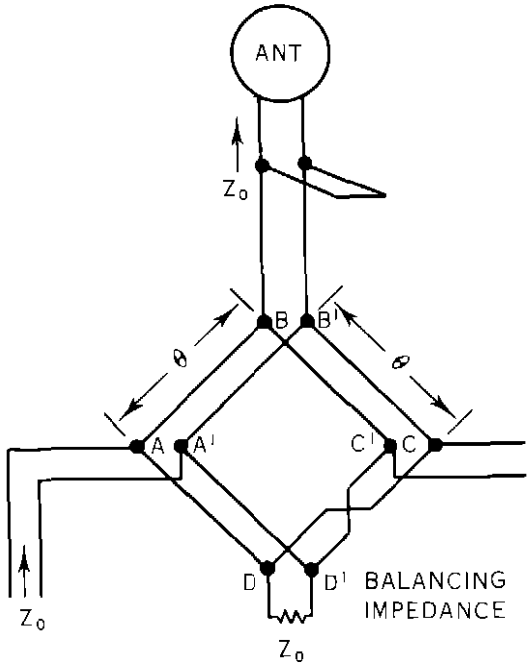

Figure 92A Schematic Diagram of Radio Frequency Bridge

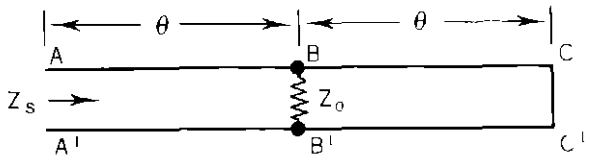

Figure 92B Equivalent Diagram of One Half of Radio Frequency Bridge

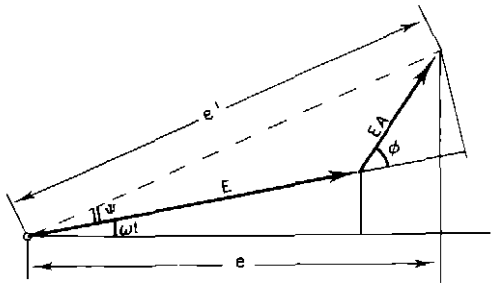

Figure 93 Vector Diagram of Carrier and Sidebands

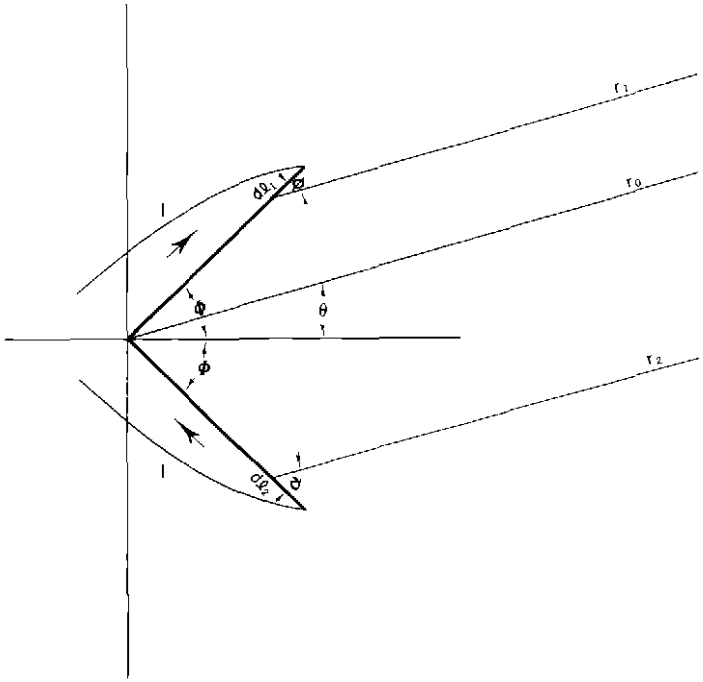

Figure 94 Geometry for Derivation of Field Patterns for V Antenna

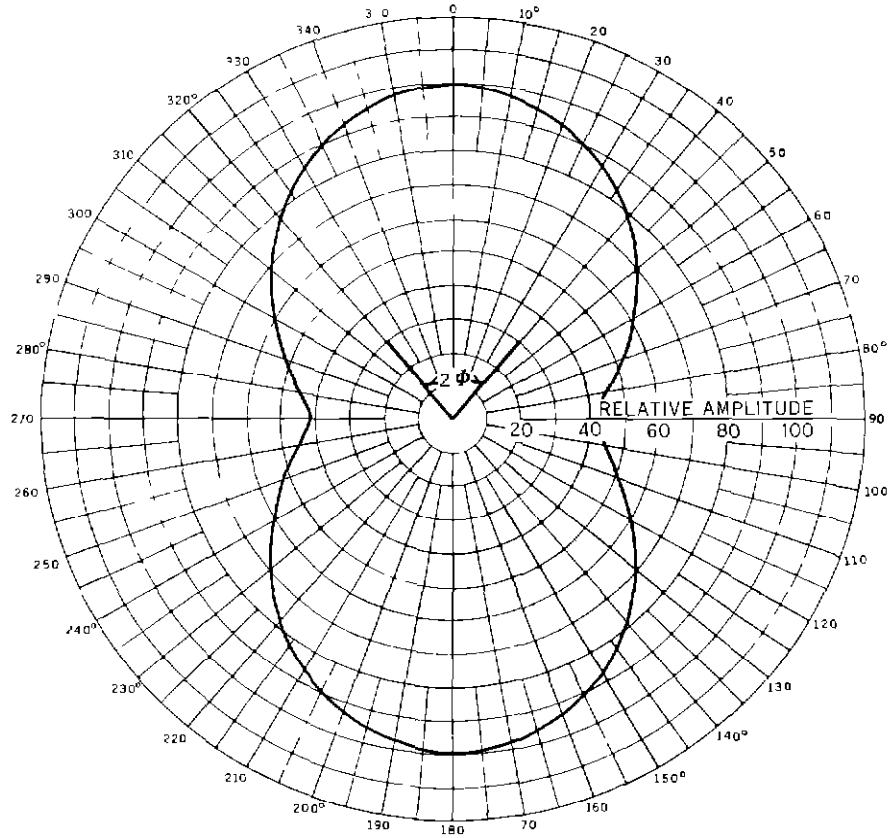

Figure 95 Calculated Pattern in Horizontal Plane for the V Antenna $2\phi=80°$

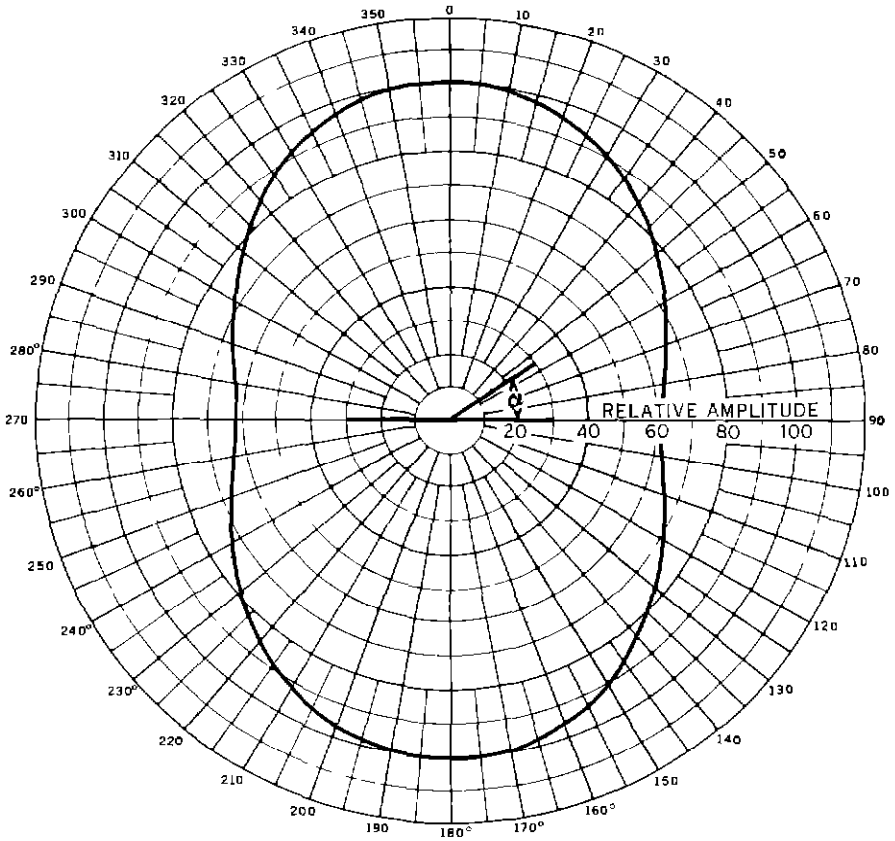

Figure 96 Calculated Pattern in Vertical Plane Through Apex Bisector for the V Antenna $2\phi=80°$